SPONSORED BY THE

Federal Ministry
of Education
and Research

Funded by

DFG Deutsche
Forschungsgemeinschaft

German Research Foundation

STATUS CONFERENCE RESEARCH VESSELS 2020

Conference transcript

SCHRIFTENREIHE PROJEKTTRÄGER JÜLICH

„Bibliographic information published by the Deutsche Nationalbibliothek.
Die Deutsche Nationalbibliothek lists this publication in the Deutsche Nationalbibliografie; detailed bibliographic data are available in the Internet at http://dnb.d-nb.de."

Für den Inhalt der einzelnen Beiträge tragen die Autoren die Verantwortung.

Published by
Forschungszentrum Jülich GmbH
Zentralbibliothek, Verlag
52425 Jülich, Germany
Phone: 02461 61 - 5368
Fax: 02461 61 - 6103
E-mail: zb-publikation@fz-juelich.de
Internet: www.fz-juelich.de/zb

Edited by and layout
Projectmanagement Jülich, Forschungszentrum Jülich GmbH

Photo credits
Titel (left to right): GEOMAR/Karen Hissmann; Manfred Schulz TV&FilmProduktion/ Max-Planck Institut Bremen; Universität Hamburg/LDF/Denecke

Schriftenreihe Projektträger Jülich Volume 13
ISBN 978-3-95806-479-9

The complete volume is freely available on the Internet on the Jülicher Open Access Server (JuSER) at www.fz-juelich.de/zb/openaccess.

STATUS CONFERENCE RESEARCH VESSELS 2020

Conference transcript

SCHRIFTENREIHE PROJEKTTRÄGER JÜLICH

FOREWORD

Dear participants,

The acquisition of research data is essential to conduct scientific working. However, to get to the bottom of a question on a research vessel, using complex sensor systems and analyzing water samples is more than just collecting data. It is a unique connection with the habitat under study, an awareness of its dimensions and variability, a moment of true "understanding". Anyone who has applied, prepared, coordinated, evaluated and documented an expedition knows that the relatively short sampling period requires careful and long advance planning. This is only possible because many people, partly unnoticed are involved. Here I would like to express my thanks to them and emphasize their importance.

Among the essential principles of science, the persistent critical exchange and the evaluation of research proposals within a discipline play an important role. For the fleet of German research vessels, since autumn 2017 the review and evaluation of the cruise proposals for all ships has been carried out by a joint review process initiated by the BMBF, DFG and HGF. As a member of the newly founded Expert Panel Research Vessels (GPF) I am pleased to welcome you to the 1st Status Conference Research Vessels 2020 at my home institute, the Institute for Chemistry and Biology of the Marine Environment (ICBM) at the University of Oldenburg. May this conference contribute to the success of marine research and offer much room for inspiration. So that future expeditions we will continue to ask questions and find answers that will help to adjust our social actions more specifically towards the protection of this unique habitat.

OLIVER ZIELINSKI
Head of the Center for Marine Sensor Technology at the Institute for Chemistry and Biology of the Marine Environment (ICBM), University of Oldenburg, and member of the GPF

TABLE OF CONTENTS

*poster contribution

*poster contribution

*poster contribution

*poster contribution

*poster contribution

*poster contribution

*poster contribution

*poster contribution

*poster contribution

*poster contribution

*poster contribution

KEYNOTE

COMPOSITION, FUNCTION AND ENVIRONMENTAL CONTROLS OF THE MICROBIOME IN THE EPIPELAGIC ATLANTIC AND PACIFIC OCEAN

AUTHORS

Institute for Chemistry and Biology of the Marine Environment, University of Oldenburg | Oldenburg, Germany
S. Meinhard

The Atlantic and Pacific Ocean cover ~80% of the world's oceans and thus are extremely important for global elemental cycles and organic matter processing in the context of climate change. Pelagic microbial communities, the microbiome, are the main drivers of these cycles. Both oceans are structured into biogeographic provinces which are distinct in hydrographic, nutrient and plankton features (Longhurst 2006). Despite quite a few investigations of the microbiome in both oceans (Sunagawa et al. 2015, Louca et al. 2016), their central and rather remote regions and in particular latitudinal gradients are still scarcely studied. Therefore, we carried out systematic investigations of south-north transects with RV Polarstern in the Atlantic (ANTXXVIII/4, -5) and RV Sonne in the Pacific (SO248/-254) from beyond the austral to beyond the northern temperate zones, covering 110° latitude and the major biogeographic provinces (Fig. 1).

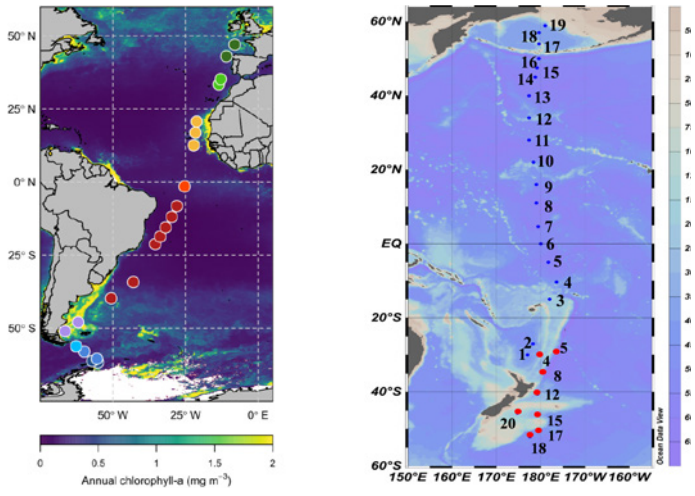

Fig. 1: Stations of cruises with RVs Polarstern in the Atlantic (left panel) and Sonne in the Pacific Ocean (right panel). Colors of the stations in the Atlantic illustrate biogeographic provinces and the background annual mean concentrations of chlorophyll a (https:// oceandata.sci.gsfc.nasa.gov). Stations in blue in the Pacific were visited during cruise SO248 and those in red during cruise SO254.

In addition to extensive analyses of the composition and functional diversity of the microbiomes by amplicon sequencing of the 16S rRNA gene and metagenomics, water masses were characterized by hydrography, nutrients, biogeochemical and microbial bulk parameters (Simon et al. 2012a and 2012b, Simon et al. 2016 and 2016).

In both oceans biogeographic provinces were well characterized and distinct on the basis of hydrography, inorganic nutrients (nitrate, phosphate, silicate) and biogeochemical properties (Fig. 2: Bacterioplankton bulk growth rate at 20 and 60 m depth, mixed layer temperature and depth across the Atlantic Ocean between 62°S and 47°N). parameters such as bacterioplankton numbers of l ow and high nucleic acid content, growth rate, turnover of amino acids, glucose and acetate also exhibited variations, not reflecting biogeographic provinces but rather regional and large scale features related to availability of substrates, stratification and to temperature gradients (Figs. 2, 3).

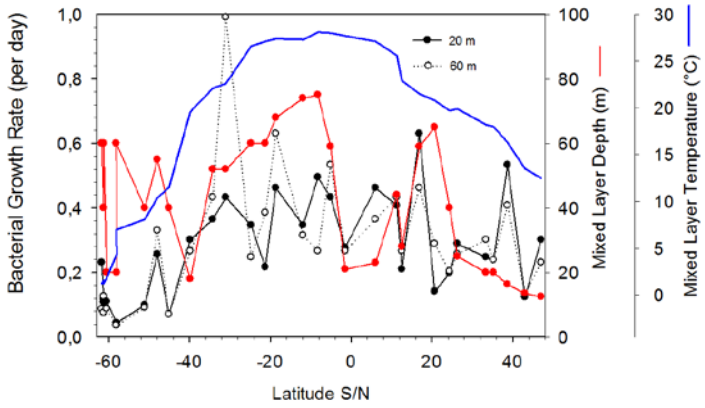

Fig. 2: Bacterioplankton bulk growth rate at 20 and 60 m depth, mixed layer temperature and depth across the Atlantic Ocean between 62°S and 47°N.

The composition of the microbiomes in both oceans reflected well the distinct biogeographic provinces with different lineages of Alpha- and Gammaproteobacteria, Flavobacteria and Cyanobacteria constituting the major components, but showing also different partitionings of sublineages in different provinces (Fig. 4). An in-depth analysis of the microbiome in the Atlantic at 20 m depth on the basis of metagenomic data identified in total more than 20,000 and at each station between 10,000 and 14,000 prokaryotic species, demonstrating a huge diversity. Also, the functional diversity exhibited distinct biogeographic patterns. Genes encoding energy metabolism, cofactors and vitamin, e. g., were relatively enriched in warm and permanently stratified provinces whereas genes encoding transporters, amino acid and carbohydrate metabolism were relatively enriched in the coldest southernmost regions. Genes encoding carbohydrate active enzymes (CAZymes) clustered into three groups with temperature optima around 5, 15 and 25°C, indicating that distinct microbial communities were well adapted to the

consumption of this important class of substrates. Temperature was identified as the strongest driver of the taxonomic and functional diversity of the Atlantic Ocean microbiome with the highest diversity in mid-latitude regions around 15–20°C and lowest values in the coldest provinces.

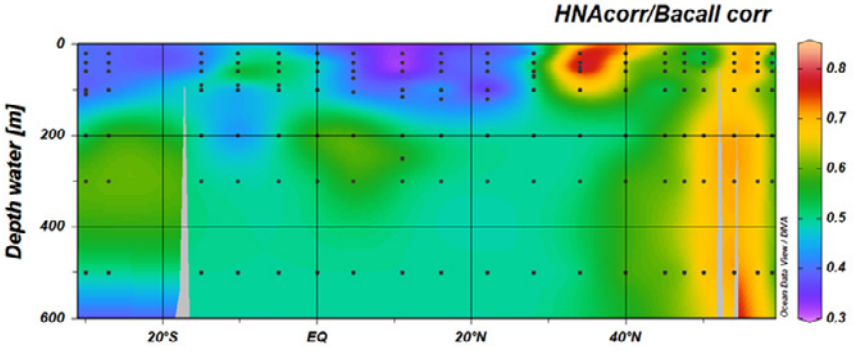

Fig. 3: Ratio of large bacteria with high nucleic acid (HNA) over total bacteria in the Pacific Ocean from 30°S to 59°N between 20 and 500 m depth.

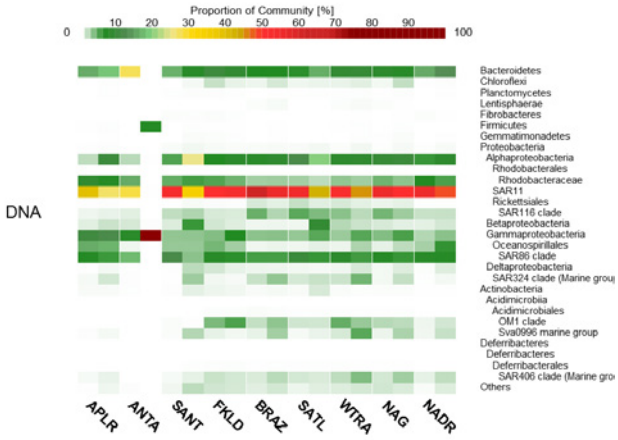

Fig. 4: Composition of the Atlantic Ocean microbiome at 20 m depth in its major biogeographic provinces between 62°S and 47°N based on 16S rRNA gene amplicon sequences (APLR: Antarctic Polar Porvince; ANTA: Antarctic Province; SANT: Subantarctic Province; FKLD: Southwest Atlantic Shelves Province; BRAZ: Brazil Current; SATL: South Atlantic gyre; WTRA: Western tropical Atlantic; NAG: North Atlantic gyre; NADR: North Atlantic Drift).

Nitrogen (N) availability had a major impact on the prokaryotic genomic G+C content and the N-content of proteomic amino acid side chains. In severely N-limited regions the genomic G+C content and N-content of amino acid side chains were significantly lower than in regions further south and north with higher N-availabilities. In addition,

N-acquisition genes exhibited a surprising biogeographic and taxonomic diversity demonstrating a well-modulated microbial exploration of the various organic and inorganic N-sources.

These detailed taxonomic and functional analyses of the oceanic microbiomes shed new light on their biogeography and on the functional significance of distinct members in the cycling of organic matter and elements.

REFERENCES

Longhurst, A. Ecological geography of the sea. (Academic Press, San Diego, 2006).

Louca, S., Parfrey, L. W. & Doebeli, M. Decoupling function and taxonomy in the global ocean microbiome. Science 2016 353: 1272–77.

Simon, M, et al. Composition and activity of the bacterioplankton communities in the Drake Passage and Antarctic Peninsula region. In: Lucassen M (ed) The expedition of the Research Vessel "Polarstern" to the Antarctic in 2012 (ANT-XXVIII/4) Reports on Polar and Marine Research 2012a, 653, 49-54, http://hdl.handle.net/10013/epic.40372.

Simon M, et al. Composition and activity of the Bacterioplankton communities in a south-north transect of the Atlantic Ocean. In: Bumke K (ed) The expedition of the Research Vessel "Polarstern" to the Antarctic in 2012 (ANT-XXVIII/5) Reports on Polar and Marine Research 2012b, 654, 30-35, http://hdl.handle.net/10013/epic.40370.

Simon M. RV SONNE SO248 BacGeoPac Cruise Report / Fahrtbericht Auckland, New Zealand, May 1st, 2016, Dutch Harbor, USA: June 3rd, 2016, PTJ, DOI 10.2312/cr_so248.

Simon M. RV SONNE SO254 PoriBacNewZ Cruise Report / Fahrtbericht Auckland, New Zealand, January 26th, 2017, Auckland, New Zealand, February 27th, 2017, PTJ, DOI 10.2312/cr_so254.

Sunagawa, S. et al. Structure and function of the global ocean microbiome. Science 2015, 348, 1261359.

M95

CURRENT IMPACT ON THE FACIES AND STRATIGRAPHY OF THE BAHAMAS CARBONATE PLATFORM (CRUISE M95, CICARB)

AUTHORS

Institut für Geologie, Universität Hamburg | Hamburg, Germany
C. Betzler, S. Lindhorst, T. Lüdmann

Research Cruise M95 achieved all the goals as formulated in the cruise proposal: By integrating swath echosounder, multichannel seismic, sedimentological, and oceanographic data it has been demonstrated how the sedimentation along the flank of Bahamian carbonate platforms is the result of the combined effects of downslope gravitative and alongslope contour current processes. Contour currents shape a periplatform drift at the foot of the Great Bahama Bank escarpment, which displays along-slope and downslope variations in sedimentary architecture. Sediments are muddy carbonate sands that coarsen basinward (Fig. 1). The drift wedge has a pervasive cover of cyclic steps. In zones of lower contour current speed, depth-related facies belts develop, whereas strike-discontinuous sediment lobes, scarps, and gullies characterize areas with higher current speed. While slope instabilities are a common pattern along all Bahamian carbonate platform slopes, different processes triggering slope failures and the formation of channels and gullies were identified. At the leeward slope of the Great Bahama Bank, extensive slope failures occurred primarily during sea-level lowering following an interglacial. These slope failures created a slope morphology that channelizes the exported platform sediments during the subsequent highstand. At the windward slope of the Cay Sal Bank, contour currents and the local tectonic regime are responsible for slope failures. During sea level lowstands, downwelling induces turbidity currents. The interaction of turbidity and contour currents leads to the formation of a system of furrows and slope-parallel sediment ridges. In the Santaren Channel, separating Great Bahama Bank and Cay Sal Bank a carbonate drift forms, which recorded the development of the Gulf Stream and oceanographic, climatic, and tectonic events since the Miocene. The new data document that the signatures of a bottom current flow in the Santaren Channel initiated about 12.3 Ma ago, as indicated by the first occurrence of sheeted drifts and moat development at the northern part of the Santaren Channel. Data also show that three types of carbonate mounds cover the slopes and toe of slopes of the carbonate banks in water depths between 285 and 685 m. Their distribution is strongly related to the present current regime. Sedimentological analyses of cores recovered during the cruise allow reconstructing different dust transport mechanisms to this part of the Caribbean: fine dust particles are delivered by the trade winds and the geostrophic winds of the Saharan Air Layer, whereas coarse dust particles travel with convective storm systems. In this context, grain-size data from the terrigenous fraction of carbonate

drifts provide a measure for past coarse dust transport, and consequently for the frequency of convective storm systems over the dust source areas and the tropical Atlantic.

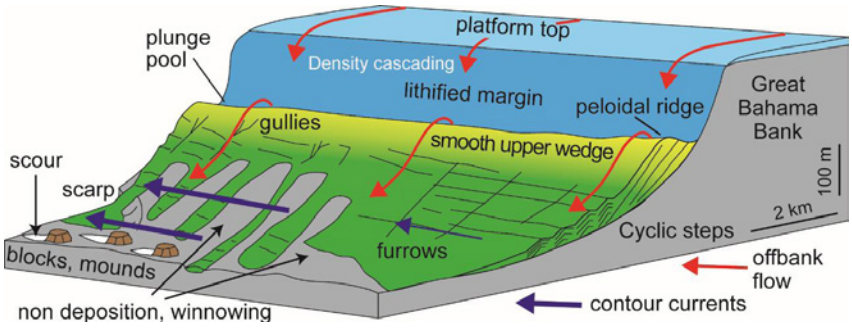

Fig. 1.: Model of the periplatform drift (Betzler et al., 2014). In areas of high alongslope current speeds, periplatform deposits are arranged in lobes infilling shallow depressions, whereas they are deposited in a sediment wedge in zones affected by weaker currents. Figure 1. Model of the periplatform drift (Betzler et al., 2014). In areas of high alongslope current speeds, periplatform deposits are arranged in lobes infilling shallow depressions, whereas they are deposited in a sediment wedge in zones affected by weaker currents.

REFERENCES

Betzler, C., Lindhorst, S., Eberli, G. P., Lüdmann, T., Möbius, J., Ludwig, J., Schutter, I., Wunsch, M., Reijmer, J. J. G., and Hübscher, C., 2014, Periplatform drift: The combined result of contour current and off-bank transport along carbonate platforms, Geology, v. 42, no. 10, p. 871–874, doi: 10.1130/G35900.1.

M101

RESULTS OF THE RHUM-RUM EXPERIMENT: SEISMOLOGICAL IMAGING OF A MANTLE PLUME UNDER RÉUNION HOTSPOT, WESTERN INDIAN OCEAN.

AUTHORS

University of Oxford | Oxford, UK
K. Sigloch

Ludwig-Maximilians-Universität München | München, Germany
K. Sigloch, H. Igel

CNRS & Institut de physique du globe Paris | Paris, France
G. Barruol

Alfred-Wegener-Institut Bremerhaven | Bremerhaven, Germany
V. Schlindwein

Goethe-Universität Frankfurt | Frankfurt, Germany
G. Rümpker

Westfälische Wilhelms-Universität Münster | Münster, Germany
C. Thomas

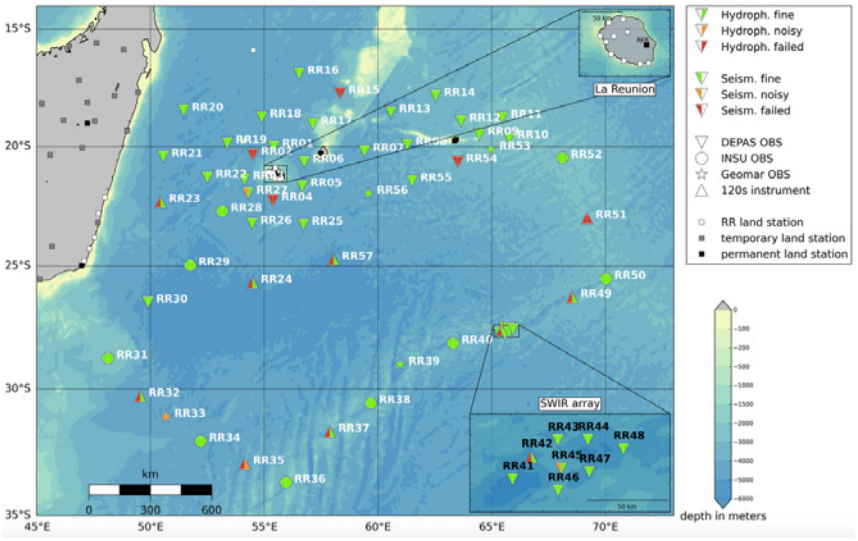

This large seismological experiment aimed at illuminating the earth's deep subsurface structure under the hotspot-type volcano island of La Réunion in the western Indian Ocean. Réunion is one of the most active volcanoes in the world. Volcanism in this absolute position has been continuously active for 65 million years and has erupted a 5500-km long hotspot track that leads to the Deccan Trap flood basalt province in India. This type of volcanism does not fit the otherwise highly successful explanatory framework of volcanism being caused by plate tectonic processes, i. e., originating from no deeper than ~100 km. Instead, hotspot-type volcanism is hypothesized to originate from the deepest possible source, through hot, buoyant "plumes" of mantle rock that rise from the earth's core-mantle boundary at 2900 km depth.

The existence and shape of mantle plumes remains controversial, as does their significance for the earth's heat budget. Sharply focused geophysical imaging of the plumes and their interactions with the oceanic lithosphere would go a long way towards settling these questions. Plumes tend to operate under the oceans, which until relatively recently could not be instrumented with long-term arrays (duration at least one year) of broadband ocean-bottom seismometers (OBS).

The RHUM-RUM experiment has been the largest attempt to geophysically image an oceanic mantle plume and to understand the results in terms of material and heat flows. With Réunion and the surrounding Indian Ocean, we instrumented a presumed type example of a volcanic hotspot underlain by a deep mantle plume.

In a close German-French collaboration funded by DFG and ANR, RHUM-RUM deployed 48 German and 9 French ocean-bottom seismometers over 2000 km x 2000 km of deep seafloor (in Oct. 2012 using R/V "Marion Dufresn e"), and successfully recovered them in Nov. 2013 using R/V "Meteor". We installed an additional 37 land seismometers between 2011 and 2015 on the islands of La Réunion, Mauritius and the Seychelles, Madagascar and the Iles Eparses. Pooling the scientific expertise, marine resources, funding, and local infrastructure of Germany and France, we could mount the largest effort so far to image an oceanic mantle plume.

Over 20 senior scientists and their groups have worked on the RHUM-RUM data, and have so far published at least 36 publications in international, peer-reviewed journals. 12 Ph.D. and M.Sc. theses have been based on the RHUM-RUM data. We will give an overview of the scientific results of RHUM-RUM, focusing on the knowledge gained about mantle structure, with mention of serendipitous by-products in marine environmental science.

REFERENCES

Barruol, G., & Sigloch, K. (2013). Investigating La Réunion Hot Spot From Crust to Core. EOS, Transactions American Geophysical Union, 94(23), pp.205–207.

Project website, including two cruise blogs, media coverage of the experiment and several short videos about ocean-bottom deployments: www.rhum-rum.net/en/

Selected media coverage:

Witze, Alexandra (2013). "Under the volcano." Nature 504, no. 7479 (2013): 206. http://www.nature.com/news/earth-science-under-the-volcano-1.14323

Choi, Charles (2013). "Mantle plumes." Proceedings of the National Academy of Sciences 110, no. 7 (2013): 2435-2435. Doi:10.1073/pnas.1300192110 http://www.pnas.org/content/110/7/2435.full

Documentary film about the RHUM-RUM project, produced by the Université de la Réunion (51 min, available in French and English versions): https://www.youtube.com/watch?v=tl2Nt-3bF5o&feature=youtu.be

M112

VENERE MUD VOLCANO, THE ACTIVE MUD VOLCANO OF THE CALABRIAN ACCRETIONARY PRISM – R/V METEOR CRUISE M112, IONIAN SEA

AUTHORS

MARUM, Center for Marine Environmental Sciences and Department of Geosciences, University of Bremen | Bremen, Germany
G. Bohrmann, M. Loher, M. Römer, T. Pape, Y. Marcon, P. Wintersteller, C. Ferreira

OGS, Borgo Grotta Gigante 42/c, Sgonico | Trieste, Italy
S. Ceramicola, D. Praeg

CEOAS, Oregon State University | Corvallis (OR), USA
M. Torres

Mud volcanoes (MV) are abundant within the eastern Mediterranean accretionary systems and the Nile deep sea fan. The Mediterranean Ridge and its eastern extensions have become one of the most intensively studied MV populations on Earth. In contrast, until recently, little was known about MVs at the Calabrian Arc (Fig. 1).

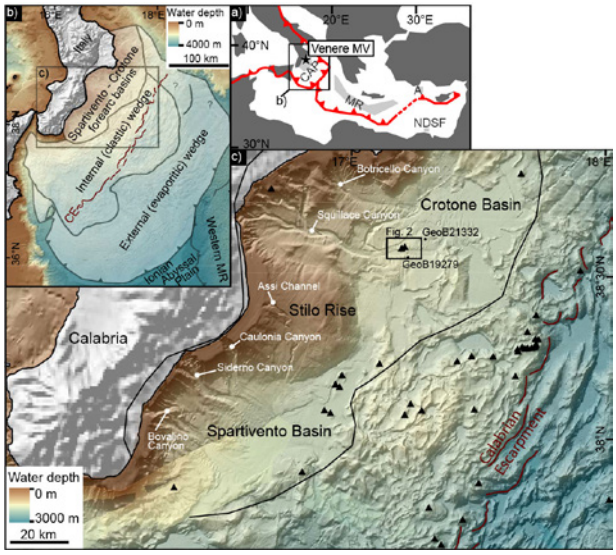

Fig. 1: (a) Map of the eastern Mediterranean region with location of Venere MV in the Calabrian Accretionary prism (CAP); (b) morphostructural domains of the CAP; CE = Calabrian Escarpment; (c) detailed bathymetric map of the Ionian-Calabrian margin showing the locations of mud volcanoes (black triangles). (Loher et al. 2018a)

By multi-beam mapping and coring Ceramicola et al. (2014) postulated 54 locations representing mud volcano buildups in the CAP, but detailed investigations about the activity of the mud volcanoes were missing. During R/V METEOR cruise M112 we explored all 54 mud volcanoes for recent or subrecent activity. Around 4,400 nautical miles of the Calabrian Arc are mapped with the EM122 multibeam and Parasound systems to find gas emission sites in the water column. Gas plumes (flares) were explored in order to localize active seepage. During Cruise M112 the bathymetry was improved from a former 100-m grid to a 30-m grid and a high resolution backscatter map of the same scale which revealed much more details of distinct seafloor features (Bohrmann et al. 2015, Loher et al. 2018b).

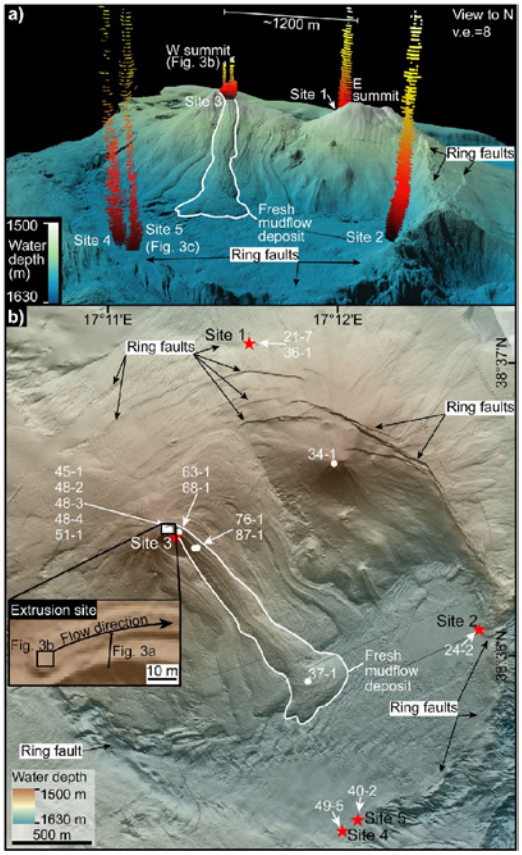

Fig. 2: AUV-derived bathymetry of Venere mud volcano (MV) and sampling locations. A fresh mudflow (outlined in white) originating from the W summit extends down to the caldera floor. (a) Perspective view of Venere MV (generated in QPS Fledermaus 7.3.2b; www.qps.nl). Note twin cones labelled as E + W summit, each up to 100 m high and ring faults defining a caldera up to 3 km across. Water column gas flares (red to yellow colours; extracted from hydroacoustic data) up to 260 m in height were observed at five sites, along the peripheral ring faults (Sites 1, 2, 4, 5) and near the W summit (Site 3); (b) Map-view of Venere MV with inset of the extrusion site of the fresh mudflow at the W summit (generated in ESRI ArcMap 10.3.1; www.esri.com). Red stars mark the flare origins and white circles indicate sampling locations with white numbers referring to the last two GeoB-identifiers of sediment cores. (Loher et al. 2018b).

A total of 70 mud volcanoes were identified and imaged (Fig.1), but only Venere MV was seen to actively emanate some gas bubbles from the seafloor into the water column at 5 distinct gas emission sites (Fig. 2). Those flares are well-associated with seeps at the rim of the mud volcano caldera or the recent mud outflow area at the western summit. Pore fluids in freshly extruded mud breccia (up to 13°C warmer than background sediments) contained methane concentrations exceeding saturation by 2.7 times and chloride concentrations up to five times lower than ambient seawater (Loher et al. 2018b). At flare locations along ring faults to the peripheral sites (Fig. 2) active seep manifestations like chemosynthetic fauna, carbonate formations and gas ebullition have been found (Bohrmann et al. 2015). The gas expelled with the mud on top of the summit shows a composition which is clearly thermogenic gas in origin, whereas the gas composition at the surrounding seeps shows a mixture of thermogenic with biogenic gas (Loher et al. 2018c). The gas and pore water analyses point to fluids sourced deep (>3km) below Venere mud volcano but do not indicate contact with chloride-rich evaporates during their ascent. The concept of an upward-branching plumbing system (Fig. 3) was proposed, to account for co-existing mud extrusion and gas seepage via multiple vents that influence the distribution of seafloor ecosystems.

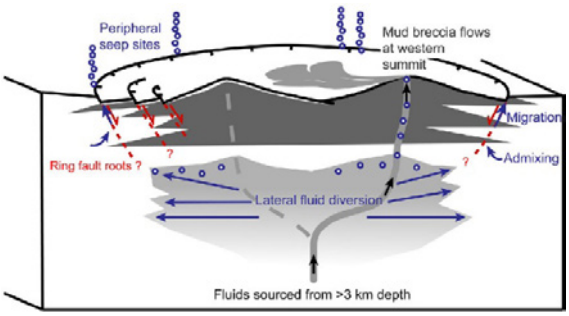

Fig. 3: Conceptional model of the upward-branching plumbing system. Gas-rich mud breccia (black arrows) through active conduit of main plumbing system from depth to the summit of the western MV cone. Gas diverted laterally from the main conduit migrates upward and may mix with gas of shallow origin. Gas discharge occurs at the peripheral seeps may mix with gas of shallow origin (Loher et al. 2018b).

Through sediment coring and tephrochronology, ages of buried mudflow deposits were determined based on the sedimentation rate and thickness of overlying hempelagic sediments. An average extrusion rate of 27,000 m^3/year over the last ~882 years was estimated. Mud breccia extrusion at the rates coeval with caldera subsidence and gas release, are best explained by excess pore fluid pressures persisting in the subsurface plumbing system. Instead of violent, short lived eruptions, the activity of Venere MV consists of a state of pressurized activity sustaining moderate extrusions over time scales of hundreds of years. The mobile mudflows and ongoing gas release in 2015 suggest that Venere MV represents one of the most active MVs on the CAP even with respect to other MVs in the forearc basins. The results of the investigation of Loher et al. (2018a)

support a three-stage evolutionary model of Venere mud volcano since ~4,000 years ago (Fig. 4). It includes the onset of quiescence at the eastern cone (after ~2,200 years ago), erosive events by may be turbidity currents following the Squillace Canyon downwards (prior to ~882 years ago) and mudflows from the eastern cone (since ~882 years).

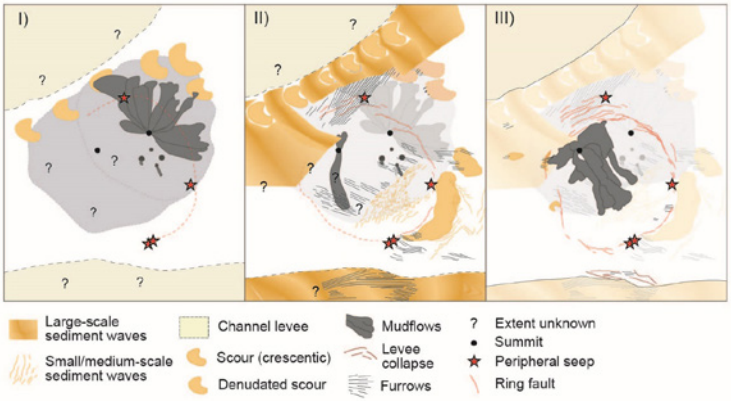

Fig. 4: Three-stage evolutionary model of Venere MV and surronded Squillace Canyon. I) Mud breccia extrusion at the eastern cone and the peripheral seepage (~4,000–2,200 years). Erosive processes at >882 years ago cause scours and seafloor furrows in old mudflow deposits, and the channel beds. III) Moderate but continuous mud breccia extrusion and peripheral gas release since ~882 years at the western cone up to 2016 (from Loher et al. 2018a).

REFERENCES

Bohrmann G, et al. (2015) Report and preliminary results of R/V METEOR cruise M112, Dynamic of Mud Volcanoes and Seeps in the Calabrian Accretionary Prism, Ionian Sea, Catania (Italy) – Catania (Italy), November 6 – December 15, 2014. Berichte, MARUM – Zentrum für Marine Umweltwissenschaften, Fachbereich Geo, Universität Bremen, 306. urn:nbn:de:gbv:46-00104282-14.

Ceramicola S, Praeg D, Cova A, Accetella D and Zecchin M (2014) Seafloor distribution and last glacial to postglacial activity of mud volcanoes on the Calabrian accretionary prism, Ionian Sea. Geo-Marine Letters 34: 111-129.

Loher, M, Ceramicola, S, Wintersteller, P, Meinecke, G, Sahling, H and Bohrmann, G (2018a) Mud volcanism in a canyon: morphodynamic evolution of the active Venere mud volcano and its interplay with Squillace Canyon, Central Mediterranean. Geochemistry, Geophysics, Geosystems. doi:10.1002/2017GC007166

Loher, M, Pape, T, Marcon, Y, Römer, M, Wintersteller, P, Praeg, D, Torres, M, Sahling, H and Bohrmann, G (2018b) Mud extrusion and ring-fault gas seepage – upward branching fluid discharge at a deep-sea mud volcano. Scientific Reports, 8(1). doi:10.1038/s41598-018-24689-1

Loher, M, Marcon, Y, Pape, T, Römer, M, Wintersteller, P, dos Santos Ferreira, C, Praeg, D, Torres, M, Sahling, H and Bohrmann, G (2018c) Seafloor sealing, doming, and collapse associated with gas seeps and authigenic carbonate structures at Venere mud volcano, Central Mediterranean. Deep Sea Research Part I: Oceanographic Research Papers, 137. 76-96. doi:10.1016/j.dsr.2018.04.006

M113/1
TECTONIC AND VOLCANIC EVOLUTION OF THE AZORES PLATEAU

AUTHORS

Institute of Geophysics, University of Hamburg | Hamburg, Germany
C. Hübscher

Department of Geosciences and Geography, University of Helsinki | Helsinki Finland
C. Beier

During RV METEOR expedition M113 we investigated the tectonic and volcanic evolution of the Azores plateau and the slow spreading Terceira Rift by means of 3.500 km multichannel seismic reflection and hydroacoustic data. The cruise was considered as a pre-site reconnaissance survey for detailed petrological sampling during the follow-up cruise M128.

We used structural geological estimates indicating the age of the Terceira Rift nucleation. A lack of magnetic chrons in a widespread area at and around the Terceira Rift limits a calculation on basis of magnetic data. According to these calculations the Terceira Rift started rifting about 1–1.5 Ma ago. This result contradicts older studies, which suggested an onset as early as 10 Ma ago. According to the prior publications, paleo-rifts further south are considered to be tectonically inactive. However, our seismic data clearly show growth faults that pierce and offset the seafloor. The vertical succession of transparent to layered reflections give evidence of several mass displacements along the rift axes.

São Jorge Island in the Azores lies south of the southern shoulder of the Terceira Rift, and raises a series of questions that we addressed in a joint study with Portuguese and French colleagues (Marques et al., 2018). The most probable mode of destruction of the successive volcanic complexes is that a major landslide occurred between ca. 1.2 and 0.8 Ma, which was responsible for the major lateral discontinuity between the older and younger volcanic complexes. Vintage palaeomagnetic and the M113 seismic data allowed for evaluating the effects of elastic rebound of the Terceira Rift`s southern shoulder on São Jorge Island. It was shown that southwestward tilting of the oldest lava flows occurred between ca. 1.2 and 0.8 Ma due to rotation of the Terceira Rifts southern shoulder during elastic rebound.

The formation or particular submarine volcanoes on the plateau was of specific interest. Based on seismic interpretation a tentative scenario for the evolution of those cones was elaborated. 1. The volcanic acoustic basement forms. 2. Pelagic sediments deposit on top of the basement. 3. Due to increased volcanic activity during arrival of a small plume

head underneath Princessa Alice bank magmas ascend and cause the deformation and bulging of the underlying and surrounding basement. 4. The upward deformation of the basement also infuences the sediments located on top of the deformed basement. They are deposited partly at the flanks and next to the convex bulging basement. Due to deposition, the internal parallel pattern changes to a chaotic, overlapping one. 5. The first explosive phase of the seamount starts, forming a small pile of volcanic sediments on top of the deformed basement. 6. More explosive volcanic phases follow and the erupted lavas and displaced volcanic sediments make the seamount grow further. 7. After the explosive phases, explosive eruptions pursue, leaving behind a more chaotic lava flow signature. 8. The top of the seamount forms, either due to a final explosive eruption or due to a sediment layer which covers the cone after the last eruption phase. 9. Fissure eruptions occur within the area surrounding the seamounts, leaving behind lava flows that eventually cover the basement and mix with pelagic sediments. 10. When the dykes cool down, the eruption centralizes to specific points along the fissures, creating small volcanic cones located on top of the lava flows. During and after the volcanic activity pelagic sediments deposit. Bottom currents already start to flow around the seamounts during the deposition of pelagic sediments, forming moats and contourite channels. With the beginning of subaerial volcanism around 4 Myr ago, the sediment composition changes and a hemipelagic sediment layer deposits on top of the pelagic sediments, which is also influenced by ocean bottom currents leaving behind moats as well as contourite channels. These valleys, formed by currents, are filled up by volcanic sediments which slid down the flanks.

The integrated interpretation of seismic (M113/1), petrological and major element, trace element and isotope geochemical data (M128) from a ~1000 m stratigraphic section of submarine lavas exposed at the western Princessa Alice bank provide evidence for intense water-rock exchange not observed anywhere in oceanic crust sampled to date (Beier et al., 2019). The immobile, incompatible trace elements show that the samples formed from higher degrees of partial melting of a mantle source that is less enriched than the source that gives rise to the islands today. The extents of melting today are very small, implying a change in melting regime since initial formation of the Princessa Alice Plateau basalts that correspond to a melting anomaly in the Azores. The extreme levels of alteration may result from a combination of intensified magmatic activity during initial formation of the Azores Plateau and the tectonic regime providing pathways for the fluids. Sites for geochemical studies of waning hydrothermal circulation were also selected from the geophysical data (Schmidt et al., 2019).

In the study of Romer et al. (2018) we combined the bathymetric and geophysical with geochemical data from Faial Island and the surrounding seafloor, providing insights into the interaction between a melting anomaly in the asthenosphere and extensional stresses in the lithosphere. Bathymetric data reveal large submarine volcanic rift zones on the western flank of Faial Island with a preferred WNW-ESE orientation partly related to the Capelinhos eruption in 1957/1958. On the basis of absolute ages, seismic imagery,

and direct observations of submarine lava formations at Capelinhos, a relative chronology of the magmatic evolution of the rift zones was developed. It was shown that melting conditions changed with time and that the different magma batches produced fed distinct volcanic rift zones and edifices. The resulting model implies that dykes efficiently transport melts along the volcanic rift zones at Faial over length scales of >12 km while plumbing systems parallel to the rift axes are distinct over a similar length scale. As progressive decrease in the plume upwelling occurs, volcanism appears to become increasingly localised along tectonically controlled lineaments in the last 10 ka exclusively erupting along fissures, alignments of elongated cones and dykes. Hence, melts erupted during the young volcanic activity on Faial focus along single rift zones, whereas the older volcanism occurs more widespread. These observations may also be applicable to other intraplate settings that have a significant extensional component.

REFERENCES

Beier C, Bach W, Busch AV, Genske FS, Hübscher C, Krumm SH, Extreme intensity of fluid-rock interaction during extensive intraplate volcanism. Geochimica et Cosmochimia Acta, 2019, 257, 26–48.

Marques FOO, Hildenbrand A, Hübscher C, Evolution of a volcanic island on the shoulder of an oceanic rift and geodynamic implications: S. Jorge Island on the Terceira Rift, Azores Triple Junction. Tectonophysics 2018, 738-739, 41–50.

Romer R, Beier C, Haase KM, Hübscher C, Correlated changes between volcanic structures and magma composition in the Faial volcanic system, Azores. Front. Earth Sci. 2018, | doi: 10.3389/feart.2018.00078.

Schmidt C, Hensen C, Wallmann K, Liebetrau V, Tatzel M, Schurr SL, Kutterolf S, Haffert L, Geilert S, Hübscher C, Lebas E, Heuser A, Schmidt M, Strauss H, Vogl J, Hansteen T, Origin of high Mg and SO4 fluids in sediments of the Terceira Rift, Azores – indications for caminite dissolution in a waning hydrothermal system. Geochemistry, Geophysics, Geosystems (G-Cubed), 2019, doi: 10.1029/2019GC008525.

M114

NATURAL HYDROCARBON SEEPAGE IN THE SOUTHERN GULF OF MEXICO – RESULTS FROM R/V METEOR CRUISE M114

AUTHORS

MARUM – Center for Marine Environmental Sciences and Department of Geosciences, University of Bremen | Bremen, Germany
G. Bohrmann, M. Römer, H. Sahling, Y. Marcon, S. Mau, F. Schubotz, P. Wintersteller, C-W. Hsu, G. Wegener

Max-Planck Institute for Marine Microbiology | Bremen, Germany
M. Rubin-Blum, C. Borowski

Florida State University | Tallahassee (FL), USA
I. MacDonald

Dept. für Geodynamik und Sedimentologie, Universität Wien | Wien, Austria
D. Smerzka

Universidad Nacional Autónoma de México | Mexico City, Mexico
E. Escobar-Briones

R/V METEOR Cruise M114 (Fig. 1) investigated seafloor manifestations related to asphalt deposits on top of submarine ridges and knolls known as salt diapirs in the Campeche Bay of the Gulf of Mexico. The cruise was successful in discovering spectacular manifestations of hydrocarbon emissions at the seafloor at various sites on top of the salt diapirs. Leg 1 focused on locating and mapping of hydrocarbon seeps by combining ship-based hydro-acoustics, deep-towed side-scan sonar, and autonomous underwater vehicle (AUV) SEAL 5000 hydro-acoustics, whereas Leg 2 focused on observing and sampling of the seeps using the remotely operated vehicle (ROV QUEST 4000m). We found numerous gas bubble emissions at knolls and ridges in the western and northern part of the study area which are accompanied in most cases by oil slicks at the sea surface visible by SAR satellite analysis (Suresh 2015). A ridge was termed UNAM Ridge after discovery of prominent hydrocarbon seepage with amazing chemosynthetic communities.

Our investigations showed that seafloor asphalt deposits previously only known from the Chapopote Knoll (Bohrmann 2016) also occur at numerous other knolls and ridges in water depths from 1230 to 3150 m (Sahling et al 2016, 2017). In particular, the deeper sites (Chapopote and Mictlan knolls) were characterized by asphalt deposits accompanied by extrusion of liquid oil in form of whips or sheets, and in some places (Tsanyao Yang,

Mictlan, and Chapopote knolls) by gas emission and the presence of gas hydrates in addition. Molecular and stable carbon isotopic compositions of gaseous hydrocarbons suggest their primarily thermogenic origin (Sahling et al. 2017).

Relatively fresh asphalt structures were settled by chemosynthetic communities including bacterial mats and vestimentiferan tube worms, whereas older flows appeared largely inert and devoid of corals and anemones at the deep sites. The gas hydrates at Tsanyao Yang and Mictlan Knolls were covered by a 5-to-10 cm-thick reaction zone composed of authigenic carbonates (Smerzka et al. 2019), detritus, and microbial mats, and were densely colonized by chemosynthetic animals.

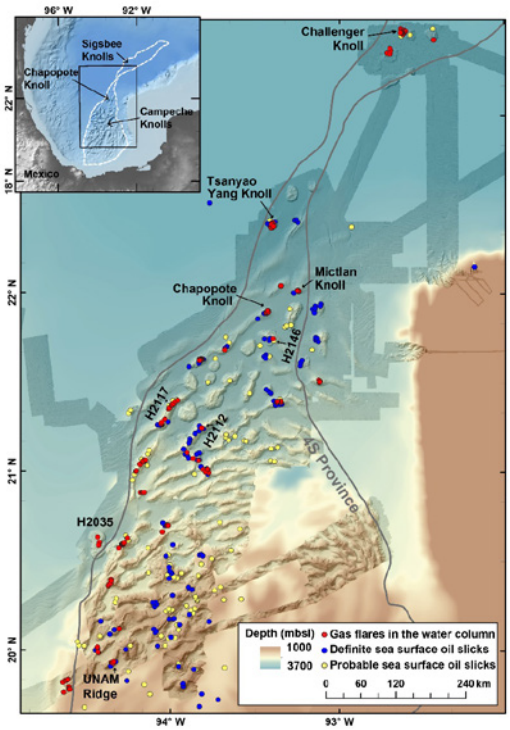

Fig. 1: Regional map of the southern Gulf of Mexico produced from swath bathymetry data draped over GEBCO bathymetry. Indicated are oil slick origins as inferred from oil slicks at the sea surface according to Williams et al. (2006), classified as definite (red dots) and probable (yellow dots) and gas flares recognized during cruise M114 (Sahling et al. 2016). Locations of persistent oil slicks correspond with seafloor ridges and knolls. Potential area of seepage covers a large portion of the Campeche Bight. Seafloor locations of hydrocarbon seepage sites investigated in our studies are also shown.

Combining data from AUV mapping and ROV navigation with powerful optical mosaicking techniques, we assembled georeferenced images of the Chapopote asphalt flows (Fig. 2). The largest image captured an area of 3,300 m^2 with over 15 billion pixels and resolved objects at centimeter scale. Augmenting this optical resolution with

microbathymetry led to the recognition that very large asphalt pavements exhibiting highly varied morphologies and weathering states comprised a series of at least three separate flow units, one on top of another.

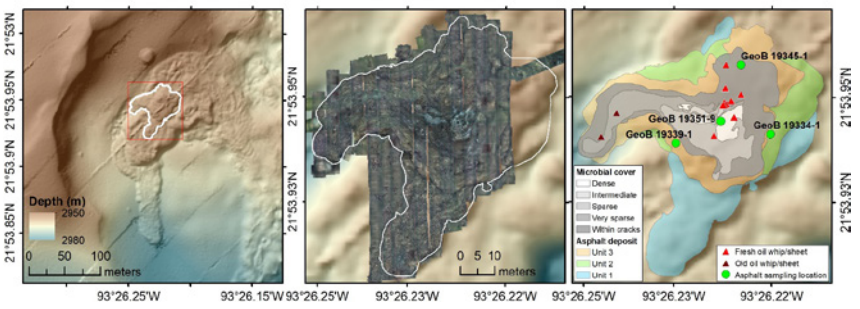

Fig. 2: Microbathymetry map of the crater of Chapopote asphalt volcano with current outline of seafloor asphalt by the white line (left). The Photomosaic and flow units of the Chapopote main asphalt field. Photomosaic overlain on area bathymetry (middle). Extent of asphalts shown in white outline. The eastern limit of the field was inferred from the bathymetry and remotely operated vehicle (ROV) footage. Extent of the main asphalt units and microbial mats (right). Colors indicate three proposed flow units – in some areas inferred by abrupt elevation changes. Gravity core locations show where targeted asphalt collections were made (Marcon et al. 2018).

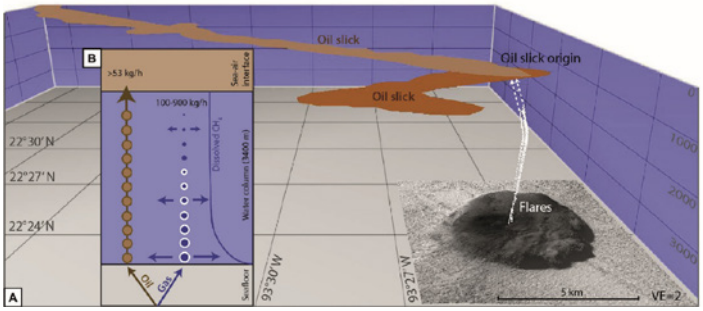

Fig. 3: Composite illustration of the Tsanyao Yang Knoll hydrocarbon seep system. (A) During R/V METEOR cruise M114 flares about 3,000 m in height originated from the main seep field on top of the knoll up to the sea surface (white dots are extracted water column anomalies from acoustic measurments, white dotted line is the projected path of bubbles in the upper 500 m), where oil and gas bubbles were observed. In 2011 oil emissions fueled extent oil slicks at the sea surface (Suresh, 2015). (B) Quantification revealed that only a minor fraction of the oil volume is required to generate an oil slick of such an extent. The oil bubble emission site was discovered at the seafloor during an ROV dive in 2015. In contrast, gas bubbles released from the seafloor contain mainly methane that is rapidly dissolved during bubble rise through the water column. Therefore, most of the carbon released through methane bubbles remained in the lowermost water column and did not reach the water-air interface (Römer et al. 2019).

The Chapopote asphalt volcano likely erupts during phases of intensified activity separated by periods of reduced activity. After extrusion, chemical and physical changes in the asphalt generate increasing viscosity gradients both along the flow path and between the flow's surface and core. This allows the asphalt to form pahoehoe lava-like shapes and to support dense chemosynthetic communities over timescales of hundreds of years. Our study at Tsanyao Yang Knoll (TYK) illustrates the amount and fate of mainly oil

and methane emanating from the seafloor structure and rising through a 3,400 m water column (Sahling et al. 2017, Römer et al. 2019). TYK was found to be one of the most active seepage structures at such a deep depth (Fig. 3). Concentrations of dissolved methane were highly elevated (30,000 nmol/L) directly above the seafloor emission site, but decreased to background concentrations (3–5 nmol/L) within the lowermost 100 m. The extent of all discovered seepage structure areas indicates that emission of complex hydrocarbons is a widespread, thus important feature of the southern Gulf of Mexico.

REFERENCES

Bohrmann, G (2016) Asphalt Volcanism. In: Harff, J, Meschede, M, Petersen, S and Thiede, J (eds.) Encyclopedia of Earth Sciences Series. Springer, 24–25. doi:10.1007/978-94-007-6238-1_1

Marcon, Y, Sahling, H, MacDonald, I, Wintersteller, P, dos Santos Ferreira, C and Bohrmann, G (2018) Slow volcanoes: The intriguing similarities between marine asphalt and basalt lavas. Oceanography, 31(2). 194–205. doi:10.5670/oceanog.2018.202

Römer M, Hsu C-W, Loher M, MacDonald IR, dos Santos Ferreira C, Pape T, Mau S, Bohrmann G and Sahling H (2019) Amount and Fate of Gas and Oil Discharged at 3400 m Water Depth From a Natural Seep Site in the Southern Gulf of Mexico.Front. Mar. Sci. 6:700.doi: 10.3389/fmars.2019.00700.

Sahling, H, Bohrmann, et al. (2017) R/V METEOR Cruise Report M114, Natural hydrocarbon seepage in the southern Gulf of Mexico, Kingston – Kingston, 12 February - 28 March 2015. Berichte, MARUM – Zentrum für Marine Umweltwissenschaften, Fachbereich Geowissenschaften, Universität Bremen, 315. 1–214. urn:nbn:de:gbv:46-00105897-18.

Sahling, H, Borowski, C, Escobar-Briones, E, Gaytán-Caballero, A, Hsu, CW, Loher, M, MacDonald, I, Marcon, Y, Pape, T, Römer, M, Rubin-Blum, M, Schubotz, F, Smrzka, D, Wegener, G and Bohrmann, G (2016) Massive asphalt deposits, oil seepage, and gas venting support abundant chemosynthetic communities at the Campeche Knolls, southern Gulf of Mexico. Biogeosciences, 13(15). 4491–4512. doi:10.5194/bg-13-4491-2016

Smrzka, D, Zwicker, J, Misch, D, Walkner, C, Gier, S, Monien, P, Bohrmann, G, Peckmann, JL and Tosca, N (2019) Oil seepage and carbonate formation: A case study from the southern Gulf of Mexico. Sedimentology. doi 10.1111/sed.12593

Suresh, Gopika (2015) Offshore oil seepage visible from space: A Synthetic Aperture Radar (SAR) based automatic detection, mapping and quantification system, Doktorarbeit: 155 Seiten/pages.

M115

LITHOSPHERIC FORMATION AT ULTRA-SLOW SPREADING RATES – CONSTRAINTS FROM M115 AND THE CAYMAN TROUGH

AUTHORS

GEOMAR Helmholtz Zentrum für Ozeanforschung | Kiel, Germany
I. Grevemeyer, A. Dannowski, C. Papenberg

Institute for Geophysics, University of Texas at Austin | Austin (TX), USA
N. W. Hayman, H. J. A. Van Avendonk,

Department of Earth Sciences, University of Durham | Durham, UK
C. Peirce

The generation of oceanic crust at ultra-slow spreading rates is fundamentally different from crustal emplacement at faster spreading rates. However, due to the remoteness of most ultra-slow ridges, the formation of crust at these magma-starved centres was poorly understood. The CAYSEIS seismic experiment conducted during M115 aboard RV METEOR provided new seismic data of excellent quality to characterize lithospheric formation at ultra-slow spreading rates at the Mid-Cayman spreading centre (MCSC) in the Caribbean Sea, where oceanic crust is formed at a full rate of ~17 mm/yr.

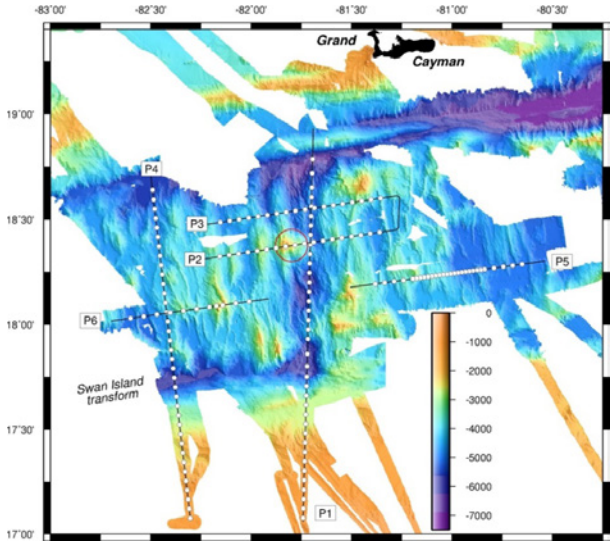

Fig. 1: Bathymetric map and location map of seismic lines shot during M115 in the Cayman Trough, Caribbean Sea; red circle marks Mt. Dent oceanic core complex.

A number of conclusions can be highlighted:

(i) Lithospheric emplacement along the median valley of the MCSC nurtures both domains of magmatic accretion and hence thin oceanic crust and areas of mantle tectonically un-roofed to the seafloor. Shallow low velocity zones (LVZ) at 3–5 km below seafloor may outline settings of volcanic activity. One LVZ is underlying the Beebe hydrothermal vent field, Earth's deepest known black smoker vent field, suggesting that hydrothermal circulation is driven by magmatism.

(ii) Seismic data from the Mt. Dent oceanic core complex can be interpreted in term of an evolutionary model, where the massif was produced by a pulse of on-axis magmatism at ca. 2 Ma, which was then followed by exhumation, cooling, and fracturing. A low seismic velocity anomaly 5 km imaged below the Von-Dann hydrothermal vent field is taken as evidence for either a cracking front mining lithospheric heat or intrusive magmatic sills, both of which could drive ongoing deep hydrothermal fluid circulation. We conclude that the transient magmatism and variable crustal thickness at ultraslow-spreading centers create conditions for long-lived hydrothermal venting that may be widespread.

(iii) Mid-ocean ridges spreading at ultra-slow rates of less than 20 mm/yr can either exhume serpentinized mantle to the seafloor, or they can produce magmatic crust. Yet, seismic imaging generally has not been able to resolve the abundance of serpentinized mantle exhumation, and instead supports 2 to 5 km of crust flowing most median valley of ridges spreading as ultra-slow rates. Based on P- to S-wave velocity (Vp/Vs) ratio derived from seismic tomography, CAYSEIS provided for the first time evidence for the occurrence of wide-spread mantle exhumation. We suggest that high Vp/Vs ratios greater than 1.9 and continuously increasing P-wave velocity, changing from 4 km/s at the seafloor to greater than 7.4 km/s at 2 to 4 km depth, indicate highly serpentinized peridotite exhumed to the seaf loor. Elsewhere, either magmatic crust or serpentinized mantle deformed and uplifted at oceanic core complexes underlies areas of high bathymetry. The Cayman Trough therefore provides a window into mid-ocean ridge dynamics that switch between magma-rich and magma-poor oceanic crustal accretion, including exhumation of serpentinized mantle covering about 25 % of the seafloor in this region.

(iv) The depth of earthquakes along mid-ocean ridges is restricted by the relatively thin brittle lithosphere that overlies a hot, upwelling mantle. With decreasing spreading rate, earthquakes may occur deeper in the lithosphere, accommodating strain within a thicker brittle layer. Data from the ultra-slow spreading MCSC illustrate that earthquakes occur deeper than along most other slow-spreading ridges. Together, the new MCSC data, a reanalysis of micro-seismicity from the Southwest Indian Ridge and a global compilation of micro-earthquake surveys support the hypothesis

that depth-seismicity relationships at mid-ocean ridges are a function of their thermal-mechanical structure as reflected in their spreading rate.

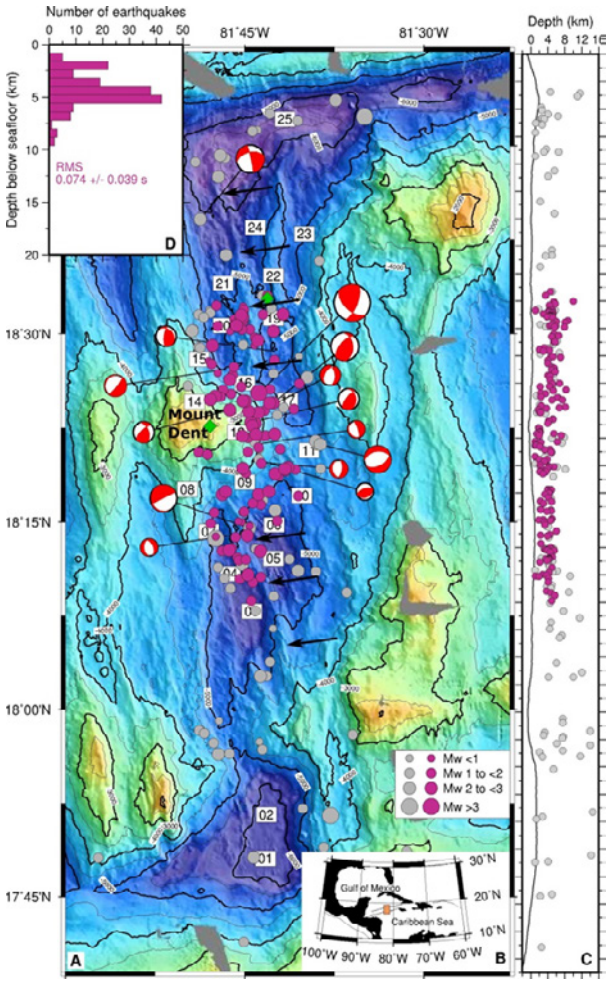

Fig. 2: A) Bathymetric map of the Cayman Trough and deployment of a local micro-earthquake monitoring network of OBSs (numbered squares), showing the Van Damm and Beebe hydrothermal vents (green diamonds), epicenters of 0.4<Mw<3.2 (circles, size scaled to magnitude) of micro-earthquakes recorded at a station gap of <180° are colored magenta, and grey circles are events with a larger gap, OBSs). The location of the axial volcanic ridge (AVR) is arrowed. Focal mechanisms are plotted in red. B) Map showing the geographic context of the study area. C) Micro-earthquakes plotted as a function of depth; colors as in Fig. 2 A. D) Histogram of the depth-distribution of well-located events (magenta events from A & C).

M116/1

RESULTS FROM METEOR CRUISE M116/1 TO THE TROPICAL NORTH ATLANTIC

AUTHORS

GEOMAR Helmholtz Centre for Ocean Research Kiel | Kiel,Germany
T. Tanhua, M. Visbeck

R/V Meteor cruise in the tropical Atlantic Ocean departed the port of Pointe-a-Pitre (Guadeloupe) on May 1, 2015 and reached Mindelo (Cape Verde) on June 03, 2015, Figure 1. The Cruise M116/1 is a contribution to the DFG Collaborative Research Project (SFB) 754: "Climate-Biogeochemistry Interactions in the Tropical Ocean" with the main goal to better understand the supply of oxygen to the oxygen minimum zone (OMZ) of the Tropical Atlantic with a particular focus on the role of regional advection, mesoscale and sub-mesoscale processes for lateral and vertical oxygen fluxes. A key method is the "Oxygen Supply Tracer Release Experiment" (OSTRE), where during M116/1 the third mapping of the tracer CF3SF5 using 82 CTD stations was done. Mapping of the water mass properties, including the distributions of oxygen, transient tracers, nutrients and the carbonate system were done mostly along 11°N. A brief detour allowed for the measurements from a 1980's cruise (TTO) to be repeated. A snapshot of the synoptic ocean circulation and mixing was accomplished by shipboard ADCP observations. The measurements support the determination of isopycnal and diapycnal mixing coefficients in the area. Ten Argo floats were deployed. One ocean-glider and one wave-glider were recovered. Finally, additional components of the cruise were dedicated to zooplankton studies, nitrogen fixation experiments and underway sampling of a broad range of biogeochemical parameters.

The M116 cruise offered the opportunity to sample (with a light carry-on meteorological instrument) central Atlantic W-E cross-section in the mineral dust outflow of Saharan dust for atmospheric aerosol and water vapor.

The cruise was the third and final mapping cruise of the tracer SF5CF3 that was injected in the end of 2012. The cruise was very successful; most systems on METEOR worked well and all planned objectives were mostly reached. The cruise was presented in a blog by the artist and trained oceanographer Anja Witt who participated the cruise. In various exhibitions her paintings bridging science and arts have been shown to the public.

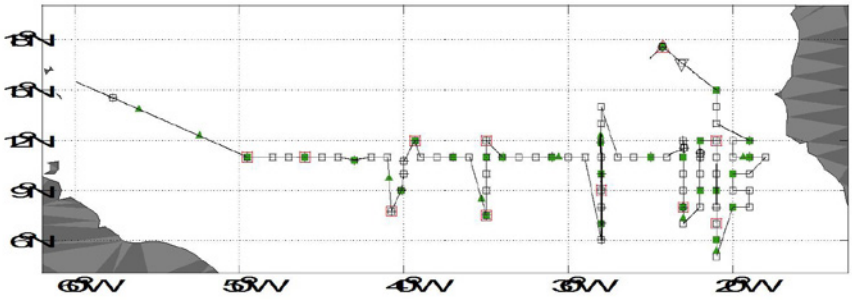

Fig. 1: The cruise track of the M116/1 cruise.

M117

BIOCHEMICAL PROCESSES IN UPWELLING ZONES OF THE BALTIC SEA

AUTHORS

Institute for Chemistry and Biology of the Marine Environment, Carl Von Ossietzky Universität Oldenburg | Wilhelmshaven, Germany
O. Wurl

Leibniz Institute for Baltic Sea Research Warnemünde | Rostock, Germany
J. Kuss, N. Loick-Wilde, M. Nausch, G. Nausch

Leibniz Institute for Tropospheric Research | Leipzig, Germany
M. van Pinxteren

The objective of cruise M117 was to observe and investigate biochemical processes in upwelling zones. Upwelled water is colder than surface waters and typically rich in nutrients and CO_2, which enhances the primary productivity of surface waters. For this reason, the phenomenon of upwelling is of interest in ocean and climate science. M117 aimed to understand potentially interconnected biochemical processes within upwelling systems of the Baltic Sea. Research activities during M117 included (1) phosphorus availability for harmful cyanobacteria blooms, (2) air-sea CO_2 exchange, (3) marine aerosol formation, (4) formation and transport of organic mercury species, and (5) energy turnover of zooplankton communities along food quality gradients. Above research activities required extensive background information about the distributions of nutrients and phytoplankton composition, and, therefore, above research activities were combined with IOW's longterm monitoring program of the Baltic Sea. The science team identified a single but well-defined upwelling system offshoreland. Later during the cruise, large cyanobacteria blooms were found and the opportunity used to investigate the blooms.

The work during M117 showed that upwelling regions (UP1 to UP4) can develop strong gradients of aqueous pCO_2 in the top surface layer caused by rich-CO_2 upwelled water (Ribas-Ribas et al., 2019). Within the gradient (UP1 to UP4) the direction of fluxes changed as upwelled water at UP1 causes the Baltic Sea to emit CO_2. At the offshore boundary of the upwelling regions, aqueous CO_2 was much lower changing the direction of the flux. With a remote-controlled catamaran, temperature anomaly between in the upper 2 cm layer and 30 cm depth was observed (Ribas-Ribas et al., 2017). Temperature anomalies were several tenths of degree in the upwelling region with the upper layer being warmer and this phenomenon was not observed outside the upwelling region. A significant higher enrichment of fluorescent dissolvent organic matter (FDOM) in the uppermost sea-surface

microlayer was observed during upwelling. Upwelling water is potentially a source of organic matter to the surface ocean, and the surface-active fraction is accumulating in the microlayer forming a surface film (Ribas-Ribas et al., 2017). These films may modify air-sea interaction as shown by low air-sea CO_2 transfer velocities in the upwelling region.

With regards to gas exchange, it was also concluded that upwelling in summer contributed to Hg^0 emission by the Baltic Sea, as "the upwelled water provides the precondition for cyanobacteria blooms and thus for mercury transformation" and the frequntly occuring upwelling usually affects large areas of up to a few hundred square kilometres (Kuss et al., 2018). In the upwelling system offshoreland, the total mercury concentration was between 0.15 and 0.20 ng L^{-1} similar to open sea surface water and the elemental mercury concentration was 11 ng m^{-3} in the cold upwelling plume and increased at first with distance from the plume to about 15 ng m^{-3}, and decreased thereafter. This was interpreted as an ongoing transformation in subsequent days with distance from the source and exposure to light as well as subsequent dilution by mixing and loss by evasion. In addition, during upwelling nutrient-depleted warm surface water is replaced by colder water that is enriched with phosphate. During mixing with warm surface water this contributed to growth of diazotrophic cyanobacteria (Wasmund et al., 2012) that in turn likely also supported the transformation of Hg(II) to Hg^0.

The concentrations of organic carbon in aerosols as well as the concentrations of methane sulfonic acid, Na^+, Mg^{2+} and Ca^{2+} (all markers for marine aerosols) were not enhanced during the upwelling periods or in the period when cyanobacteria were present. Therefore, no direct correlation between enhanced biological activity in the ocean and the organic matter observed in the PM1 aerosol particles were observed. However, this does not rule out a connection between biological activity and organic matter abundance on the aerosol particles. The missing correlations could be due to a delay in response between biological organic matter production and its transfer to the aerosol particles (Rinaldi, et al. 2013; van Pinxteren, et al. 2017). Large quantities of transferable organic carbon can be released during the decay phase of the bloom and are therefore not directly correlated to blooming conditions (O'Dowd, et al. 2015). In addition, sea state was calm during the observations in the upwelling regions leading to low abundance of marine aerosols typically generated by sea-spray.

The cellular C:P ratios of 94–154 of the filamentous cyanobacteria indicated a good P nutrition status. In the upwelling areas of land and offshore the Finnish coast the P status was even more favourable (C:P ratios of 71 and 43). In the eastern and western Gotland Basin, however, the surface water was DIP-depleted, and C:P ratios of the cyanobacteria were between 170–308 indicating a lower P content compared to the "DIP- rich" stations. The comparison of the C:P ratios with the respective polyphosphate (PolyP), adenosine triphosphate (ATP), phospholipids (PL) concentrations shows that all of these three cell components decrease with an increase in the C:P ratio. However, the decreases are slower from a C:P ratio of 150 than from a C:P ratio below 150. It can therefore be concluded that

PolyP, ATP and PL are also affected when C:P ratios of cyanobacteria change. Incubations experiments, conducted with cyanobacteria under deficiency of dissolved inorganic phosphate, showed that PolyP content of the cyanobacteria increased and reached its maximum after 24 hours before declining again. Cyanobacteria that had grown under sufficient DIP used little added phosphate and the PolyP content increased only slightly. The change of PolyP concentration could be shown in SEM and NanoSIMS for single cells of N. spumigena filaments (Braun et al. 2018) collected from the experiments with the natural community. It can be clearly seen that PolyP is only formed in vegetative cells and not in heterocytes. Furthermore, P is located inside the cell and not, like N, already on the cell surface. In comparison to vegetative cells, heterocytes store only little P, which is diffusely distributed in them and not accumulated as PolyP granules. Overall, the upwelling system offshore land might have provided favourable conditions for blooms of cyanobacteria.

Furthermore, investigations during M117 suggest that a relatively small increase in sea surface temperature of 4°C may restrict temperate mesozooplankton keystone species from diazotrophic N based food webs in the mixed layer in future oceans. For the first time, strong evidence was found that zooplankton species in suboxic waters below a cyanobacterial bloom relied on a local, mesopelagic food web. Together the data suggest that indirect feeding on diazotrophs and mesopelagic food webs will be principal ways of amino acid supply for epi- and mesopelagic zooplankton species in future enhanced stratified aquatic systems (Eglite et al. 2018). The supply of essential amino and fatty acids in mesozooplankton at times of unpalatable, lipid poor cyanobacterial blooms was mainly covered by feeding on mixo- and heterotrophic dinoflagellates and flagellates as well as on detrital complexes in and below cyanobacterial blooms as revealed by a multi-tracer approach combining stable carbon isotope data in amino and fatty acids with fatty acid trophic marker, taxonomy and environmental data. The continuous warming trend and simultaneous feeding of epi- and ascending mesopelagic keystone copepods may lead to competition on the preferred diet of key copepods below the thermocline in highly stratified systems (Eglite et al. 2019).

The cruise M117 provided also additional insights in the evolution of the Major Baltic Inflow, which occurred in December 2014 with the intrusion of large amount of water from the North Sea. This inflow caused a strong increase in the bottom water salinity in the eastern Gotland Basin (Gotland Deep) by May 2015, but showed a slight decrease during M117 in July 2015. In addition, the oxygen concentration in the Gotland Deep increased by May 2015 with bottom concentrations of 2.09 ml L^{-1} and the typical anoxic intermediate layer was found only sporadically. At the time of M117, the whole water column was oxic.

REFERENCES

Braun P D, Schulz-Vogt H N, Vogts A, Nausch M, Differences in the accumulation of phosphorous between vegetative cells and heterocysts in the cyanobacterium Nodularia spumigena. Scientific Reports 2018, 8, 56521–56527, doi 10.1038/s41598-018-23992-1

Eglīte E, Graeve M, Dutz J, Wodarg D, Liskow I, Schulz-Bull D, Loick-Wilde N, Metabolism and foraging strategies of mid-latitude mesozooplankton during cyanobacterial blooms as revealed by fatty acids, amino acids and their stable carbon isotopes. Ecology and Evolution 2019, 9(17), 9916–9934, doi: 10.1002/ece3.5533

Eglīte E, Wodarg D, Dutz J, et al., Strategies of amino acid supply in mesozooplankton during cyanobacteria blooms: a stable nitrogen isotope approach. Ecosphere 2018, 9(3), e02135, doi: 10.1002/ecs2.2135

Kuss J, Krüger S, Ruickoldt J, Wlost K P, High-resolution measurements of elemental mercury in surface water for an improved quantitative understanding of the Baltic Sea as a source of atmospheric mercury. Atmospheric Chemistry and Physicis 2018, 4361–4376. doi 10.5194/acp-18-4361-2018.

O'Dowd C, Ceburnis D, Ovadnevaite J et al., Connecting marine productivity to sea-spray via nanoscale biological processes: Phytoplankton Dance or Death Disco? Scientific Reports 2015, 5, 14883, doi: 10.1038/srep14883

Ribas-Ribas M, Mustaffa N I H, Rahlff J, Stolle C, Wurl O, Sea Surface Scanner (S3): A catamaran for high-resolution measurements of biogeochemical properties of the sea surface microlayer. Journal of Atmospheric and Oceanic Technology 2017, 34, 1433–1448, doi: 10.1175/JTECH-D-17-0017.1

Ribas-Ribas M, Battaglia G, Humphreys M P, Wurl O, Impact of nonzero intercept gas transfer velocity parameterizations on global and regional ocean-atmosphere CO_2 fluxes. Geosciences 2019, 9, 230. doi:10.3390/geosciences9050230

Rinaldi M, Fuzzi S, Decesari S et al., Is chlorophyll-a the best surrogate for organic matter enrichment in submicron primary marine aerosol? Journal of Geophysical Research: Atmospheres 2013, 118(10), 4964–4973.

van Pinxteren, M., Barthel, S., Fomba, et al., The influence of environmental drivers on the enrichment of organic carbon in the sea surface microlayer and in submicron aerosol particles–measurements from the Atlantic Ocean. Elementa: Science of the Anthropocene 2018, 5, 35.

Wasmund N, Nausch G, Voss M, Upwelling events may cause cyanobacteria blooms in the Baltic Sea. Journal of Marine Systems 2012, 90(1), 67–76. doi: 10.1016/j.jmarsys.2011.09.001.

M120 & M131

HEAT BUDGET AND CIRCULATION VARIABILITY OFF ANGOLA AND NAMIBIA (BENGUELA HEAT I & II)

AUTHORS

GEOMAR Helmholtz Centre for Ocean Research Kiel | Kiel, Germany
P. Brandt, M. Dengler

R/V Meteor cruises M120 and M131 carried out a physical oceanography research program with a biogeochemical component in the eastern boundary upwelling region off Angola and Namibia. The program was an integral component of the EU collaborative project PREFACE ("Enhancing prediction of tropical Atlantic climate and its impacts") and the BMBF collaborative projects SACUS ("Southwest African Coastal Upwelling System and Benguela Niños") and RACE ("Regional Atlantic Circulation and Global Change"). The major aim of the cruise was (1) to determine the variability of eastern boundary current transport, water masses variability and wave propagation along the coastal wave guide; (2) to quantify physical processes controlling the mixed-layer heat and freshwater budget in the eastern boundary region, including the loss of heat due to turbulent mixing; and (3) to investigate upper-ocean water mass variability associated with the variability of the meridional overturning circulation along a transatlantic transect at about 11°S. The work program of both cruises included recoveries and redeployments of moorings positioned along the continental slope of Angola and Namibia. High-resolution hydrographic, velocity and turbulence profiling was conducted along 7 sections between 6°S and 23°S and autonomous observing platforms were deployed and recovery in three key regions of the eastern boundary upwelling systems. The observational program was complemented by underway measurements of climate-sensitive trace gas concentrations (CO_2, N_2O, CH_4 and CO_2 isotopes) and measurements of the size distribution of aerosols. Additionally, a capacity program for students and colleagues from southern African counties was carried out.

For the first time ever, velocity data describing the variability of the Angola Current and eastern boundary coastal waves off Angola are now available. Analysis of the multi-year velocity observations of the Angola Current revealed alternating poleward and equatorward flow having periods of a few months with superimposed high-frequency velocity pulses (Kopte 2017, Kopte et al. 2017). However, while the strength of the variable flow is in agreement with previous synoptic measurements, the mean poleward flow is weak and amounts to only 0.3 Sverdrup (Kopte et al. 2017; Tchipalanga et al. 2018).

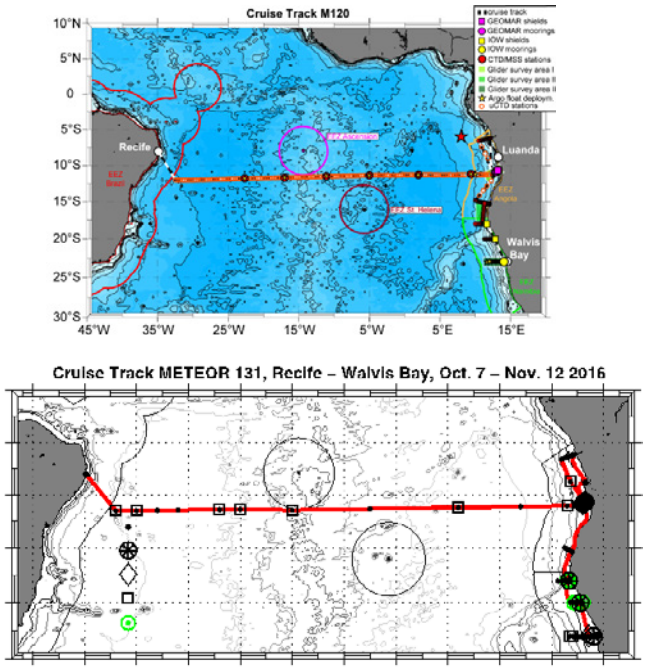

Fig. 1: Left panel shows ship track of R/V METEOR cruise M120 including locations of conductivity, temperature, depth (CTD) and oxygen and microstructure (CTD/MSS) stations, mooring and bottom shield recoveries and redeployments, glider survey areas, Argo float deployments and underway-CTD (uCTD) profiles. Territorial waters of different countries are marked with coloured solid lines. Right panel shows ship track of R/V Meteor cruise M131 (red line) with locations of CTD/LADCP (black dots) and Dredge/van Veen grab stations (green dots/circles), mooring deployments (stars) and recoveries (circles), Argo float deployments (squares) and glider deployments/ recoveries (diamonds). Also included are the exclusive economic zones of Brazil, Saint Helena, Ascension, Angola, and Namibia (black lines). Depth contours are drawn at 6000, 5000, 4000, 3000, 2000, 1000, and 500.

The moored time series of currents, hydrography and oxygen allowed a description of the variability of the boundary current circulation and water masses. During austral summer the southward Angola Current is concentrated in the upper 150 m. It strengthens from north to south reaching a velocity maximum just north of the Angola Benguela Front. During austral winter the Angola Current is weaker, but deeper reaching. While the southward strengthening of the Angola Current can be related to the wind forcing, its seasonal variability is most likely explained by coastally trapped waves (Tchipalanga et al. 2018). The hydrographic sections combined with the shipboard meteorological measurements and the autonomous measurements contribute to determining seasonal and interannual variability of the mixed layer heat and fresh water budgets (Lüdke 2015). On interannual timescales, the hydrographic data reveals remarkable variability in subsurface upper ocean heat content that apears to be related to Benuela Niños (Tchipalanga et al. 2018). Junker et al. (2019) used current observations of three moorings on the Namibian shelf (18°S, 20°S, 23°S) to examine the alongshore velocity signal for signatures of coastal trapped waves. Typical time and length scales of these waves range between 2 and 50 days, and 800 to 7000km, respectively. It turns out that

the wave properties differ significantly within a few hundred kilometers along the coast which is likely explained by variations in the bottom topography.

REFERENCES

Junker, T., V. Mohrholz, M. Schmidt, L. Siegfried, and A. van der Plas, Coastal trapped wave propagation along the southwest African shelf as revealed by moored observations, J. Phys. Oceanogr., 49, 851-866, doi:10.1175/JPO-D-18-0046.1, 2019.

Kopte, R., The Angola Current in a tropical seasonal upwelling system, Ph.D. thesis, Christian-Albrechts-Universität zu Kiel, 135 pp., 2017.

Kopte, R., P. Brandt, M. Claus, R. J. Greatbatch, and M. Dengler, Role of basin-mode resonance for the seasonal variability of the Angola Current, J. Phys. Oceanogr., 48, 261-281, doi:10.1175/JPO-D-17-0111.1, 2018.

Lüdke, J., Seasonal Mixed Layer Heat and Salinity Budget in the South Eastern Tropical Atlantic Ocean, Master thesis, Christian-Albrechts-Universität zu Kiel, Kiel, Germany, 88 pp., 2016.

Tchipalanga, P., M. Dengler, P. Brandt, R. Kopte, M. Macuéria, P. Coelho, M. Ostrowski, and N. S. Keenlyside, Eastern boundary circulation and hydrography off Angola – building Angolan oceanographic capacities, Bull. Amer. Meteor. Soc., 99, 1589-1605, doi:10.1175/BAMS-D-17-0197.1, 2018.

M121

TRACE ELEMENTS AND THEIR ISOTOPES IN THE SOUTHEASTERN ATLANTIC OCEAN: FIRST RESULTS OF CRUISE M121 (GEOTRACES CRUISE GA08)

AUTHORS

GEOMAR Helmholtz Centre for Ocean Research Kiel | Kiel, Germany
M. Frank, E. Achterberg

Department of Physics and Earth Sciences, Jacobs University Bremen | Bremen, Germany
A. Koschinsky

Research cruise M121 on RV Meteor (Walvis Bay-Walvis Bay, Nov–Dec 2015) was carried out in the southeastern (SE) Atlantic Ocean. The focus of the cruise were trace metal biogeochemical and chemical oceanographic investigations that also included physical and biological oceanographic components. The main goal of the cruise was to determine in detail the distributions of trace elements and their isotopes (TEIs) in the water column of the SE Atlantic in order to constrain TEI supply and removal mechanisms, their biogeochemical cycling, and their interaction with the nitrogen cycle in the study region. The research focused on three main research topics that can ideally be combined in the study area. The first focus was the detailed investigation of the distribution of the TEIs, some of which act as limiting micronutrients for primary productivity and diazotrophy. The TEI distribution is affected by the distribution and mixing of the water masses of the Benguela upwelling region and their properties with respect to oxygen levels and exchange with the anoxic shelves. The relationships between the supply strengths of key TEIs (e. g. Fe, Co, Mn, Mo) that drive ocean productivity, N_2 fixation and N-loss processes (anammox and denitrification), were assessed as water column N:P ratios in the study region show strong deviations from the classical Redfield ratio, with potential consequences for productivity in downstream regions of the Atlantic. Secondly, the fluxes and supply pathways of TEIs via dust (Namibian Desert), sediments and major rivers, mainly the Congo and Orange Rivers were investigated. The third focus was the investigation of the offshore distribution of the TEIs as a function of major ocean circulation and water mass mixing. This is particularly important because some of these TEIs are applied as paleo water mass tracers but knowledge on their present day distribution in the study area is scarce. These objectives are of global significance and their achievement provides improved understanding of the role of diverse processes in controlling the chemical environment in which ecosystems operate worldwide.

The cruise was officially part of the internationally coordinated program GEOTRACES (Cruise Number GA08). A total of 51 full water column stations were sampled for the

different dissolved TEIs, which was accompanied by sampling for particulates and radium isotopes using in-situ pumps and by trace metal clean surface water sampling using a towed fish (Fig. 1).

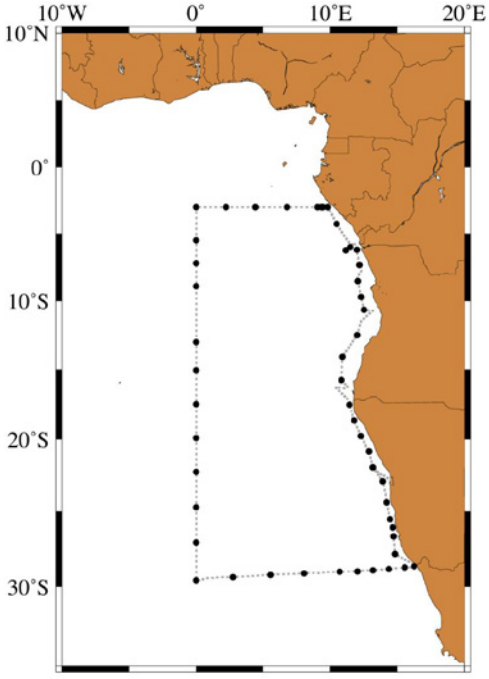

Fig. 1: Cruise track of R/V METEOR Cruise M121 (GEOTRACES Cruise GA08) and locations of sampled stations provided as black dots.

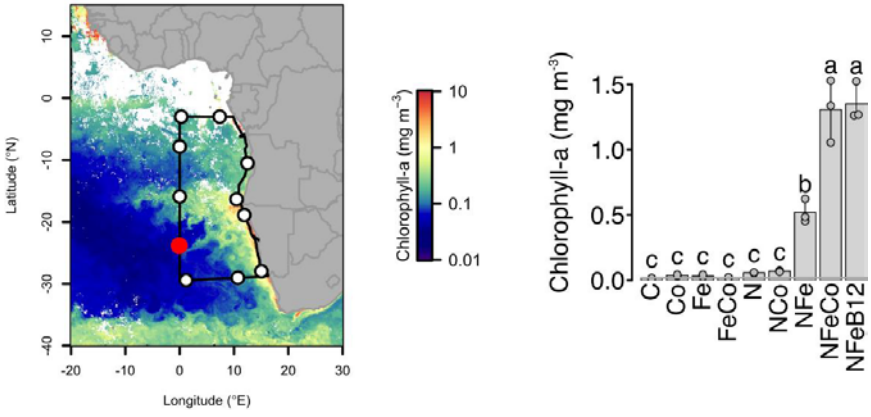

Fig. 2: Experiments conducted along the southeast Atlantic GEOTRACES GA08 cruise track (left panel) demonstrated that both nitrogen and iron had to be added to surface waters to significantly stimulate phytoplankton growth (example experiment in the right panel). Supplementary addition of cobalt (or cobalt-containing vitamin B12) stimulated significant additional growth (Browning et al., 2017).

One of the highlights published so far are the results achieved on nutrient and micronutrient co-limitation of bioproductivity. These data demonstrated that separate nitrogen and iron addition to seawater in the study area did not result in elevated diatom bioproductivity, whereas the combination of the two raised chlorophyll a levels by up to a factor of 40 and was even further increased by addition of Co (Fig. 2). This finding has very important implications for the factors controlling ocean bioproductivity and their accurate representation in biogeochemical modeling and was published by Browning et al. (2017).

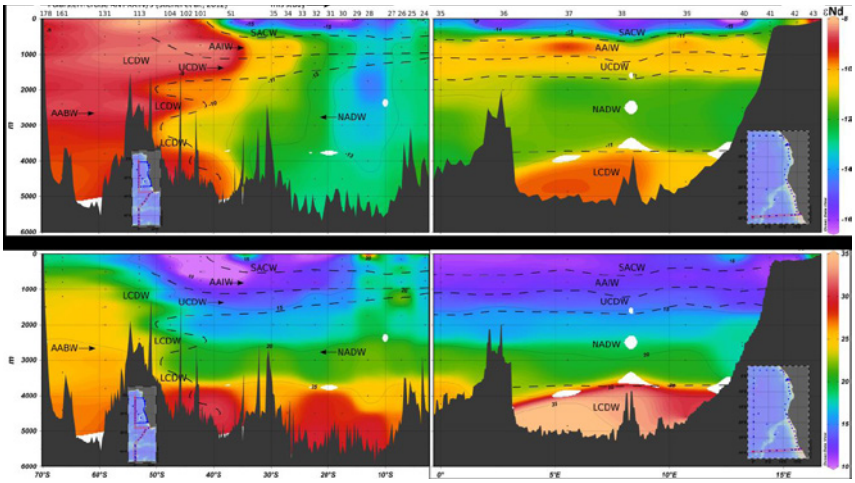

Fig. 3. Nd isotopic compositions and Nd concentrations of the Angola Basin and Cape Basin obtained for Cruise M121, together with data from cruise ANT-XXIIV/3 (Stichel et al., 2012). Dashed lines indicate approximate boundaries of the prevailing water masses. The figure has been adopted from Rahlf et al. (2020).

Radiogenic Nd isotopes have been widely used as water mass tracers in the present and past ocean but their detailed water column distribution and relationship to water mass mixing in the SE Atlantic, in particular the restricted Angola Basin has been unconstrained due to an almost complete lack of data. The Nd isotope distributions now show that the near surface waters in the study area were affected by water masses charged with dissolved metals of a coastal plume in the western Angola Basin and by surface waters carrying signature of old Archean terrains of southern Africa in the Cape Basin (Rahlf et al., 2020). As supported by Ra isotope measurements, the Nd isotope inputs from the Congo River are still clearly traceable in the surface waters more than a 1000 km north of the Congo mouth whereas the subsurface waters deeper than 200 m do not show any impact of the river waters. Except in the central Angola Basin the deep water Nd isotope signatures reflect water mass mixing (Fig. 3).

A first comprehensive set of Cd elementary and isotopic distributions in the study area was published (Guinoiseau et al., 2019) and showed that water mass mixing largely

controls deep ocean Cd isotope signatures whereas Cd isotope fractionation in surface waters can be modelled as an open system at steady-state buffered by organic ligand complexation. In the oxygen deficient zone ODZ, stronger Cd depletion relative to PO_4 is associated with a shift in $\delta^{114}Cd$ towards heavier values, which is indicative of CdS precipitation.

The distribution of dissolved aluminum concentrations can be used as a tracer for atmospheric deposition fluxes and the dissolved Al data of GA11 are part of a paper on an improved reconstruction of the atmospheric inputs into the Atlantic Ocean (Menzel Barraqueta et al., 2019). The new data agree well with previous estimations in the Atlantic but deviate from atmospheric dust deposition model flux estimates in regions influenced by riverine Al inputs and in upwelling regions.

Further publications on the dissolved and particulate distributions of other trace metals, their speciation and of Ra isotopes are currently in preparation.

REFERENCES

Browning TJ, Achterberg EP, Rapp I, Engel A, Bertrand EM, Tagliabue A and Moore CM, Nutrient co-limitation at the boundary of an oceanic gyre. Nature 2017, 551, 242–246. doi:10.1038/nature24063

Menzel Barraqueta JL, Klar JK, Gledhill M, Schlosser C, Shelley R, Planquette HF, Wenzel B, Sarthou G and Achterberg EP, Atmospheric deposition fluxes over the Atlantic Ocean: a GEOTRACES case study. Biogeosciences 2019, 16, 1525–1542, doi:10.5194/bg-16-1525-2019

Rahlf P, Hathorne E, Laukert G, Gutjahr M, Weldeab S and Frank M, Tracing water mass mixing and continental inputs in the southeastern Atlantic Ocean with dissolved neodymium isotopes. Earth and Planetary Science Letters 2020, in press, doi:10.1016/j.epsl.2019.115944

Guinoiseau D, Galer SJG, Abouchami W, Frank M, Achterberg EP and Haug GH, Importance of cadmium sulfides for biogeochemical cycling of Cd and its isotopes in Oxygen Deficient Zones – a case study of the Angola Basin. Global Biogeochemical Cycles 2019, in press.

Stichel T, Frank M, Rickli J, and Haley BA, The hafnium and neodymium isotope composition of seawater in the Atlantic sector of the Southern Ocean. Earth and Planetary Science Letters 2012, 317–318, 282–294, doi:10.1016/j.epsl.2011.11.025

M121*

SOURCES AND DISTRIBUTION OF DISSOLVED MOLYBDENUM, VANADIUM AND URANIUM IN THE SOUTHEASTERN ATLANTIC OCEAN

AUTHORS

Department of Physics and Earth Sciences, Jacobs University Bremen | Bremen, Germany

I. Velasquez, S. Poehle, K. Kunde*, A. Koschinsky

*Ocean and Earth Science, National Oceanography Centre Southampton, University of Southampton

The spatial distributions of dissolved molybdenum (Mo), uranium (U) and vanadium (V) were determined from 23 stations in the Southeastern Atlantic Ocean during the GEOTRACES cruise GA11 (M121) to understand their possible supply and removal mechanisms and biogeochemical cycling in the study region. The sampling sites covered areas of major external input sources e. g. dust from the Namib Desert, exchange with the West African continental margin and with the oxygen-depleted shelf sediments of the Benguela upwelling as well as the influence of the plume of the Congo River.

Molybdenum and U are often considered to behave conservatively in the open ocean, while V was reported to exhibit conservative (Firdaus et al., 2008; Sohrin et al., 1987, 1999) and nutrient-like distributions (Smrzka et al., 2019) in seawater. However, it is known that all three metals can adsorb on Mn-Fe oxide particles and form insoluble precipitates in anoxic regions. The concentrations of Mo, U and V from the study sites (Figure 1) ranged from 96 to 127 nM, 10 to 13 nM and 29 to 49 nM respectively, and their mean concentrations (Mo 109 nM; U 12.8 nM; V 36.7 nM) were comparable to published values for seawater (Smrzka et al., 2019). Similar concentrations of Mo, V, and U in 0.2 µm and 0.015 µm filtered samples indicate that the soluble fractions of the three elements dominate their abundance in the water column. Vertical distributions of dissolved Mo, U and V were highly variable in the upper 200 m with a near homogenous distribution down the water column. The upper 200 m of the shelf stations in the Angola Basin have marginally higher average concentrations of dissolved Mo, U and V than in in the shelf stations in the Cape Basin (Figure 2). This may be indicative of desorption from Mn-Fe-oxyhydroxides or release from the sediments coming from the Congo River (Audry et al., 2006; Algeo and Tribovillard, 2009; Rickli et al., 2010, Bauer et al., 2017).

Our results conform to the presence of high unradiogenic Nd isotope signals observed in the Angola Basin due to riverine input and a trace metal enriched plume originating from the African coast (Noble et al., 2012, Zheng et al., 2016, Rahlf et al., 2019).

Differences in concentrations and depth profiles of Mo, U and V in deep stations 1285 compared to stations along the 28°S west-east transect (1289, 1296, 1304 and 1313) illustrate signatures of the mixture of different water masses in the waters of the Angola and Cape Basins (Rahlf et al., 2019). Our data imply that dissolved Mo, U and V do not behave strictly conservative in the SE Atlantic Ocean. Their concentrations vary in a limited range between distinct areas with specific environmental conditions (e. g. impact of riverine input like particles and suspended sediments, and dust input into the waters along the shelf as well as oxygen depletion in the subsurface layer of the upwelling region).

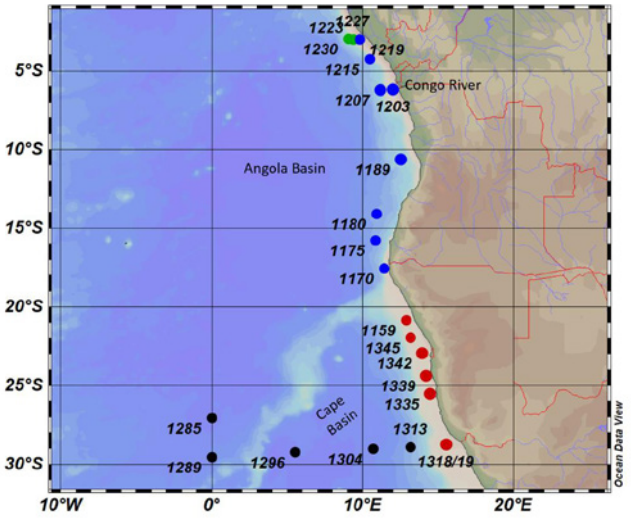

Fig. 1: Sampling stations of cruise M121 in the SE Atlantic for which Mo, V, and U data have been analysed for the study; blue dots represent Angola Basin stations shown in Figure 2 and red dots represent Cape Basin stations in Figure 2.

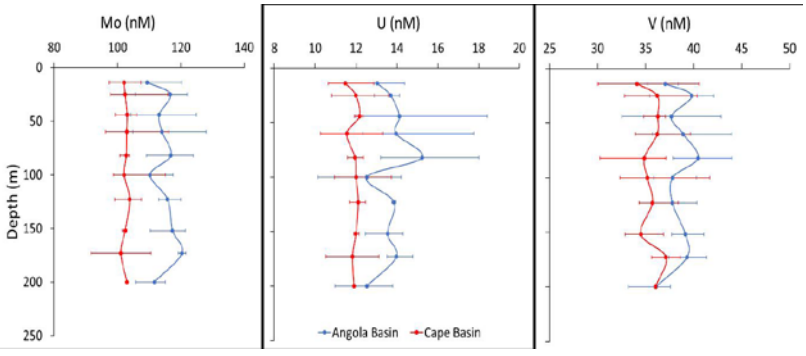

Fig. 2: Plot showing higher average concentrations of Mo, U and V in the upper 200m of Angola Basin (stations 1219, 1215, 1203, 1207, 1180, 1189, 1175 and 1170, see Figure 1) compared to Mo, U and V in the waters of Cape Basin (stations 1157, 1159, 1345, 1342, 1339, 1335 and 1318). Concentration ranges for each sampling depth are presented using horizontal bars.

REFERENCES

Algeo TJ, Tribovillard N, Environmental analysis of paleoceanographic systems based on molybdenum-uranium covariation, Chemical Geology 2009, 268, 211–225.

Audry S, Blanc G, Schafer J, Chaillou G, Robert S, Early diagenesis of trace metals (Cd, Cu, Co, Ni, U, Mo, V) in freshwater reaches of a macrotidal estuary, Geochimica et Cosmochimica Acta 2006, 70, 2264–2282.

Bauer S, Blomqvist S, Ingri J, Distribution of dissolved and suspended particulate molybdenum, vanadium and tungsten in the Baltic Sea, Marine Chemistry 2017, 196, 135–147.

Firdaus ML, Norisuye K, Nakagawa Y, Nakatsuka S, Sohrin Y, Dissolved and labile particulate Zr, Hf, Nb, Ta, Mo and W in the Western North Pacific Ocean, Journal of Oceanography 2008, 64, 247–257.

Noble AE, Lamborg CH, Ohnemus DC, Lam PJ, Goepfert TJ, Measures CI, Saito MA, Basin-scale inputs of cobalt, iron, and manganese from the Benguela-Angola front to the South Atlantic Ocean. Limnol. Oceanogr. 2012, 57 (4), 989–1010. https://doi.org/10.4319 /lo.2012.57.4.0989.

Rahlf P, Hathorne E, Laukert G, Gutjahr M, Weldeab S, Frank M, Tracing water mass mixing and continental inputs in the southeastern Atlantic Ocean with dissolved neodymium isotopes, Earth and Planetary Science Letters 2019, https://doi.org/10.1016/j.epsl.2019.115944.

Rickli J, Frank M, Baker AR, Aciego S, de Souza G, Georg RB, Halliday AN, Hafnium and neodymium isotopes in surface waters of the eastern Atlantic Ocean: implications for sources and inputs of trace metals to the ocean. Geochim. Cosmochim. Acta 2010, 74 (2), 540–557, https://doi.org/10.1016/j.gca.2009.10.006.

Smrzka D, Zwicker J, Bach W, Feng D, Himmler T, Chen D, and Peckmann J, The behavior of trace elements in seawater, sedimentary pore water, and their incorporation into carbonate minerals: a review, Facies 2019, 65:41, doi.org/10.1007/s10347-019-0581-4.

Sohrin Z, Isshiki K, Kuwamoto T, Nakazama E, Tungsten in north pacific waters, Marine Chemistry 1987, 1, 95–93.

Sohrin Y, Matsui M, Nakayama E, Contrasting behavior of tungsten and molybdenum in the Okinawa Trough, the East China Sea and the Yellow Sea, Geochimica et Cosmochimica Acta 1999, 63(19-20), 3457–3466.

Zheng XY, Plancherel Y, Saito MA, Scott PM, Henderson GM, Rare earth elements (REEs) in the tropical South Atlantic and quantitative deconvolution of their non-conservative behavior. Geochim. Cosmochim. Acta 2016, 177, 217–237. https://doi.org/10.1016/j.gca.2016.01.018.

M121*

TRACING WATER MASS MIXING AND CONTINENTAL INPUTS IN THE ANGOLA AND CAPE BASINS WITH DISSOLVED NEODYMIUM AND HAFNIUM ISOTOPES

AUTHORS

GEOMAR Helmholtz Centre for Ocean Research Kiel | Kiel, Germany

P. Rahlf, E. Hathorne, G. Laukert, M. Gutjahr, M. Frank

In the frame of GEOTRACES cruise GA08 on RV Meteor (cruise M121), we determined 49 full seawater profiles of dissolved radiogenic neodymium (Nd) isotope signatures (ε_{Nd}) and neodymium concentrations as well as 20 profiles of dissolved hafnium (Hf) isotope signatures (ε_{Hf}) and hafnium concentrations of the restricted Angola Basin, the well ventilated northern Cape Basin and along the coast of Angola and Namibia (Fig. 1). Radiogenic Nd and Hf isotopes are used to investigate water mass mixing and provenance as well as exchange processes between seawater and sediments.

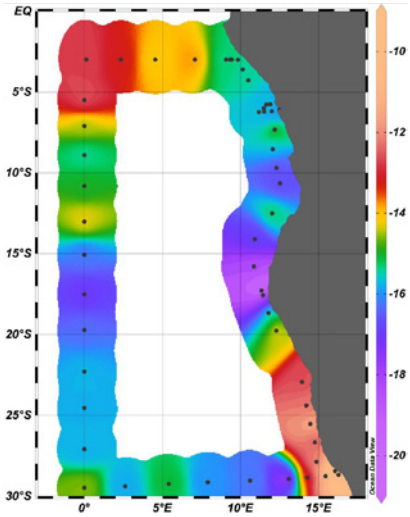

Fig. 1: Dissolved surface water Nd isotopic compositions of the research area with the most negative εNd values reaching -21 at 11 °E and 17 °S.

Nd isotope compositions of deep water masses in both basins primarily reflect conservative water mass mixing, except the central Angola Basin, which is significantly overprinted by regional terrestrial inputs (ε_{Nd} = -14) (Fig. 2). Bottom waters of the Cape Basin show some excess Nd concentrations released from detrital sediments, however,

without significantly changing their Nd isotopic compositions ranging between ε_{Nd} -9.6 and -10.5 (Fig. 2). Given that bottom waters within the Cape Basin today are enriched in Nd, non-conservative Nd isotopic effects may have been resolvable under past glacial boundary conditions when bottom waters were more radiogenic.

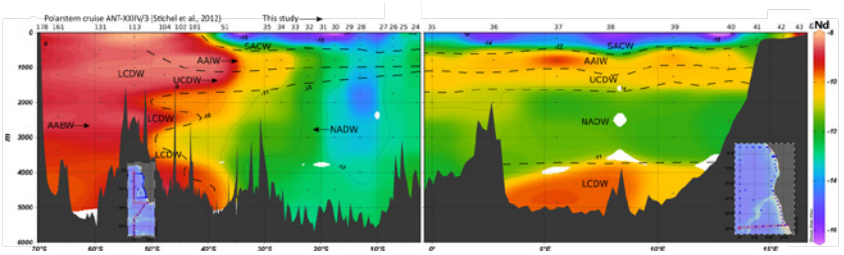

Fig. 2: Nd isotopic compositions of the Angola Basin and Cape Basin obtained for Cruise M121, together with data from cruise ANT-XXIII/3 (Stichel et al., 2012). Dashed lines indicate approximate boundaries of the prevailing water masses. The figure has been adopted from Rahlf et al. (2020).

Highly unradiogenic εNd signatures of up to -17 in the upper water column of the western Angola Basin are primarily the consequence of the admixture of a coastal plume originating near 15 °S and carrying an unradiogenic Nd signal (ε_{Nd} = -21) that is likely caused by the dissolution of Fe-Mn coatings of particles formed in river estuaries or near the West African coast (Fig. 3). The unradiogenic ε_{Nd} signatures of up to -17.7 in the upper water column of the northern Cape Basin, in contrast, originate from old Archean terrains of southern Africa and are introduced into the Mozambique Channel via rivers like the Limpopo and Zambezi. These signatures allow tracing the advection of shallow waters via the Agulhas and Benguela currents into the southeastern Atlantic Ocean.

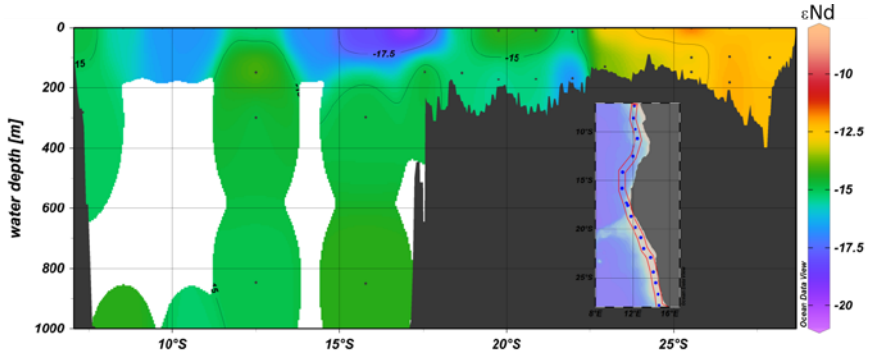

Fig. 3: Nd isotopic compositions along the coast of Namibia and Angola. Between 10 and and 15 °S. Unradiogenic Nd is released from particles and is advected westward into the Angola Basin.

North of the above mentioned coastal plume the Congo River discharges into the northern Angola Basin at 6 °S. We find high Nd and Hf concentrations of up to 4000 pmol/kg

and 54 pmol/kg, respectively, in low salinity surface waters of the Congo river mouth. Nd isotope compositions of the river endmember seasonally vary between -15.6 and -16.4 and Hf isotope compositions (ε_{Hf}) vary between 0.35 and -1.4. REEs and Hf are efficiently removed by coagulation at low salinities but are still enriched in surface waters up to 1000 km to the northwest of the river mouth (Fig. 4). In contrast to the Nd isotope compositions of the surface waters that indicate close to conservative behavior, Hf isotopes indicate significant influence by exchange by particulate matter. Based on mass balance calculations we find that up to 50 % of the dissolved Hf but max. 2 % of the dissolved Nd in surface waters near the mouth of the Congo River plume is released from suspended particulate matter, mainly from Fe-hydroxides.

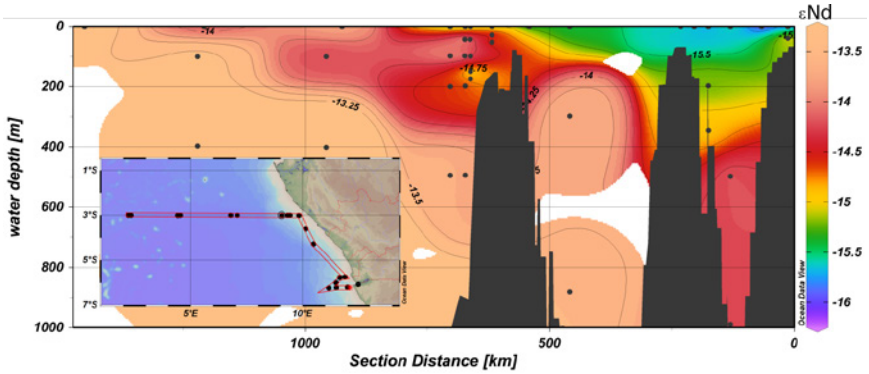

Fig. 4. Nd isotopic compositions of the Congo River plume, which is traced up to 1000 km northwestward.

REFERENCES

Rahlf P, Hathorne E, Laukert G, Gutjahr M, Weldeab S and Frank M, Tracing water mass mixing and continental inputs in the southeastern Atlantic Ocean with dissolved neodymium isotopes. Earth and Planetary Science Letters 2020, in press, doi:10.1016/j.epsl.2019.115944

Stichel T, Frank M, Rickli J, and Haley BA, The hafnium and neodymium isotope composition of seawater in the Atlantic sector of the Southern Ocean. Earth and Planetary Science Letters 2012, 317–318, 282-294, doi:10.1016/j.epsl.2011.11.025

M122

PRESENT AND PAST COLD-WATER CORAL ECOSYSTEMS IN THE SE ATLANTIC

AUTHORS

MARUM – Center for Marine Environmental Sciences, University of Bremen | Bremen, Germany

D. Hebbeln, C. Wienberg, RV Meteor Cruise M122 participants

During R/V METEOR expedition M122, hitherto unknown occurrences of thriving as well as fossil framework-forming cold-water corals (CWC) have been discovered off Namibia and Angola, a region characterised by a distinct oxygen minimum zone (OMZ). Especially the presence of vivid coral reefs off Angola (Fig. 1) shed new light on the adaptive capacities of the two main reef-forming CWC species: Lophelia pertusa and Madrepora oculata, which thrive in the center of the Angolan OMZ under the lowest dissolved oxygen concentrations (<0.8 mL L^{-1}) ever observed for CWC.

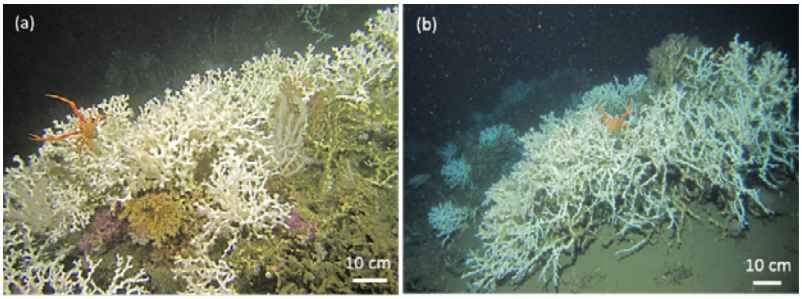

Fig. 1: (a, b) Vivid Lophelia pertusa-reefs are present in the center of the oxygen minimum zone (OMZ) off Angola OMZ (~350 m water depth; ROV images ©MARUM).

In addition, with partly >12°C also the observed temperatures off Angola are close to the assumed upper tolerable limit for CWC, especially for L. pertusa. As the occasional advection of slightly better ventilated waters by the activity of internal tides goes along with higher temperatures and vice versa (Fig. 2), these two stressors seem to balance each other to some extent. However, the widespread occurrence of vivid L. pertusa-reefs indicates that the presumed negative effects of hypoxic conditions and high temperatures on the proliferation of CWC seemingly can be compensated by significantly enhanced food supply controlled by the local upwelling regime. These findings triggered new ideas about the interaction of multiple stressors, by showing that one environmental constraint providing an optimal setting may balance the impact of another one providing an unfavourable setting.

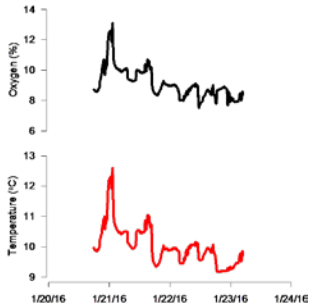

Fig. 2: Benthic lander data obtained over a 4-day period in January 2016 by the NIOZ Albex Lander at 340 m water depth close to the thriving cold-water coral reefs at the Angolan margin. The data clearly document the effect of internal tides.

Studying the long-term development of the Angolan CWC documented their almost continuous presence throughout the last approximately 35 kyr, covering cold glacial as well as warm interglacial periods (Fig. 3). This is in contrast to most other CWC sites known from the Atlantic, which almost exclusively reveal CWC occurrence patterns paced by large, i. e. , glacial/interglacial, climate variability. So far, a similar pattern as observed off Angola only has been found off Brazil, highlighting the specific role of the South Atlantic for the basin-wide development of CWC under changing global climates.

On even longer timescales, the CWC seem to benefit from tectonic activities off Angola, resulting in vertical movements creating distinct morphologies. A key feature is the Anna Fault, which borders a subsiding graben feature in the east to a salt block in the west (Fig. 4). This fault affected the local hydrodynamic regime triggering the deposition of a complex Contourite Depositional System to the east. At some point, the corals started to benefit from the enhanced hydrodynamics and built up the Anna Ridge, a coral mound/ridge reaching a height of >100 m (Fig. 4), which appears in the seismic data as a contorted to chaotic body.

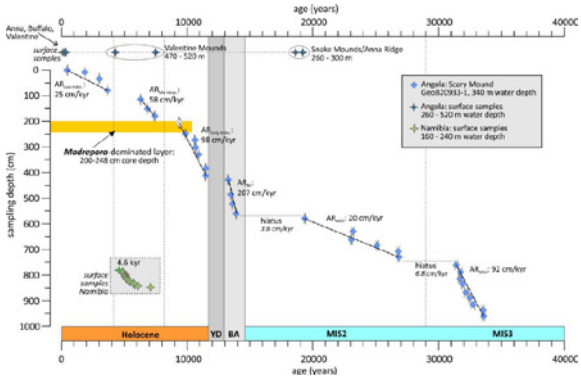

Fig. 3: U/Th-dating results from the Angolan margin largely based on corals collected from sediment core GeoB 20933-1 plotted versus core depth. Along seemingly continuous and undisturbed core sections mound aggradation rates (AR) are presented.

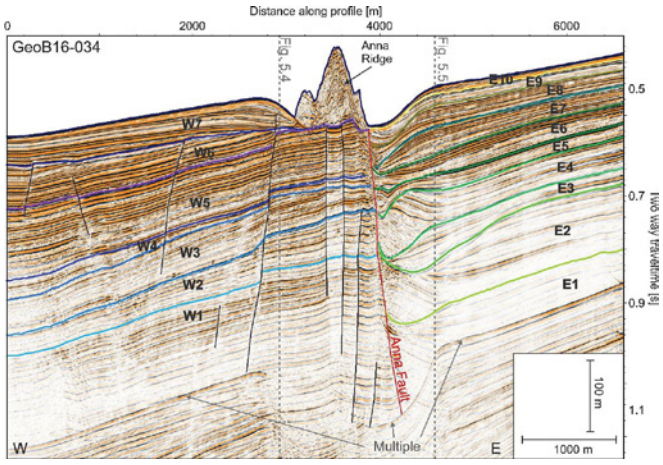

Fig. 4: Multi-Channel Seismic profile GeoB16-034 crossing Anna Ridge off Angola in E-W direction.

Off Namibia, >2000 smaller coral mounds have been found between 160 and 260 m water depth in even less ventilated intermediate waters (>0.5 mL L^{-1}). These mounds are densely covered with coral rubble and dead coral framework, while no living corals were observed (Fig. 5).

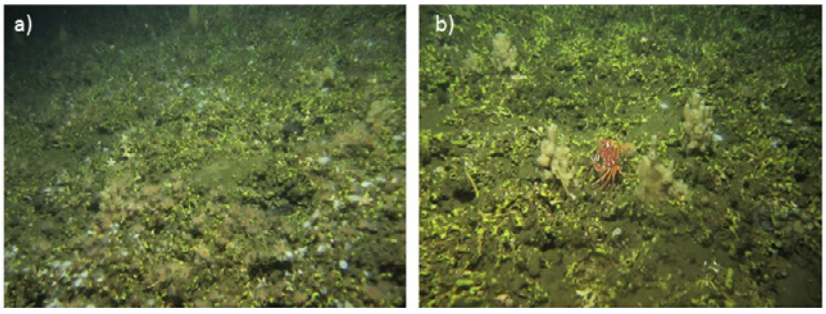

Fig. 5: ROV images showing the surface of cold-water coral mounds off Namibia. (a, b) Dead coral framework and rubble entirely consisting of Lophelia pertusa. The framework is intensely colonized by the yellow bryozoan Metropriella sp. (ROV images ©MARUM).

Nevertheless, these mounds testify the presence of environmental conditions suitable for CWC off Namibia in the geological past. Dating of CWC collected from the mounds' surfaces as well as of a full mound record reveal that formerly thriving CWC vanished from the region approximately 4.5 kyr ago. At that time, latitudinal movements of the Southern Westerlies resulted in a strengthening of the regional OMZ, most likely pushing the ambient ventilation state below a level bearable for the Namibian CWC (see abstract by Tamborrino et al.).

Known as biodiversity hotspots in the deep sea, CWC reefs can provide space, shelter, and food and, thus, attract many other organisms. However, the thriving reefs of Angola and even more the fossil, but still exposed reefs off Namibia show much less biodiversity as known from other CWC reefs, e. g. , in the North Atlantic. This is most likely due to the overall very low concentrations of dissolved oxygen in the SE Atlantic OMZ. Nevertheless, compared to the surrounding seabed, also in these coral mound settings the biodiversity is high, even revealing species new to science as e. g. , the mussel Neocardia kandeli n. sp.

M122*

MID-HOLOCENE EXTINCTION OF COLD-WATER CORALS ON THE NAMIBIAN SHELF STEERED BY THE BENGUELA OXYGEN MINIMUM ZONE

AUTHORS

MARUM, Center for Marine Environmental Sciences, University of Bremen | Bremen, Germany
L. Tamborrino, C. Wienberg, J. Titschack, P. Wintersteller, J. Haberkern, D. Hebbeln

Senckenberg am Meer | Wilhelmshaven, Germany
J. Titschack, A. Freiwald

Department of Geosciences, University of Bremen | Bremen, Germany
P. Wintersteller, J. Haberkern

NIOZ-Royal Netherlands Institute for Sea Research and Utrecht University | Den Burg, Netherlands
F. Mienis

IUP-Institute of Environmental Physics, Heidelberg University | Heidelberg, Germany
A. Schröder-Ritzrau

Centro Oceanográfico de Baleares, Instituto Español de Oceanografia | Palma, Spain
C. Orejas

GEOMAR–Helmholtz Centre for Ocean Research | Kiel, Germany
W.-C. Dullo

Cold-water coral (CWC) ecosystems have been widely documented along the continental slopes around the Atlantic Ocean, but still new areas are awaiting their discovery. Frameworks built by colonial scleractinian CWC, like Lophelia pertusa, have the capacity to baffle bypassing sediments supporting the development of impressive three-dimensional seabed structures known as “coral mounds”, which form over geological time scales. Here, we present the discovery of a new large coral mounds province, extending over a remarkable distance of (at least) 80 km along the northern Namibian shelf (~20-21°S). More than 2,000 coral mounds varying in height between a few metres up to 20 m were

detected in 160–270 m water depth (Fig. 1) during the RV Meteor M122 cruise (Hebbeln et al., 2017). The Namibian coral mounds (NCM) occur in three main areas: Squid Mounds, Coral Belt Mounds and Escarpment Mounds (Fig.1) Observation with the remote operated vehicle MARUM SQUID and sediment sampling confirmed that no living L. pertusa is occurring in the NCM province.

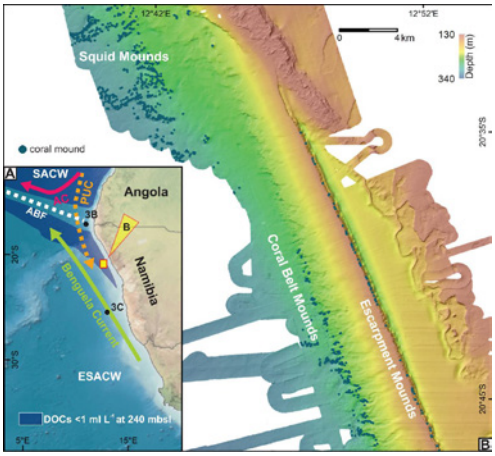

Fig.1: (A) Overview map showing oceanographic circulation patterns off southwestern Africa (ABF-Angola Benguela Front; AC-Angola Current; PUC-poleward undercurrent; SACW-South Atlantic Central Water; ESACW-Eastern South Atlantic Central Water; mbsl-meters below sea level). Spatial extent of oxygen minimum zone (dissolved oxygen concentrations [DOCs] <1 ml L^{-1} in 240 m water depth; dark-blue shading) is based on Schmidt and Eggert (2016). Corresponding DOCs at the ABF are <2 ml L^{-1}. Yellow square and arrow indicate the Namibian coral mound province shown in B. "3B" and "3C" refer to data sets presented in Fig. 2, (B) and (C), respectively. (B) Bathymetric map showing the distribution of coral mounds.

Uranium-series datings obtained from various surface coral samples revealed that L. pertusa became regionally extinct at ~4.5 ka (Fig. 2), resulting in a simultaneous cessation in mound development within the entire NCM province.

Nowadays, in the area of the NCM the Benguela oxygen minimum zone (OMZ, Fig. 1) causes very low dissolved oxygen concentrations (Hanz et al., 2019), suggesting a possible cause for the absence of living CWC. Their Mid-Holocene demise is indeed coincident with an intensification of the upwelling and the northward migration of the Angola-Benguela Front, driven by a change of the wind stress (Fig. 2). Higher productivity (and consequent high consumption of dissolved oxygen through the water column due to the high amount of decaying organic matter) combined with less mixing effect of the Angola-Benguela Front intensified the Benguela OMZ since the Mid-Holocene until today. The resulting extremely depleted OMZ off Namibia represented a hostile environment for the CWC, although until the Mid-Holocene, they have benefitted of the abundant food supply, which guaranteed high mound aggradation rates (158 cm $k.y^{-1}$, Tamborrino et al., 2019).

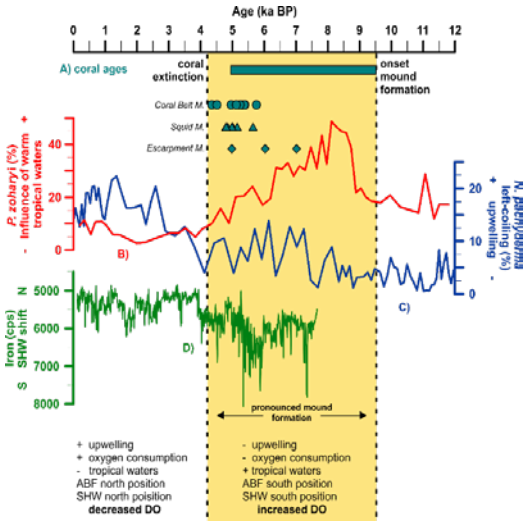

Fig. 2: Uranium-series cold-water coral ages (A) obtained from 19 surface sediment samples (green symbols) collected from various Namibian shelf coral mounds differentiated into three mound settings, and the age range derived from one gravity core fully penetrating one Coral Belt Mound (green bar). Coral ages reveal a pronounced period in mound formation restricted to the early to mid-Holocene. This coincides with enhanced influence of warm tropical waters (indicated by high percentages of the tropical dinoflagellate Polysphaeridium zoharyi; Shi et al., 2000) (B), and weakened upwelling (indicated by low percentages of the planktonic foraminifera Neogloboquadrina pachyderma [left coiling];) (Farmer et al., 2005) (C), pointing to southward displacement of the Angola-Benguela Front (ABF) due to southward displacement of the Southern Hemisphere westerlies (SHW; indicated by enhanced iron contents in Chilean margin sediments;) (Lamy et al., 2001). (D). M.-Mounds; DOC-dissolved oxygen concentration; cps-counts per second. Locations for B and C are indicated in Fig. 1A.

Due to the further increase in ocean deoxygenation expected over the coming decades as a consequence of ongoing global climate change (e. g. Stramma et al., 2008), our results from the NCM might serve as an example highlighting how marine benthic ecosystems suffer from such a development. For regions with CWCs that currently thrive under OMZ (Georgian et al., 2016; Wienberg et al., 2018), further decreasing dissolved oxygen concentrations might wipe out biodiversity hotspots engineered by CWCs within the coming decades to centuries.

REFERENCES

GENUS (Geochemistry and Ecology of the Namibian Upwelling System) Project, 2017, How does the Benguela Upwelling System work?: Podcast video, https://www.youtube.com/watch?v=8C9p6_qxgEI&t=1s.

Farmer, E. C., deMenocal, P. B., and Marchitto, T. M., 2005, Holocene and deglacial ocean temperature variability in the Benguela upwelling region: Implications for low-latitude atmospheric circulation: Paleoceanography, v. 20, no. 2.

Georgian, S. E., DeLeo, D., Durkin, A., Gomez, C. E., Kurman, M., Lunden, J. J., and

Cordes, E. E., 2016, Oceanographic patterns and carbonate chemistry in the vicinity of cold-water coral reefs in the Gulf of Mexico: Implications for resilience in a changing ocean: Limnology and Oceanography, v. 61, no. 2, p. 648–665.

Hanz, U., Wienberg, C., Hebbeln, D., Duineveld, G., Lavaleye, M., Juva, K., Dullo, W. C., Freiwald, A., Tamborrino, L., Reichart, G. J., Flögel, S., and Mienis, F., 2019, Environmental factors influencing benthic communities in the oxygen minimum zones on the Angolan and Namibian margins: Biogeosciences, v. 16, no. 22, p. 4337–4356.

Hebbeln, D., Wienberg, C., Bender, M., Bergmann, F., Dehning, K., Dullo, W.-C., Eichstädter, R., Flöter, S., Freiwald, A., Gori, A., Haberkern, J., Hoffmann, L., Mendes João, F., Lavaleye, M., Leymann, T., Matsuyama, K., Meyer-Schack, B., Mienis, F., Bernardo Moçambique, I., Nowald, N., Orejas Saco del Valle, C., Cordova, C. R., Saturov, D., Seiter, C., Titschack, J., Vittori, V., Wefing, A.-M., Wilsenack, M., and Wintersteller, P., 2017, ANNA - Cold-Water Coral Ecosystems off Angola and Namibia. Cruise M122 – December 30, 2015 – January 31, 2016 – Walvis Bay (Namibia) – Walvis Bay (Namibia). METEOR-Berichte/Reports, M122, 66 pp, DFG-Senatskommission für Ozeanographie.

Lamy, F., Hebbeln, D., Röhl, U., and Wefer, G., 2001, Holocene rainfall variability in southern Chile: a marine record of latitudinal shifts of the Southern Westerlies: Earth and Planetary Science Letters, v. 185, no. 3, p. 369–382.

Schmidt, M., and Eggert, A., 2016, Oxygen cycling in the northern Benguela Upwelling System: Modellingoxygen sources and sink: Progress in Oceanography, v. 149, p. 145–173.

Shi, N., Dupont, L. M., Beug, H.-J., and Schneider, R., 2000, Correlation between Vegetation in Southwestern Africa and Oceanic Upwelling in the Past 21,000 Years: Quaternary Research, v. 54, no. 1, p. 72–80.

Stramma, L., Johnson, G. C., Sprintall, J., and Mohrholz, V., 2008, Expanding oxygen-minimum zones in the tropical oceans: Science, v. 320, p. 655.

Tamborrino, L., Wienberg, C., Titschack, J., Wintersteller, P., Mienis, F., Schröder-Ritzrau, A., Freiwald, A., Orejas, C., Dullo, W.-C., Haberkern, J., and Hebbeln, D., 2019, Mid-Holocene extinction of cold-water corals on the Namibian shelf steered by the Benguela oxygen minimum zone: Geology, v. 47, no. 12, p. 1185–1188.

Wienberg, C., Titschack, J., Freiwald, A., Frank, N., Lundälv, T., Taviani, M., Beuck, L., Schröder-Ritzrau, A., Krengel, T., and Hebbeln, D., 2018, The giant Mauritanian cold-water coral mound province: Oxygen control on coral mound formation: Quaternary Science Reviews, v. 185, p. 135–152.

M122*

ON DETERMINING THE LIVING CONDITION THRESHOLDS OF THE EASTERN ATLANTIC COLD-WATER CORALS WITH HIGH-RESOLUTION IN SITU OBSERVATIONS

AUTHORS

GEOMAR Helmholtz Centre for Ocean Research Kiel | Kiel, Germany
K. Juva, J. Karstensen, P. Linke, W.-C. Dullo, S. Flögel

Marum Center for Marine Environmental Sciences | Bremen, Germany
D. Hebbeln

Cold-water corals (CWCs) cover distinct part of the water column on continental margins. Several environmental factors, such as near sea-floor flow velocities, water mass characteristics and carbon chemistry, are believed to set the ideal environmental conditions for CWC growth. These parameter ranges are used in global habitat suitability models, but how these individual factors control and limit the development of CWCs is not yet fully understood.

Our goal is to investigate the impact of varying ocean dynamics on CWC habitats and to explain why CWCs have such confined settling areas. For this purpose, high-resolution physical, biogeochemical, and ecosystem data from seven CWC sites on the eastern margin of the Atlantic, from the sub-arctic to the subtropical southern hemisphere are used. The southernmost sites on Angolan and Namibian margins, visited during the M122-ANNA cruise, add valuable information on the less-studied conditions of the modern southern Atlantic CWC sites.

We found that across all sites, a distinct tidal flow is observed and that high tide flow and its relaxation are not symmetric. Living and healthy corals are concentrated at sites, where high tide creates local upwelling that allow recycling of sinking material with each tidal cycle. This process links hydrodynamics to several environmental factors and supports energy and food supply for filter-feeding corals. Our analysis provides new insights on CWC occurrences in the modern ocean, and might help to understand the CWC growth and distribution of a changing ocean, in the past and in the future.

M122*

PERSISTENT GLACIAL COOLING AND AGING OF THE MID-DEPTH BENGUELA CURRENT REVEALED THROUGH COLD-WATER CORALS RECOVERED DURING M122

AUTHORS

Institute of Environmental Physics, Heidelberg University | Heidelberg, Germany
N.Frank, C. Roesch, E. Beisel, A.-M. Wefing, F. Hemsing, M. Lausecker, J. M. Link, A.Schröder-Ritzrau, S. Therre

Institute for Earth Sciences, Heidelberg University | Heidelberg, Germany
N.Frank

Laboratory for Ion Beam Physics, ETH Zürich | Zürich, Switzerland
A.-M. Wefing

Institute for Geosciences, University Potsdam | Potsdam, Germany
J. Fohlmeister

Curt-Engelhorn-Center Archaeometry, D6, 3 | Mannheim, Germany
R. Friedrich

Senckenberg am Meer, Marine Research Department | Wilhelmshaven, Germany
A. Freiwald

GEOMAR- Helmholtz Centre for Ocean Research | Kiel, Germany
W.-C. Dullo

MARUM – Center for Marine Environmental Sciences, University of Bremen | Bremen, Germany
C. Wienberg, D. Hebbeln

The Benguela current (BC) is an important player in the climate system. It feeds cold and nutrient rich waters into the South Atlantic gyre, fueling high rates of phytoplankton growth in the upwelling centers off Namibia and Angola. Its thermocline waters spread and cool the entire South Atlantic basin. The Li/Mg elemental ratio and 14C content of framework forming cold-water corals from north of today's Angola-Benguela Front (9°49.3′ S; 12°46.6′ E, 338 m) now reveal a massive glacial upper thermocline water cooling by up to 6.5 ± 1.7°C and synchronous water mass aging by ~400 years

(R = 970±160 years) if compared to the Holocene. These changes are persistent between 31'000 to 18'950 years BP. Regional sea surface temperature reconstructions point to moderate < 3°C glacial surface water cooling contrasting intensified regional upwelling and leading to an augmented vertical temperature gradient and thus thermal stratification. To explain the observations we propose a substantial increase of the northward advection of cold and aged mid-depth waters of polar origin via the Benguela Current. This implies a northward shift of the southern hemisphere Hadley cell and a blocking of warm water leakage from the Agulhas retro-flexion during the last glacial.

M122*

OCCURRENCE AND DENSITY OF THE COLD-WATER CORAL MADREPORA OCULATA IN THE HYPOXIC WATERS OFF ANGOLA (SE ATLANTIC)

AUTHORS

Instituto Español de Oceanografía, Centro Oceanográfico de Baleares | Palma, Mallorca, Spain
C. Orejas,

MARUM- Center for Marine Environmental Sciences, University of Bremen | Bremen, Germany
C. Orejas, C. Wienberg, J. Titschack, L. Tamborrino, D. Hebbeln

Senckenberg am Meer | Wilhelmshaven, Germany
A. Freiwald

Madrepora oculata is together with Lophelia pertusa one of the two main reef-forming cold-water corals in the Atlantic Ocean. Although the information for M. oculata is much less abundant than for L. pertusa, results from ecophysiological experiments as well as from paleo-oceanographic records point out to high adaptation and accommodation capabilities for this species. Recent discoveries of M. oculata populations in the South East Atlantic along the Angolan continental margin during RV Meteor expedition M122 revealed exceptional large colonies of this species with heights of more than 1.2 meters, never documented before in any other area. Furthermore, these colonies thrive under extreme hypoxic conditions with average densities of 0.53 colonies m-2 ± 0.37 (SD), comparable to average densities previously documented from areas without any oxygen constraints. These results are discussed considering the specific environmental envelope off Angola and compared to previous results gained in the North Atlantic and Mediterranean Sea.

M123
CLIMATE ARCHIVES IN COASTAL WATERS OF SOUTHERN AFRICA

AUTHORS

MARUM – University of Bremen | Bremen, Germany
M. Zabel

University of KwaZulu Natal | Durban, South Africa
A.N. Green

Council for Geoscience | Cape Town, South Africa
Nelson Mandela Metropolitan University | Port Elisabeth, South Africa
H. Cawthra

And: Science party M123

As the water problems in parts of South Africa in recent years have shown, southern Africa is very sensitive to the impacts of climate change and therefore depend on accurate regional climate predictions (IPCC 2007). However, well-dated, continuous, high-resolution paleorecords are scarce and unevenly distributed (Nash and Meadows 2012). This is in part due to the strongly seasonal climate with frequent episodes of fluvial or eolian erosion that inhibit the accumulation of long terrestrial sedimentary sequences making marine records particularly important. But, despite various previous expeditions, among others with German research vessels, there were hardly any sediment archives from the east coast of southern Africa before METEOR cruise M123.

Our main scientific objective of this expedition, the search for and sampling of sediment archives with the highest possible resolution in nearshore waters along the south and east coasts of southern Africa, was met with considerable reservations by the reviewers of our first proposal. Despite the undoubtedly difficult conditions due to the well-known strong coastal current (Agulhas Current), the close cooperation with South African scientists and their local knowledge made it possible to find appropriate deposits. As expected, very sandy sediments predominate in the working area, which are neither suitable for studies to reconstruct previous climate conditions, nor for investigations of sediment provenance. By using existing maps for the distribution and description of the shallow water sediments, as well as the ship's own acoustic systems, it was possible to identify and sample a few patches of fine-grained sediments in areas in front of different river estuaries. The results of the investigations to date have allowed new insights into sedimentation dynamics, for example, in connection with the deposition of sediments introduced into the Indian Ocean by the Limpopo (Schüürman et al. 2018). The Parasound profiles of this cruise, which have been evaluated and published so

far, reveal as yet unknown details of morphodynamics in individual sections of the shelf (De Lecea et al. 2017, Cawthra et al. 2019, Pretorius et al. 2019). The analysis of further profiles is in progress and will be submitted for publication shortly.

For the underlying research project RAiN this trip was an essential component and a complete success with regard to the results. Thus, local relationships between marine sediment archives and samples from different potential terrestrial source regions could be identified for the reconstruction of paleo-environmental conditions (e. g. Hahn et al. 2018, Miller et al. 2019).

Last but not least, it should be remembered that this trip also had the task of introducing students and young scientists to the planning and implementation of marine geoscientific techniques and working methods (students : scientists = 13/12). As can be seen from the documentation and the number of qualifications, the expedition was also successful in this respect.

REFERENCES

Cawthra HC, Frenzel P, Hahn A, Compton JS, Gander L, Zabel M. Seismic stratigraphy of the inner to mid Agulhas bank, South Africa. Quat. Sci. Rev. 2019 (in press)

De Lecea, AM, Green AN, Strachan KL, Cooper JAG, Wiles EA. Stepped Holocene sea-level rise and its influence on sedimentation in a large marine embayment: Maputo Bay, Mozambique. Estuarine, Coastal and Shelf Science 2017, 193:25–36.

Hahn A, Miller C, Andó S, Bouimetarhan I, Cawthra HC, Garzanti E, Zabel M. The provenance of terrigenous components in marine sediments along the east coast of southern Africa. Geochemistry, Geophysics, Geosystems 2018, 19 (7):1946–1962.

IPCC et al. (2007) Synthesis Report, IPCC, Geneva, Switzerland, 104.

Miller C, Hahn A, Liebrand D, Zabel M, Schefuß E. Mid- and low latitude effects on eastern South African rainfall over the Holocene. Quaternary Science Reviews (in press).

Nash DJ, Meadows ME, Quat. Environ. Change in the Tropics, In: Metcalfe & Nash (eds), Wiley, London, 2012, 79–150.

Pretorius L, Green AN, Cooper JAG, Hahn A, Zabel M. Outer-to inner-shelf response to stepped sea-level rise: Insights from incised valleys and submerged shorelines. Marine Geology 2019, 416, 105979.

Schüürman J, Hahn A, Zabel M. In search of sediment deposits from the Limpopo (Delagoa Bight, southern Africa): Deciphering the catchment provenance of coastal sediments. Sedimentary geology 2018, 380:94–104.

M123*

THE PROVENANCE OF TERRIGENOUS COMPONENTS IN MARINE SEDIMENTS ALONG THE EAST COAST OF SOUTHERN AFRICA

AUTHORS

MARUM – University of Bremen | Bremen, Germany
A. Hahn, C. Miller, I. Bouimetarhan, E. Schefuß, M. Zabel

University of Milano-Bicocca | Milan, Italy
S. Andó, E. Garzanti, G. Radeff

Council for Geoscience | Cape Town, South Africa
H. C. Cawthra

Nelson Mandela University | Port Elizabeth, South Africa,
H. C. Cawthra

University of KwaZulu-Natal | Durban, South Africa
A. N. Green

Terrestrial signals in marine sediment archives are often used for paleoclimatic reconstructions. It is therefore important to know the origin of the different terrestrial sedimentary components. The proximity to a river mouth is often the key location to determine the source. Especially in regions with strong ocean currents, such an assumption might, however, lead to considerable misinterpretations. To investigate the source of various terrigenous sediment fractions in southeastern Africa, a region with strong sediment redistribution, we have performed an extensive comparison between terrestrial material (pollen, plant lipids, detrital modes, and heavy minerals as well as bulk inorganic geochemical composition) from potential source regions and the same components in the adjacent coastal and continental shelf sediments. Onshore the proxy-indicators reflect small-scale diversity in sampling locations and associated environments (riverbank sediments, flood deposits, suspension loads, and soils). Nevertheless, the overall trends reflect significant environmental gradients along a SW to NE transect. We note a general comparability of the studied parameters between the continental and marine sediments regardless of their specific differences in transport and depositional characteristics. We propose that the influence of the Agulhas Current affects sediment deposition and distribution only seaward of the midshelf and that pockets of sediment remain preserved in the lee of coastal protrusions where they are protected from erosion. This study provides the essential prerequisite to allow the attribution of temporal variations of compositional changes in marine sediment cores to environmental changes in southeastern Africa.

M123*

MID- AND LOW LATITUDE EFFECTS ON EASTERN SOUTH AFRICAN RAINFALL OVER THE HOLOCENE

AUTHORS

MARUM – University of Bremen | Bremen, Germany
C. Miller, A. Hahn, M. Zabel, E. Schefuß, D. Liebrand

Climate variability and its forcings in eastern South Africa during the late Quaternary remain poorly understood with data suggesting temporal variability and spatial heterogeneity. To constrain the variability and the drivers of past climate, we explore vegetation (C3/C4) and hydrological change using stable carbon and hydrogen isotopes of plantwaxes and X-ray florescence (XRF) analysis in marine core GeoB20610-2 offshore the Limpopo River. We find evidence for two climatic phases: an initial arid phase (c. 7–3 cal. kyr BP), followed by a wetter phase (c. 3–0 cal. kyr BP). To put our findings into a regional context, we investigate a latitudinal transect of sites along eastern South Africa and divide the region into three distinct hydro-climatic zones, with significantly different climate drivers. During the last ca. 3 cal. ka BP, wet climatic conditions dominated the northern summer rainfall zone (SRZ) and the southern South African zone (SSAZ), whereas arid conditions prevailed in the central and eastern SRZ. In the northern SRZ the climate was driven by local insolation, where heightened insolation resulted in more precipitation. The aridity during the last c. 3 cal. ka BP in the central and eastern SRZ and the increased humidity in the SSAZ are attributed to an equatorward displacement of the southern hemisphere westerlies, the South African high-pressure cell and the South Indian Ocean Convergence Zone (SIOCZ). For the Holocene we find little evidence for an Indian Ocean SST control on climate. The results for the Limpopo River catchment region highlight the spatial heterogeneity of Holocene climate conditions in eastern South Africa and indicate significant latitudinal differences in climate drivers.

M124

STUDIES IN THE SOUTH ATLANTIC DURING THE "MYSCIENCE CRUISE" METEOR M124

AUTHORS

GEOMAR Helmholtz Centre for Ocean Research Kiel | Kiel, Germany
J. Karstensen

Marum, Research Faculty, Universität Bremen | Bremen, Germany
R. Morard

Ecole Normal Superior | Paris, France
S. Speich

Deutsche Gesellschaft für Internationale Zusammenarbeit GmbH | Bonn, Germany
A. Schneider

The research cruise M124 (29. Feb.–18. Mar. 2016) was proposed to a call for South Atlantic transit cruises which only short station time. Most observations during the cruise were acquired from underway systems, operated during transit of the vessel. On average every 4° (about 400 km) a mulitnet/CTD rosette station provide profiles in the upper 700 to 2000 m depth. The multinet catches were analyzed under the microscope for planktonic foraminifera abundances and characteristics. Underway sampling was targeted to estimate the hydrographic (temperature, salinity) structure of the upper layer using an underway CTD system as well as Expandable Bathythermographs (XBTs). The ADCP surveyed upper ocean currents down to about 1500 m depth. The thermosalinograph recorded continuous temperature and salinity at about 5 m depth.

The main science objectives of M124 were: Diversity, ecology and extent of the transoceanic gene flow in planktonic foraminifera between Indian, Pacific and South Atlantic Ocean; Upper ocean meridional heat/freshwater transport across the South Atlantic AX18 section; Long term variability in Antarctic Bottom Water temperature/salinity in the Vema Channel, and occurrence of persistent pollutants in South Atlantic surface waters. The cruise also introduced the "MyScience cruise" concept for Bachelor to PhD level students. The MyScience cruise concept is a mix of hands-on training in ocean observing activities (e. g. 4/8h watch cycle) but combined with work on the student's-own science project. For M124 (in combination with M133; SC: Martin Visbeck, GEOMAR, Kiel) about 60 applications for participation were received from students from France, Togo, Argentina, Uruguay, Brazil, South Africa and Germany. The proposals were evaluated considering scientific quality, feasibility, gender and country and a cohort of 9 students was selected for the M124 cruise.

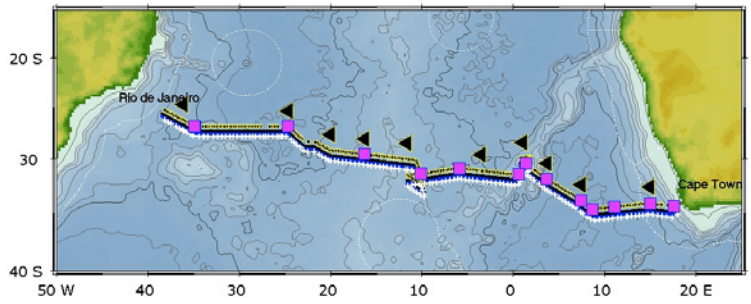

Fig. 1: RV Meteor M124 cruise track and sampling. Yellow dots : uCTD Stations (0–450m), magenta squares: CTD-rosette (0–2000m), black triangle: Multinet/CTD (0–700m), blue and black lines: ADCP recordings, white stars: XBT launches (0–700m). Symbols for the instrument groups are shifted by 1° in latitude.

Unassigned diversity of planktonic foraminifera from environmental sequencing revealed as known but neglected species by Morard et al (2019), Most research on extant planktonic foraminifera has been directed towards larger species (>0.150 mm) which can be easily manipulated, counted and yield enough calcite for geochemical analyses. This has drawn attention towards the macroperforate clade and created an impression of their numerical and ecological dominance. Drawing such conclusions from the study of such "giants" is a dangerous path. There were times in the evolutionary history of planktonic foraminifera when all species were smaller than 0.1 mm and indeed numerous small taxa, mainly from the microperforate clade, have been formally described from the modern plankton. The significance of these small, obscure and neglected species is poorly characterized and their relationship to the newly discovered hyperabundant but uncharacterized lineages of planktonic foraminifera in metabarcoding datasets is unknown. To determine who is hiding in the metabarcoding datasets, we carried out an extensive sequencing of 18S rDNA targeted at small and obscure species. The sequences of the newly characterized small and obscure taxa match many of the previously uncharacterized lineages found in metabarcoding data.

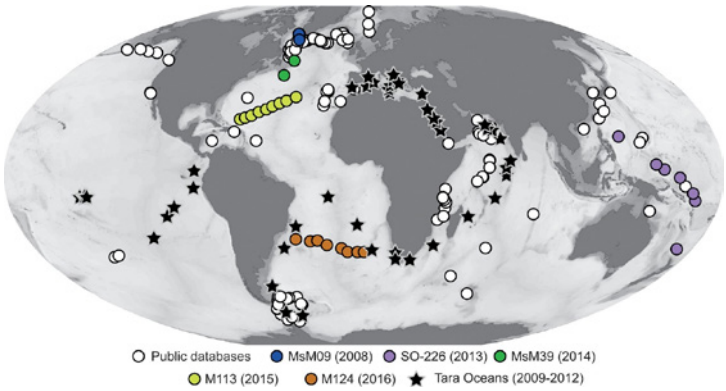

Fig. 2: Morard et al (2019) showing the location of samples analyzed in the study (M124 red dots).

This indicates that most of the modern diversity in planktonic foraminifera has been taxonomically captured, but the role of the small and neglected taxa has been severely underestimated. Vertical distribution of planktonic foraminifera in the Subtropical South Atlantic: depth hierarchy of controlling factors by Lessa et al. (in discussion), temperature appears to be the best predictor of species composition of planktonic foraminifera communities, making it possible to use their fossil assemblages to reconstruct sea surface temperature (SST) variation in the past. However, the role of other environmental factors potentially modulating the spatial and vertical distribution of planktonic foraminifera species is poorly understood. This is especially relevant for environmental factors affecting the subsurface habitat. If such factors play a role, changes in the abundance of deeper dwelling species may not solely reflect SST variation. In order to constrain the effect of subsurface parameters on species composition, we here characterize the vertical distribution of living planktonic foraminifera community across the subtropical South Atlantic Ocean, where SST variability is small but the subsurface water mass structure changes dramatically. Four planktonic foraminifera communities could be identified across the top 700 m of the E-W transect. Gyre and Agulhas Leakage faunas were predominantly composed of Globigerinoides ruber, Globigerinoides tenellus, Trilobatus sacculifer, Globoturborotalita rubescens, Globigerinella calida, Tenuitella iota and Globigerinita glutinata, and only differed in terms of relative abundances (community composition). Upwelling fauna was dominated by Neogloboquadrina pachyderma, Neogloboquadrina incompta, Globorotalia crassaformis and Globorotalia inflata. Thermocline fauna was dominated by Tenuitella fleisheri, Globorotalia truncatulinoides and Globorotalia scitula in the western side, and by G. scitula in the eastern side of the basin. The largest part of the standing stock was consistently found in the surface layer, but SST was not the main predictor of species composition, neither for the total fauna at each station nor in analyses considering each depth layer separately. Instead, we identified a consistent vertical pattern in parameters controlling species composition at different depths, in which the parameters appear to reflect different aspects of the pelagic habitat. Whereas productivity appears to dominate in the mixed layer (0–60 m), physical-chemical parameters are important at depth immediately below (60–100 m), followed by parameters related to the degradation of organic matter (100–300 m), and parameters describing the dissolved oxygen availability (>300 m). These results indicate that the seemingly straightforward relationship between assemblage composition and SST in sedimentary assemblages reflects vertically and seasonally integrated processes that are only indirectly linked to SST. This also implies that fossil assemblages of planktonic foraminifera should also contain a signature of subsurface processes, which could be used for paleoceanographic reconstructions.

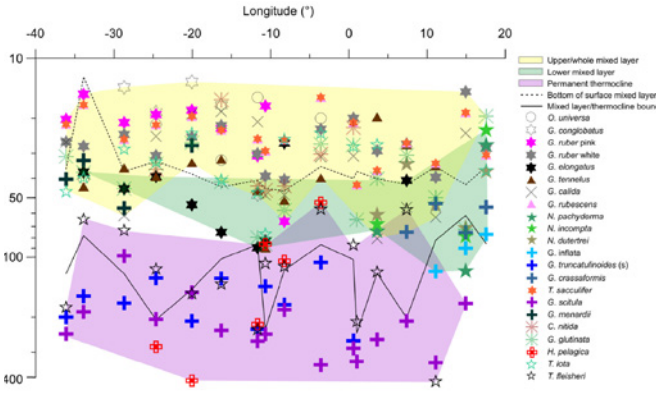

Fig. 3: Lassa et al.: Average Living Depth (ALD) of the most abundant species along the transect in the South Atlantic. Depth groups are highlighted by different color filling. Note the ALD separation above and beneath 100 m and the lower mixed layer group that is more evident on the eastern side.

REFERENCES

Morard R, Vollmar NM, Greco M, Kucera M (2019) Unassigned diversity of planktonic foraminifera from environmental sequencing revealed as known but neglected species. PLoS ONE 14(3): e0213936. https://doi.org/10.1371/ journal.pone.0213936s

Lessa, D., Morard, R., Jonkers, L., Venancio, I. M., Reuter, R., Baumeister, A., Albuquerque, A. L., and Kucera, M.: Vertical distribution of planktonic foraminifera in the Subtropical South Atlantic: depth hierarchy of controlling factors, Biogeosciences Discuss., https://doi.org/10.5194/bg-2019-355, in review, 2019.

Sobotka J. A., Schink A., Lammel G., Vrana B., Organic pollutants (PAHs, OCPs, PCBs, PBDEs, HBCDs) in South Atlantic surface seawater (in prep.)

Manta G., S. Speich, R. Laxenaire, J. Karstensen, et al., Water mass transport and properties along the SAMBA/SAMOC Line (in prep.)

M125

SOUTH AMERICAN HYDROLOGICAL BALANCE AND PALEOCEANOGRAPHY DURING THE LATE PLEISTOCENE AND HOLOCENE (SAMBA)

AUTHORS

Institute of Earth Sciences, Heidelberg University | Heidelberg, Germany
A. Bahr, A. Hou, K. Meier

Institute of Geosciences, University of Frankfurt | Frankfurt, Germany
S. Voigt

Programa de Geociências (Geoquímica), Universidade Federal Fluminense | Niterói, Brazil
C. Chiessi

School of Arts, Sciences and Humanities, University of São Paulo | São Paulo, Brazil
A. Albuquerque

And: M125 Participants

The main scientific objective of R/V METEOR cruise M125 was to investigate the influence of changes in ocean circulation and insolation on the continental climate in eastern Brazil. The hydrological cycle in this region strongly depends on the intensity of the South American Summer Monsoon (SASM). Especially in NE Brazil, precipitation is extremely seasonal with a long (8 months) drought season and a short rainy season. The long dry season make this region highly sensitive to changes in rainfall amount with potentially severe effects on terrestrial ecosystems, agriculture and energy supply (90% of Brazil's energy derives from water power). Considering that NE Brazil frequently experiences severe dry spells, the paleoclimatic insights gathered from the material retrieved during the M125 cruise will help to constrain potential impacts of future climate change.

The western tropical Atlantic (WTA) supplies warm and saline waters to the upper-limb of the Atlantic Meridional Overturning Circulation (AMOC) and may store excess heat and salinity during periods of AMOC slowdown (Schmidt et al., 2004). To study the long-term dynamics of the WTA, stable isotope and Mg/Ca analyses on the surface dwelling foraminifer Globigerinoides ruber (pink) were performed on piston core M125-55-7 covering the past ~330 kyr (Hou et al., under review). The Mg/Ca-derived sea surface temperature (SST) record indicates that the WTA was relatively stable across the past three

glacial/interglacial cycles. The observed variability appears to be mostly driven by the level of atmospheric pCO_2 concentrations, however, its influence was strongly diminished during Marine Isotope Stage (MIS) 6. A relatively stable cross-equatorial heat distribution over the past ~330 kyr suggests that glacial-interglacial variations in AMOC strength did not drive past WTA SST changes at these timescales. The zonal SST contrast within the (sub) tropical South Atlantic, on the other hand, displayed a clear glacial-interglacial mode of variability, which can be attributed to low-frequency fluctuations in the strength of the southeast trade winds. In this respect the anomalously warm MIS 6 SSTs observed in the WTA can be attributed to strong trade winds during this time interval.

X-Ray Fluorescence (XRF) core scanning were performed on the same core (M125-55-7) to investigate whether long-term changes in the oceanic heat distribution had a noticeable impact on the SAMS. We utilized the XRF-derived Ti/Ca ratio and δ18Oseawater (a proxy for salinity) to trace rainfall variability in the Doce River drainage basin. The generated data is the first continuous record of SASM variability covering multiple glacial/interglacial cycles from the eastern domain of the SASM. The data shows a clear precession beat, indicating that insolation-forcing is the unifying pacemaker of large-scale shifts in the monsoonal system in South America and world-wide (Trenberth et al., 2000; Wang et al., 2017). These results is remarkable given the despite the spatial complexity of the SASM. Glacial/Interglacial changes in the interhemispheric SST gradient appear to influence SASM intensity as well, however, to a distinctly lesser degree than insolation. A persistent negative response of SASM rainfall intensity to greenhouse gas forcing can be detected as well. Based on this observation, an increase in greenhouse gas concentration results in a weakening of the tropical atmospheric circulation cell and a decrease in SASM convection and rainfall. These findings indicate that the intensity of SASM rainfall in tropical E Brazil will likely decline in response to increasing greenhouse gas concentrations related to anthropogenic activities. Ongoing work at Heidelberg University (PhD Thesis A. Hou) concentrates on extending the SST and SASM record to 900 kyrs by means of foraminiferal and sediment geochemistry on core M125-73-3 from central E Brazil. This record will allow unprecedented insights into the long-term variability of the SASM and WTA during the mid- to Late Pleistocene.

Continental and marine paleoclimate archives from NW and NE South America recorded positive precipitation anomalies during Heinrich Stadials (HS). To decipher the impact of HS on the SASM, geochemical proxy data have been generated on piston core M125-95-3 collected off eastern South America (11°S), combined with results from an atmosphere-ocean general circulation model for South American HS conditions (Campos et al., 2019). The obtained /K data show increases during HS 1-6 as well as during the Younger Dryas, representing the southernmost record from the South American continental margin that unequivocally records HS-related positive precipitation anomalies. The new data suggests that austral summer precipitation increases only over eastern South America while the rest of tropical South America experienced precipitation increases during the winter, challenging the widely held assumption of a strengthened monsoon.

Interestingly the enhanced continental hydrological cycle during HS appears to fuel cold water coral growth on the southern E Brazilian margin, as revealed by coral-bearing sediments retrieved during M125 (Raddatz et al., accepted).

Recently generated Mg/Ca-derived SST data from core M125-35-3 (southern E Brazil), covering HS 1 in high resolution, further suggest that strong fluctuations of the Brazil Current during Heinrich Stadials (PhD Thesis K. Meier, Heidelberg University). The SST variations are notably antiphased to those from northern South America (Tobago Basin core M78/1-235-1 (Bahr et al., 2018). This finding for the first time substantiates an hypothesized anti-phasing of Brazil Current and North Brazil Current in response to alterations of the AMOC strength. This see-saw behavior is likely the driver for the concomitant high-frequency variations in SASM intensity in E Brazil (Stríkis et al., 2015).

The strong spatio-temporal variability of the SASM in the Holocene becomes obvious from the comparison of the moisture availability recorded in Core M125-67-4 (close to the Jequitinhonha River) sediments with the speleothem-based monsoonal rainfall records from E Brazil. The combination of the new and published data thus argues for a substantial variability of the rainfall distribution with a general drying trend for central E Brazil. A continuation of this trend in the future would increase the risks of "mega-droughts" in E Brazil with potentially hazardous ecological and economic consequences.

The influence of anthropogenic pollution and major element cycling has been investigated in marine sediments on the E Brazilian continental margin. In the case of the strongly polluted Doce River shelf suboxic to anoxic conditions were observed, possibly due to sediment isolation caused by the rapid mud deposition from a recent catastrophic break of the tailings dam of an iron ore mine. Major, minor and trace element distribution in cores from the vicinity of the Doce River mouth suggest at least two distinct contamination events. Ongoing 210Pb dating will enable to establish the timing of the events of heavy metal enrichments in recent history. Notably, the iron-rich sediments also appear to affect benthic faunal communities, as benthic foraminifera are showing a distinct red color attributed to the incorporation of Fe into the test.

These studies were further complemented by in-depth proxy calibrations, e. g. by using benthic foraminiferal faunal assemblages to reconstruct bottom current variability as well as stable carbon isotopes on benthic foraminifera to assess the carbon pump efficiency.

REFERENCE

Bahr, A, Hoffmann, J, Schönfeld, J, et al., Low-latitude expressions of high-latitude forcing during Heinrich Stadial 1 and the Younger Dryas in northern South America, Global and Planetary Change 2018, 160, 1–9.

Campos, M, Chiessi, C, Prange, M, et al., A new mechanism for millennial scale positive precipitation anomalies over tropical South America, Quaternary Science Reviews 2019, 225, 105990.

Hou, A, Schmidt, S, Strebl, C, et al., Forcing of western tropical South Atlantic SST across three glacial-interglacial cycles, Global and Planetary Change, under Review.

Raddatz, J, Titschack, J, Frank, N, et al., Solenosmilia variabilis-bearing cold-water mounds off Brazil, Coral Reefs (accepted).

Schmidt, M, Spero, H, Lea, D, Links between salinity variation in the Caribbean and North Atlantic thermohaline circulation, Nature 2004, 428, 160–163.

Stríkis, N, Chiessi, C, Cruz, F, et al., Timing and structure of Mega-SACZ events during Heinrich Stadial 1, Geophysical Research Letters 2015, 42, 5477–5484.

Trenberth, K, Stepaniak, D, Caron, J, The global monsoon as seen through the divergent atmospheric circulation, Journal of Climate 2000, 13, 3969–3993.

Wang, P. X., Wang, B., Cheng, et al., The global monsoon across time scales: Mechanisms and outstanding issues, Earth-Science Reviews 2017, 174, 84–121.

M127

METAL FLUXES AND RESOURCE POTENTIAL AT THE SLOW-SPREADING TAG MID-OCEAN RIDGE SEGMENT (26°N, MAR)

AUTHORS

GEOMAR – Helmholtz Centre for Ocean Research Kiel | Kiel, Germany
S. Petersen, J. Bialas, S. Graber, S. Martins

NGU Geological Survey of Norway | Trondheim, Norway
F. Szitkar

National Oceanography Centre | Southampton, UK
R. A. Gehrmann

Memorial University of Newfoundland | St. John's, Newfoundland, Canada
J. Jamieson

Introduction

Increasing demand for resources and growing challenges of discovery on land are encouraging the search for alternatives in the oceans. Many countries are actively exploring for metals in the deep oceans. Others (Papua New Guinea, Fiji, Tonga) have leased portions of their EEZs for exploration of seafloor hydrothermal ore deposits. Because the oceans cover more than 70 % of the Earth's surface, many expect them to contain vast quantities of mineral resources. Even among skeptics, the resource potential of the deep sea is considered to be huge, but only a tiny fraction of the 360 million km^2 of ocean floor has been explored (Petersen et al., 2017). There are many unsubstantiated assessments of the actual amount of resources that may be available and, compared to the late 1970s, there is far greater sensitivity to the potential environmental impacts of their exploitation, with increasing calls for internationally binding standards and research-based management to ensure protection of the oceans. In order to address the uncertainties of global metal inventory in the oceans, the EU-FP7 project "Blue Mining: Breakthrough Solutions for the Sustainable Deep Sea Mining Value Chain" looked at specific technology and research aspects regarding the nature and resource potential of marine minerals, especially seafloor massive sulfides (SMS) along mid-ocean ridges. As part of the project, the seagoing activities of the "Blue Mining" project focused on the slow-spreading Mid-Atlantic Ridge that is known to host large accumulations of submarine massive sulfides.

Results

During cruise M127 high-resolution AUV-based mapping (Fig. 1), including the co-registration of magnetic and self-potential data, has been used together with information derived from seismic reflection and refraction studies to determine the local geological controls of current and past hydrothermal fluid flow in the area (Fig. 2). They document complex tectonic patterns that drive fluid flow in this area. The presence of short detachment faults and corrugations, not visible on ship-based data, suggests an even more prominent role of these tectonic processes in focusing fluid flow at slow-spreading ridges than previously thought, as these small structures can only be seen in high-resolution (meter-scale) datasets that are usually not available (Fig. 3; Szitkar et al., 2019).

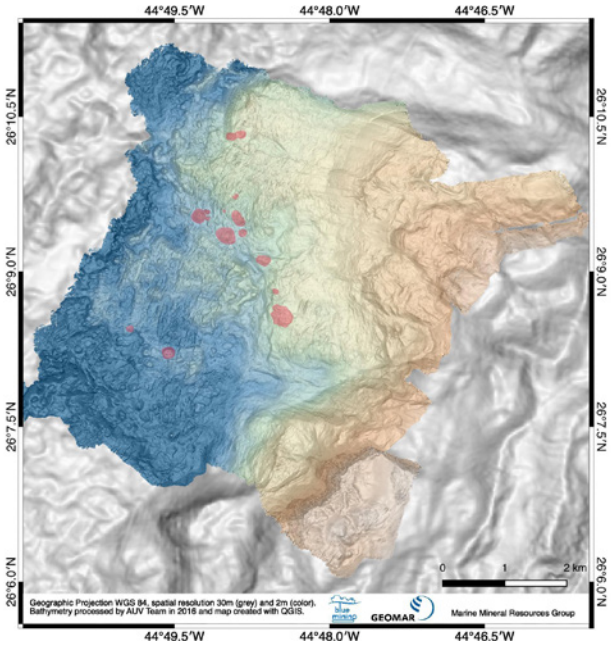

Fig. 1: High-resolution (2m) bathymetric map of the Mid-Atlantic Ridge segment hosting the TAG hydrothermal field. Active and inactive sulfide occurrences are indicated with red polygons.

The presence of a dozen inactive sulfide mounds of various sizes, topography and apparent age as well as the occurrence of thick metalliferous sediments covering large areas between the mounds contribute to a substantial metal resource being present within the TAG hydrothermal field (Murton et al., 2019). The sulfide accumulation rate is around 500 t/y, assuming episodic hydrothermal activity, and is comparable to those of other modern seafloor vent fields. The TAG district is, therefore, not characterized by a different or more powerful type of hydrothermal activity when compared to most other vent sites. Instead, our observations suggest that the overall

tectonic complexity at the TAG segment is unusual for a slow-spreading mid-ocean ridge segment. This complexity and the resulting longlivety of the system confine sulfide formation into a rather small area over long periods of time (>100.000 years) and are responsible for the substantial sulfide accumulation at this site (Graber et al., 2020).

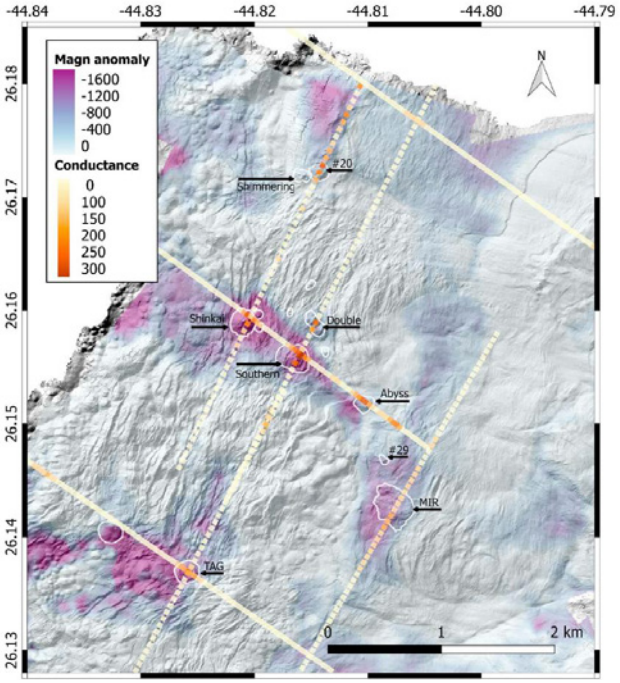

Fig. 2: Reduced-to-the-pole magnetic anomaly map overlain by bathymetry hill shading, conductance for six profiles, and highlighted seafloor massive sulfide deposits identified from the AUV-based bathymetry and verified with video footage or sampling. TAG = Trans-Atlantic Geotraverse. From Gehrmann et al. (2019).

The AUV-based high-resolution topography has been used as a complementary dataset to investigate the controls on the seafloor exposure of detachment fault surfaces and the genesis of corrugated fault surfaces at detachments in general. Our data provide evidence for a blanketing of the detachment surface under an apron of hanging wall material if the detachments are emerging from the seafloor at angles less than 13°. It is therefore likely, that many moderate-offset, hidden detachment faults may exist along slow mid-ocean ridges, that do not feature an exposed fault surface. Overall, cruise M127 has shown that high-resolution AUV-based mapping is a powerful tool for investigating important tectonic processes and the formation and evolution of hydrothermal activity over time. The combination of multiple datasets (including seismic and electromagnetic data) being acquired in a small area has provided important ground truthing information and imaging of the internal structure of inactive sulfide mounds and the complex tectonic patterns at slow-spreading ridges.

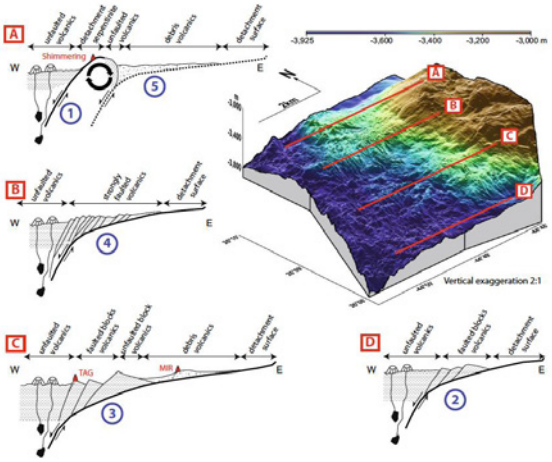

Fig. 3: Schematic cross sections; A–D and their location on a 3D bathymetric view of the study area. On the sections, thick black lines mark the detachment faults and surfaces (dashed: abandoned); thin black lines, other faults. On the left, at the ridge axis, thin black lines symbolize dykes rising from transient magma bodies to volcanoes. Red triangles represent known hydrothermal systems projected on the section. Patterns indicate volcanic edifices (horizontal dotted lines) and volcanic debris (random points). From Szitkar et al. (2019).

REFERENCES

Gehrmann RAS, North LA, Graber S, Szitkar F, et al. Marine mineral exploration with controlled-source electromagnetics at the TAG hydrothermal field, 26°N Mid-Atlantic Ridge, Geophysical Research Letters 2019, 46(11), 5808-5816, doi: 10.1029/2019GL082928.

Graber S, Petersen S, Yeo I, et al. Structural control and evolution of massive sulfide deposits in the TAG hydrothermal field, Gcubed 2020, (submitted).

Murton B, Lehrmann B, Dutrieux A, et al. Geological fate of seafloor massive sulphides at the TAG hydrothermal field (Mid-Atlantic Ridge), Ore Geology Reviews 2019, 107, 903–925.

Petersen S, Hannington M, and Krätschell A, Technology developments in the exploration and evaluation of deep-sea mineral resources, Annales des Mines – Responsab. & Environ. 2017, 85(1), 14–18.

Szitkar F, Dyment J, Petersen S, Bialas J, et al. Detachment tectonics at Mid-Atlantic Ridge 26°N, Scientific Reports 2019, 9, 11830, doi: 10.1038/s41598-019-47974-z.

ACKNOWLEDGEMENTS

This study is based on data collected during research cruise M127, which was part of the EU-funded project “Blue mining: Breakthrough Solutions for the Sustainable Deep Sea Mining Value Chain” under grant agreement No. 604500. We thank all cruise participants as well as the captains and crew for their support. GEOMAR is thanked for additional financial support.

M127*

METAL RESOURCE POTENTIAL AND FLUXES AT A SLOW-SPREADING MID-OCEAN RIDGE SEGMENT M127 – BLUE MINING @ SEA SEISMIC AND MAGNETIC INVESTIGATIONS

AUTHORS

GEOMAR Helmholtz-Zentrum für Ozeanforschung Kiel | Kiel, Germany
J. Bialas, S. Petersen, A. Dannowski

Geological Survey of Norway | Trondheim, Norway
F. Szitkar

Uppsala Universitet | Uppsala, Sweden
A. Gil

National Oceanographic Centre | Southampton, Great Britain
B. Murton

And: the M-127 scientific crew

Cruise M-127 "Blue Mining @ Sea" was proposed to support the "Blue Mining" project funded through the EU 7th Framework program. "Blue Mining" sets out to advance sea mining technology for marine minerals in a combined effort of academic and industry partners. Besides production technology, the exploration and imaging of marine deposits for minerals is a key question both in scientific investigations and economic analyses. "Blue Mining @ Sea" has its focus on Seafloor Massive Sulfides (SMS), which were found at volcanic plate margins and mid-ocean spreading ridges. They contain the worlds largest reservoirs of Cu, Pb, Zn and precious metals. Individual drill holes have been used to estimate volumes of resources and their lateral extent. Continuous lateral imaging of such deposits is missing due to the large water depth and thin thickness of depositional layers. Exploration activity currently attracts active hydrothermal vent fields only and most probably underestimates the storage potential of inactive SMS fields.

Among other technologies, high-resolution seismic applications, high-resolution AUV bathymetry and near seafloor magnetic measurements were undertaken to investigate the technological capabilities and limits imaging SMS deposits at mid ocean ridges. The well-known TAG hydrothermal vent field at the Mid-Atlantic Ridge (MAR) was chosen because previous investigations provided an overview of hydrothermal mound locations. Core sampling and drilling provided a conceptual model of the main vent structure TAG mound.

Seismic profiling was applied to provide high-resolution images and velocity depth information of the vent fields. Due to the complex seafloor morphology, 3D multichannel seismic measurements would be required to enable reduction of side reflections by migration processing of the data. However, the available work time did not allow such time-consuming measurements. A foreseen deep towed streamer was successfully tested on a previous cruise but failed on M127 due to electrical failures during deployment. A 2D surface streamer with short group offsets (1.5 m) was applied recording seismic signals from a high-frequency GI airgun and a larger volume G-gun cluster. Velocity-depth modelling was based on ocean-bottom seismometers that were densely deployed across several mound structures at variable offsets. To ensure closest and most precise seafloor positions right at the top of the structures a video-controlled deployment was completed by active positioning using ROV HYBIS for the central stations. Additional deployments were undertaken by deep sea cable with USBL guided release about 10 m above ground. The AUV ABYSS was equipped with a new self-potential device and magnetometer. Dives were undertaken at 40 to 100 m altitudes above the seafloor and provided high-resolution magnetic data acquisition.

Seismic and magnetic datasets were combined to investigate the block formation and detachment tectonics at TAG hydrothermal vent field at a new scale of resolution. Wide-angle reflection events observed by the densely deployed OBS allowed us to achieve first velocity depth models for the mounds in the TAG hydrothermal field (Murton et al., 2019). Combined analyses of near seafloor magnetic and 2D multichannel seismic revealed a new block structure (Szitkar et al., 2019).

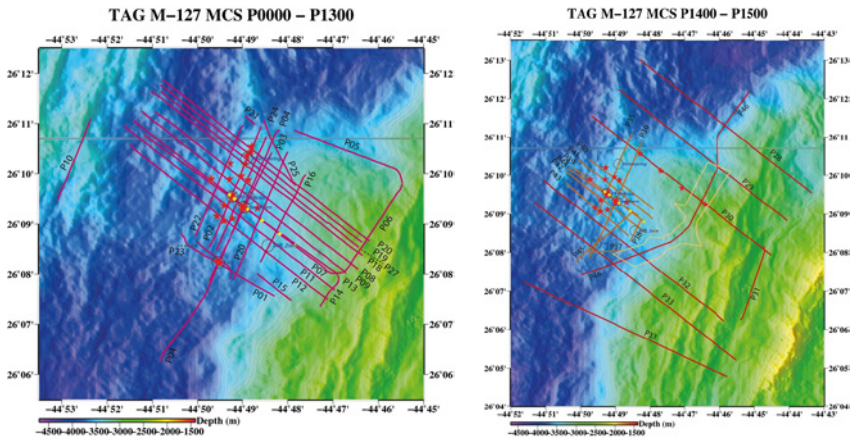

Fig. 1: Overview maps of the 2D multichannel seismic profiling (red lines). OBS deployment positions are indicated by red stars. Yellow boxes indicate MT stations to be recovered with the follow-up cruise of RRS James Cook

REFERENCES

Murton, B.J., Lehrmann, B., Dutrieux, A.M., Martins, S., la Iglesia, de, A.G., Stobbs, I.J., Barriga, F.J.A.S., Bialas, J., Dannowski, A., Vardy, M.E., North, L.J., Yeo, I.A.L.M., Lusty, P.A.J., and Petersen, S., Ore Geological Reviews 2019, Geological fate of seafloor massive sulphides at the TAG hydrothermal field (Mid-Atlantic Ridge): v. 107, p. 903–925, doi: 10.1016/j.oregeorev.2019.03.005.

Szitkar, F., Dyment, J., Petersen, S., Bialas, J., Klischies, M., Graber, S., Klaeschen, D., Yeo, I., and Murton, B.J., Scientific Reports 2019, Detachment tectonics at Mid-Atlantic Ridge 26°N, v. 9, no. 1, p. 4163–8, doi: 10.1038/s41598-019-47974-z.

ACKNOWLEDGEMENTS

This study is based on data collected during research cruise M127, which was part of the EU-funded project "Blue mining: Breakthrough Solutions for the Sustainable Deep Sea Mining Value Chain" under grant agreement No. 604500. We thank all cruise participants as well as the captains and crew for their support. GEOMAR is thanked for additional financial support.

M127*

GEOLOGICAL AND STRUCTURAL MAPPING OF THE TAG HYDROTHERMAL FIELD

AUTHORS

GEOMAR – Helmholtz Centre for Ocean Research | Kiel, Germany
S. Graber, S. Petersen, M. Rothenbeck

National Oceanography Centre | Southampton, UK
I. Yeo

Introduction

The growing demand for raw material, fostered by the technological developments and the shift to greener energies in the last decades, has led to the search for additional sources for some of the key elements. The focus of the industry but also of the scientific world turned to the seafloor. The seafloor might have the potential to become a significant contributor to a secure metal supply for some elements in the future. However, we have only investigated a fraction of the seafloor in a detail that would allow for a reliable assessment of its resources.

Seafloor massive sulfides (SMS), polymetallic ores, formed at hot hydrothermal vent sites are one type of seafloor resource considered for the future extraction. They form mainly at active plate boundaries, and at volcanoes in arc as well as back-arc environments. Large deposits tend to be more common along slow-spreading and ultra-slow-spreading ridges that make up the majority of the global mid-ocean ridge system (German et al. 2016). However, where these deposits from and what controls the location in a larger perspective is not well understood.

During research cruise M127 onboard of RV Meteor in May 2016 we studied the area of TAG hydrothermal field on the slow-spreading central Mid-Atlantic Ridge at 26°N. This field hosts one large active mound, a few low-temperature venting areas as well as several inactive mounds with varying sizes. Mapping the entire ridge segment with the ship-born multibeam system (Figure 1a), as well as the area of the hydrothermal field in high-resolution with GEOMAR's AUV Abyss 6000 (Figure 1b), gave us the opportunity to study the structural control of the hydrothermal field on a larger scale but also in more detail.

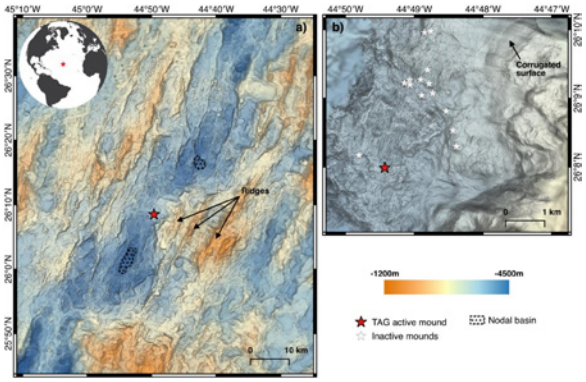

Fig. 1: Bathymetric data collected during cruise M127 in the central Atlantic. a) Ship-based bathymetric map (30m resolution) of the TAG segment. b) High-resolution AUV bathymetry (2m resolution) covering the hydrothermal field at the intersection of the volcanic valley floor and the eastern ridge flank.

Geological Setting

The TAG hydrothermal field is located at 26°08'N, in the center of a short segment (<40 km). This segment shows a strong asymmetry, where the eastern flank, formed by a massif of three ridges, protrudes towards the west. The asymmetry is mainly caused be the highly complex morphology and fault pattern on the eastern ridge side (Figure 2). The major faults, bounding the three eastern ridges, are environed by multiple, smaller faults with varying dipping directions. Previous studies have proposed that the TAG hydrothermal field is located on the hanging wall section of a large oceanic detachment system (Tivey et al. 2003), where the permeability of the hanging wall is increased by intersecting faults and fissures (Humphris and Kleinrock 1996). However, no clear evidence such as corrugations or shallow dipping faults can be seen in the ship-based bathymetry. While volcanoes are dispersed over the entire area, no continuous neovolcanic zone could be observed. Instead, the location of most recent volcanism is marked by separated small neovolcanic ridges. Four of these ridges occur along the TAG segment.

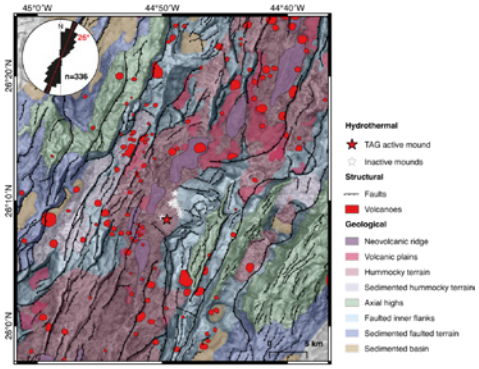

Fig. 2: Geological interpretation of the TAG segment. The overall fault orientation (rose diagram upper left corner) coincides with the general trend of the spreading axis (indicated by the dashed red line).

Structural control of the TAG hydrothermal field

The eastern section of the segment, hosting the active and the inactive SMS deposits, was mapped by the AUV in 2m resolution. The high-resolution dataset shows morphologically distinct areas and lineaments populations (Figure 3). The valley floor is characterized volcanic terrains, which are partially dissected by faults, while other areas remain intact. Axis-parallel faults and obliquely striking fissures are the most prominent lineaments. These populations occur in corridors and well-defined areas that are caused by temporal changes in the dominating stress regime and may locally be driven by shallow, propagating dikes. The active TAG mound is located on the boundary between areas affected by axis-parallel faulting and an area characterized by oblique fissuring. The inactive mounds also align along an area which is dominated by intersecting fault generations and directions. The low-temperature mounds occur on the edge of major fault scarps. However, also related to fault intersections. Therefore, the occurrences of SMS mounds related to a structural control are striking. The presence of a 600m wide corrugated surface in the north (only visible in AUV-based data) increases the structural complexity of the hydrothermal field and might confirm the former geophysical studies, implying that the highly dissected hanging wall enables focused hydrothermal fluid flow over a prolonged period at a few spots, defined by the intersection of fault and fissure populations.

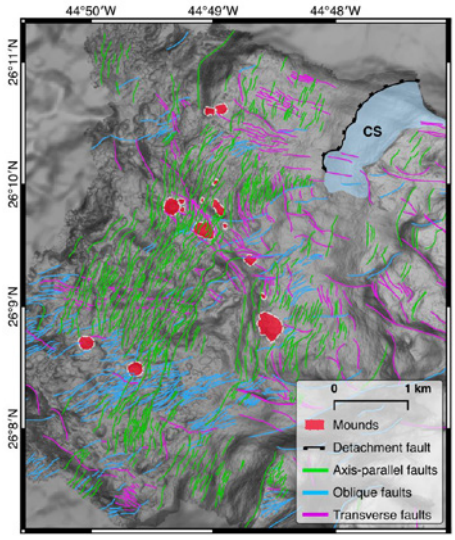

Fig. 3: Structural interpretation of the TAG hydrothermal field. The strike of lineaments can be grouped in three distinct populations. (CS = Corrugated surface).

REFERENCES

German CR, Petersen S, and Hannington MD, Hydrothermal exploration of midocean ridges: Where might the largest sulfide deposits be forming? Chemical Geology 2016, 420, 114–126.

Humphris SE and Kleinrock MC, Detailed morphology of the TAG Active Hydrothermal Mound: Insights into its formation and growth. Geophys. Res. Lett. 1996, 23, 3443–3446.

Tivey M, Schouten H, and Kleinrock MC, A near-bottom magnetic survey of the Mid-Atlantic Ridge axis at 26°N: Implications for the tectonic evolution of the TAG segment. J. Geophys. Res. Solid Earth 2003, 108 (B5), 13 p.

ACKNOWLEDGEMENTS

This study is based on data collected during research cruise M127, which was part of the EU-funded project "Blue mining: Breakthrough Solutions for the Sustainable Deep Sea Mining Value Chain" under grant agreement No. 604500. We would also like to gratefully thank the AUV team of GEOMAR for their performance and level of professionalism, without which the collection of this data would not have been possible.

M128

THE FORMATION AND EVOLUTION OF OCEANIC PLATEAUS: A CASE STUDY FROM THE AZORES FROM RV METEOR CRUISE M128

AUTHORS

GeoZentrum Nordbayern, Friedrich-Alexander-Universität Erlangen-Nürnberg | Erlangen, Germany
C. Beier, K. M. Haase, R. H.W. Romer

Department of Earth and Planetary Sciences, University of Helsinki | Helsinki, Finland
C. Beier

Westfälische Wilhelms-Universität Münster | Münster, Germany
Felix S. Genske

Submarine oceanic plateaus are formed by large volumes of magma erupting within relatively short time periods of few million years (Kerr, 2014). Their emplacement may have a large impact on regional and global ecoystems (Coffin & Eldholm, 2005). The mechanisms that control the ascent of large quantities of melt are transported through the oceanic and continental crust are poorly understood and the extent to which pre-existing and syn-tectonic fault systems control the ascent of magmas may be spatially and temporarily variable. The amount of excess melt produced underneath large igneous provinces likely results from thermal or chemical intraplate melting anomalies or a combination of these (Morgan, 1971, Bonatti, 1990, Farnetani & Samuel, 2005). The formation of oceanic plateaus is believed to reflect the arrival of a mantle plume head underneath or close to an active spreading axis and to cause shallow melting in the mantle (Cannat et al., 1999, Gente et al., 2003). The temporal and spatial changes associated with changes in the melting regime of the mantle plume will result in distinct geochemical changes directly observed in the composition of the rocks erupted. The formation of large submarine igneous provinces will also act as an ecosystem barrier in which shallow water ecosystems may develop in areas that otherwise commonly defined by deep-sea ecosystems.

The Azores are ideally suited to improve our understanding of the formation and evolution of submarine large igneous provinces and the impact of structural features on the formation and ascent of melts. The Azores Plateau is situated at the triple junction between the Eurasian, African and American Plates (Fig. 1) and is bordered by the seismically inactive East Azores Fracture Zone in the south and the slow spreading Terceira Rift axis in the North. The scientific programme of RV Meteor cruise M128 Azores Plateau during July 2016 targeted research questions related to the a) tectonic and structural evolution

of the Azores, b) structural and magmatic processes related to the emplacement of large igneous provinces, c) processes of magma evolution and crustal transport in intraplate regimes that are situated in an extensional stress field, and d) large igneous provinces acting as stepping stones for marine organisms as a result of the reduced water depth compared to the normal ocean floor. The results from the petrological, geochemical and hydroacoustic post-cruise programme have shown that the length scales over which the magmatic processes influence the composition of magmas vary. Chemical changes observed on scales of ~30 km or more reflect changes in the larger scale melting regime of the mantle, i. e. decreasing degrees of partial melting over several million years (Romer et al., 2018) produce melts that are distinctively enriched in their incompatible trace element ratios. We interpret this to be an effect of a decreasing influence of the mantle plume, whereas changes of 15-20 km may be related to the transport of melts at crustal levels in magma systems and dykes. The stress regime observed at <15 km around a submarine intraplate edifice is influenced by the local magma plumbing system underneath the volcanoes (Romer et al., 2018). Our results also show that the initial composition of magmas that form the basis of the large central volcanoes observed today are alkaline in composition indicative for relatively low degree mantle melts that are focussed along structures where lithospheric extension is strongest (Romer et al., 2018, Romer et al., 2019).

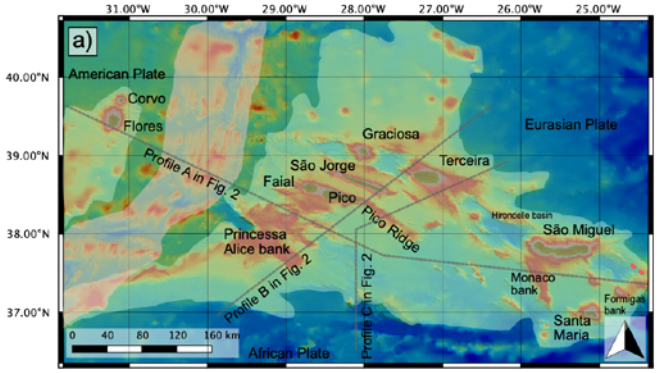

Fig. 1: Main working areas of cruise M128 Azores Plateau and main structural features of the Azores Plateau including the Terceira rift axis and East Azores Fracture Zone. Focus areas of publications by Beier et al. (2019), Romer et al. (2019) and Romer et al. (2018) are marked with red squares.

Few of our samples represent the earliest stages of the emplacement of the Azores Plateau at 10–13 Ma revealed from Ar-Ar age determinations and may be related to the arrival of a mantle plume head (Cannat et al., 1999, Gente et al., 2003, Beier et al., 2015, Beier et al., 2018, Beier et al., 2019), evidence for tholeiitic melts from such a magmatic stage remains sparse. Our new results from three stratigraphic ROV profiles along the Terceira Rift in the northern part of the Azores Plateau suggest that the opening of slow spreading rift systems occurs periodically with phases of tectonic dominance and phases of predominant magmatic activity, respectively. The three profiles cover ages from 13–12

Ma in the western part of the Terceira rift between Terceira and Graciosa, to 2.02 to 1.55 Ma east of Terceira, and ~7 Ma to 5.5 Ma southwest of São Miguel covering almost the entire age spectrum available in the Azores. Along the Easter Azores Fracture Zone in the southern part of the platform, we recovered peridotites that are compositionally and petrographically similar to altered mid-ocean ridge peridotites at the southern part of the Azores Plateau implies that the area covered by the intraplate lavas may be smaller than previously thought. In the western part of Princessa Alice Bank we did find evidence that the duration of magmatic emplacement in large igneous provinces may lead to the highest water-rock ratios observed in oceanic environments so far (Beier et al., 2019). We propose that the duration of hydrothermal activity rather than temperature during water-rock interaction processes can drastically change the composition of intraplate oceanic crust and may change the elemental fluxes from the igneous crust to the seawater during emplacement of large igneous provinces. We did not find evidence for active hydrothermal systems at water depths >300m as proposed prior to the cruise. Bacterial mats at Serreta Ridge west of Terceira, however, imply that hydrothermal activity was active during and after eruption but is relatively short-lived (<15–20 years).

We conclude that the rock samples recovered during M128 Azores Plateau cover almost the entire evolutionary history of this relatively small igneous province. The processes of magma ascent and evolution vary on distinct length scales that are influenced by the strong structural regime in the Azores. The occurrence of tholeiitic, depleted magmas remains ambiguous indicating that the majority of magmas from the Azores are enriched and alkaline.

REFERENCES

Beier, C., Haase, K. M. & Abouchami, W. (2015). Geochemical and geochronological constraints on the evolution of the Azores Plateau. In: Neal, C. R., Sager, W. W., Sano, T. & Erba, E. (eds.) Geological Society of America Special Papers. The Geological Society of America, 27–88.

Beier, C., Bach, W., Blum, M., Cerqueira, T., Ferreira, P. J., Genske, F. S., Haase, K. M., Kausche, A. H., Kemner, F., Klügel, A., Krumm, S. H., Kueppers, U., Leymann, T., Mai, A., Petry, F., Ratmeyer, V., Raeke, A., Rentsch, H., Romer, R. H. W., Sampaio, Í., Schade, T., Schleifer, B., Schröder, M. K., Skambraks, T. O., Storch, B., Vittori, V. F. & Wefer, G. (2018). Azores Plateau – Cruise No. M128 – July 02, 2016 – July 27, 2016 – Ponta Delgada (Portugal) – Ponta Delgada (Portugal). METEOR-Berichte: DFG-Senatskommission für Ozeanographie, 41. | Related to cruise M128 Azores

Beier, C., Bach, W., Busch, A. V., Genske, F. S., Hübscher, C. & Krumm, S. H. (2019). Extreme intensity of fluid-rock interaction during extensive intraplate volcanism. Geochimica et Cosmochimica Acta 257, 26–48. doi:10.1016/j.gca.2019.04.017 | Related to cruise M128 Azores

Bonatti, E. (1990). Not so hot “hot spots” in the oceanic mantle. Science 250, 107–111.

Cannat, M., Briais, A., Deplus, C., Escartín, J., Georgen, J., Lin, J., Mercouriev, S., Meyzen, C., Muller, M., Pouliquen, G., Rabain, A. & Silva, P. d. (1999). Mid-Atlantic Ridge - Azores hotspot interactions: along-axis migration of a hotspot-derived event of enhanced magmatism 10 to 4 Ma ago. Earth and Planetary Science Letters 173, 257–269.

Coffin, M. F. & Eldholm, O. (2005). Large Igneous Provinces. Scientific American, 315-323.

Farnetani, C. G. & Samuel, H. (2005). Beyond the thermal plume paradigm. Geophysical Research Letters 32, L07311. doi:doi: 10.1029/2005gl022360

Gente, P., Dyment, J., Maia, M. & Goslin, J. (2003). Interaction between the Mid-Atlantic Ridge and the Azores hotspot during the last 85 Myr: Emplacement and rifting of the hot spot-derived plateaus. Geochemistry, Geophysics, Geosystems 4, Q8514. doi:10.1029/2003GC000527

Kerr, A. C. (2014). Oceanic Plateaus. In: Carlson, R. W. (ed.) Treatise on Geochemistry 2nd Edition. Amsterdam: Elsevier, 631–667.

Morgan, W. J. (1971). Convection plumes in the lower mantle. Nature 230, 42–43.

Romer, R. H. W., Beier, C., Haase, K. M. & Hübscher, C. (2018). Correlated Changes Between Volcanic Structures and Magma Composition in the Faial Volcanic System, Azores. Frontiers in Earth Science 6, 78. doi:10.3389/feart.2018.00078 | Related to cruise M128 Azores

Romer, R. H. W., Beier, C., Haase, K., Klügel, A. & Hamelin, C. (2019). Progressive changes in magma transport at the active Serreta Ridge, Azores. Geochemistry, Geophysics, Geosystems. doi:10.1029/2019GC008562 | Related to cruise M128 Azores

M129

THE ROLE OF THE BANC D'ARGUIN AND SINE SALOUM AS SINK FOR MATTER FLUXES AND SOURCE FOR PRODUCTIVITY OF THE SOUTHERN CANARY CURRENT SYSTEM – BASS

AUTHORS

ZMT Leibniz-Zentrum für Marine Tropenökologie | Bremen, Germany
W. Ekau, J. Bachmann, E. Bahlmann, S. Bröhl, S. Flotow, T. Heimbach, A.-K. Hornidge, J. Mawick, C. Müller, P. Müller, K. Otto, C. Reymond, T. Rixen, H. Sloterdijk, F. Wischnewski

GEOMAR Helmholtz-Zentrum für Ozeanforschung Kiel | Kiel, Germany
T. Klenz, W. Martens

IdGM Instituto di Geologia Marina | Bologna, Italy
M. Taviani

USBG Universität Salzburg | Salzburg, Austria
A. Sinner, P. Wenta, S. Wickham

TI Thünen Institut für Seefischerei | Hamburg, Germany
G. Börner, M. Tiedemann

CRODT Centre de Recherche Oceanographique Dakar-Thiaroye | Dakar, Senegal
B. Balde, C. Howes

IMROP Institut Mauritanien de Recherches Océanographiques et des Pêches, Nouadhibou, Mauretania
M. Ndiaye, A. K. Sleymane

The marine ecosystem on the shelf in the upwelling off Mauritania and Senegal is of great scientific and economic interest: (1) As the highest eutrophic regional tropical ecosystem worldwide, which additionally is strongly affected by the CO_2-enriched upwelled waters, it is a textbook example of natural eutrophication and acidification; it is a scenario for the changes expected for the future seas. (2) It is one of the most productive fisheries grounds on earth that at the same time shows severe consequences of overfishing.

The expedition focused on biogeochemical processes, trophic networks and productivity, and the interaction between shallow waters, the shelf and the open ocean. From a total of

95 ship stations, the physical water profiles were assessed at 68 stations using a CTD. Different size fractions of plankton were caught with a variety of nets: 43 vertically towed multinet-midi casts, 60 oblique hauls with mulitnet-maxi, 24 neuston and 63 GULF-net hauls together with 4 dinghy operations with a towed catamaran for neuston and ring trawl tows. To understand the interactions between protists and phyto- and zooplankton, 6 long-term experiments were set up on board. For classifying sediments and macrobenthos in depths of <200 m, 8 box corer and 40 van Veen grab samples were collected. Moreover, underway CO_2 measurements were performed to estimate the pCO_2 distribution and daily collections of dust (with a dust sampler) were realised.

REFERENCES

Ekau, W, Bachmann, J, Bahlmann, E, Balde, B, Börner, G, Bröhl, S, Flotow, S, Heimbach, T, Hornidge, A-K, Howes, C, Klenz, T, Martens, W, Mawick, J, Müller, C, Müller, P, Ndiaye, M, Otto, K,

Reymond, C, Rixen, T, Sinner, A, Sleymane, A K, Sloterdijk, H, Taviani, M, Tiedemann, M, Wenta, P, Wickham, S, Wischnewski, F (2016) RV-Meteor M129 cruise report: https://doi.pangaea.de/10013/epic.47318.d006

M129*

ASSEMBLAGE STRUCTURE OF MESOPELAGIC FISHES IN THE CANARY AND BENGUELA CURRENTS

AUTHORS

Marine Ecosystems, Johann Heinrich von Thünen Institute for Sea Fisheries | Braunschweig, Germany
S. Duncan, H. Fock

Marine Zoology, University of Bremen | Bremen, Germany
S. Duncan, H. Wilhelm

GLOMAR – Bremen International Graduate School for Marine Sciences, University of Bremen | Bremen, Germany
S. Duncan

Mesopelagic fishes play a vital role in ocean ecosystems due to their high biomass, position in the food web as prey for upper trophic levels such as tuna and predators of zooplankton, as well their role in the ocean's biological pump by transporting carbon from surface waters to greater depths through diel vertical migrations. The aim of this study was to compare the community composition of mesopelagic fishes between the Canary and Benguela Currents. These areas of high primary productivity not only have sections that are associated with an oxygen minimum zones, but also have may have seen shifts in biological activity take place such as changes in the biomass and composition of mesopelagic fishes, due to high fisheries pressure during the last century on top predators and a changing climate. For this study, mesopelagic fishes were collected using a rectangular midwater trawl (8 m^2) on the R/V Meteor M129 cruise in the Canary Current and on the Meteor M153 cruise in the Benguela Current. Samples were counted, identified to species level, and combined with oceanographic data in order to compare the community composition from the differing sampling regions with the hydrographical measurements. Results showed that while the Canary Current was dominated by bristlemouths, Cyclothone sp. (Gonostomatidae), the Benguela Current is dominated by a variety of lanternfish species (Myctophidae). While Myctophids were an important part of both systems, the species composition differed greatly which may demonstrate that myctophids may have effective niche-partitioning, with each species playing an important role in its habitat. Because mesopelagic fishes may become an important fisheries resource, it is important to gain information on not only the abundane but also species composition of mesopelagic changes, in order to see how these may change in the face of fishing pressure as well as expanding oxygen minimum zones. This study sheds light on the assemblage structure of these fishes in some of the world's most highly productive regions.

M119 & M130

OXYGEN AND CIRCULATION VARIABILITY IN THE CENTRAL AND WESTERN TROPICAL ATLANTIC – SCIENTIFIC RESULTS FROM METEOR CRUISES M119 AND M130

AUTHORS

GEOMAR Helmholtz Centre for Ocean Research Kiel | Kiel, Germany
P. Brandt, M. Dengler

And: the shipboard parties of M119 and M130

The research cruises were part of the collaborative research center (SFB) 754 „Climate – biogeochemistry interactions in the tropical ocean" funded by the Deutsche Forschungsgemeinschaft and the BMBF cooperative project "Regional Atlantic circulation and global change" (RACE). A regional focus of the SFB 754 related physical-biogeochemical investigations was the oxygen minimum zone (OMZ) in the eastern tropical north Atlantic. Here, the measurement program aimed at advancing quantification of the oxygen budget in the oxygen minimum zone. Further objectives were investigating the role of zooplankton and its vertical migration for fluxes of particulate and dissolved matter to the OMZ as well as advancing quantitative understanding of nitrogen fixation in the near-surface layers of the tropical Atlantic.

A second regional focus of the measurement program was in the western tropical South Atlantic. Here, the cruise focused on providing shipboard and moored velocity and hydrographic observations to investigate long-term variability of the western boundary current transports and T-S characteristics. In combination with data from previous cruises, the research objectives were to relate the variability of the North Brazil Undercurrent (NBUC) and Equatorial Undercurrent (EUC) transport to Atlantic Meridional Overturning Circulation (AMOC) changes, to variability of the Atlantic's subtropical cell (STC) as well as to tropical Atlantic climate modes.

We achieved major scientific progress in most of the cruise objectives. Hydrographic and oxygen data from the cruises was used in combination with data from previous cruises, to analyze the decadal variability of the ETNA OMZ and associated changes in the oxygen budget. Along 23°W section between 6°N and 14°N from 2006 to 2015, oxygen decreased with a rate of -5.9±3.5 µmol kg^{-1} $decade^{-1}$ within the depth range of the deep oxycline (200–400 m), while below the OMZ core (400–1000 m) oxygen increased by 4.0±1.6 µmol kg^{-1} $decade^{-1}$ on average. Within the improved oxygen budget, the zonal advective oxygen supply stands out as the most probable budget term responsible for the decadal oxygen changes (Hahn et al. 2017).

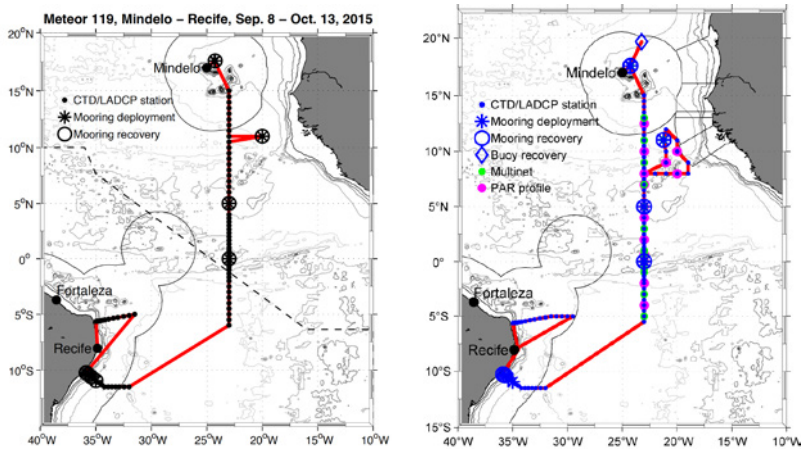

Fig. 1: Bathymetric maps with cruise tracks (red lines) of R/V METEOR cruises M119 (left) and M130 (right) including locations of CTD/LADCP stations, mooring recoveries and redeployments, multinet and photosynthetically active radiation (PAR) profile stations. Territorial waters of different countries are marked with thin black solid lines.

The data also advanced understanding of the role of the interannual variability of the North Equatorial Undercurrent (NEUC) in ventilating the OMZ of the eastern tropical Atlantic. Burmeister et al. (2019) found that the NEUC transport variability is dominated by sporadic intraseasonal events. Some of these events are associated with high oxygen levels suggesting an enhanced but rare eastward oxygen supply by intraseasonal variability that are responsible for local oxygen maxima.

The cruise also contributed to the census of low-oxygen eddies in the ETNA. Locally increased oxygen consumption within eddy cores enhances the total oxygen consumption in the open ETNA and likely contributes to the formation of the shallow OMZ at about 100 m depth (Schütte et al. 2016).

Top-to-bottom velocity measurements at CTD stations with lowered ADCPs or by using moored observation were carried out in the equatorial region and at the continental slope off the Brazilian coast. The long-term mooring at the equator, 23°W was successfully recovered and redeployed during both cruises now providing an unprecedented dataset of the equatorial circulation since December 2001. Using mooring data and idealized numerical simulations, it could be shown that the equatorial deep jets (EDJs), which are suggested to impact surface conditions and climate by upward energy propagation, are maintained against dissipation in the deep equatorial ocean by the meridional flux of intraseasonal zonal momentum, i. e. energy for the EDJs is provided by downward energy propagation of intraseasonal waves (Greatbatch et al. 2018). Tuchen et al. (2018) analyzed the deep intraseasonal meridional velocity fluctuations at the equator. Elevated intraseasonal kinetic energy with periods between 30–40 days was observed down to 2000m depth. The fluctuations are best described as Yanai waves, which in turn supply their energy to the equatorial deep jets (Greatbatch et al., 2018).

Recent evidence from the analysis of the mooring data from the equator, 23°W revealed that semi-annual and longer time scale equatorial current variability is close to being resonant with equatorial basin modes. This work was expanded by Kopte et al. (2018) who showed that the equatorial basin modes also affect the eastern boundary circulation off Angola as far as 12°S.

The complete recovery and redeployment of the 11°S mooring array off Brazil during the second part of the cruise ensured the continuation of the transport time series of the Deep Western Boundary Current and the North Brazil Undercurrent as an important contribution to the Atlantic Meridional Overturning observing system. The western boundary current measurements are an integral part of the Tropical Atlantic Observing System (Foltz et al. 2019) and of global observations of boundary current systems (Todd et al. 2019).

A recent analysis of the STC from observations revealed find that the thermocline layer convergence is dominated by the southern hemisphere water mass transport (9.0±1.1 Sv from the southern hemisphere compared to 2.9±1.3 Sv from the northern hemisphere) and that this transport is mostly confined to the western boundary (Tuchen et al., 2019). Compared to the asymmetric convergence at thermocline level, the wind-driven Ekman divergence in the surface layer is more symmetric, being 20.4±3.1 Sv between 10°N and 10°S.

Another focus of the cruises was the role of zooplankton and particles for oxygen consumption and biogeochemical cycles. High primary productivity in the equatorial Atlantic was found to fuel a substantial flux of particulate matter towards the abyssal ocean. The increase in particle abundance and flux at depths of 300 to 600m at the Atlantic equator could be attributed to faecal pellet production by zooplankton and nekton migrating vertically within a daily cycle. The snowfall of particles is focused in the equatorial ocean likely due to the presence of off-equatorial large-vertical-scale eastward jets at 2°N/S producing potential vorticity barriers that strongly reduce lateral mixing between the equatorial and off-equatorial ocean at depth (Kiko et al. 2015).

Additional studies that were not part of the original cruise proposal focused on epi- and mesopelagic communities of macrozooplankton and micronekton (a project of the Cluster of Excellence "Future Ocean") or on the quantification of N2 fixation. During M119, the gelatinous, flux-feeding polychaete of the genus Poeobius (Christiansen et al. 2018) and the orangeback flying squid Sthenoteuthis pteropus (Merten et al. 2017) were studied. Observed elevated abundances of Poeobius sp. in anticyclonic mode water eddies showed that a single zooplankton species can completely intercept the downward particle flux by feeding with their mucous nets, thereby substantially altering the biogeochemical setting within the eddy.

REFERENCES

Burmeister K, Lübbecke J F, Brandt P, Duteil O, Interannual variability of the Atlantic North Equatorial Undercurrent and its impact on oxygen, J. Geophys. Res., 2019, 124, pp. 2348–2373. DOI 10.1029/2018JC014760.

Christiansen, S., H.-J. Hoving, F. Schütte, H. Hauss, J. Karstensen, A. Körtzinger, S.-M. Schröder, L. Stemmann, B. Christiansen, M. Picheral, P. Brandt, B. Robison, R. Koch, R. Kiko, Particulate matter flux interception in oceanic mesoscale eddies by the polychaete Poeobius sp., Limnology and Oceanography, 63, 2093–2109, doi:10.1002/lno.10926, 2018.

Foltz G R, Brandt P, Richter I, et al., The tropical Atlantic observing system, Front. Mar. Sci., 6, 206, DOI 10.3389/fmars.2019.00206, 2019.

Greatbatch R J, Claus M, Brandt P, Matthießen J D, Tuchen F P, Ascani F, Dengler M, Toole J, Roth C, Farrar J T, Evidence for the maintenance of slowly varying equatorial currents by intraseasonal variability. Geophys. Res. Lett., 2018, 45, 1923–1929. DOI 10.1002/2017GL076662.

Kopte R, Brandt P, Claus M, Greatbatch R J, Dengler M, Role of Equatorial Basin-Mode Resonance for the Seasonal Variability of the Angola Current at 11°S. J. Phys. Oceanogr., 2018, 48, 261–281. DOI 10.1175/JPO-D-17-0111.1.

Merten V., B. Christiansen, J. Javidpour, U. Piatkowski, O. Puebla, R. Gasca, H.-J. T. Hoving, Diet and stable isotope analyses reveal the feeding ecology of the orangeback squid Sthenoteuthis pteropus (Steenstrup 1855) (Mollusca, Ommastrephidae) in the eastern tropical Atlantic, PLoS ONE 12(12): e0189691, doi:10.1371/journal.pone.0189691, 2017.

Schütte, F., J. Karstensen, G. Krahmann, H. Hauss, B. Fiedler, P. Brandt, M. Visbeck, and A. Körtzinger, Characterization of "dead-zone" eddies in the eastern tropical North Atlantic, Biogeosciences, 13, 5865–5881, doi:10.5194/bg-13-5865-2016, 2016.

Todd R E, Chavez F P, Clayton S, et al, Global Perspectives on Observing Ocean Boundary Current Systems, Front. Mar. Sci., 2019, 6, 423, DOI 10.3389/fmars.2019.00423.

Tuchen F, Brandt P, Claus M, Hummels R, Deep Intraseasonal Variability in the Central Equatorial Atlantic. J. Phys. Oceanogr., 2018, 48, 2851-2865. DOI 10.1175/JPO-D-18-0059.1.

Tuchen F, Lübbecke J F, Schmidtko S, Hummels R, Böning C W, The Atlantic Subtropical Cells inferred from observations. J. Geophys. Res., 2019, 124, 7591–7605, DOI 10.1029/2019JC015396.

M132

MESO-TO SUBMESOSCALE DYNAMICS AT THE BENGUELA EASTERN BOUNDARY UPWELLING SYSTEM

AUTHORS

University of Hamburg, Institute of Oceanography | Hamburg, Germany
K. Jochumsen, J. Dräger-Dietel, R. North

Leibniz-Institut für Ostseeforschung Warnemünde (IOW) | Warnemünde, Germany
L. Umlauf

The cruise with R/V METEOR took place from Nov 15 to Dec 11, 2016, departing from Walvis Bay (Namibia), heading westward on the Namibian shelf and performing a zig-zagging track until the vessels' departure toward Cape Town (South Africa). An upwelling filament was identified in a satellite SST image (Fig. 1a) and subsequently sampled. Data was obtained using several underway systems (e. g. Scanfish, ADCP, underway-CTD), autonomous platforms (gliders, drifters) and station-based measurements (CTD, MSS). A catamaran equipped with an ADCP and a thermistor chain was deployed and towed in the wake of the ship to study the uppermost layer of the ocean without the ship induced turbulence. The multi-platform approach allowed us to identify the filament formation as a process where two main eddies with opposing rotation orientation, one originating from the Agulhas region, draw cold-water offshore and allows to characterize energy transfer from meso- to turbulent dissipation scales. The underway systems capture the horizontal and vertical variability across the filaments and the upwelling front.

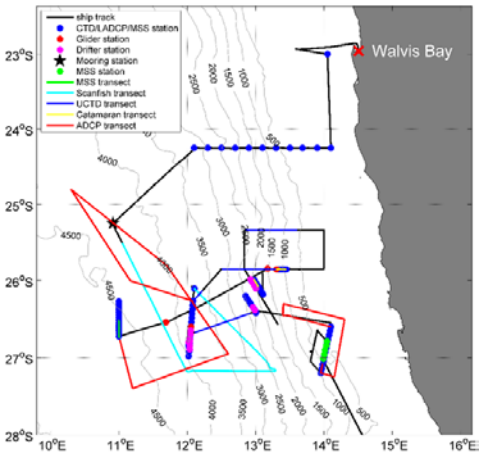

Fig. 1: Cruise track of M132, with stations and instruments used.

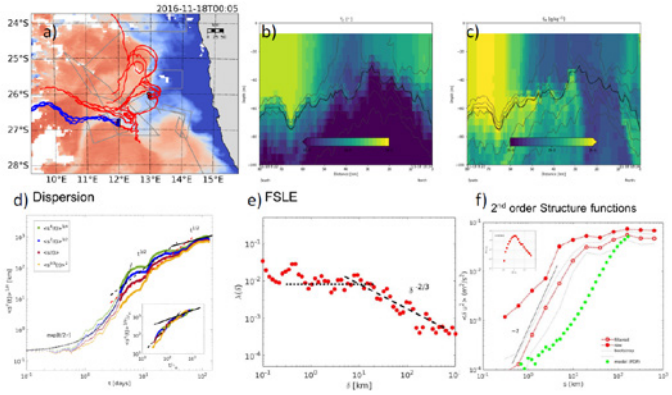

Fig. 2: a) Satellite SST image showing the filament, transects and drifter deployments in two main groups: Northern (red) and southern (blue). b),c) depth dependence of temperature and salinity across the filament, d) Lagrangian moments sn(t) of relative dispersion for northern deployment and rescaled plot (inlay), e) FSLE as a function of separation distance δ for the northern deployment, f) Northern deployment: second order longitudinal structure function versus separation distance from raw (full red circles) and filtered (open circles) drifter-trajectories and from numerical simulations (POP-model) (full green circles) and skewed PDF of velocity differences (inlay).

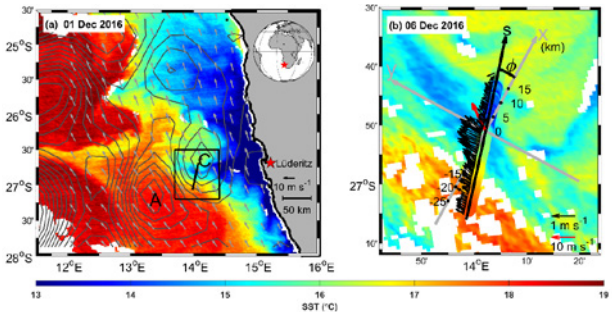

Fig. 3: (a) Overview map of the Benguela upwelling system with satellite sea surface temperature (SST, in color), sea surface height anomaly (SSHA, black contour lines at 0.01 m intervals), and wind field (arrows), all from 01 December 2016. The study area for the investigations is marked by a black rectangle, and the main ship transect by a black line. The white arrows shows a second filament that is subject to ongoing research. (b) Expanded view of study area with satellite SST from 06 December 2016. Also shown are ship-based SST measurements (colored markers) and near-surface velocities (arrows) along the ship track. The red arrow indicates the wind speed, averaged over the transect.

REFERENCES

Dräger-Dietel, J., D. Balwada, and A. Griesel, in prep: Two-point velocity statistics from ocean surface drifter observations in the Benguela upwelling system.

Dräger-Dietel, J., K. Jochumsen, A. Griesel, and G. Badin, 2018: Relative dispersion of surface drifters in the Benguela upwelling region. J. Phys. Oceanogr., 48:2325–2341.

Peng, J.-P., P. L. Holtermann, and L. Umlauf, submitted: Frontal instability and energy dissipation in a submesoscale upwelling filament. J. Phys. Oceanogr., in press.

M133
SURVEYING THE SOUTH ATLANTIC GYRE AT 34.5°S

AUTHORS

GEOMAR Helmholtz Centre for Ocean Research Kiel | Kiel, Germany
M. Visbeck, P. Handmann

MARUM, Center for Marine Environmental Sciences | Bremen, Germany.
M. Siccha

The cruise M133 SACROSS (South Atlantic Crossing) left the port of Cape Town (South Africa) on 15th December, 2016 and reached the port of Stanley (Falklands) on 13th January, 2017. M133 was a multidisciplinary ocean survey of the South Atlantic gyre roughly along 34.5°S. This transect is covered by the international SAMOC moored array and also the path of the internationally agreed AX18 XBT line. Most of the measurements were based on using underway methods including near-surface water sampling for the determination of SST, and SSS as well as shipboard ADCP current observations. Moreover, an underway CTD allowed to sample the upper 300-400 m every hour. Chemical analysis of surface waters as well as atmospheric parameters was of scientific interest to both, compare different regions with each other but also to document long term trends. At the western and eastern boundary current regime full water column water mass properties were measured. Upper ocean 10–700m plankton assemblages allow improving the calibration of sediment proxies. Water samples for later lab-based biodiversity analysis were taken. The M133 cruise offered the opportunity to sample (with a light carry-on meteorological instrument) an Atlantic Southern Ocean cross-section for atmospheric aerosol and water vapor.

The collection of single cell-foraminifera together with environmental samples during the cruise M133 contributed to an effort of global synthesis of the cryptic diversity of planktic foraminifera. Specifically, the collection of single-cell foraminifera are used to produce a collection of barcodes, which is part of a global synthesis effort that will enable the establishment of a reference database crucial for the interpretation of metabarcoding datasets. This global effort will be a stepping-stone to constrain the diversity and ecology of planktonic foraminifera to improve significantly the quality of paleoceanographic reconstruction to achieve better projection of climate change.

The cruise had a strong educational and capacity building component. A number of smaller student projects were carried out as part of a global ocean learning and capacity building effort. As Ocean Observations are one of the cornerstones for understanding, assessing and predicting ocean change the MyScience-Cruise provided the unique

opportunity of a practical hands on-training on ocean observation and ocean research in the South Atlantic for 7 students from 6 different nations. Students from Bachelor to PhD level attended. During the cruise an "expert training" on a variety of observing instrumentation as well as lectures covering a range of topics in oceanography as well as instrumental applications were provided. All scientists as well as all students gave talks about their background, science interests and current projects. The three CTD/uCTD/XBT/rapid cast/MICROTOPS shifts were covered with one expert and three MyScience cruise students each. At the beginning of the cruise the "experts" primarily trained the students but soon the experts took over to the observer's position and the students were fully operating the shifts.

During the cruise daily reports by the students about life at sea and their experiences have been published on the MyScience Cruise blog (http://www.oceanblogs.org/mysciencecruise/) which is embedded in a network called "Oceanblogs" (operated by GEOMAR and the Kiel network Future Ocean with Kiel University) and which was shared on a variety of social media. On Christmas a radio feature on the German radio program NDR 90,3 was reporting on the cruise.

Finally, continuous swath bathymetry mapping was made, and a number of floats and drifters were launched in support of the global ocean observing system arrays. The cruise was very successful, all objectives were reached, and the measurements were carried out as planned.

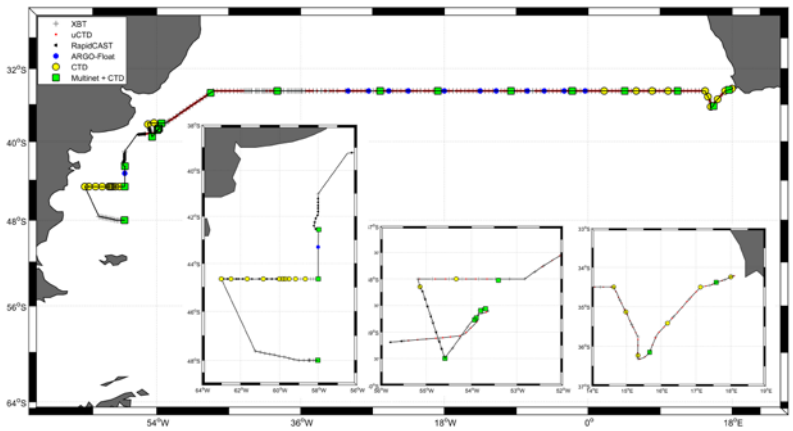

Fig. 1: Cruise track of METEOR cruise M133 with locations of CTD stations (yellow circles), MultiNet-CTD (Green Box), UCTD (red dots), XBT (gray cross), RapidCast (black triangle) and Argo Float Deployments (Blue dots).

M133*

CHARACTERIZATION OF A NOVEL AUTONOMOUS ANALYZER FOR SEAWATER TOTAL ALKALINITY: RESULTS FROM THE M 133 AND MSM 68/2 CRUISE

AUTHORS

GEOMAR Helmholtz Centre for Ocean Research Kiel | Kiel, Germany
K.Seelmann, A. Körtzinger

Kongsberg Maritime Contros GmbH | Kiel, Germany
S. Aßmann

Christian-Albrechts-Universität zu Kiel | Kiel, Germany
K. Seelmann, A. Körtzinger

Introduction

Total alkalinity (A_T) is one of four key parameters, together with dissolved inorganic carbon (C_T), pH and partial CO_2 pressure (pCO_2), characterizing the carbonate system of the ocean. In times of global warming, deoxygenation and especially acidification, an intensive monitoring of the marine carbon system is of very high importance. Due to thermodynamic relationships between the four named variables, a full characterization of the oceanic carbon cycle is possible by measuring only two of these four (Millero 2007). One common measuring parameter within the oceanographic community is AT. Nowadays, the traditional measurement way is discrete sampling and subsequent analysis with manually operated analyzer in the home lab. This procedure is time-consuming, cost-intensive and only provides spatial and temporal low resolution data. To overcome these problems, Kongsberg Maritime Contros GmbH (Kiel, Germany) developed an autonomous wet-chemical analyzer for seawater total alkalinity, called CONTROS HydroFIA® TA. In order to evaluate the measuring performance of this analyzer under long-term semi-continuous measurement conditions (real field conditions), we participated in the M 133 research cruise on the RV Meteor from Cape Town, South Africa to Port Stanley, Falkland Islands (15.12.2016–13.01.2017), and the MSM 68/2 research cruise on the RV Maria S. Merian from Emden, Germany to Mindelo, Cape Verde (03.11.–14.11.2017).

Installation onboard

We used one analyzer during the M 133 cruise and two systems in parallel during the MSM 68/2 cruise. The set-ups for both cruises are shown in Fig. 1. To get information about the behavior of the system under semi-continuous measurement conditions the A_T of steady pumped sea-surface water (underway, depth □ 5 m) was measured every 10 minutes. For this purpose, the analyzer was connected to the seawater pump of the respective ship.

Fig. 1: The installation of the CONTROS HydroFIA® TA analyzers during (a) the M 133, and (b) the MSM 68/2 cruise, respectively.

Methods

In order to monitor the precision and accuracy of the system over the whole semi-continuous period Certified Reference Material (CRM) was measured daily in the morning and evening (each five repetitive measurements). Additionally, discrete samples were taken during the entire cruise with a sampling of four to five times per day in order to determine the accuracy of the system. They were measured with a reference measuring system in the lab of the GEOMAR Helmholtz Centre for Ocean Research Kiel following the requirements of Dickson et al. (2007).

Results

To give an overview of the measured underway AT in the monitored regions, Fig. 2a shows the time series over the course of each cruise. The red filled circles in Fig. 2a represent the discrete samples taken during each cruise. Figure 2b illustrates the track of the M 133 and MSM 68/2 cruise, respectively. The scientific interpretation of these underway data is not part of this study as the focus here lies on the assessment of instrument performance under typical field deployment conditions.

Due to a malfunction (leaking degasser) of the M 133 analyzer and one of the MSM 68/2 analyzers, only the performance results of the second functional MSM 68/2 system are shown, because these observations are representative for the analyzers behavior. Anyway, the observed behavior of both leaking analyzers is important for future malfunction detections.

For evaluating the precision of the analyzer, the standard deviation (σ) of the five repetitive CRM measurements (twice a day) was calculated and the results are shown in Fig. 3. The σ distributed from around 0.2 up to 2.8 µmol kg^{-1}, and an averaged σ of 1.2 µmol kg^{-1} was calculated. For evaluating the accuracy of the system, the bias (ΔA_T) between the AT value measured by the analyzer and the reference value of the CRM, and the discrete sample, respectively, was calculated. By plotting this bias against the measurement counter of the system (see Fig. 4a), a linear drift to higher values was observable. Due to the system ran without any malfunctions, this behavior must be typical and, as we hypothesize, is caused

by deposits in the optical pathway, which cannot be prevented. However, due to the linear drifting character, this can be corrected for by regular reference measurements giving consistent measurement results. Fig. 4b shows the results of this correction. Finally, the analyzer featured an accuracy of – 0.3 ± 2.8 µmol kg^{-1}.

Compared to the performance of traditional A_T measuring methods, for which a precision of 1 µmol kg^{-1} and an accuracy of ± 2 µmol kg^{-1} are required (Dickson et al. 2007), the CONTROS HydroFIA® TA provides AT data with similar high quality.

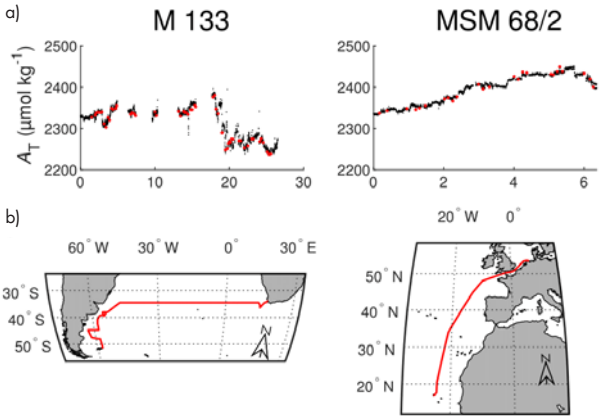

Fig. 2: (a) Time-series of the measured AT values during the M 133 and MSM 68/2 cruise, respectively. Each filled red circle represents the AT value of a discrete sample taken at a certain time during the cruise. (b) Track of the M 133, and MSM 68/2 cruise.

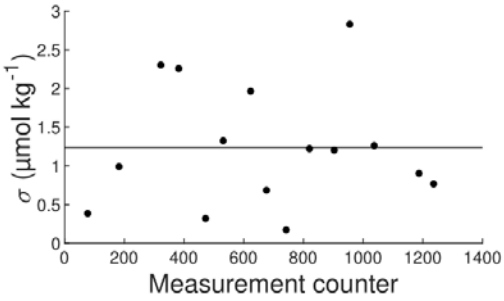

Fig. 3: Standard deviation σ of repeated CRM measurements as a function of the measurement counter of the analyzer during the cruise MSM 68/2. The horizontal black line indicates the averaged σ (here: 1.2 µmol kg^{-1}).

Conclusion

All in all, it can be said, that the field characterization of the novel autonomous analyzer CONTROS HydroFIA® TA during the M 133 and MSM 68/2 cruises was successful. Although two of the three tested systems featured a malfunction, the gained knowledge can be used for future malfunction detection procedures and troubleshooting during

long-term deployments. Furthermore, the results observed with the functional analyzer confirm the comparability of the measurement quality to traditional methodologies. In summary, the novel autonomous AT analyzer CONTROS HydroFIA® TA is suitable for autonomous underway measurements of the marine carbonate system and for ocean acidification observations, and, at the same time, overcomes the disadvantages of the traditional methods.

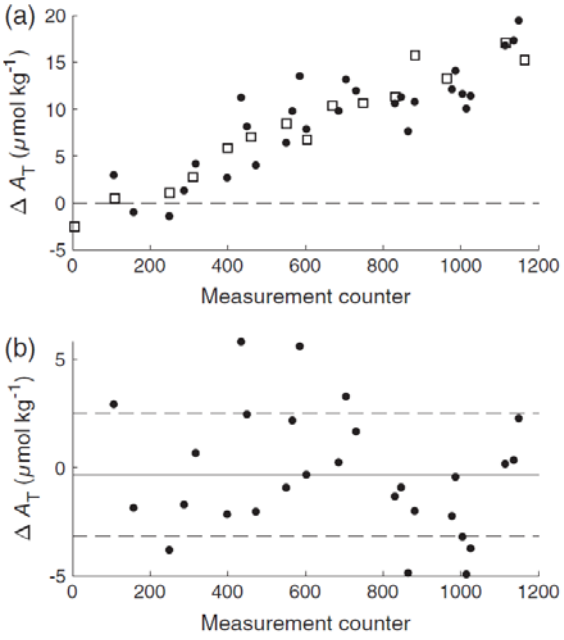

Figure 4: (a) Bias plot for the intercomparison of A_T measurements between the analyzer and the reference samples during the cruise MSM 68/2, where open squares represent the CRM and filled circles represent the discrete samples measured in the laboratory. The horizontal dashed line indicates ΔA_T = 0 µmol kg^{-1}. (b) Bias plot (discrete samples) after a linear drift correction using the CRM measurements. The horizontal black line indicates the mean bias, $\Delta A_{T,m}$, while the dashed lines indicate $\Delta_{AT,m} \pm \sigma$ (here: − 0.3 ± 2.8 µmol kg^{-1}).

REFERENCES

Dickson A G, Sabine C L, Christian J R, Guide to best practices for ocean CO_2 measurements, PICES Special Publications 3 2007, 191 pp.

Millero F J, The Marine Inorganic Carbon Cycle, Chemical Reviews 2007, 107(2), 308–341, doi: 10.1021/cr0503557.

M134

METHANE EMISSIONS AROUND SOUTH GEORGIA – R/V METEOR CRUISE M134

AUTHORS

MARUM – Center for Marine Environmental Sciences and Department of Geosciences, University of Bremen | Bremen, Germany
M. Römer , G. Bohrmann, T. Pape, S. Mau, P. Wintersteller

AWI, Alfred-Wegener-Institut Helmholtz-Zentrum für Polar-und Meeresforschung | Bremerhaven, Germany
S. Kasten

CEOAS, Oregon State University | Corvallis (OR), USA
M. Torres

GEOMAR Helmholtz Centre for Ocean Research Kiel | Kiel, Germany
W. Weinrebe

British Antarctic Survey | Cambridge, UK
K. Linse, O. Hogg

Emissions of free gas from sediments in glacial troughs into the water column were first discovered at the northern shelf of South Georgia during R/V POLARSTERN Cruise ANT29-4 in 2013. Preliminary but not systematically conducted surveys for flare mapping have shown that the emissions are exclusively related to the cross-shelf trough systems and probably sourced from the post-glacial sediments by biogenically produced methane (Römer et al., 2014; Geprägs et al. 2016).

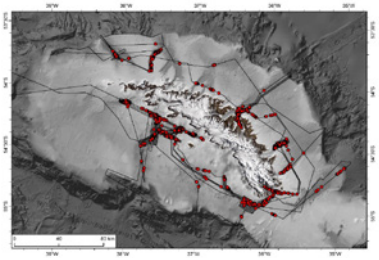

Fig. 1: Map of South Georgia and the surrounding shelf investigated during M134. The track is shown as black line and red dots indicate locations of gas emission sources detected during the cruise.

During M134 with R/V METEOR eight cross-shelf troughs were mapped for detecting the distribution of gas emission sites. 2,647 nautical miles were mapped around South Georgia by using Parasound and multi-beam systems EM710 and EM122. More than 1,600 gas emissions sites were detected by acoustic anomalies in the water column data (Fig. 1). The emission sites and the zones of blanking within sediment echo-sounder records correlate well and are predominantly concentrated to the inner fjords and cross-shelf troughs, where higher rates of organic material seems to become deposited and leads to the formation of methane under anoxic sediment conditions.

Continuous atmospheric methane measurements were carried out to investigate the influence of seafloor seeps to the atmospheric methane concentration. The highest methane concentrations were detected at and around acoustically detected flares, for example in the King Haakon Trough, Church Trough and the Cumberland Bay. This result points to an influence of gas seepage at the seafloor to the atmospheric methane concentration (Lange et al., 2018).

Because of the cold bottom waters, methane hydrates are theoretically stable in areas deeper than 370 m water depth and have been sampled during M134 in sediment cores of Church Trough and Annenkov Trough (Fig. 2). These findings represent the first gas hydrates recovered south of the Polar Front. Using samples taken by the dynamic autoclave piston corer in combination of pore water analysis revealing negative chloride concentrations, gas hydrate saturations were quantified to reach 2-8 % of the pore space (Bohrmann et al. 2017).

Fig. 2: Photograph of sediments recovered at Church Trough containing methane hydrate.

Fig. 3: Ikaite crystals found in sediment samples around South Georgia.

In total, 21 gravity cores and 14 multicorer were acquired along the shelf, within the troughs and fjords off South Georgia. They have been taken to sample gas-rich sediments for gas analysis, testing the potential presence of gas hydrates, and studying the biogeochemistry of pore fluids not only related to methane-influenced diagenesis. Besides authigenic carbonate precipitates sampled close to seep sites, ikaite crystals of different

shape and size (Fig. 3) have been found at various locations and probably seem to be widely distributed in these deposits around South Georgia. Diagenesis of iron was obvious in sediment cores by strong colour changes. Sediments taken within the fjords were characterized by high amounts of interstitial Fe^{2+}, whereas those investigated outside the fjords were dominated by hydrogen sulfide. Pore-water data sampled at seep sites in the fjords demonstrate that iron reduction occurs within the methanogenic zone below the sulfate methane transition zone (SMT). These findings suggest that deep iron and manganese reduction represent important diagenetic processes in the deeper subsurface sediments of South Georgia fjords, possibly linking the biogeochemical cycles of methane, iron, manganese and sulfur. Water samples from 31 CTD/hydrocast stations, 12 bottom water sampler and 8 GoFlo stations have been taken to reconstruct the methane distribution and its fate in the water column. Water samples have also been taken in order to investigate iron transport to the ocean where iron as micronutrient is fertilizing high phytoplankton productivity.

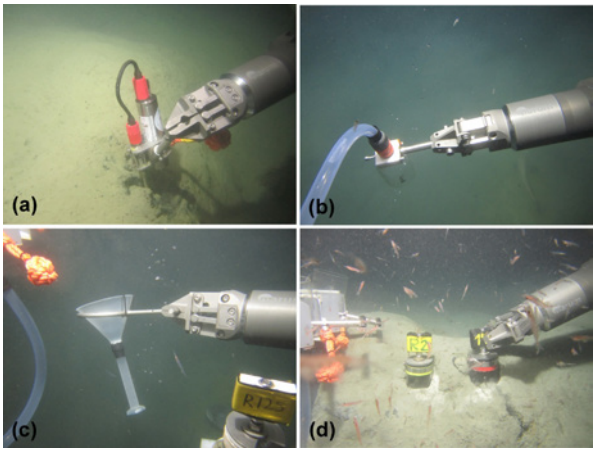

Fig. 4: Photographs taken with ROV MARUM-SQUID illustrating the main tools used during M134: a) Temperature measurements, b) Sampling of free gas bubbles, c) Bubble flux quantification, d) Push corer sampling. (Bohrmann et al., 2017)

Furthermore, 10 dives with MARUM's ROV SQUID have been used to investigate methane emission sites at the seafloor. Besides visual seep investigations, sediment and gas sampling, fluid flux quantifications and temperature measurements were performed (Fig. 4 a–d). The dives additionally aimed to assess the in situ benthic assemblages at South Georgia and to test if the seeps have an effect of benthic assemblage distributions (Fig. 5). The acquired data facilitates the assessment of the interaction between biodiversity and habitat classifications to create a map of conservation priorities for the region (Hogg et al., 2016). The government of South Georgia and the South Sandwich Islands as part of the UK has already identified the shelf areas around South Georgia as a maritime protection area and is currently implementing its regulations (http://www.gov.gs/south-georgia-and-the-south-sandwich-islands-mpa-enhancements/).

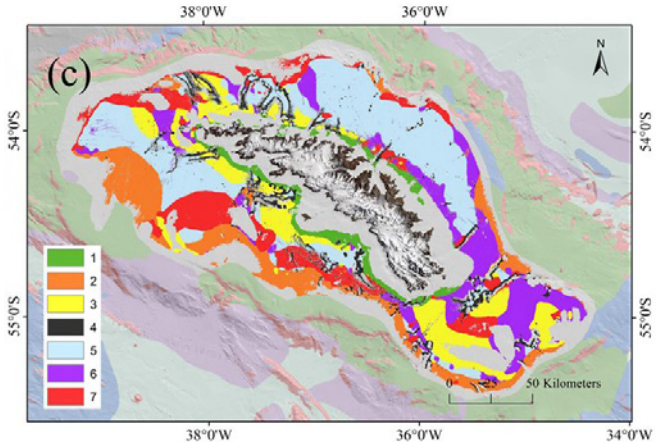

Fig. 5: Hierarchically nested marine landscape map showing the results of landscape mapping around South Georgia. (Hogg et al., 2016)

REFERENCES

Bohrmann G, et al. RV METEOR cruise report M134 – Emissions of free gas from cross-shelf troughs of South Georgia: Distribution, quantification, and sources for methane ebullition sites in sub-Antarctic waters. Berichte, MARUM – Zentrum für Marine Umweltwissenschaften, Fachbereich Geowissenschaften, Universität Bremen, 317, 2017. 1–220. urn:nbn:de:gbv:46-00106081-12.

Geprägs, P, Torres, ME, Mau, S, Kasten, S, Römer, M and Bohrmann, G, Carbon cycling fed by methane seepage at the shallow Cumberland Bay, South Georgia, sub-Antarctic. Geochemistry, Geophysics, Geosystems, 2017, 17(4). doi:10.1002/2016GC006276.

Hogg, O., Huvenne, V., Griffiths, H. et al. Landscape mapping at sub-Antarctic South Georgia provides a protocol for underpinning large-scale marine protected areas. Sci Rep 2016, 6, 33163, doi:10.1038/srep33163.

Lange, M, Does methane from shallow seep sites reach the atmosphere? A case study of the shelf of Subantarctic South Georgia. Department of Geosciences, University of Bremen. Master thesis at Department of Geosciences, 2018, University Bremen.

Römer, M, Torres, ME, Kasten, S, Kuhn, G, Graham, AGC, Mau, S, Little, CTS, Linse, K, Pape, T, Geprägs, P, Fischer, D, Wintersteller, P, Marcon, Y, Rethemeyer, J, Bohrmann, G, First evidence of widespread active methane seepage in the Southern Ocean, off the sub-Antarctic island of South Georgia. Earth and Planetary Science Letters 2014, 403, doi:10.1016/j.epsl.2014.06.036

M135

RESULTS FROM METEOR CRUISE M135 TO THE UPWELLING SYSTEM OFF CHILE AND PERU

AUTHORS

GEOMAR Helmholtz Centre for Ocean Research Kiel | Kiel, Germany
T. Tanhua, M. Visbeck

R/V METEOR departed from Valparaiso, Chile in the evening of 1 March 2017 and reached the port of Callao, Peru on 8 April, 2017, Figure 1. Cruise M135 was a contribution to the DFG Collaborative Research Project (SFB) 754: "Climate-Biogeochemistry Interactions in the Tropical Ocean" with the overall goal to understand the coupling of tropical climate variability and circulation with the ocean's oxygen and nutrient budget. In particular, this cruise supported the objectives of TP A3, with the main goal to better understand the the role of diffusive and advective pathways connecting water within the bottom boundary layer (i. e. the water directly affected by sediment processes) to the pelagic and surface ocean in the eastern tropical South Pacific. To achieve this, a conservative tracer (CF3SF5) within the bottom boundary layer at three different sites along the Peruvian coast at a depth of about 350 m had been injected in October 2015. The mixing and advection of the traver after one and a half years was mapped during M135. Tracer sampling was carried out by measuring water samples from the CTD-rosette water bottles. In total 144 CTD casts were carried out off the coast of Peru and Chile. From 132 CTD profiles 2828 samples for CF3CF5 investigations were gained and on most stations the tracer was detected. Additionally, 48 trace metal CTD stations were sampled for trace metal and chemicals. Overall 166 CTD stations (trace metal and regular CTD) were probed for oxygen and on 94 CTD profiles nutrient samples were collected. All CTD data were provided in near real time to the Argo-network project and were publically available for forecasting and assimilation modeling via CORIOLIS. Calibrated data are available via PANGEA. The station distribution in the area closed a gap in the poorly sampled southern boundary of the tropical South Pacific oxygen minimum zone, giving for the first time a complete snapshot of the extent, volume and severity of the oxygen deficit.

In addition, microstructure measurements were made on 24 stations and two gliders were deployed. For geological investigations at five locations multicorer and long gravity cores were taken. Also, continuous ADCP and thermosalinograph recording was made on 37 days. Continuous measurements of the climate-relevant trace gases carbon dioxide (CO_2), nitrous oxide (N_2O) and carbon monoxide (CO) were conducted in surface waters throughout the M135 cruise. These measurements were part of a comprehensive survey carried out within the context of the SFB 754 and spanned a total of four cruises

(March–July 2017) in the eastern tropical South Pacific. Given the data paucity in eastern boundary upwelling ecosystems (EBUEs) such as the Humboldt Current (HC) system off Peru-Chile, this survey represented a crucial contribution to the improvement of observational and modelling-based approaches aiming to accurately estimate the oceanic source/sink dynamics of these gases. Several manuscripts with results from this cruise are presently in preparation. So far published are data from M135 to investigate deglacial to Holocene ocean temperatures in the Humboldt Current system, the influence of intraseasonal eastern boundary circulation variability on the hydrography and biogeochemistry off Peru and the influence of decadal oscillations on the oxygen and nutrient trends off Peru.

The overall scientific goal of the SFB 754 is to understand the coupling of tropical climate variability and circulation with the ocean's oxygen and nutrient budgets, to quantitatively evaluate the functioning of oxygen-sensitive microbial processes and their impact on biogeochemical cycles, and to assess potential consequences for the ocean's future. The cruise M135 contributed to this goal and the improved knowledge of the coupling of tropical climate variability and circulation with the ocean's oxygen and nutrient budgets will probably be paid increasing interest by public media in regards to ongoing awareness of the impact on climate change on society.

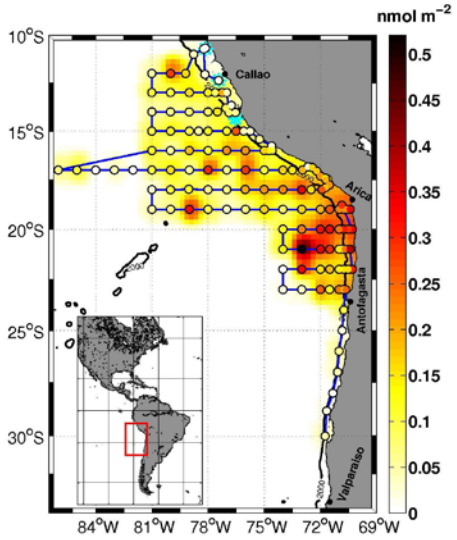

Fig. 1: The cruise track of the M135 cruise. The color coding is the column inventory of the deliberately released tracer CF3SF5 in nmol m^{-2}.

M136 & M137

COUPLED BENTHIC AND PELAGIC OXYGEN, NUTRIENT AND TRACE METAL CYCLING, VENTILATION AND CARBON DEGRADATION IN THE OXYGEN MINIMUM ZONE AT THE PERUVIAN CONTINENTAL MARGIN (SFB 754). SCIENTIFIC RESULTS FROM METEOR CRUISES M136 AND M137

AUTHORS

GEOMAR Helmholtz Centre for Ocean Research Kiel | Kiel, Germany
S. Sommer, M. Dengler

The Meteor cruises M136 (April 11 to May 3, 2017) and M137 (May 6 to 29, 2017) in the oxygen minimum zone off central Peru were conducted within the framework of the Kiel collaborative research center SFB 754 (Climate – Biogeochemistry Interactions in the Tropical Ocean). They addressed the major goal of the SFB 754, namely the understanding of the sensitivities and feedbacks linking low or variable oxygen (O_2) and nitrate (NO_3-) levels, organic matter dynamics, and key nutrient (N, P, Fe) source and sink mechanisms in the benthos and in the water column. Further objectives were to determine ventilation rates by sub-mesoscale processes, quantify export fluxes of particulate organic matter, determine production and decay rates of dissolved organic material, and investigate mechanisms of iron stabilization, removal and cycling. During the cruise M137 the focus shifted slightly towards benthic element cycling to resolve the extent how benthic N, P and S fluxes are coupled and controlled by filamentous sulfide oxidizing bacteria Marithioploca and Beggiatoa, which represent a key faunal component of the Peruvian shelf and upper slope sediments as well as by denitrifying foraminifera and to experimentally determine the magnitude and pathways of benthic element fluxes in response to enhanced availability of NO_3- and O_2.

The multidisciplinary working program of both cruises focused on a depth transect at 12°S perpendicular to the Peruvian coast (Figure 1). Additionally, during M136, a transect at 14°S was completed and a sub-mesoscale process study in an upwelling filament structure was carried out in the region of 15°S, 77°W. The coordinated sampling scheme included CTD profiling and water sampling stations, shipboard turbulence and velocity observations, a glider swarm experiment, moored velocity and hydrography observations, in situ benthic flux measurements using landers, sediment retrieval with a multiple corer, drifting sediment trap deployments and in situ pump deployments.

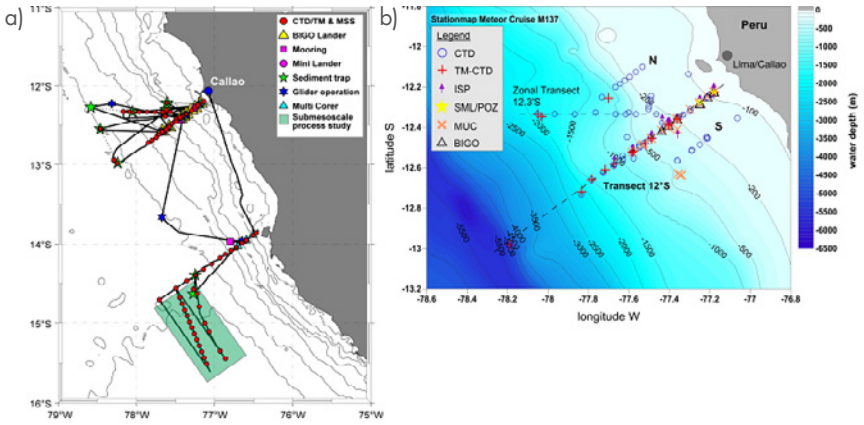

Fig. 1: Station maps of Meteor cruises M136 (panel a) and M137 (panel b) off Peru.

The hydrodynamic conditions at the 12°S study site off Peru during April/May 2017 (austral autumn) were distinct from those encountered during previous SFB 754 cruises carried out in austral summer. Most prominent differences were anomalously warm and saline waters in the upper 200m and increased poleward circulation associated with a strengthened Peru-Chile Undercurrent (Lüdke et al. 2019). The intensification of the Peru-Chile Undercurrent was caused by a downwelling coastal trapped wave. The associated increase of poleward water mass advection resulted in low N-deficit waters in the OMZ off Peru demonstrating the importance of alongshore advection for the cumulative strength of N-cycling in the Peruvian OMZ.

The sub-mesoscale process study showed enhanced nutrient and chlorophyll concentrations within a filament suggesting an offshore transport of nutrients. In conjunction with an evaluation using Regional Ocean Model System (ROMS) simulations (Hauschildt 2017), it was found that the net effect of sub-mesoscale frontal processes on biogeochemistry in the Peru-Chile upwelling system is increased oxygen subduction and increased offshore transport of nutrients, which in turn reduce primary production in the upwelling region.

Bacterial heterotrophic activity in the suboxic core of the OMZ (O_2 levels ≤ 5 µmol kg^{-1}) was not significantly lower than in oxygenated waters (O_2 levels 5–60 µmol kg^{-1}) (Maßmig et al. 2019). Moreover, bacterial abundance in the OMZ was slightly and leucine aminopeptidase activity even significantly higher in suboxic waters compared to the upper oxycline suggesting no impairment of bacterial organic matter degradation in the core of the OMZ. However, particulate organic carbon (POC) fluxes determined from sediment traps agree with the idea that POC flux attenuation is lower in OMZs. POC attenuation with depth measured by the sediment traps in the upwelling region varied largely from 0.35 to 0.91, and was on average b = 0.65 ± 0.22, lower than the original ocean composite value (b = 0.86). However, large variability in particle fluxes was observed, suggesting that particle flux attenuation is not always low in OMZs as was previously thought.

Benthic element cycling (N, P, Si, (see Poster by Dale et al.), TM, and carbon), was determined along the 12°S depth transect using benthic lander and pore water gradients. The bottom water at the shelf was weakly ventilated and NO_3- and nitrite (NO_2-) was available at higher levels. This was in contrast to the cruise M92 in 2013, where flux measurements at the shelf were conducted under stagnant bottom water conditions depleted in O_2, NO_3- and NO_2- resulting in the seabed release of sulfide (Sommer et al. 2016). Focusing on the benthic N-cycle, the Peruvian shelf sediments represent a major source for ammonium (NH_4+) to the bottom water, sustained by high rates of dissimilatory nitrate reduction to ammonium (DNRA). During DNRA major part of the sedimentary NO_3- uptake is channeled into the oxidation of sulfide by sulfur bacteria releasing high amounts of NH_4+ into the bottom water fueling water column anammox. Irrespective of the distinct differences in the bottom water availability of NO_3- in 2013 and 2017, the magnitude of NH_4+ fluxes determined during both time periods was similar (21.2 and 26.0 mmol m^{-2} d^{-1} respectively, Sommer et al. 2016, Clemens et al. in prep.). In 2013 and 2017, organic carbon degradation was equally high and strongly driven by sulfate reduction leading to the accumulation of high porewater sulfide concentrations. During conditions of enhanced availability of O_2 and NO_3- encountered in 2017, the benthic shelf ecosystem apparently retained its full functionality. On the shelf NO_3- was channeled into DNRA supporting constantly high release rates of NH_4+ and the efficient sulfide detoxification of the sediment. In contrast, the sulfur bacteria community encountered in 2013 survived on their dwindling intracellular NO_3- reservoir to survive the stagnation period (Dale et al. 2016).

A study in the Peruvian OMZ during M77-1 indicated that foraminifera are responsible for up to 40 to 50% of total benthic NO_3- loss at certain stations (Glock et al. 2013). Similar to the sulfur bacteria, foraminifera can accumulate NO_3- internally. In effect, both organisms represent a major NO_3- reservoir that responds to variable environmental redox conditions that can become uncoupled from the pelagic input and mineralization of organic matter. To assess the significance of foraminiferal denitrification in the Peruvian N-cycle, denitrification rates of 10 benthic foraminifer species were measured along the 12°S transect. Results shows that foraminifera not only switch from aerobic respiration to denitrification when bottom water O_2 becomes depleted, but even have a metabolic preference of NO_3- over O_2 (Glock et al., 2019).

The joint analysis of foraminiferal denitrification with DNRA allowed to address the question to what extent foraminifera and sulfur bacteria compete for NO_3- and NO_2- resulting into the prevalence of fixed N loss versus recycling. Between denitrifying foraminifera and sulfur bacteria exists a clear niche separation minimizing competition for NO_3- between these two major groups (Clemens et al. in prep.).

M137 enabled further scientific results, which cannot be presented here. But we hope, that the joined future synthesis including the data from previous SFB cruises bears a high scientific potential and impact.

REFERENCES

Dale AW, Sommer S, Lomnitz U, Bourbonnais A, Wallmann K. Biological nitrate transport in sediments on the Peruvian margin mitigates benthic sulfide emissions and drives pelagic N loss during stagnation events, Deep-Sea Res. I. 2016, 112, doi.org/10.1016/j.dsr.2016.02.013.

Hauschildt J, Observed and modeled biogeochemistry of filaments off Peru. 2017, Master Thesis, Christian-Albrechts-Universität Kiel, 110 pp, http://oceanrep.geomar.de/id/eprint/41369.

Glock N, Roy A-S, Romero D, Wein T, Weissenbach J, Revsbech NP, Høgslund S, Clemens D, Sommer S, Dagan T. Metabolic preference of nitrate over oxygen as an electron acceptor in foraminifera from the Peruvian oxygen minimum zone, PNAS 2019, 116, doi/10.1073/pnas.1813887116.

Glock N, Schönfeld J, Eisenhauer A, Hensen C, Mallon J, Sommer S. The role of benthic foraminifera in the benthic nitrogen cycle of the Peruvian oxygen minimum zone, Biogeosciences 2013, 10, doi:10.5194/bg-10-4767-2013.

Graco MI, Purca S, Dewitte B, Castro CG, Morón O, Ledesma J, Flores G, Gutiérrez D. The OMZ and nutrient features as a signature of interannual and low-frequency variability in the Peruvian upwelling system, Biogeosciences 2017, 14, doi.org/10.5194/bg-14-4601-2017.

Gutiérrez D, Enriquez E, Purca S, Quipúzcoa L, Marquina R, Flores G, Graco M. Oxygenation episodes on the continental shelf of central Peru: Remote forcing and benthic ecosystem response, Progress in Oceanography, 2008, 79, doi:10.1016/j.pocean.2008.10.025.

Lüdke J, Dengler M, Sommer S, Clemens D, Thomsen S, Krahmann G, Dale AW, Achterberg EP, Visbeck M. Influence of intraseasonal eastern boundary circulation variability on hydrography and biogeochemistry off Peru, 2019, Ocean Sci. Discuss., https://doi.org/10.5194/os-2019-93.

Maßmig M, Lüdke J, Krahmann G, Engel A. High bacterial organic carbon uptake in the Eastern Tropical South Pacific oxygen minimum zone, 2019, Biogeosciences Discuss., https://doi.org/10.5194/bg-2019-237, accepted.

Sommer S, Gier J, Treude T, Lomnitz U, Dengler M, Cardich J, Dale AW. Depletion of oxygen, nitrate and nitrite in the Peruvian oxygen minimum zone cause an imbalance of benthic nitrogen fluxes, Deep-Sea Res I 2016, 112, doi.org/10.1016/j.dsr.2016.03.001

M137*

RECYCLING AND BURIAL OF BIOGENIC SILICA IN THE PERUVIAN OXYGEN MINIMUM ZONE

AUTHORS

GEOMAR Helmholtz Centre for Ocean Research Kiel | Kiel, Germany
A. W. Dale (Corresponding author), U. Schroller-Lomnitz, D. Clemens, F. Scholz, K. Wallmann, S. Geilert, C. Hensen, A. Plaß, U. V. Liebetrau, P. Grasse, S. Sommer

Department of Environmental Sciences, University of Helsinki | Helsinki, Finland
M. Paul

The availability of silicic acid (H_4SiO_4), or silicate, in the ocean exerts a major control on primary production by certain groups of phytoplankton such as diatoms, radiolaria and silicoflagellates. The dissolved silicate is biomineralized to amorphous biogenic silica (BSi, biogenic opal) that constitutes the hard exoskeletons and tests of these organisms. Most BSi that is synthesized in the surface ocean is solubilized back to silicate in situ, with around one-third of new production surviving dissolution in the ocean interior to reach the seafloor (Tréguer and De La Rocha, 2013). Around 80–90 %
of the deposited flux is recycled back to silicate, such that only a minor fraction (<5 %) of newly synthesized BSi is permanently buried in the sediment. Yet, the oceanic residence of silicate with regard to burial is short enough (~15 kyr), that the Si inventory will respond to changes in the global burial flux over glacial-interglacial timescales (Tréguer and De La Rocha, 2013). A sound understanding of BSi recycling efficiency is thus crucial for the biological carbon and silicon pumps, the assessment of paleo-productivity from the sedimentary BSi archive, and for more accurate global models (Mortlock et al., 1991; Heinze et al., 2003).

An extensive data set of BSi fluxes is presented for the Peruvian continental margin at 11 °S and 12 °S. Primary production here is intense and dominated by diatoms (Franz et al., 2012). Microbial respiration of sinking biogenic detritus leads to the formation of an oxygen minimum zone (OMZ) between ca. 100 and 500 m where dissolved oxygen is depleted down to levels that are functionally anoxic (Thamdrup et al., 2012). The sediments underlying the OMZ are classified as hemipelagic diatomaceous ooze (DeMaster, 1981). They accumulate massive amounts of particulate organic carbon at rates that are 5–6 times higher than the average continental margin value (Dale et al., 2015).

Each sampling transect extends from the shelf to the upper slope (~1000 m). BSi accumulation and recycling fluxes are highest on the shelf with mean preservation

efficiencies (35 ± 15 %) that exceed the global mean of 10–20 %. The preservation efficiency was apparently not controlled by the detrital content. Comparison with existing global data, most of which are from deep waters (>1000 m), suggests that the main control on BSi preservation is the rate at which reactive BSi is transported away from undersaturated surface sediments by burial and bioturbation to underlying saturated layers where further dissolution of BSi is thermodynamically inhibited. BSi preservation is highest on the inner shelf (up to 56 %), decreasing to 7 and 12 % under anoxic waters and below the OMZ, respectively. Low preservation is argued to be related to few bioturbating macrofauna. In contrast, particulate organic carbon preservation tends to increase with water depth. This divergence may have important implications for the reconstruction of paleo-productivity from sediment archives. Existing data permit a simple relationship between BSi rain rate to the seafloor and the accumulation of unaltered biogenic silica, giving the possibility to reconstruct rain rates from the sediment archive. BSi burial across the entire Peruvian margin between 3 °S to 15 °S and down to 1000 m water depth is estimated to be 0.1–0.2 Tmol yr-1; equivalent to 3–6 % of the global burial on continental margins.

ACKNOWLEDGEMENTS

This work is a contribution of the Sonderforschungsbereich 754 "Climate – Biogeochemistry Interactions in the Tropical Ocean" (www.sfb754.de) which is supported by the Deutsche Forschungsgemeinschaft.

REFERENCES

Dale A. W., Sommer S., Lomnitz U., Montes I., Treude T., Liebetrau V., Gier J., Hensen C., Dengler M., Stolpovsky K., Bryant L. D. and Wallmann K. (2015) Organic carbon production, mineralisation and preservation on the Peruvian margin. Biogeosciences 12, 1537–1559.

DeMaster D. J. (1981) The supply and accumulation of silica in the marine environment. Geochim. Cosmochim. Acta 5, 1715–1732.

Franz J., Krahmann G., Lavik G., Grasse P., Dittmar T. and Riebesell U. (2012) Dynamics and stoichiometry of nutrients and phytoplankton in waters influenced by the oxygen minimum zone in the eastern tropical Pacific. Deep-Sea. Res. I 62, 20–31.

Heinze C., Hupe A., Maier-Reimer E., Dittert N. and Ragueneau O. (2003) Sensitivity of the marine biospheric Si cycle for biogeochemical parameter variations. Global Biogeochem. Cycles 17, 12–21.

Mortlock, R.A., Charles, C.D., Froelich, P.N., Zibello, M.A., Saltzmann, J., Hays, J.D., Burckle, L.H. (1991) Evidence for lower productivity in the Antarctic ocean during the last glaciation. Nature 351, 220–222.

Thamdrup B., Dalsgaard T. and Revsbech N. P. (2012) Widespread functional anoxia in the oxygen minimum zone of the Eastern South Pacific. Deep-Sea. Res. I 65, 36–45.

Tréguer P. and De La Rocha, Christina L. (2013) The World Ocean Silica Cycle. Ann. Rev. Mar. Sci. 5, 477–501.

M137*

BENTHIC FORAMINIFERA FROM THE PERUVIAN OXYGEN MINIMUM ZONE: THE ROLE IN NUTRIENT CYCLING AND A METABOLIC PREFERENCE FOR NITRATE AS AN ELECTRON ACCEPTOR

AUTHORS

GEOMAR Helmholtz Centre for Ocean Research Kiel, Marine Geosystems | Kiel, Germany
N. Glock, D. Clemens, S.Sommer

Institute of Microbiology, Kiel University | Kiel, Germany
A.-S. Roy, T. Wein, J. Weissenbach, T. Dagan

IMARPE, Dirección General de Investigaciones Oceanográficas y Cambio Climático | Callao, Peru
D. Romero

Faculty of Biology, Technion – Israel Institute of Technology, Haifa | Haifa, Israel
J. Weissenbach

ABSTRACT

Benthic foraminifera populate a wide and diverse range of marine habitats. Their ability to use alternative electron acceptors – nitrate or oxygen – makes them keyplayers within the benthic nitrogen cycle (Risgaard-Petersen et al., 2006; Piña-Ochoa et al., 2010; Glock et al. 2013; Woehle and Roy et al., 2018). Nevertheless, the metabolic scaling of the two alternative respiration pathways were yet unknown. On RV Meteor cruise M137 we measured the denitrification and oxygen respiration rates for ten benthic foraminiferal species sampled in the Peruvian oxygen minimum zone (OMZ). These species were able to use both nitrate and oxygen as an electron acceptor. Various characteristics of any organism scale with their body size (e. g. energy consumption, population growth rate, …). Scaling of these characteristics can be described by a power function (Eq1) with a scaling exponent α (Kleiber 1932):

Eq1: $Y = Y0.S^{\alpha}$

(Y = Rate of interest; Y0 = Normalization constant; α = Scaling exponent; S = Body size)

Kleiber hypothesized that the scaling exponent α = 0.75 in all mammals and birds (Kleiber, 1932). More recent studies showed that α can vary between different taxa and a higher α indicates a higher metabolic efficiency (DeLong et al. 2010).

Our results from M137 show that denitrification and oxygen respiration rates of the Peruvian benthic foraminifera significantly scale with the cell volume (Glock et al., 2019). The scaling for oxygen respiration ($\alpha = 0.41$) is lower than for denitrification ($\alpha = 0.68$), indicating that their nitrate metabolism during denitrification is more efficient than their oxygen metabolism during aerobic respiration in foraminifera from the Peruvian OMZ (Glock et al. 2019). The oxygen respiration rate is stronger correlated with the surface/volume ratio than the denitrification rate, most probably due to the presence of intracellular nitrate storage in denitrifying foraminifera. Oxygen can be toxic in higher intracellular concentrations and thus not be stored in vacuoles. Furthermore, we observe increasing cell volume in foraminifera from the Peruvian margin, under higher nitrate availability. This suggests that the cell size of denitrifying foraminifera is not limited by oxygen rather by nitrate availability. Our findings show that nitrate is the preferred electron acceptor in foraminifera from the OMZ, where the foraminiferal contribution to denitrification is governed by the ratio between nitrate and oxygen (Glock et al. 2019).

In addition, during cruise M137 we measured intracellular nitrate and phosphate contents of five different benthic foraminiferal species and the in situ nitrate uptake rates of six additional samples. Both macronutrients were strongly enriched within the foraminifera and significantly correlated with the cell volume of the analyzed foraminifera (PNitrate = 3.10-9 and PPhosphate = 3.10-14). To assess the foraminiferal in situ nitrate uptake rates, we analyzed the ratio of labeled to unlabeled nitrate stored within benthic foraminifera two different experiments within biogeochemical observatories (BIGO). The biogeochemical observatories are described in detail by Sommer et al. (2009). All analyzed foraminifers took up labeled nitrate and the ratio of labeled to unlabeled nitrate reached up to 0.98, indicating that benthic foraminifera are able to completely exchange their intracellular nitrate storage within the time of incubation (36 hours). The calculated in situ nitrate uptake rates of the foraminifera during the experiment showed that were in average more than two times higher than their species specific denitrification rates. Benthic foraminifera can reach very high living abundances at the Peruvian OMZ (up to 617 ind cm^{-2} after Glock et al. 2013). Our new results from M137 and a comparison of the total benthic fluxes with the total benthic foraminiferal rates and intracellular nutrient storage suggest that benthic foraminifera play a previously underestimated role within both the benthic nitrogen and phosphorous cycling.

REFERENCES

DeLong, J.P., Okie, J.G., Moses, M.E., Sibly, R.M., and Brown, J.H., Shifts in metabolic scaling, production, and efficiency across major evolutionary transitions of life, Proceedings of the National Academy of Science USA 2010, 107, 12941–12945, doi: 10.1073/pnas.1007783107.

Glock, N., Schönfeld, J., Eisenhauer, A., Hensen, C., et. al., The role of benthic foraminifera in the benthic nitrogen cycle of the Peruvian oxygen minimum zone, Biogeosciences 2013, 9, 17775–17817, doi: 10.5194/bg-10-4767-2013.

Glock, N., Roy, A.-S., Romero, D., Wein, T., et al, Metabolic preference of nitrate over oxygen as an electron acceptor in foraminifera from the Peruvian oxygen minimum zone, Proceedings of the National Academy of Science USA 2019, 116, 2860–2865, doi: 10.1073/pnas.1813887116.

Kleiber, M., Body size and metabolism, Hilgardia 1936, 6, 315–353.

Piña-Ochoa, E., Høgslund, S., Geslin, E., Cedhagen, et al., Widespread occurence of nitrate storage and denitrification among Foraminifera and Gromiida, Proceedings of the National Academy of Science USA 2010, 107, 1148–1153, doi: 10.1073/pnas.0908440107.

Risgaard-Petersen, N., Langezaal, A. M., Ingvardsen, S., Schmid, M. C., et al., Evidence for complete denitrification in a benthic foraminifer, Nature 2006, 443, 93–96, doi:10.1038/nature05070.

Sommer, S., Linke, P., Pfannkuche, O., Schleicher, T., et al., Seabed methane emissions and the habitat of frenulate tubeworms on the Captain Arutyunov mud volcano (Gulf of Cadiz), Marine Ecology-Progress Series 2009, 382, 69–86, doi:10.3354/meps07956.

Woehle, C., Roy, A.-S., Glock, N., Wein, T., et al., 2018, A novel eukaryotic denitrification pathway in foraminifera, Current Biology 2018, 28, 2536–2543, doi: 10.1016/j.cub.2018.06.027.

M137*

BENTHIC NITROGEN CYCLING IN THE PERUVIAN OXYGEN MINIMUM ZONE IN RELATION TO VARIABLE BOTTOM WATER REDOX CONDITIONS – A SYNTHESIS OF SFB 754 METEOR CRUISES M92, M136, M137

AUTHORS

GEOMAR Helmholtz Centre for Ocean Research Kiel | Kiel, Germany
D. Clemens, A. Dale, M. Dengler, J. Lüdke, K. Wallmann, S. Sommer

The magnitude and timing of processes involved in the nitrogen cycle of oxygen minimum zone (OMZ) sediments in response to variable bottom water redox conditions has been hardly constrained, yet would allow for the better up-scaling and predictive capability of the benthic-pelagic coupling in the Peruvian OMZ at various time scales. Bottom water redox conditions at the upper boundary of the Peruvian OMZ are highly variable. Intermittent oxygenation events between 10 and 90 m water depth were observed over a period of 13 years (1992–2005) (Gutiérrez et al., 2008). Such oxygenation events are strongly associated with the passage of coastal trapped waves that occur more frequently during positive El Nino Southern Oscillation periods (Gutiérrez et al. 2008) and are associated with a significant deepening of the thermo- and oxycline. Concentrations of nitrate (NO_3^-) and nitrite (NO_2^-) also strongly fluctuated in the bottom water at 100 m depth clearly indicating a seasonal cycle during most years (Graco et al. 2017).

We compare previous measurements of the benthic nitrogen turnover from austral summer (January 2013, Meteor cruise M92), where the bottom water on the shelf has been depleted of oxygen (O_2), NO_3^- , NO_2^- and even sulfide has been released due to persistent stagnant current conditions (Sommer et al. 2016), with measurements obtained in austral autumn (April/May 2017, Meteor cruises M136/M137). In 2017 investigations were conducted during the passage a coastal trapped wave, which enhanced the southward transport of NO_3^- and NO_2^- and caused a slight ventilation of the bottom water on the shelf. During both campaigns, solute fluxes of NH_4^+, NO_3^- and NO_2^- across the sediment water interface were measured at 9 stations along a depth transect (70 to 1000 m) at 12° S in the Peruvian OMZ using benthic lander in situ incubations. During nitrogenous conditions in 2017 the NO_3^- uptake by the sediment on the shallow shelf was elevated (up to 8 mmol m^{-2} d^{-1}). Despite the significantly different bottom water geochemistry, the NH_4+ fluxes measured in 2017 were similar to 2013 with values reaching 21 mmol m-2 d-1 at the shallowest station. As in 2013, the high NH_4^+ fluxes measured in 2017 were predominantly caused by filamentous, vacuolated sulfur bacteria (Marithioploca, Beggiatoa), forming extended mats on the sediment surface, via the dissimilatory nitrate reduction to ammonium pathway (DNRA). Elevated DNRA rates in

2013 and 2017 were sustained by high sulfide pore water fluxes due to the intense organic carbon degradation using sulfate as terminal electron acceptor. In contrast to 2013, during conditions of enhanced availability of NO_3^- and O_2 encountered in 2017, the benthic (microbial) shelf ecosystem apparently retained its full functionality. A major proportion of NO_3^- was channeled into DNRA supporting constantly high release rates of NH_4^+ and the efficient sulfide detoxification of the sediment. In contrast, the sulfur bacteria community encountered in 2013 survived on their dwindling intracellular NO_3^- reservoir to survive the stagnation period (Dale et al. 2016). We explore implications of enhanced transport of NO_3^- and NO_2^- for the nitrogen budget as well as reasons for the unchanged NH_4+ release from shelf sediments considering new findings, which indicate that sulfidic events off Peru occur more frequently than previously thought.

REFERENCES

Dale AW, Sommer S, Lomnitz U, Bourbonnais A, Wallmann K. Biological nitrate transport in sediments on the Peruvian margin mitigates benthic sulfide emissions and drives pelagic N loss during stagnation events, Deep-Sea Res. I. 2016, 112, doi.org/10.1016/j.dsr.2016.02.013.

Graco MI, Purca S, Dewitte B, Castro CG, Morón O, Ledesma J, Flores G, Gutiérrez D. The OMZ and nutrient features as a signature of interannual and low-frequency variability in the Peruvian upwelling system, Biogeosciences 2017, 14, doi.org/10.5194/bg-14-4601-2017.

Gutiérrez D, Enriquez E, Purca S, Quipúzcoa L, Marquina R, Flores G, Graco M. Oxygenation episodes on the continental shelf of central Peru: Remote forcing and benthic ecosystem response, Progress in Oceanography, 2008, 79, doi:10.1016/j.pocean.2008.10.025.

Sommer S, Gier J, Treude T, Lomnitz U, Dengler M, Cardich J, Dale AW. Depletion of oxygen, nitrate and nitrite in the Peruvian oxygen minimum zone cause an imbalance of benthic nitrogen fluxes, Deep-Sea Res I 2016, 112, doi.org/10.1016/j.dsr.2016.03.001

M138*

SURFACE VARIABILITY OF CLIMATE-RELEVANT TRACE GASES (N_2O, CO_2, CO) IN THE TROPICAL EASTERN SOUTH PACIFIC OCEAN

AUTHORS

Chemical Oceanography Department, GEOMAR Helmholtz Centre for Ocean Research Kiel | Kiel, Germany

D. L. Arévalo-Martínez, T. Steinhoff, H. W. Bange

Given the climatic relevance of marine-derived trace gases, the investigation of their distribution and emissions from key oceanic regions is a crucial need in our efforts to better understand potential responses of the ocean and the overlying atmosphere to environmental changes such as warming and deoxygenation. Low-oxygen waters connected to coastal upwelling systems and the associated oxygen minimum zones (OMZ) are well-recognized strong sources of several trace gases (Capone and Hutchins, 2013). Our main goal during the M135-M138 cruises was to assess the distribution of different gases which are relevant for the biogeochemical cycling of carbon and nitrogen in the OMZ off Peru, as well as the spatial and temporal variability of their sea-air fluxes.

To this end, we conducted continuous measurements of dissolved N_2O, CO_2 and CO in seawater by means of an autonomous equilibrator headspace setup (GO-System; General Oceanics, Inc.) coupled to an off-axis integrated cavity output spectroscopy analyzer (model DLT-100, Los Gatos Research, Inc.), as described in Arévalo-Martínez et al. (2019). The combined setup is shown in Fig. 1. Water was drawn into the system at ca. 3 L min^{-1} by using a LOWARA submersible pump installed in the R/V Meteor's hydrographic well at about 6 m depth. In order to correct for potential warming of the seawater between intake and equilibrator, the water temperature at the equilibrator was constantly monitored by means of a high accuracy digital thermometer (Fluke) and at the intake by a Seabird SBE38 thermometer. Ambient air measurements were carried out every six hours by drawing air into the system from a suction point located at about 30 m high. Control measurements and calibration procedures were performed every ~6 and 24 h respectively, by means of three standard gas mixtures (Deuste Steininger GmbH) bracketing the expected concentrations in this area.

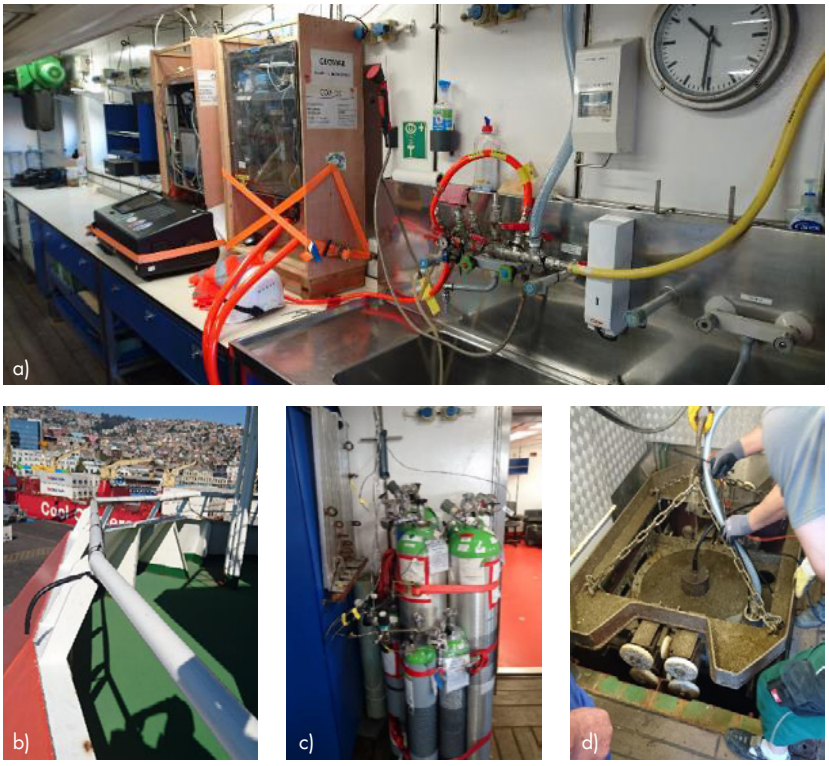

Fig. 1: Setup for along-track measurements of trace gases during M135-M138. (a) Equilibration system and gas analyzers, (b) inlet for ambient air measurements, (c) reference gases, (d) submersible pump, and SBE38 thermometer for measuring intake seawater temperature.

The along-track measurements during M135-M138 provided a unique record of the surface distribution of N_2O, CO_2 and CO during the autumn-winter period off Peru, supplementing similar measurements conducted in the region since 2008 within the framework of the BMBF-funded SOPRAN (Surface Ocean Processes in the Anthropocene, http://sopran.pangaea.de/home) project and the DFG-funded Collaborative Research Centre SFB754 (www.sfb754.de).

The strong cross-shelf variability in the region is exemplified by the N_2O and CO_2 data shown in Fig. 2. As can be seen, a marked decrease in sea surface temperature (SST) coincided with an enhanced outgassing of N_2O to the atmosphere and simultaneous uptake of CO_2. Although previous observations in this area (and under the occurrence of upwelling) have provided evidence that the distribution of both gases is often similar in the shelf area (i. e. CO_2 tends to be emitted to the atmosphere as well), the fact that CO_2 diverges from this pattern suggests a strong biological drawdown, which in turn drives partial pressures of CO_2 below atmospheric equilibrium. Since there is not such a biological sink for N_2O in surface waters, the solubility effect seemed to be dominant along this section.

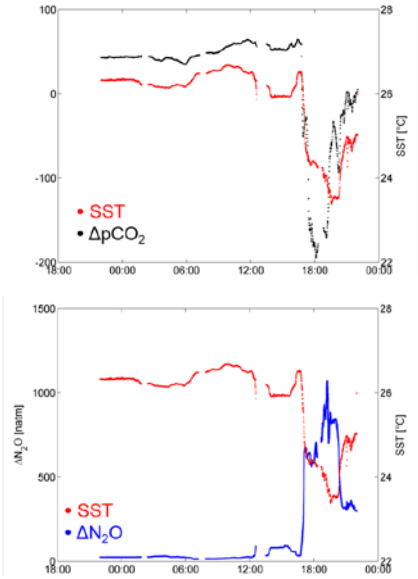

Fig. 2: Cross-shelf section of ΔpCO_2 (pCO_2 seawater – pCO_2 air; left) and ΔN_2O (N_2O seawater – N_2O air; right) at about 17°S. Positive values indicate that seawater is oversaturated with respect to the atmosphere (i. e. the ocean acts as a source for these gases). Along-track SST is displayed in red in both panels.

In addition to cross-shelf gradients, large meridional as well as sub-km variability in N_2O, CO_2 and CO could be observed off Peru. Fig. 3 shows the distribution of these three gases along the cruise track as well as the recorded SST. The Peruvian upwelling acted as a strong source of N_2O and CO_2 in June 2018, in particular in the near-coastal area between 9°S and 16°S where seawater values surpassed atmospheric equilibrium (~329 ppb for N_2O und ~ 408 ppm for CO_2) by about one order of magnitude. In agreement with past surveys which took place during the R/V Meteor M91 and R/V SONNE SO-243 cruises (December 2012 and October 2015, respectively) the highest N_2O and CO_2 values were consistent with the location of the upwelling cells off Chimbote, Callao and Pisco. Episodic undersaturation of CO_2 was observed at discrete locations along the coast (c. f. also Fig. 2), suggesting strong biological drawdown in response to enhanced primary production after upwelling events. Our observations also showed that the coastal waters off Peru were a net source of CO to the atmosphere. Thus, despite the clearly dominant diurnal variability (production enhanced at noon, microbial consumption at dawn and night), a cross-shelf gradient in CO could be observed along the cruise track (Fig. 3).

These results are an important contribution for future improvements in the representation of the nitrogen and carbon processes from coastal ecosystems in global biogeochemical models. Likewise, they highlight the relevance of employing high-resolution, autonomous methods during ship surveys in order to extend the temporal and spatial coverage of measurements of climate-relevant trace gases.

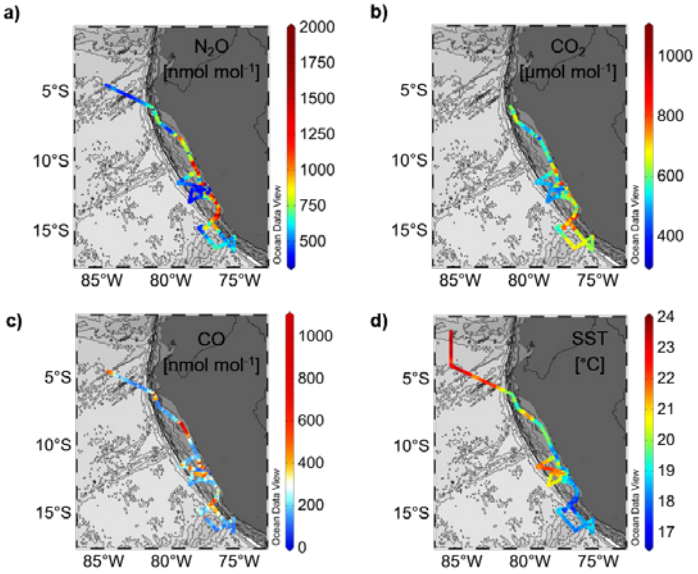

Fig. 3: Surface distribution of dissolved N_2O (a), CO_2 (b) and CO (c) during M138. Along-track SST as measured by the R/V Meteor's thermosalinograph is shown in (d).

REFERENCES

Capone, D.G., and Hutchins, D.A.: Microbial biogeochemistry of coastal upwelling regimes in a changing ocean, Nature Geoscience, 6, 711–717, 2013, doi:10.1038/ngeo1916.

Arévalo-Martínez, D. L., Steinhoff, T., Brandt, P., Körtzinger, A., Lamont, T., Rehder, G., and Bange, H. W.: N_2O emissions from the northern Benguela upwelling system, Geophysical Research Letters, 46, 3317–3326, 2019, doi:10.1029/2018GL081648.

M139

DEEP-SEA MICROBIAL FOOD WEBS OF THE ATLANTIC AND CARIBBEAN

AUTHORS

University of Cologne, Biocenter, Department for Biology, Institute for Zoology, General Ecology | Cologne, Germany
Hartmut Arndt

And: the scientific crew of M139

Although the dark ocean represents the largest environment on this planet, microbial life in the deep sea is still a relatively uncharted territory. This is in striking contrast to its potential importance regarding the global carbon flux. The biological focus within this expedition was set on the diversity and activity of deep-sea microbes (protists and prokaryotes) sampled from the benthic and pelagic realm at different deep-sea basins (one in the Caribbean, two in southern North Atlantic) by means of a Multicorer system and a specific water sampler ISMI, the in-situ microbial incubator, which can be used to analyse the activity in non-decompressed samples. Metabarcoding analysis based on the V9 region of the 18S ribosomal DNA of the benthic protist communities investigated on a small and large spatial scale showed an unexpected highly unique, distinct and diverse deep-sea community at each sampled spot with a great proportion of so far unknown and potentially new taxa. Diplonemids, kinetoplastids were much more diverse than the traditionally considered foraminiferans. The incorporation of data in our global benthic deep-sea dataset and the comparison to global surface water metabarcoding studies (Tara Ocean) revealed distinct microbial deep-sea communities with certain specificity to basins and regions. Direct microscopic studies immediately after sampling allowed a quantification and qualification of living deep-sea protists. We were able to establish monoclonal cultures of different protists from deep-sea sediments which revealed several new species. Most striking was the establishment of cultures of deep-sea ciliates, the first ever cultivated ciliates from the abyssal. Pressure incubations on board revealed their specific pressure adaptation supported by later behavioural studies. Genotypes of isolates of deep-sea protists could be recovered from metabarcoding studies and used for global analysis of respective genotypes. Our studies clearly indicate that potentially active unicellular eukaryotes are much more diverse than assumed up to now.

Another very important finding was that sea surface microbial communities sampled with the ISMI sampler exhibited reduced leucine incorporation rates under elevated pressure as compared to atmospheric pressure conditions. Results indicate that the ISMI works reliably and allows determining the metabolic activity of dark ocean microbes under in situ hydrostatic pressure. The abundance, percentage and the diversity of genes encoding secretory enzymes consistently increased from epipelagic to bathypelagic waters as did the corresponding enzymes, indicating that prokaryotic metabolism is predominately particle-associated in the bathypelagic realm. In cooperation with geologists on board, the OFOS-system allowed us to quantify the sedimentation of macroalgae to the deep-sea floor, and later video-analyses in a short distance from the deep-sea floor (1.5 m) at two abyssal stations (one with macrophyte sedimentation) and one seamount revealed high abundances of diverse megafauna communities.

The geological focus laid on the geology of the oceanic crust (BrightFlows), which is virtually unknown and even basic knowledge of bathymetry is missing in most areas. During the transit Barbados – Mid-Atlantic Ridge during cruise M127 (May 2016), an area of 20 Ma seafloor was crossed which showed high acoustic reflectivity linked to the presence of several small cones, implying the presence of lava flows. Calculations of acoustic attenuation by sediment at the sonar frequencies used had shown that these lava flows have a maximum sediment cover of 2 m (and possibly much less). Thus, we investigated the geology of the deep-sea floor in this special region (A3/4) with lava flows in the western North Atlantic to determine their age and composition and map out their full areal extent to estimate the magma volumes erupted. The discovery of the recent lava fields and their detailed sampling and mapping was one highlight of the cruise, because the lava flows could clearly be classified as much younger compared to the surrounding, old oceanic crust which is very exciting.

The public could follow our scientific investigations and life on board at the oceanblogs.org homepage. In addition, we created a facebook page for the expedition to gain more readers from social media. A hint to the new findings of the expedition was visible for several weeks at the startpage of the University of Cologne.

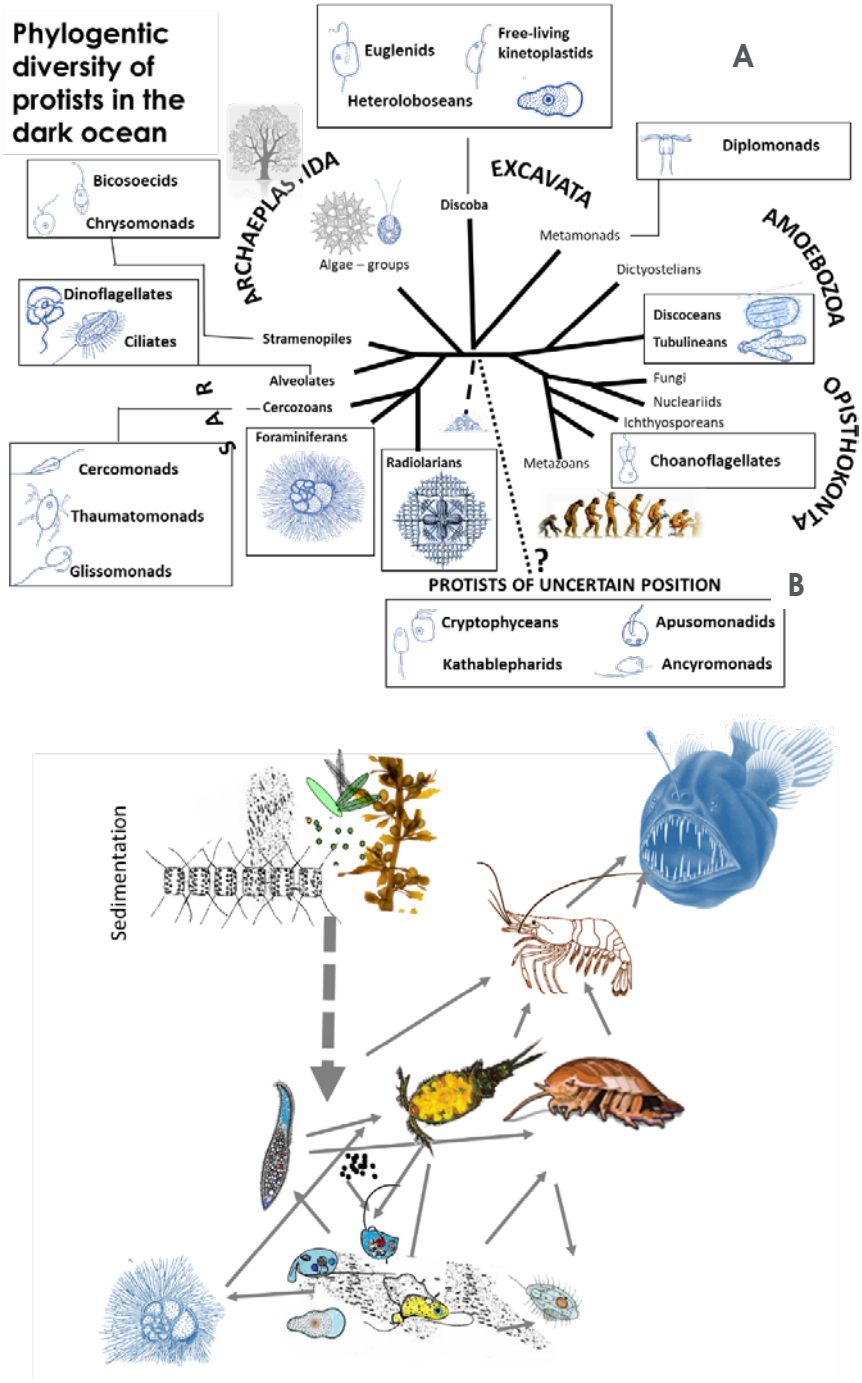

Fig. 1: Conceptual framework of the role of nano- and microprotists in deep-sea microbial food webs. (A) Phylogenetic diversity of protist groups detected or observed during M139. (B) Nanoprotists in addition to foraminiferans should be considered as fundamental components of deep-sea food webs.

M139*
A NEW STYLE OF OCEANIC INTRAPLATE VOLCANISM

AUTHORS

GEOMAR Helmholtz Centre for Ocean Research Kiel | Kiel, Germany
N. Augustin, C.W. Devey, T.M. Herrero, M. Schade, F.M. van der Zwan, C. Böttner

Institute of Oceanography, Dep. of Marine Geology, University Gdańsk | Gdańsk, Polandy
D. Palgan

Institut für Mineralogie, Universität Hannover | Hannover, Germany
R.R. Almeev

Although the dark ocean represents the largest environment on this planet, microbial Studies of active volcanism on the seafloor traditionally focused along plate boundaries and hotspots where volcanic activity is frequent, and the structures constructed are clearly detectable. The rest of the seafloor remains largely uninvestigated, as the abyssal plains in general were believed to be geologically inactive. A large group of bright bathymetric-backscatter anomalies have recently been identified on 20 Ma old oceanic crust in the NW-Atlantic (Figure 1) and detailed investigated for their nature. The anomalies have identified as wide spread lava fields by seafloor observations (by video and hydroacoustics) and sampling (dredging, sediment coring) and have been named as Balerion Lava Fields. Apart from very small cones that presumably mark their eruption centres, they have no bathymetric signature and can only be detected by their acoustic reflectivity relative to the surrounding seafloor. Radiocarbon dating of overlaying sediments indicate a Late Pleistocene age of the flows of less than 50 ky. Balerion glasses have compositions different from other oceanic magmas, being Si-saturated basaltic andesites (MgO ca. 5.9–6.6 wt.%, SiO2 ca. 54.3–55.3 wt.%, total alkalies 3.3–3.9 wt.%) with anomalous depletions in Ca and Fe. Relative to MORB, their incompatible trace element concentrations patterns are steep but HREE depleted, with trace element concentrations lower than in ocean island basalt (OIB) magmas or, with the exception of the heaviest REE, in petit-spot magmas. Such small-volume, high-Si, mafic and highly incompatible-element-enriched magmas will not be formed by simple melting of a peridotite in anhydrous, hydrous or carbonated conditions, in contrast, for example, with the melting process envisaged for petit-spots. Instead they appear to require interactions between a deep-formed alkalic mantle melt and shallow harzburgite. These flows may represent magmas from the lithosphere-asthenosphere boundary and such eruptions may be common in intraplate areas and thus effect

global geochemical budgets, subdbucted plate composition and the availability of hard substrate and chemosynthetic habitats in intraplate regions.

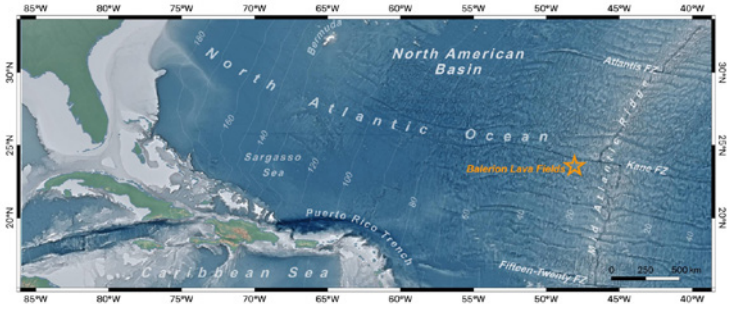

Fig. 1: The position of the Balerion Lava Fields in the framework of the western Atlantic Ocean. The age of the ocean crust is shown by thin white isochrones. The lava fields, sampled during Meteor cruise M139, are located on the 20 Ma old crust but date <50 ka.

M139*

HORIZONTAL AND VERTICAL SMALL-SCALE PATTERNS OF BENTHIC PROTIST COMMUNITIES AT THE ABYSSAL SEAFLOOR

AUTHORS

University of Cologne, Biocenter, Department for Biology, Institute of Zoology, General Ecology | Cologne, Germany

M. Hohlfeld, A. Schoenle, K. Hermanns, H. Arndt

The deep-sea floor is the largest benthic habitat on our planet, covering 65 % of its surface. As it is also the most remote habitat, the deep sea is widely uncharted territory. However, in the last decade it became clear that deep-sea ecosystems are subject to frequent and sudden environmental changes forming an extremely heterogeneous habitat. Bathymetric features such as seamounts, trenches and mid-ocean ridges form a highly complex landscape (Watling et al. 2013).

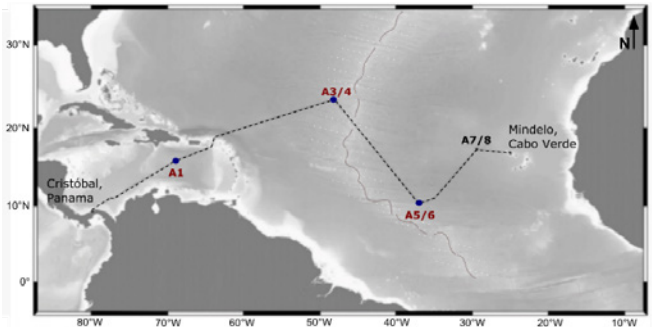

Fig. 1: Station map of Meteor cruise M139 from Cristóbal (Panama) to Mindelo (Cape Verde Islands) in July/ August 2017.

Large-scale sedimentation events of organic material (e. g. macroalgae) have a potential high impact on deep-sea ecosystems as regular carbon input (reviewed by Krause-Jensen and Duarte 2016, Baker et al. 2018). However, how these heterogeneous conditions influence species diversity and distribution in this vast environment is still not known yet, even though this knowledge would possibly give major insights into the ecological function of deep-sea ecosystems and their response to environmental changes. In the present study, we investigated the diversity and distribution of benthic deep-sea nanofauna communities at both, small and large horizontal spatial scales, as well as along a vertical sediment depth gradient at abyssal plains in the Caribbean Sea (15°53.22'N/ 68°53.22'W), the northwestern Atlantic (23°33.23'N/ 48°05.03'W)

and the central Atlantic Ocean (20°38.31'N/ 57°75.68'W) sampled in July and August 2017 during R/V Meteor cruise M139 (Fig. 1).

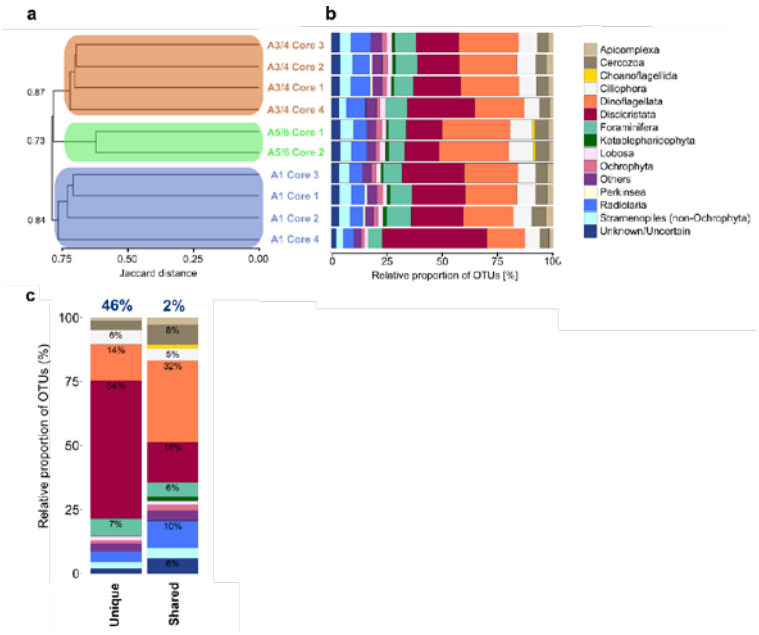

Fig. 2: Deep-sea protist diversity and distribution at horizontal scales. (a) Clusterdendrogram of all surface sediment samples based on the Jaccard index and UPGMA clustering with bootstrap values given at the branching points of the clusters. (b) The relative proportion of OTUs belonging to the major taxonomic groups. (c) Relative proportions of shared and unique OTUs between surface sediment samples assigned to the major taxonomic groups. "Others" = Taxa with a relative abundace of < 1 %. "Unknown/Uncertain" = OTUs which could not be assigned to a taxonomic group. Blue numbers above the bars show the amount of shared and unique OTUs as percentage of the total OTU number.

Illumina HiSeq sequencing of the V9 SSU rDNA resulted in 23,978,215 assembled and filtered reads and 28,166 OTUs assigned to heterotrophic protists. The low average similarity of sequences to reference sequences from the database, show that most benthic deep-sea eukaryotic V9 rDNA diversity have not been molecularly described, yet (Fig. 3). The majority of OTUs were affiliated to Dinoflagellata and Discicristata (Fig. 2, b). Cluster analysis based on the Jaccard index revealed the formation of three main clusters, which represent the three sampling areas, demonstrating differences between the protistan communities of the three deep-sea sites (Fig. 2, a). Only around 2 % of OTUs were found to be shared between all surface sediment samples, whereas 46 % of OTUs only occurred in a single sample (Fig. 2, c). Most of the OTUs shared between sediment cores were affiliated to the group of dinoflagellates (Fig. 2, c),indicating that this group is commonly distributed, whereas most of the OTUs which were unique to one sediment core belonged to the Discicristata (Fig. 2, c), indicating that this group is strongly influenced by the heterogeneity of the deep seafloor.

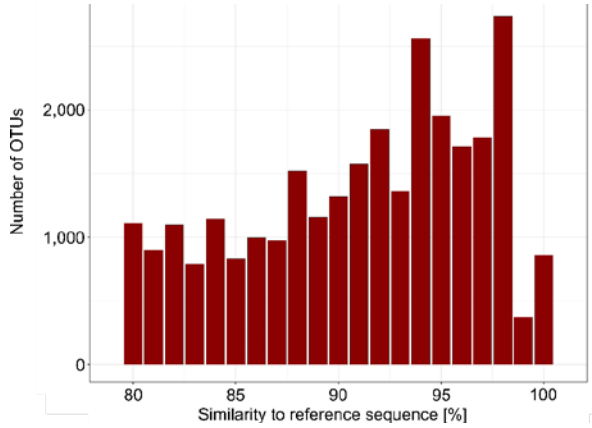

Fig. 3: Relative sequence similarity of OTUs to reference sequences from the PR2 database.

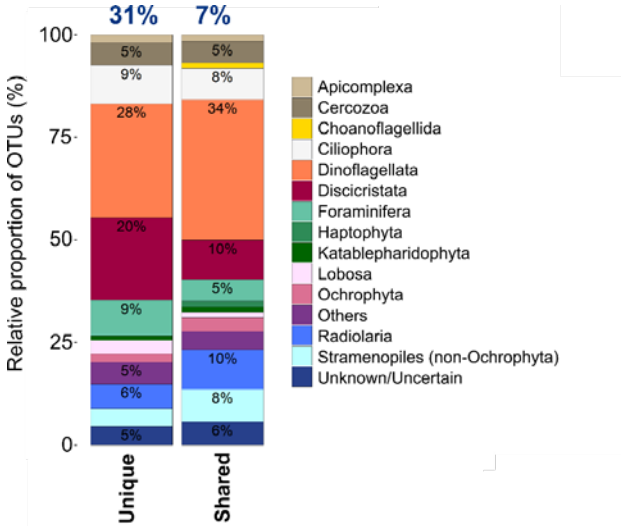

Fig. 4: Relative proportions of shared and unique OTUs between sediment depth layers. OTUs were assigned to the major taxonomic groups. "Others" = Taxa with a relative abundace of < 1 %. "Unknown/Uncertain" = OTUs which could not be assigned to a taxonomic group. Blue numbers above the bars show the amount of shared and unique OTUs as percentage of the total OTU number.

The extremely low amount of OTUs ubiquitously distributed and the high amount of OTUs unique to a single sediment core indicate patterns in the community structure of protists at small spatial scale. Protist community structure was also found to vary along a vertical sediment depth gradient. The amount of OTUs shared between the four different sediment depth layers was low with only 7 % and the proportion of OTUs unique to a single sediment layer was high with around 31 % (Fig. 4), indicating that sediment depth might be a factor shaping protist community composition, possibly leading to unique communities in different depth layers.

REFERENCES

Baker P, Minzlaff U, Schoenle A, Schwabe E, Hohlfeld M, Jeuck A, Brenke N, Prausse, D, Rothenbeck M, Brix S, Frutos I, Jörger KM, Neusser TP, Koppelmann R, Devey C, Brandt A, Arndt H, Potential contribution of surface-dwelling Sargassum algae to deep-sea ecosystems in the southern North Atlantic. Deep Sea Res Part II, 2018, 148, 21–34.

Krause-Jensen D and Duarte CM, Substantial role of macroalgae in marine carbon sequestration, Nature Geoscience 2016, 9, 737–742.

Watling L, Guinotte J, Clark MR and Smith CR, A proposed biogeography of the deep ocean floor, Progress in Oceanography 2013, 111, 91–112.

M139*

VERTICAL DISTRIBUTION OF PARTICLE-ASSOCIATED PROTISTS FROM MARINE PLANKTON COMMUNITIES IN THE NORTH ATLANTIC OCEAN

AUTHORS

University of Cologne, Biocenter, Department for Biology, Institute of Zoology, General Ecology | Cologne, Germany

C. Meyer, A. Schoenle, M.Hohlfeld, R. Meißner, K.Hermanns, H.Arndt

Marine plankton communities play a crucial role in global biogeochemical cycles and eukaryotic microbes are an integral part of them. While the role and importance of phototrophic protists has been widely recognized, the complex ecological functions and food web interactions of heterotrophic protists are still only poorly resolved. Cultivation-based studies have laid the foundation of our knowledge on protist morphology, ecology and taxonomy. The emergence of cultivation independent methods, indicated that cultivation-based approaches are able to recover only a fraction of protist diversity, though isolates can be studied in detail regarding its morphology, physiology and molecular identity. While next-generation sequencing studies have unveiled a vast and hitherto hidden protist diversity in the world's oceans, they too are prone to a range of biases. This study therefore combined a molecular approach based on Illumina HiSeq sequencing of the V9-region of SSU rDNA and a cultivation-based approach in order to study the vertical distribution of heterotrophic protists in marine plankton communities. A total of ten stations, including three open ocean stations in the Caribbean and southern North Atlantic as well as seven stations around the islands of the Azores Archipelago, were examined (Fig. 1). Samples were recovered from a range of depths from surface waters to bathypelagic waters shortly above the sea floor. Both approaches revealed depth-dependent patterns of protist diversity and community structure. The cultivation-based approach recovered a total of 45 distinct morphospecies, which were mainly assigned to Cercozoa, Neobodonida and Bicosoecida. It also yielded in the isolation of 15 strains, most of them belonged to new species. In contrast, the molecular based approach recovered a total of 12073 OTUs, with the majority of them assigned to the Syndiniales, a parasitic order belonging to the Alveolata. Other important taxonomic groups included Dinophyceae, Radiolaria and Euglenozoa.

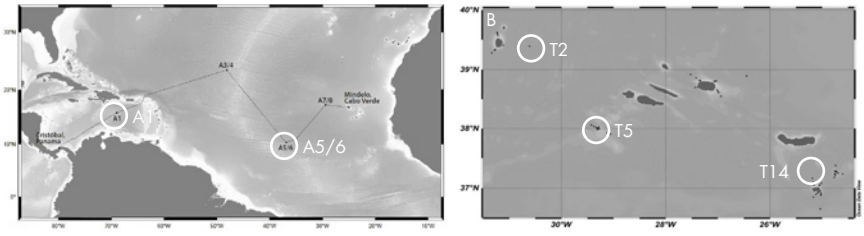

Fig. 1: Station maps of (A) expedition M139, RV Meteor in the North Atlantic Ocean and Caribbean Sea and (B) expedition M150, RV Meteor around the islands of the Azores Archipelago. Water samples were taken at stations A1 and A5/6 (M139) and at stations Flores Island (T2), Princess Alice Bank (T5) and Santa Maria Island (T14). Maps were created with Ocean Data View (Schlitzer, 2012).

We sampled plankton with a CTD-rosette-system at different stations in the Caribbean Sea and for comparison in the North Atlantic during the research cruises M139 and M150 with RV Meteor in 2017 and 2018 (Fig. 1). Abundances of cultivable aggregate-dwelling protists were estimated based upon on positive cultures for the respective morpho-species following MPN methodology (Fig. 2). Genotypes were determined using Sanger sequencing based on the SSU rDNA gene. In parallel, the vertical differences in the community structure based on metabarcoding (Illumina Hiseq, variable V9 region of SSU rDNA, with an enlarged reference database) was studied for the deep chlorophyll maximum layer and bathypelagic depths (Fig. 3).

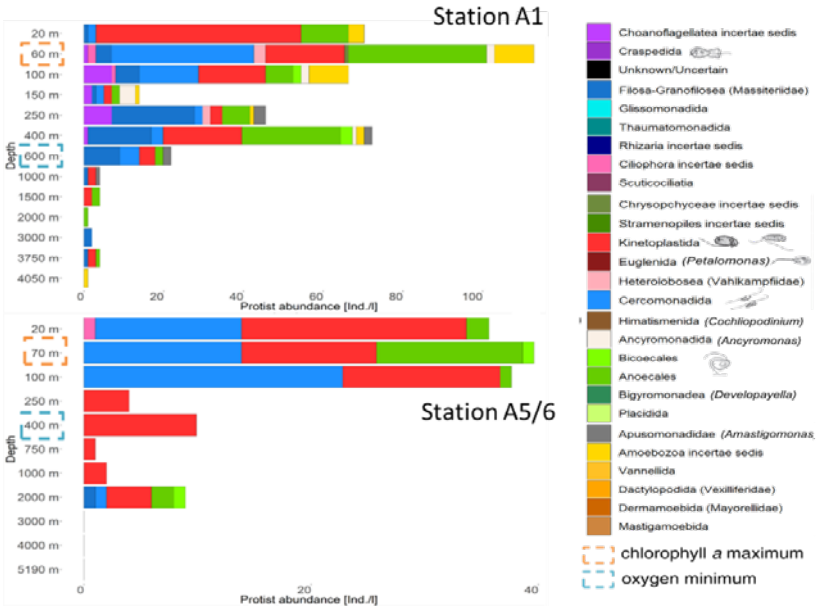

Fig. 2: Vertical depth profiles of protist abundance and community structure at sampling site A1 and A5/6. For each sampled depth 30 culture flasks were qualified and observed morphotypes were noted. Depths corresponding to the chlorophyll a maximum and the oxygen minimum are circled with orange / blue boxes, respectively.

The dominant morphotypes recorded from the depth profiles included rhizarians (mainly cercomonads as well as Massisteria-like specimen) and kinetoplastids (mainly Neobodo and Rhynchomonas) as well as stramenopiles (mainly Cafeteria). The depth profiles from cruise M139 and M150 recorded very similar results (Fig. 3, lower panel). In contrast to earlier studies from the Mediterranean (Arndt et al. 2003), we did not only predominantly observe bodonids and stramenopiles but also many morphotypes belonging to cercozoans. In a few cases we could identify similar morpho- and genotypes in different depth (e. g. Neobodo sp. in 60, 1000 and 1500m depth; Cafeteria burkhardae in 1500 and 2000m depth).

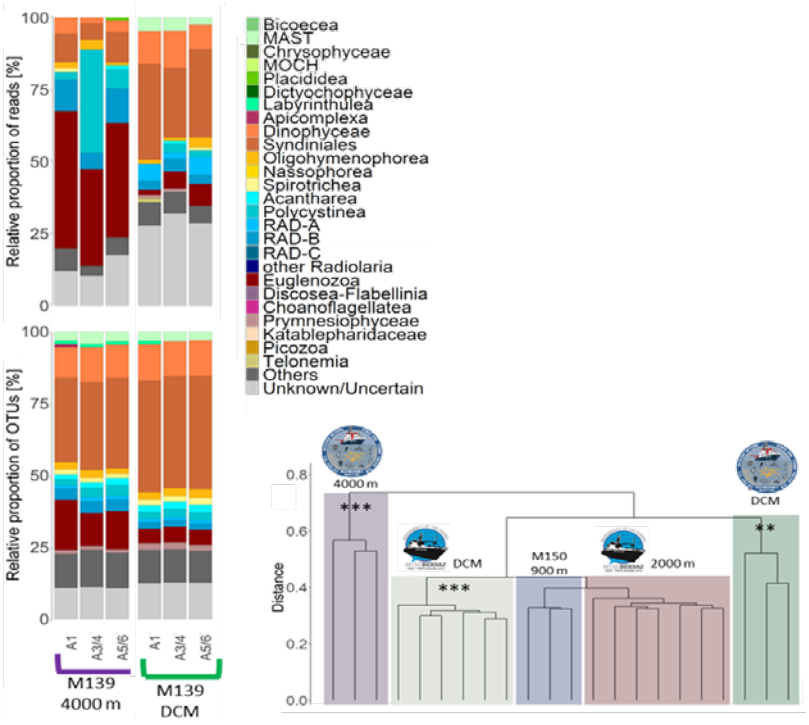

Fig. 3: Community structure of eukaryotes in pelagic samples collected during cruise M139 using NGS metabarcoding. Left: Relative proportions of reads (upper graph) and relative proportions of OTUs (lower graph) with regard to taxonomic composition. Phototrophic divisions, plants (Streptophyta), Fungi and Metazoa were excluded from the dataset. "Unknown": reads/OTUs which could not be assigned to a taxonomic division. "Others": taxa with a relative abundance of < 1 % in reads. Below: Cluster dendrogram based on Jaccard distance for taxonomic composition of community structures obtained from M139 and M150, using rarefied reads and the unweighted pair group method with arithmetic mean (UPGMA). Asterisks indicate significant clusters revealed through PERMANOVA (levels of significance: ** = $p \leq 0.01$, *** $p = \leq 0.001$).

REFERENCES

Alldredge AL, Silver MW, Characteristics, Dynamics and Significance of Marine Snow. Prog. Oceanogr. 1988, 20, 41–82.

Arndt H, Hausmann K, Wolf M, Deep-sea heterotrophic nanoflagellates of the Eastern Mediterranean Sea: qualitative and quantitative aspects of their pelagic and benthic occurrence, Marine Ecology Progress Series 2003, 256, 45–56, doi: 10.3354/meps256045.

Caron DA, Davis PG, Madin LP, Sieburth JM. Heterotrophic bacteria and bacterivorous protozoa in oceanic macroaggregates. Science, 1982; 218(4574):795–7.

de Vargas C, Audic S, Henry N, Decelle J, Mahé F, et al. Eukaryotic plankton diversity in the sunlit ocean. Science 2015, 348, 1261605, doi: 10.1126/science.1261605.

Schlitzer R, Ocean Data View, 2012, http://odv.awi.de.

M139*

OCCURRENCE OF ABYSSAL MEGAFAUNA IN THE SOUTHERN NORTH ATLANTIC

AUTHORS

University of Cologne, Biocenter, Department for Biology, Institute of Zoology, General Ecology | Cologne, Germany
D. Scepanski, J. Werner, H. Arndt

GEOMAR Helmholtz Centre for Ocean Research Kiel | Kiel, Germany
N. Augustin

CIIMA – Interdisciplinary Centre of Marine and Environmental Research University of Porto | Porto, Portugal
J. R. Xavier

Deep-sea ecosystems, limited by their inability for primary production as a source of carbon, rely on other sources to maintain life. According to observations made during our last expedition crossing the southern North Atlantic (VEMA Transit expedition SO237 in 2015, Brandt et al. 2018, Baker et al. 2018, Devey et al. 2018), we hypothesized that sedimentation of large mats of the surface dwelling brown algae Sargassum is an underestimated phenomenon that can cause potential regular carbon input to deep-sea ecosystems. The importance of organic material as both a food source and habitat for sessile taxa on the ocean's deep-sea floor was highlighted by several authors (e. g. Grassle & Morse-Porteous 1987, Johnson et al. 2007). Usually the origin of such organic material is not well defined. To determine the potential for this carbon flux, a literature survey of previous studies was conducted that estimated the abundance of surface water Sargassum (Baker et al. 2018). We compared these estimates with quantitative analyses of sedimented Sargassum appearing on photos taken with the OFOS camera system during the M139 expedition. The OFOS camera system was equipped with a camera in a downward looking position to collect close-up views of the megafauna and sedimented algae of the deep-sea floor. Laser pointers allowed the quantification of the observed seafloor areas. Furthermore, we quantified the associated megafauna and analyzed the vertical distribution of megafauna along a mapped seamount west of the Cape Verde islands.

Four benthic surveys were conducted using the OFOS camera system at station A3/4 (two surveys, about 4000 m depth), station A5/6 (one survey, about 5100 m depth) and station A7/8 (one survey on a seamount from 1355 down to 3218 m depth) (Fig. 1). During each dive, 4–8 hours of video recording from high definition videos (calibrated

screen by the presence of lasers) were taken. In the home laboratory, hundreds of still images were captured manually in order to estimate the abundance and biovolume of Sargassum and megafauna species abundance and diversity along each transect. Annotated data per still image included taxa occurrence, position, depth and substrate type. The still images covered about 90 % of the total length of transects at the bottom. Collected footage was of high quality due to a wide visual field (4–10 m^2) and waters of low turbidity. Organisms were counted and identified to the lowest possible taxon level.

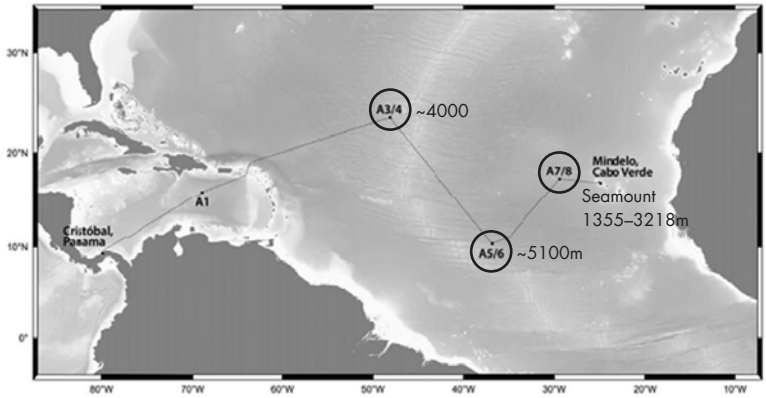

Fig. 1: Station map of Meteor cruise M139 from Cristóbal (Panama) to Mindelo (Cape Verde Islands) in July/August 2017. Red circles mark the areas of OFOS deployments

The analysis of the videos taken from the abyssal communities at areas A3/4, A5/6 and A7/8 revealed a relatively diverse megafauna (Figs. 2,3). The megafauna (we considered organisms generally larger than 10 cm in length) observed comprised anemones, glass sponges, holothurians, starfish, crinoids, shrimps, coryphaenoid fish among others.

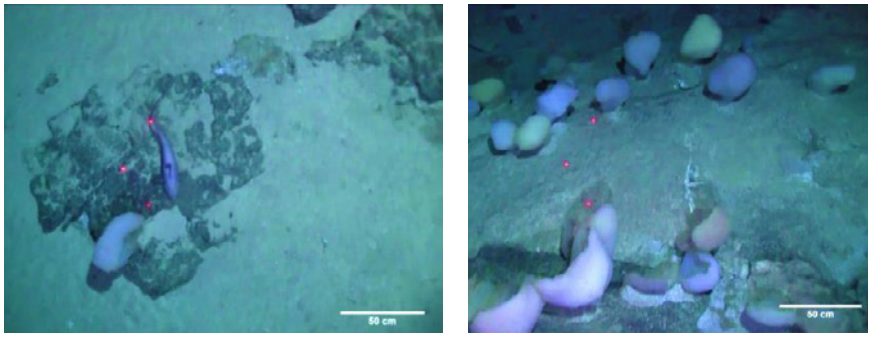

Fig. 2: OFOS video-graphs from the deep-sea floor at area A7/8 showing glass sponges (Poliopogon amadou) and a coryphenoid fish.

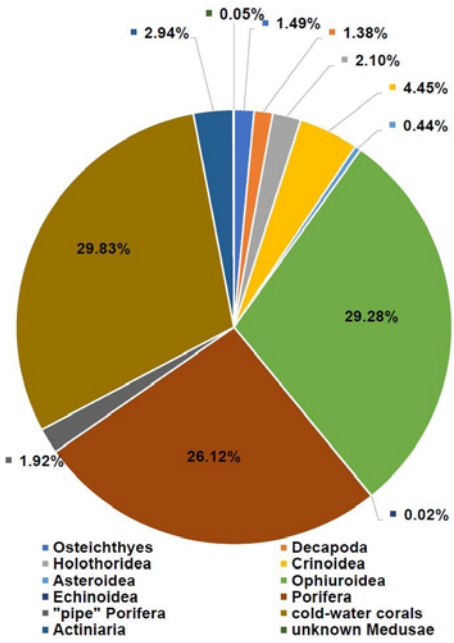

Fig. 3: Megafauna composition recorded from the four OFOS deployments in the southern North Atlantic.

Significantly higher megafauna abundances were observed at the seamount (Fig. 4) including inter alia dense aggregation of Poliopogon amadou (Hexactinellida) and cold-water corals. Cold-water corals and Poliopogon amadou, dominating different seamount areas, were associated with specific fauna (specific fish species, sponges, and holothurians). In addition, we could report on habitat/substrate preferences for Osteichthyes, Ophiuroidea, Crinoidea, Holothuroidea, cold-water corals and sponges. Sargassum may serve as a habitat and a food source (e. g. Holothuroidea) for abyssal (epi-) megafauna. The data indicated a relatively high abundance of megafauna associated to Sargassum flocs. (Scepanski et al., in manus). Especially in area A5/6, we observed high densities of Sargassum. Interestingly, all stages of degradation of Sargassum were observed comprising freshly sedimented mats, algal mats which were sucked into the sediment by megafauna, and mats with surrounding anaerobic microbial mats. These different stages of degradation indicated the continuous sedimentation process. We could observe the process of sequential degradation and sedimentation in the deep sea for the first time. The accumulation of Sargassum represents a potentially large and consistent carbon flux to deep-sea ecosystems (Baker et al. 2018). While the particular abundance and nature of holopelagic Sargassum is relatively unique to the North Atlantic (particularly the Sargasso Sea), the mechanism of large-scale sedimentation of macrophytes as a carbon flux is an important finding and could be translated through the world's oceans (Krause-Jensen & Duarte 2016). This relatively high input of carbon could than also lead to relatively high abundances of megafauna at regions receiving high input. We intend to apply for a separate expedition to investigate this unexplored phenomenon in future.

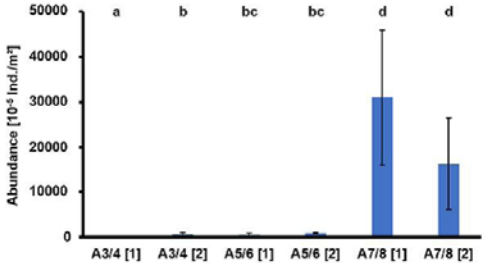

Fig. 4: Total megafauna abundance of the abyssal seafloor stations (Mean ± SE); Letters above the bars mark significant differences between the total megafauna abundances of each area; ANOVA (P-value < 0.001, F-value 64.89, n=3).

REFERENCES

Baker P, Minzlaff U, Schoenle A, Schwabe E, Hohlfeld M, Jeuck A, Brenke N, Prausse, D, Rothenbeck M, Brix S, Frutos I, Jörger KM, Neusser TP, Koppelmann R, Devey C, Brandt A, Arndt H, Potential contribution of surface-dwelling Sargassum algae to deep-sea ecosystems in the southern North Atlantic. Deep Sea Res Part II, 2018, 148, 21–34.

Brandt A, Frutos I, Bober S, Brix S, Brenke N, Guggolz T, Heitland N, Malyutina M, Minzlaff U, Riehl T, Schwabe E, Zinkann A-C, Linse K, Composition of abyssal macrofauna along the Vema Fracture Zone and the hadal Puerto Rico Trench, northern tropical Atlantic. Deep Sea Research Part II, 2018,148, 35–44.

Devey CW, Augustin N, Brandt A, Brenke N, Köhler J, Lins L, Schmidt C, Yeo IA, 2018. Habitat characterization of the Vema Fracture Zone and Puerto Rico Trench. Deep Sea Res Part II, 2018, 148, 7–20

Grassle JF, Morse-Porteous LS, Macrofaunal colonization of disturbed deep-sea environments and the structure of deep-sea benthic communities. Deep Sea Research Part A 1987, 34, 1911–1950.

Johnson NA, Campbell JW, Moore TS, Rex MA, Etter RJ, McClain CR, Dowell MD, The relationship between the standing stock of deep-sea macrobenthos and surface production in the western North Atlantic. Deep. Res. Part I, 2007, 54, 1350–1360.

Krause-Jensen D, Duarte CM, Substantial role of macroalgae in marine carbon sequestration, Nature Geoscience 2016, 9, 737–742.

M139*

GLOBAL COMPARISON OF BICOSOECID CAFETERIA-LIKE FLAGELLATES FROM THE DEEP OCEAN AND SURFACE WATERS

AUTHORS

University of Cologne, Biocenter, Department for Biology, Institute of Zoology, General Ecology | Cologne, Germany
A. Schoenle, M. Hohlfeld, M. Rosse, P. Filz, F. Nitsche, H. Arndt

Friedrich-Loeffler-Institut, Federal Research Institute for Animal Health, Institute of Diagnostic Virology | Greifswald – Insel Riems, Germany
C. Wylezich

Cafeteria species are very common and might be ecologically significant heterotrophic nanoflagellates as bacterial consumers due to its high abundances in the marine environment (e. g. Fenchel and Patterson 1988).

We could isolate and cultivate 29 Cafeteria-like strains from surface waters and from the deep sea at different parts of the ocean including the Atlantic Ocean, Mediterranean Sea, Indian Ocean, Pacific and Baltic Sea. This gave us the chance to reanalyze the taxonomy and the phylogenetic relationships within the Cafeteriaceae. Morphological characterization obtained by high resolution microscopy revealed only small differences between the strains (Fig. 1). Sequencing the type material of the type species C. roenbergensis (CCAP 1900/1) and molecular analyses (18S rDNA, 28S rDNA) of newly isolated strains resulted in a revision and separation of the Cafeteriaceae into two known species (C. roenbergensis, C. mylnikovii) and six new species (C. maldiviensis, C. biegae, C. loberiensis, C. chilensis, C. graefeae, C. burkhardae). Many deposited Cafeteria sequences at GenBank and most of our own sequences clustered within one clade (C. burkhardae) with a p-distance of 5% to strain CCAP 1900/1. Only C. maldiviensis clustered together with the type species C. roenbergensis. A strain from the Angola Basin had a p-distance of 10% to Cafeteria species and clustered separately within the Anoecales requiring the erection of a new genus, Bilabrum gen. nov., with B. latius sp. nov. as type species.

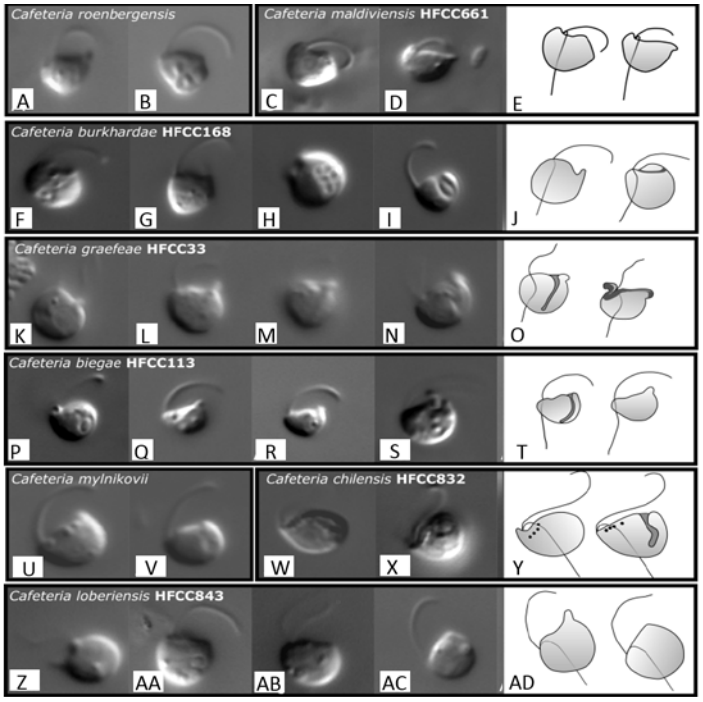

Fig. 1: Differential interference contrast micrographs of Cafeteria roenbergensis CCAP 1900/1 (A, B; type population), C. maldiviensis HFCC661 (C-E), C. burkhardae HFCC168 (F-J), C. graefeae HFCC33 (K-O), C. biegae HFCC113 (P-T), C. mylnikovii CCAP 1900/2 (U-V), C. chilensis HFCC832 (W-Y), C. loberiensis HFCC843 (Z-AD). Scale bar represents 1 µm. Adapted from Schoenle et al., in revision, European Journal of Protistology.

Furthermore, we analyzed the read abundance of operational taxonomic units (OTUs) taxonomically assigned to Cafeteria species with a V9 sequence similarity of 100% to investigate the distributional pattern of the different Cafeteria species within our own next-generation-sequencing (NGS) deep-sea dataset. This deep-sea dataset consisted of reads obtained from deep-sea sediment samples at 20 stations (Fig. 2 A) in the Atlantic (M139, SO 237) and Pacific Ocean (SO 223T) from bathyal, abyssal and hadal regions.

Concerning ecology and distribution of the members of the Cafeteriaceae, the clade of Cafeteria biegae could only be isolated from the Mediterranean Sea, while the two strains of C. graefeae (HFCC33 and HFCC772) were only found in samples from the Atlantic Ocean. While C. maldiviensis (HFCC661) could only be isolated from the Indian Ocean, we could recover V9 sequences with 100% sequence similarity to C. maldiviensis in 19 out of 20 deep-sea stations (Fig. 2 A–E). Cafeteria burkhardae, on the other hand, seems to have a cosmopolitan distribution in brackish and marine environments, in surface waters as well as in the deep sea, which is underlined by our cultivation approach as well as by our next-generation-sequencing results of sediment at 20 different deep-sea stations (Fig. 2).

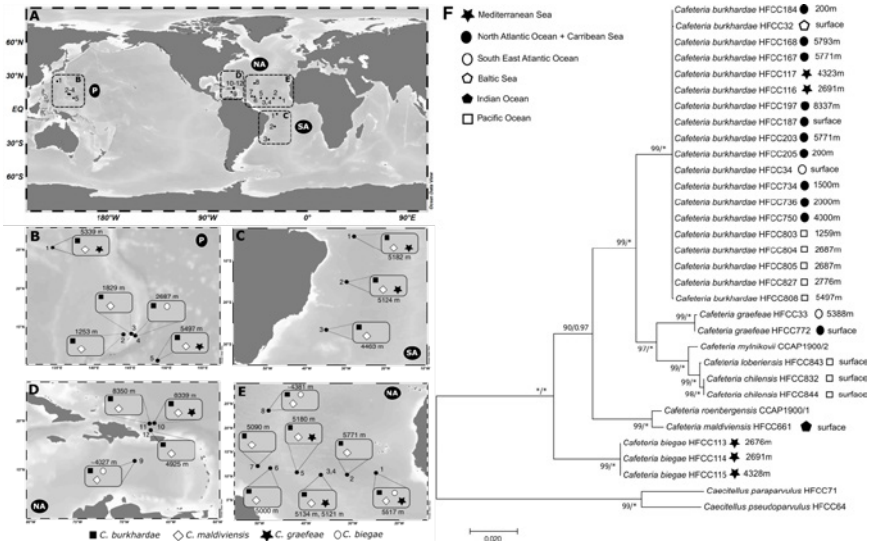

Fig. 2: Differential interference contrast micrographs of Cafeteria roenbergensis CCAP 1900/1 (A, B; type population), C. maldiviensis HFCC661 (C-E), C. burkhardae HFCC168 (F-J), C. graefeae HFCC33 (K-O), C. biegae HFCC113 (P-T), C. mylnikovii CCAP 1900/2 (U-V), C. chilensis HFCC832 (W-Y), C. loberiensis HFCC843 (Z-AD). Scale bar represents 1 µm. Adapted from Schoenle et al., in revision, European Journal of Protistology.

We found that a great proportion of environmental sequence V9 reads from our 20 analyzed deep-sea communities belonged to Cafeteria burkhardae with a 100% sequence similarity. A high proportion of reads obtained by next-generation sequencing (NGS) could also be assigned to Cafeteria burkhardae within the Tara Ocean global eukaryotic plankton survey (see Supplement Database W5 in de Vargas et al. 2015). Our phylogenetic/evolutionary placement analysis (EPA) revealed that most of the OTU representative sequences assigned to Cafeteria (sequence similarity 80–100%) within our deep-sea study and the Tara Ocean project could actually be placed to the C. burkhardae clade.

The discovery and analysis of new bicosoecids and utilizing more sequences and comparative morphological descriptions as well as multigene analysis are essential to reconstruct a more robust evolutionary relationship within the bicosoecids and might result in a higher resolution e. g. of Bilabrum latius strain HFCC35.

Cafeteria and related species are very common and might be the ecologically most significant heterotrophic nanoflagellates in marine environments.

REFERENCES

de Vargas C, Audic S, Henry N, Decelle J, Mahé F, Logares R, Lara E, Berney C, et al., Eukaryotic plankton diversity in the sunlit ocean. Science 2015, 348, 1261605, doi: 10.1126/science.1261605.

Fenchel T, Patterson DJ, Cafeteria roenbergensis nov. gen., nov. sp., a heterotrophic microflagellate from marine plankton. Mar. Microb. Food Webs 1988, 3, 9–19.

Schlitzer R, Ocean Data View, 2012, http://odv.awi.de.

Živaljić S, Schoenle A, Nitsche F, Hohlfeld M, Piechocki J, Reif F, Shumo M, Weiss A, Werner J, Witt M, Voss J, Arndt H (2018) Survival of marine heterotrophic flagellates isolated from the surface and the deep sea at high hydrostatic pressure: Literature review and own experiments. Deep-Sea Res Part II Top Stud Oceanogr 148: 251–259. http://doi.org/10.1-016/j.dsr2.2017.04.022

M139*

HIGH AND SPECIFIC DIVERSITY OF BENTHIC PROTISTS IN DEEP-SEA BASINS

AUTHORS

University of Cologne, Biocenter, Department for Biology, Institute for Zoology, General Ecolog | Cologne, Germany

A. Schoenle, M. Hohlfeld, K. Hermanns, F. Nitsche, H. Arndt

Marine heterotrophic flagellates are a major component within the microbial food web and are important nutrient remineralizers in biogeochemical cycles in surface waters (Caron et al., 1999). Considering the order of geographic magnitude of the deep sea and the potentially importance of protists within these vast ecosystem, the ecological function, species-level distribution and diversity of deep-sea protist communities is scant. Genetic approaches like Next-Generation Sequencing (NGS) and clone libraries have turned out to be reliable tools in identifying previously unknown protistan lineages in surface waters and the deep sea (e. g. Edgcomb et al., 2011; Massana et al., 2014). Most benthic deep-sea studies focused on assumed hot spots in the deep-sea like hydrothermal vents, cold seeps and anoxic basins at bathyal depths (e. g. Edgcomb et al., 2009; Stoeck et al., 2003). Investigations on benthic deep-sea protists from the abyss (3–6 km), covering 54% of the Earth's surface, and hadal regions (< 6 km) are scarce (Scheckenbach et al., 2010).

To assess their diversity we collected 27 sediment samples at 20 stations from deep-sea basins in the Atlantic (M139, SO 237) and Pacific Ocean (SO 223T) (Fig. 1A, B) to conduct a comparative analysis from benthic deep-sea protist communities on a global and local spatial scale approach at different depths (mainly abyssal regions) by sequencing the hypervariable V9 region of the 18S rDNA. Clustering and filtering led to a final eukaryotic dataset of 46,694 OTUs (~70 million reads) of which 87% (40,623 OTUs, ~55 million reads) could be assigned to protists (excluding ~2,300 phototrophic protist OTUs) using an in-house reference database called V9_DeepSea.

Of our final protist OTUs only 2.4% were 100% identical to reference sequences. On average protist OTUs had only a 90.4% match with reference sequences indicating the existence of new lineages and the potential of a specific protist fauna in the deep sea, especially within the Discoba (Fig. 1D).

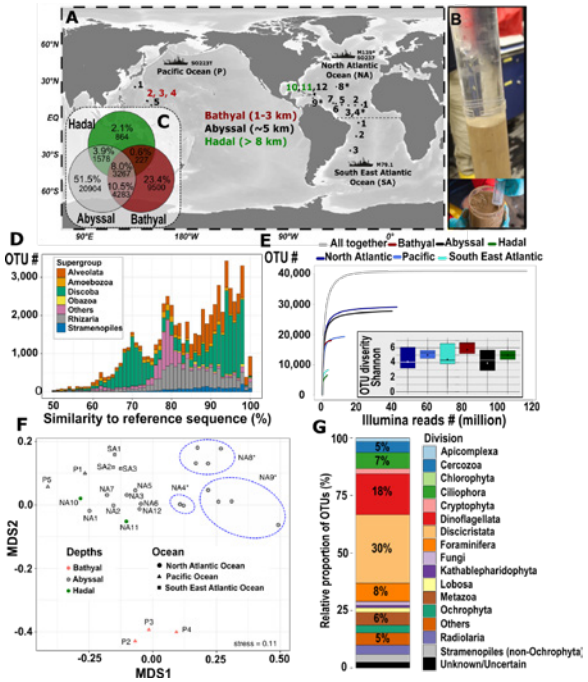

Fig. 1: Heterotrophic deep-sea protist diversity and distribution. (A) Sampling map of the 20 examined deep-sea stations from bathyal, abyssal and hadal regions. Multiple sediment samples were taken at stations marked with an asterisk for the investigation of small scale distribution patterns. In the North Atlantic Ocean (NA) samples were collected during two expeditions (one in summer (marked with asterisk), one in winter). (B) Only the upper 2 mm of undisturbed sediment from cores of the Multi-Corer (MUC) were taken with a sterile syringe. (C) Venn-Diagram showing the number of unique and shared OTUs between the three different depth zones. (D) Similarity of rDNA richness to total referenced eukaryotic rDNA diversity in the V9_DeepSea database. Proportion of OTUs per eukaryotic supergroup is color-coded. (E) V9 rDNA protist OTUs rarefaction curves and overall diversity (Shannon index, inset) from either region dependent or depth dependent clustering of all stations. (F) Grouping of deep-sea protist communities according to taxonomical compositional similarity (binary Jaccard distances) using nonlineal multidimensional scaling. (G) Relative proportion of OTUs of all the 27 deep-sea sediment samples (20 stations) related to the major taxonomic protist groups.

We almost reached sampling saturation of heterotrophic protist OTUs considering all sampled stations (Fig. 1E). Only 8% of the OTUs were shared between the three different depth zones, while over half of them (51.5%) could only be detected in abyssal sediments (Fig. 1C). The incidence-based clustering using nonlinear multidimensional scaling of the 27 sediment samples showed a high dissimilarity between all the stations (Fig. 1F). In all 27 stations Discicristata, Dinoflagellata, Foraminifera and Ciliophora showed the highest protist richness (number of OTUs, Fig. 1G). Only 0.6% of the total protist OTUs were shared among all 27 sediment samples, while about 59% of the OTUs detected in this study were unique to one station indicating the potential existence of highly endemic protist communities in deep-sea sediments. The majority of shared OTUs with 29% belonged to the Dinoflagellata, while half of the unique OTUs could be assigned to Discicristata including e. g. diplonemids, euglenids and kinetoplastids. This relative proportion of unqiue OTUs was also consistent within the three depth zones.

Within our study there exists an extremely high diversity of protists in the deep sea with large local differences between individual sediment samples. This indication of a potentially high global diversity of protists with a major fraction of heterotrophic protists might make them good indicators of changes in environmental conditions in the abyss. Investigating the diversity and distribution of natural microbial communities in Earth's largest habitat is critical to our understanding of global biogeochemical cycles. Unique techniques and large-scale studies, as well as long-term surveys/time series, may further elucidate the diverse composition of deep-sea microbial communities over both space and time.

REFERENCES

Caron D, Peele E, Lim E, Dennett M, Picoplankton and nanoplankton and their trophic coupling in surface waters of the Sargasso Sea south of Bermuda. Limnology and Oceanography 1999, 44, 259–272, doi: 10.4319/lo.1999.44.2.0259.

Edgcomb V, Orsi W, Leslin C, Epstein S, Bunge J, Jeon S, Yakimov M, Behnke A, Stoeck T, Protistan community patterns within the brine and halocline of deep hypersaline anoxic basins in the eastern Mediterranean Sea. Extremophiles 2009, 13, 151–167, doi: 10.1007/s00792-008-0206-2.

Edgcomb, V., Orsi, W., Taylor, GT, Vdacny, P, Taylor, C, Suarez, P, Epstein, S, 2011. Accessing marine protists from the anoxic Cariaco Basin. ISME Journal 5, 1237, doi: 10.1038/ismej.2011.10.

Massana R, del Campo J, Sieracki M, Audic S, Logares R, Exploring the uncultured microeukaryote majority in the oceans: reevaluation of ribogroups within stramenopiles, ISME Journal 2014, 8, 854–866, doi: 10.1038/ismej.2013.204.

Scheckenbach F, Hausmann K, Wylezich C, Weitere M, Arndt H, Large-scale patterns in biodiversity of microbial eukaryotes from the abyssal sea floor, Proceedings of the National Academy of Sciences of the United States of America 2010, 107, 115–120, doi: 10.1073/pnas.0908816106.

Schoenle A, Nitsche F, Werner J, Arndt H, Deep-sea ciliates: Recorded diversity and experimental studies on pressure tolerance. Deep-Sea Research Part I, 2017, 128: 55–66, doi: 10.1016/j.dsr.2017.08.015.

Stoeck, T, Taylor, GT, Epstein, SS, Novel eukaryotes from the permanently anoxic Cariaco Basin (Caribbean Sea). Applied and Environmental Microbiology 2003, 69, 5656–5663, doi: 10.1128/AEM.69.9.5656.

M139*

INFLUENCE OF HYDROSTATIC PRESSURE ON THE BEHAVIOUR OF THREE CILIATE SPECIES ISOLATED FROM THE DEEP SEA

AUTHORS

University of Cologne, Institute of Zoology, General Ecology | Cologne, Germany
S. Živaljić, A. Schoenle, A. Scherwass, M. Hohlfeld, F. Nitsche, H. Arndt

The deep sea is an extreme environment with uniform conditions such as low temperatures and food resources, permanent darkness and high pressure. Despite these extreme conditions, the deep sea is inhabited by a large variety of organisms which have become evolutionary adapted to this environment. It is well known, that in shallow benthic and pelagic ecosystems protists are very important for the energy transfer in aquatic food webs. Regarding protists in the deep sea and their potential importance within the deep-sea microbial food web, little is known. Aside from some heterotrophic flagellates, only a very few ciliates and foraminiferans isolated from surface waters and the deep sea were able to survive high hydrostatic pressures (Turley et al. 1988; Schoenle et al. 2017, 2019; Živaljić et al. 2018). Concerning ciliates, it was shown that deep-sea strains of Pseudocohnilembus persalinus and Uronema sp. and one surface strain of P. persalinus were able to survive better at 557 bar at lower temperature (2 °C) than at higher temperature (13 °C) (Schoenle et al. 2017). Still, there is a lack of pressure studies on protists isolated from the deep sea, because most studies were based on protists inhabiting the euphotic zone. So far, only a few ciliates have been collected from the deep sea and cultivated later successfully under laboratory conditions. Data on ciliates isolated from the deep sea are scarce and mostly based on molecular surveys (Schoenle et al. 2017, Živaljić et al. in revision). However, metagenome data already indicated that ciliates may form a very diverse component of deep-sea communities (Edgcomb et al. 2002).

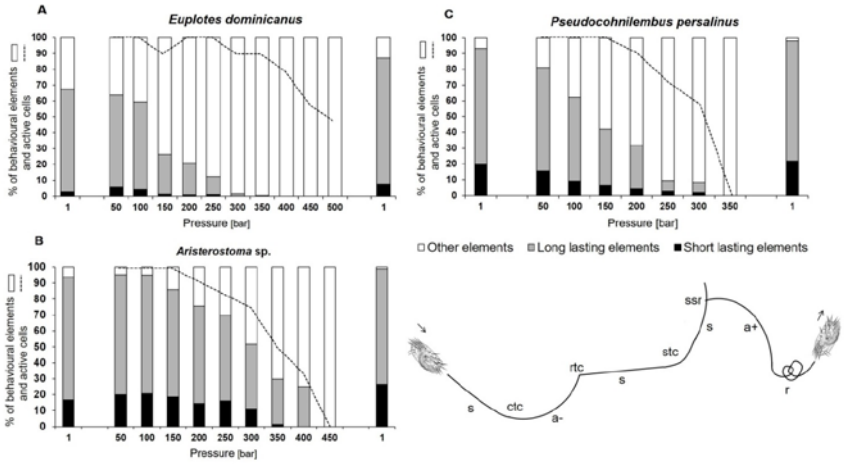

Fig. 1: A-C The percentage of behavioural elements and active cells recorded for total observation time for three deep-sea ciliates Euplotes dominicanus (A), Aristerostoma sp. (B) and Pseudocohnilembus persalinus (C) during pressure and control treatments (1 bar) (Temp.= 4°C, n = 10–12). The behavioural elements are indicated as columns and active cells as dashed lines. The schematic drawing below the legend shows the short lasting elements (continuous trajectory change, ctc; smooth trajectory change, stc; rough trajectory change, rtc; side-stepping reaction, ssr) and the long lasting elements (linear segment, s; rightward arc, a+; leftward arc, a-). The rotation (r) is an example for other elements (from Živaljić et al. subm.)

Three species of ciliates were isolated from the deep sea (≥ 4000 m) during the cruise M139: Pseudocohnilembus persalinus, Euplotes dominicanus and Aristerostoma sp. Locomotion is considered to be the main form of expression of ciliate behaviour regarding their overall life activity. But how ciliates behave under deep-sea conditions is still unclear. Data on the occurrence of ciliates in the deep sea are scarce and mostly based on molecular studies. We observed the behaviour of the three deep-sea isolates directly under high hydrostatic pressures up to 500 bar using a pressure chamber system that allows for direct observation using an inverted microscope equipped with a high-speed camera system. For all three ciliates, the typical behavioural elements were observed at least at a pressure of up to 200 bar. For all three isolated deep-sea ciliates, additional long-term survival experiments were carried out within 6 days at 200, 350 and 430 bar. Several specimens showed an ability to survive for several days at the highest pressure and to recover from pressure release (returning to their normal movement) indicating their barotolerance. Our results suggest that ciliates are active in the deep sea even in regions deeper than 2000 m and might be an important part of the deep-sea microbial food web.

REFERENCES

Edgcomb VP, Kysela DT, Teske A, de Vera Gomez A, Sogin ML, Benthic eukaryotic diversity in the Guaymas Basin hydrothermal vent environment, Proceedings of the National Academy of Sciences of the United States of America 2002, 99, 7658–7662, doi: 10.1073/pnas.062186399.

Schoenle A, Nitsche F, Werner J, Arndt H, Deep-sea ciliates: Recorded diversity and experimental studies on pressure tolerance, Deep-Sea Research Part I Oceanographic Research Papers 2017, 128, 55–66, doi: 10.1016/j.dsr.2017.08.015.

Schoenle A, Živaljić S, Prausse D, Voß J, Jakobsen K, Arndt H, New phagotrophic euglenids from deep sea and surface waters of the Atlantic Ocean (Keelungia nitschei, Petalomonas acorensis, Ploeotia costaversata), European Journal of Protistology 2019, 69, 102-116, doi: 10.1016/j.ejop.2019.02.007.

Turley CM, Lochte K, Patterson DJ, A barophilic flagellate isolated from 4500 m in the mid-North Atlantic, Deep-Sea Research 1988, 35, 1079–1092, doi: 10.1016/0198-0149(88)90001-5.

Živaljić S, Scherwass A, Schoenle A, Hohlfeld M, Quintela-Alonso P, Nitsche F, Arndt H (in revision) A barotolerant ciliate isolated from the abyssal deep-sea of the North Atlantic: Euplotes dominicanus sp. n. (Ciliophora, Euplotia) (in revision)

Živaljić S, Schoenle A, Nitsche F, Hohlfeld M, Piechocki J, Reif F, Shumo M, Weiss A, Werner J, Witt M, Voss J, Arndt H, Survival of marine heterotrophic flagellates isolated from the surface and the deep sea at high hydrostatic pressure: Literature review and own experiments. Deep-Sea Research Part II Topical Studies in Oceanography 2018, 148, 251–259, doi: 10.1-016/j.dsr2.2017.04.022.

M139*

THE FIRST BAROTOLERANT CILIATE ISOLATED FROM THE ABYSSAL DEEP-SEA OF THE NORTH ATLANTIC: EUPLOTES DOMINICANUS SP. N. (CILIOPHORA, EUPLOTIA)

AUTHORS

University of Cologne, Institute of Zoology, General Ecology | Cologne, Germany
S. Živaljić, A. Scherwass, A. Schoenle, M. Hohlfeld, F. Nitsche, H. Arndt

Complutense University of Madrid, Faculty of Biology, Department of Genetics, Physiology and Microbiology | Madrid, Spain
P. Quintela-Alonso

The deep-sea benthic environment is one of the most diverse and extended habitats on Earth with a high richness of deep-sea micro-eukaryotes as revealed from environmental DNA surveys (Scheckenbach et al. 2010). Ciliates are considered as a major and active microeukaryote group in microbial mats of cold-seep sediments based on environmental DNA/RNA surveys. Still, very little is known about the benthic eukaryotic communities from abyssal depths, though our recent survey of available data indicated that ciliates may form a very diverse component of deep-sea communities (Schoenle et al. 2017). So far, only a very few ciliates have been collected from the deep sea and cultivated later successfully in laboratory conditions. The reason for this may be the potentially low abundances of ciliates in the deep sea, or the hydrostatic stress during sampling (deep sea to the surface). Using multiple cultivation efforts on board as well as high resolution light and electron microscopy in the home laboratory, we were able to isolate and cultivate several deep-sea ciliates. To our knowledge, this is the first time that Euplotes dominicanus, a new ciliate species from abyssal depths (>4000 m) was isolated, successfully cultivated and morphologically characterized alive. Moreover, the 18S rRNA was analyzed to estimate the phylogenetic position of E. dominicanus. In addition, the survival ability at high hydrostatic pressure (up to 500 bar) of the newly described Euplotes species was investigated. We also analyzed its occurrence based on the V9 region of the 18S rRNA in metabarcoding data sets obtained from 12 deep-sea basins of the North-Atlantic, South-West Atlantic and Pacific Ocean (M139, M79, S223T, SO 237) to check the possible occurrence in other deep-sea regions.

Euplotes dominicanus sp. n. is characterized by a small body size (29–40 × 17–27 µm in vivo), 18–22 adoral membranelles, 10 frontoventral, five transverse and two left marginal cirri and one caudal cirrus, five or six dorsolateral kineties with 7–9 dikinetids in mid-dorsolateral kinety (DK3), and dorsal silverline system of the

double-eurystomus type (Fig. 1A-D). Phylogenetic analyses inferred from 18S rRNA sequences show that Euplotes dominicanus sp. n. is most closely related to E. curdsi, with a sequence similarity of 97.6%. Euplotes dominicanus sp. n. was able to survive hydrostatic pressures up to 500 bar indicating its barotolerance (Fig. 2). The hypervariable V9 region of the 18S rRNA used to target environmental diversity of microbial eukaryotes was used in next generation sequencing studies to search for the presence of E. dominicanus in sediments of different deep-sea basins. We could confirm that sequences being 100% identical to the V9 region of the 18S rRNA of E. dominicanus were present in six out of 12 deep-sea basins in the Atlantic and in the Pacific Ocean Fig. 3). A 100% identity regarding the V9 region does not mean that sequences belong to exactly the same species, however, our study might indicate that Euplotes species at least very similar to E. dominicanus are not seldom and might be a component of deep-sea microbial communities. In contrast, we did not find sequences being 100% identical to the V9 region of the 18S rRNA of E. dominicanus in the database of surface-water samples from the Tara Ocean project. We compared the similarity of the V9 region of E. dominicanus sequence with all other Euplotes sequences available in GenBank. Our results show that E. dominicanus has a unique and specific V9 region, only found in this species of all currently available sequences from species within the genus Euplotes.

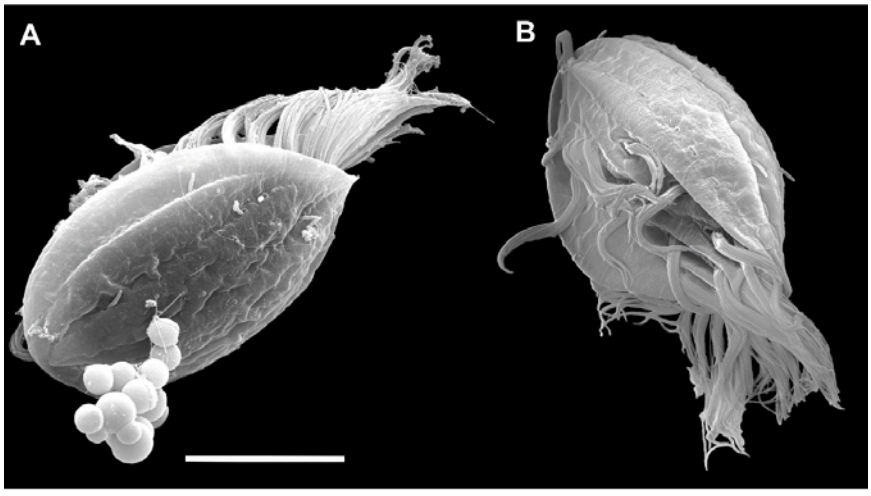

Fig. 1: Euplotes dominicanus sp. n. Scale bars = 10 µm. SEM preparation.

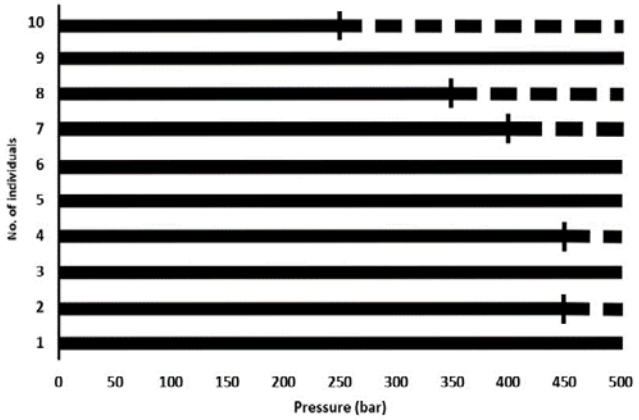

Fig. 2: Survival rates of Euplotes dominicanus sp. n. exposed up to a maximum pressure of 500 bar (n = 10). The filled sections of the bars indicate the range of pressure at which survival was observed for the different individuals.

Our studies indicate that ciliates should be considered as important components in deep-sea microbial food webs.

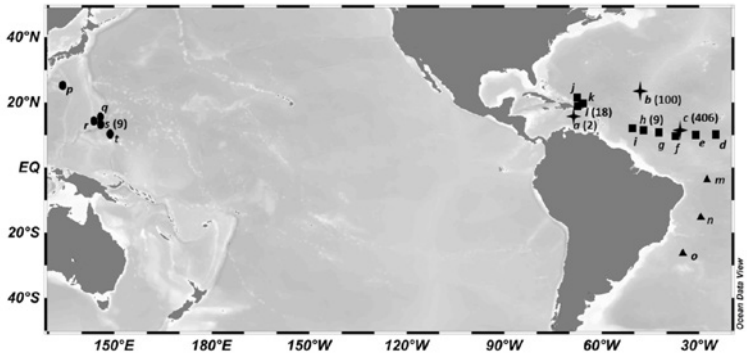

Fig. 3: Survival rates of Euplotes dominicanus sp. n. exposed up to a maximum pressure of 500 bar (n = 10). The filled sections of the bars indicate the range of pressure at which survival was observed for the different individuals.

REFERENCES

Scheckenbach F, Hausmann K, Wylezich C, Weitere M, Arndt H, Large-scale patterns in biodiversity of microbial eukaryotes from the abyssal sea floor. Proc. Natl. Acad. Sci. U.S.A., 2010, 107, 115–120. https://doi.org/10.1073/pnas.0908816106

Schoenle A, Nitsche F, Werner J, Arndt H, Deep-sea ciliates: Recorded diversity and experimental studies on pressure tolerance. Deep-Sea Res. Part I, 2017, 128, 55–66. https://doi.org/10.1016/j.dsr.2017.08.015

M140

POPULATION DYNAMICS, ECOLOGY AND PHYSIOLOGY OF PLANKTONIC FORAMINIFERA IN THE EASTERN TROPICAL ATLANTIC

AUTHORS

MARUM, Universität Bremen | Bremen, Germany
M. Kucera, M.Siccha, J. Meilland, L. Jonkers, R. Morard, C. Schmidt

Département des Sciences de la Terre, Université de Genève | Geneva, Switzerland
M. Weinkauf

NIOZ, Royal Netherlands Institute for Sea Research | Texel, Netherlands
G.-J. Brummer

Atmosphere and Ocean Research Institute, The University of Tokyo | Tokyo, Japan
H. Takagi

Planktonic foraminifera shells in marine sediments are the principle source of information on the state of past oceans. To unlock the signals preserved in these shells, the ecology of the organisms that produced them have to be constrained in detail. Yet, despite decades of research, many aspects of the life cycle and habitat of planktonic foraminifera remain unknown. To improve the applicability of foraminifera for paleoceanographical studies and stimulate new research and the SCOR/IGBP Working Group 138 was established. The group identified research priorities, which then motivated the main aspect of the research programme of the RV METEOR cruise M140 (11.8.2017 Mindelo–5.9.2017, Las Palmas). Combining observations from sediment traps, plankton samples and on-board experiments, the main aims of the foraminifera-related programme were to investigate the extent and scale of population patchiness, ontogenetic and diel vertical migration, synchronisation of reproduction, symbiont presence and physiology and the extent of genetic diversity in the group. To this end, the cruise followed a transect in the central western Atlantic between oligotrophic waters of the subtropical gyre and the productive coastal waters off Mauretania affected by coastal upwelling. To characterise population dynamics, ecology and physiology of planktonic foraminifera, we obtained a series of fourteen vertically resolved plankton net profiles along the cruise track, together with profiles of physical and chemical properties of the ambient water masses. Live foraminifera extracted from these profiles were used to quantify photosynthetic activity of selected species and determine their photoadaptation. High-resolution spatial and temporal sampling of the upper 300 m over 24 hours was carried out at two locations (recovering 41 and 46 vertical profiles), allowing the characterisation of patchiness and daily vertical migration of planktonic foraminifera.

First analysis of vertical distribution of foraminifera in one of the hyper-replicated sampling regions allowed us to show that the vertical habitats of species are stable on daily time scale, and that the foraminifera do not participate in diel vertical migration (Meilland et al., 2019). Our hyper-replicated sampling showed that the highest cell concentrations remained in the top 50 m and, based on robust data analysis, we could safely reject the existence of DVM in this group. This conclusion applies to the total concentration of foraminifera, as well as to the individual concentrations of individual species representing different sizes, life strategies and vertical habitats. Instead, we observe that concentrations of planktonic foraminifera varied laterally by as much as two orders of magnitude. This variability could not be linked to any temporal rhythm and thus hints at the existence of considerable patchiness at the scale of tens of km.

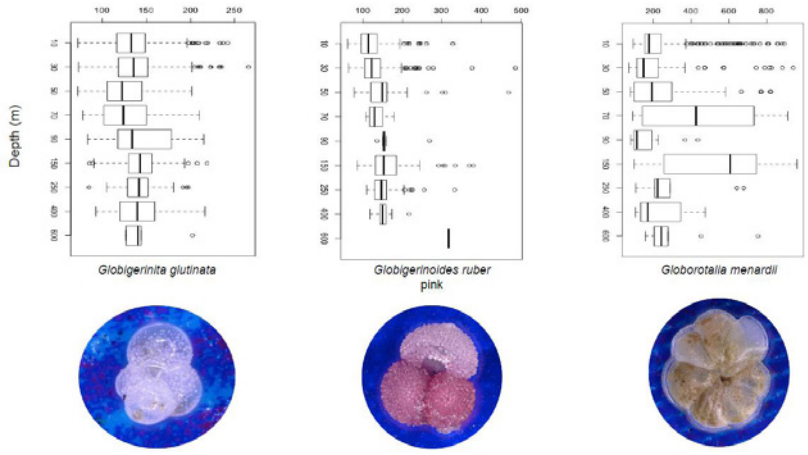

Fig. 1: Overall distribution of shell sizes among cytoplasm-bearing specimens of three selected species of planktonic foraminifera collected from vertical profiles taken during M140 south of the Cabo Verde. The profiles show no evidence for ontogenetic vertical migration that would lead to large shells being found only at the migration target depth.

Material from vertically resolved daily monitoring of population composition provided direct observations on the temporal evolution of the depth habitat and reproductive cycle of multiple species of planktonic foraminifera in the tropical North Atlantic Ocean. We have for the first time combined individual counts with size measurements (Fig. 1). Our results reveal a consistent vertical distribution of planktonic foraminifera with highest densities in the upper 80 m. The largest total standing stock was observed during the black moon while the lowest ones were sampled around the 3rd quarter. No clear differences between the ratio of living and dead specimens along the lunar cycle could be observed, suggesting continuous mortality across the population. The temporal pattern of vertical shell size distribution (Fig. 1), vertical abundance distribution and incidence of empty shells provides no support for synchronised reproduction occurring in phase with the lunar cycle. Instead, we observe that individuals of different sizes

(and ages) occur at all times in similar proportions across the species-specific stable depth habitats.

The high abundance of planktonic foraminifera allowed us to isolate hundreds of specimens across a range of species and use these to provide the first comprehensive characterization on the presence and strength of functional photosymbiosis and photoadaptation in planktonic foraminifera (Takagi et al., 2019). Since the photosynthetic activity of the symbionts can affect the geochemistry of foraminiferal tests, the understanding of the photosymbiotic ecology of planktonic foraminifera species is an essential prerequisite for their use in paleoceanographic studies. The presence of photosymbiosis also yield strong functional constraints on the habitat depth of species, allowing us to better understand the vertical distribution and population dynamics of planktonic foraminifera. During this cruise, we evaluated the photosynthetic performance of intracellular algae by conducting on-board photophysiological assessments using fast repetition rate and pulse amplitude modulation fluorometry. Fifteen species showed potential photosynthetic activity at a level consistent with functional photosymbiosis. We found that light absorbance efficiency varied, contrasting high-light adapted species against low-light-adapted and hence deeper dwelling species. This is the first time that the presence of photosymbiosis in planktonic foraminifera has been constrained by direct functional measurements, allowing us to unambiguously detect symbionts, quantify their amount, activity and photoadaptation. Combining these results allowed us to formulate a new model of photosymbiosis in planktonic foraminifera.

REFERENCES

Meilland J, Siccha M, Weinkauf MFG, Jonkers L, Morard R, Baranowski U, Baumeister A, Bertlich J, Brummer G-J, Debray P, Fritz-Endres T, Groeneveld J, Magerl L, Munz P, Rillo MC, Schmidt C, Takagi H, Theara G, Kucera M, Highly replicated sampling reveals no diurnal vertical migration but stable species-specific vertical habitats in planktonic foraminifera, Journal of Plankton Research, 2019, 41(2): 127–141. doi: 10.1093/plankt/fbz002

Takagi H, Kimoto K, Fujiki T, Saito H, Schmidt C, Kucera M, Moriya K, Characterizing photosymbiosis in modern planktonic foraminifera, Biogeosciences, 2019, 16: 3377–3396. doi: 10.5194/bg-16-3377-2019

M141/2

URANIUM ISOTOPE FINGERPRINTING OF MEDITERRANEAN OUTFLOW WATER DURING M141/2

AUTHORS

Institut für Umweltphysik, Universität Heidelberg | Heidelberg, Germany
N.Frank, E. C. Border

The U-isotopic composition of $^{234}U/^{238}U$ of seawater has been found to vary little due to the conservative nature of U. However, it is well admitted that in regions of strong freshwater runoff or groundwater discharge on can observe a deviation from the global ocean mean value of $^{234}U/^{238}U$, with typically higher than average values. The global ocean mean value given as ‰ deviation from secular radioactive equilibrium is $\delta^{234}U_{sw}$ = 146.7±0.1 ‰ and is of relevance regarding the quality control and precision of marine carbonate dating via Th/U methods (Wefing et al., 2017), but also to trace changes in global weathering and runoff patterns through time (Chen et al., 2016). We have recently found that the Mediterranean Outflow Water (MOW) has a significantly higher isotopic composition of ~149±0.5 ‰. As the Mediterranean Sea is predominantly fed by Atlantic water this was a surprising observation. The deviation from the global average value reflects strong a significant river or submerged groundwater discharge of ^{234}U, which however is unknown today. During M141/2 we have collected large volume seawater samples along the path from the Azores (Ponta Delgada) to the Black Sea (Varna) to trace the evolution of $\delta^{234U}{}_{MOW}$, to verify our observation and to possibly identify the origin of this deviation. Through the 6 stations that could be sampled along the 3000 nm transit of RV Meteor to the ship yard, we have now resolved a continuous east-west gradient of the MOW U-isotopic composition at a sub-‰ precision level. However its origin remains still unknown as we were not allowed to sample water in the Marmara and Black Sea, where we suspect elevated ^{234}U levels.

REFERENCES

Chen, T. Y., Robinson, L. F., Beasley, M. P., Claxton, L. M., Andersen, M. B., Gregoire, L. J., Wadham, J., Fornari, D. J., and Harpp, K. S., 2016, Ocean mixing and ice-sheet control of seawater U-234/U-238 during the last deglaciation: Science, v. 354, no. 6312, p. 626–629.

Wefing, A. M., Arps, J., Blaser, P., Wienberg, C., Hebbeln, D., and Frank, N., 2017, High precision U-series dating of scleractinian cold-water corals using an automated chromatographic U and Th extraction: Chemical Geology, v. 475, p. 140–148.

M142

DRILLING GAS HYDRATES IN THE DANUBE DEEP-SEA FAN, BLACK SEA

AUTHORS

GEOMAR Helmholtz Centre for Ocean Research Kiel | Kiel, Germany
M. Riedel, M. Haeckel, K. Wallmann, J. Bialas

MARUM-Center for Marine Environmental Sciences and Department of Geosciences, University of Bremen | Bremen, Germany
G. Bohrmann, T. Freudenthal, T. Pape

The overarching goal of Expedition M142 was to increase our knowledge about gas hydrate (GH) in the Danube deep sea fan, Black Sea. In 1974, GH was found in the Black Sea for the first time (Yefremova and Zhizchenko, 1974). Since then a number of research projects studied the occurrence and distribution of GH in the continental margins of the Black Sea. Numerous gas expulsion sites and indicators for gas and GH were found (Naudts et al., 2006; Popescu et al., 2007; Vassilev and Dimitrov, 2002). According to current temperature and salinity conditions in the Black Sea, GH is stable in water depths > 670 m. Depending on the depth of the seafloor, GH is expected to be stable within the upper 200 m to 300 m below the seafloor (Bialas et al., 2014). This defines upper and lower limits of the distribution of the bottom-simulating reflector (BSR), as mapped by Popescu et al. (2007) or Zander et al., (2017). Based on seismic data (Bialas et al., 2014), four drill sites were selected for drilling with the MARUM MeBo200 seafloor drill rig (Freudenthal and Wefer, 2013) during expedition M142 (Figure 1).

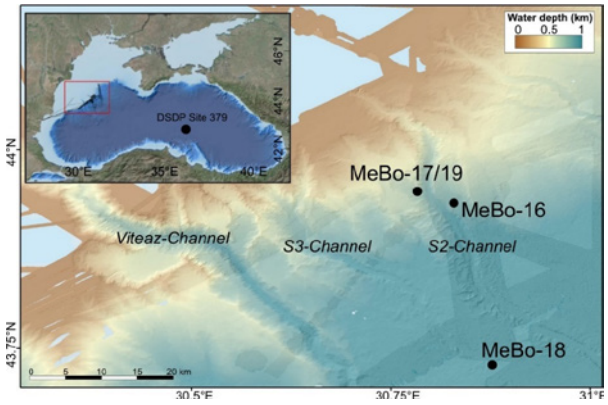

Fig. 1: Map showing overview of study region of expedition M142 in the Black Sea with all four drill sites visited with the MARUM MeBo200 seafloor drill rig.

At the first drill site (GeoB22603-1, MeBo-16) in ~860 m water depth on the eastern flank of the S2 Channel (Figure 2), a sediment depth of 147.4 m was reached. Below the typical Holocene sediment sequence, glacial slump deposits and spill-over turbidite layers were cored with more than 85 % core recovery rate. In order to reach the base of GH stability, a second Site (GeoB22605-1, MeBo-17) was drilled on the western flank of the S2 Canyon in 765 m water depth at the base of a larger slump-feature (Figure 2). The fine-grained sediment sequence down to 144.1 m was drilled with an 84 % recovery rate. At MeBo-17, geophysical borehole logging was conducted and natural gamma ray and P-wave velocity data were acquired. A second hole was drilled (GeoB22620-1, MeBo-19), ~40 m to the south, for selected spot coring between 50 and 100 m below seafloor (mbsf) and the use of a second logging tool for electrical resistivity measurements. Another drill site in ~1400 m water depth within the S2 channel was visited (GeoB22609-2, MeBo-18), but only three cores up to a maximum depth of ~18 mbsf were taken and the site abandoned. During MeBo coring, in situ temperature measurements were carried out defining an average thermal gradient of ~24°C/km at the sites visited. Downhole temperature measurements were supported by heat-probe measurements around the MeBo drill sites.

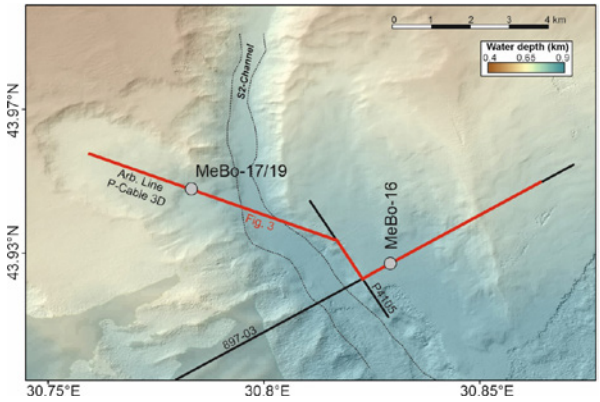

Fig. 2: Map showing locations of the drill sites around the S2 channel and the combined seismic line (red) shown in Figure 3.

Using the wealth of seismic data available in the region, a splice was created across the S2 channel and the drill sites MeBo-16 and MeBo-17/-19 highlighting the continuous levee-stratigraphy and BSR in the region (Figure 3). As seen on the seismic data, sediments at Site MeBo-17/19 are basically from the same levee sequence drilled at MeBo-16 (below 40 mbsf), but represent a younger sequence, which has been eroded at MeBo-16. On all recovered cores, a full suite of pore-water geochemical analyses was conducted including (but not limited to) measurements of sulfate, chlorinity, alkalinity, phosphate, and ammonium. Usually, the presence of GH is seen in pore-water chlorinity by freshening from a defined background trend. However, in the sediment sequence cored below ~ 20 mbsf, the in situ

pore fluid composition reflects a fresh-water phase of the Black Sea and pore fluid salinity is already overall low (2–3 psu). Void-gas samples were taken from the core prior to splitting and used to analyze the gas composition combined with sediment headspace sampling. Regular sediment cores were also imaged with an infra-red (IR) camera on deck immediately after extraction from the MeBo outer barrels to identify potential zones of GH occurrence that show up as 'cold spots'. Afterwards, all cores were curated, and split into a working half (for extraction of pore water and core-based physical property measurements) and archive half (for imaging and sedimentological description). Additionally, several pressure cores (MDP) were taken to determine in-situ gas volumes contained in sediments by controlled degassing experiments. As an example of work accomplished by M142, sediment physical property, pore-fluid composition, gas composition, and geophysical logging data are given for Site MeBo-17 in Figure 4.

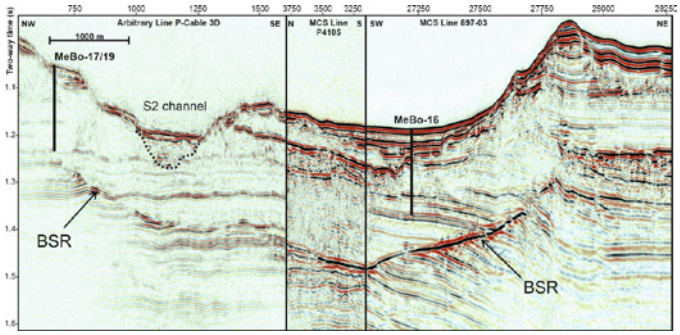

Fig. 3: Splice of seismic lines connecting the drill sites MeBo16 and MeBo17. Drill depths are indicated by black lines (location see Figure 2).

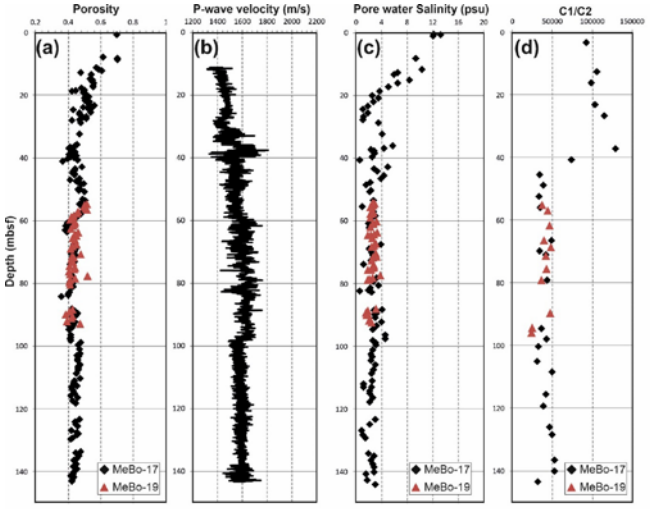

Fig. 4: Collection of data acquired at Site MeBo-17/-19: (a) sediment porosity, (b) logging-based P-wave velocity, (c) pore fluid salinity, (d) void-gas methane (C1) to ethane (C2) ratio.

REFERENCES

Freudenthal T, Wefer G, 2013, Drilling cores on the sea floor with the remote-controlled sea floor drilling rig MeBo. Geos. Instr., Methods & Data Systems, 2(2), 329–337.

Bialas J, Klaucke I, Haeckel M, 2014. FS MARIA S. MERIAN Cruise Report MSM-34 / 1 & 2 – SUGAR Site, GEOMAR Report, No. 15, 109 pages.

Yefremova A G, Zhizchenko B P, 1974, Occurrence of crystal hydrates of gases in the sediments of modern marine basins. Akademii Nauk SSSR 214, 1179–1181

Naudts L, Greinert J, Artemov Y, Staelens P, Poort J, Van Rensbergen P, De Batist M, 2006, Geological and morphological setting of 2778 methane seeps in the Dnepr paleo-delta, northwestern Black Sea. Marine Geology 227, 177–199.

Popescu I, Lericolais G, Panin N, De Batist M, Gillet H, 2007, Seismic expression of gas and gas hydrates across the western Black Sea. Geo-Marine Lett. 27, 173–183.

Vassilev A, Dimitrov L I, 2002, Spatial and quantity evaluation of the Black Sea gas hydrates, Russian Geology and Geophysics 43, 672–684.

Zander T, Haeckel M, Berndt C, Chi W-C, Klaucke I, Bialas J, Klaeschen D, Koch S, Atgin O, 2017, On the origin of multiple BSRs in the Danube deep-sea fan, Black Sea, Earth and Planet. Sci. Lett., 462, 15–25.

M143

SLOPE FAILURES AND ACTIVE GAS EXPULSION ALONG THE ROMANIAN MARGIN

AUTHORS

GEOMAR Helmholtz Centre for Ocean Research Kiel | Kiel, Germany
M. Riedel, P. Urban, L. Hähnel, J. Bialas, J. Greinert

MARUM-Center for Marine Environmental Sciences and Department of Geosciences, University of Bremen | Bremen, Germany
G. Bohrmann, P. Wintersteller

Expedition M143 in the Black Sea was a short-term replacement for an expedition originally scheduled to recover marine geodetic instrumentation in the Sea of Marmara. With less than two months preparation time and associated restrictions for permitting, transport, and limited personnel availability, expedition M143 was defined as a "mapping only" exercise directly following expedition M142 in the same study area of the Romanian sector of the Danube Delta deep-sea fan. Using the onboard acoustic multibeam and PARASOUND systems, seafloor mapping was extended from efforts conducted during M142 and previous expedition MSM34. Additional emphasis was on acoustic mapping of gas release from the seafloor and quantification of gas emission rates with a calibrated EK80 sounder system deployed through the moon-pool of the vessel.

Research topics on the data acquired focus on two themes:

(a) Quantification of gas emissions with acoustic tools

The use of a calibrated single-beam EK80 echosounder and coincident acquisition of multibeam data (Figure 1) allowed for the first time the transfer of methods known for single-beam-based gas emission rate quantification (e. g. Veloso et al., 2015) to multibeam data. Gas flow rate estimates from multibeam data are consistent through repeated surveys (Figure 2). They further correlate linearly with gas flow estimates from the calibrated single-beam echosounder.

Using this method thereby increases the areal coverage that can be achieved by a single cruise by more than ten times compared to single-beam echosounder surveys and enables a much more detailed flow rate estimate of a given research area.

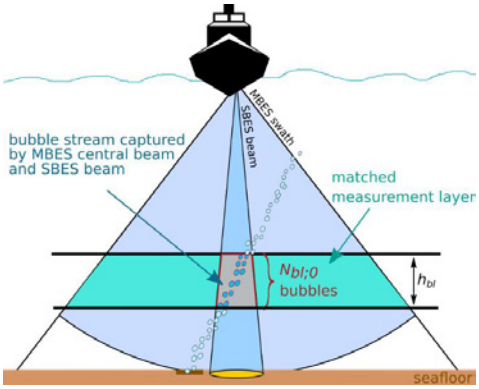

Fig. 1: Comparison of a typical water column survey conducted during M143 with simultaneous recording of the single beam (SBES) and multibeam system (MBES) across a gas bubble stream (from Urban et al., submitted). For the chosen acoustic flare map layer (10–30 m above seafloor), the MBES coverage (80° swath) is more than 10 times the coverage of the SBES beam cone (7°).

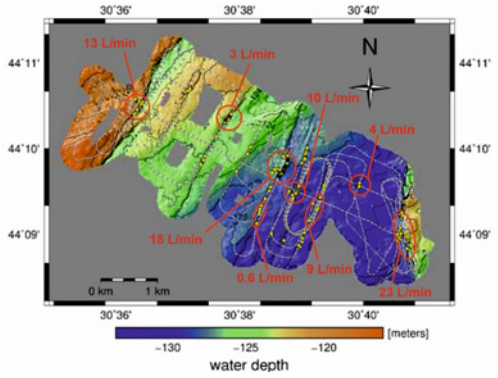

Fig. 2: Map of survey on the shelf of the Danube Delta (water depth ~ 125 m) with prominent gas bubble sites. Volumetric gas flow rates were defined for all flare sites with individual flow rates ranging from < 1 L/min to 23 L/min. The total flow rate for this region is ~ 80L/min.

(b) Seafloor structures indicating past slope failure and zone of potential future seafloor instabilities as well as linkages to free gas emission patterns

Individual gas flare locations determined from the multibeam acoustic data were merged with the bathymetric data to see whether a structural control for gas emission exists, or gas venting is a (spatially) random process (Figure 3). More than 2,400 individual flare locations were determined from the M143 data set. Gas seepage mostly occurs in water depths shallower than 700 m and thus outside the zone of gas hydrate stability. An emerging pattern of gas seepage was identified along canyon walls and ridges. The gas release is either tied to the erosional walls of the canyon by exposing gas bearing strata or gas migration and ultimate release into the water column is structurally focused to the ridges (i. e. highest elevation). As proposed for the southern Black Sea region by Xu et

al. (2018), there is also a spatial link between gas seepage and elongated seafloor depressions, that may be sites of future seafloor instability and slope failure.

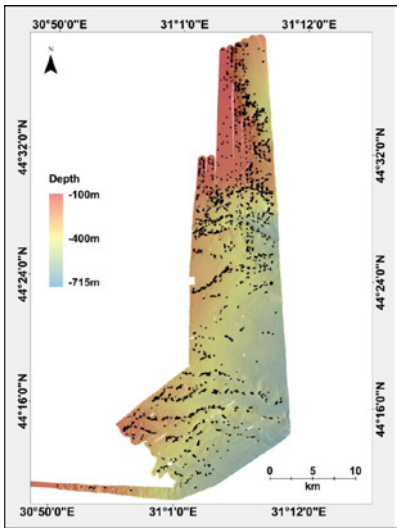

Fig. 3: Map of the distribution of observed gas flares (black dots) in the M143 survey area (modified from Hähnel, 2018).

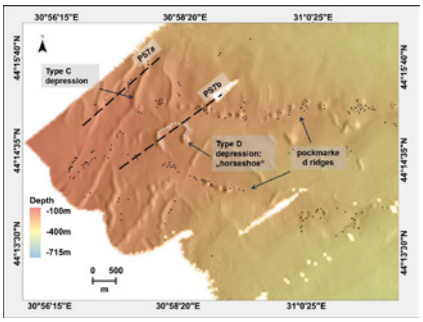

Fig. 4: Region of elongated depressions systems (modified from Hähnel, 2018).

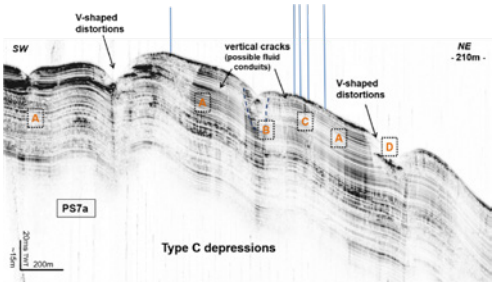

Fig. 4: Region of elongated depressions systems (modified from Hähnel, 2018).

REFERENCES

Hähnel L, Seafloor structures controlling gas flare distributions – Romanian margin, Black Sea, 2018, BSc thesis, Christian-Albrechts-University (CAU) Kiel, 79 pp.

Veloso M, Greinert J, Mienert J, De Batist M, A new methodology for quantifying bubble flow-rates in deep-water using splitbeam echo-sounders: examples from the Arctic offshore NW-Svalbard, Limnol. Oceanogr., 2015, 267–287, doi:10.1002/lom3.10024

Xu C, Greinert J, Haeckel M, Bialas J, Dimitrov L, Zhao G, The Character and Formation of Elongated Depressions on the Upper Bulgarian Slope, Journal of Ocean University of China, 2018,17: 555-562, https://doi.org/10.1007/s11802-018-3460-7

M144/2
IODP-TARGETS IN THE IONIAN SEA

AUTHORS

Institute of Geophysics, Center for Marine and Climate Research, University of Hamburg | Hamburg, Germany
C. Hübscher

Deciphering exact mechanisms for the formation of massive dolomite deposits remains an outstanding enigma in sedimentary geology. However, the common association of dolomite with salt giant deposits has long been recognized. A noteworthy 33.5 m-thick dolomite sequence capping the salt giant of the Messinian Salinity Crisis (MSC: 5.97–5.33 Ma) was recovered during drilling across the Miocene/Pliocene boundary at DSDP Leg 42A, Site 374 in the Ionian Abyssal Plain. The Messinian Salinity Crisis in the Mediterranean Realm (5.97–5.33 Ma) represents the most recent deposition of a major salt giant complex in Earth's history. It has been proposed, that at the location of DSDP Leg 42A, Site 374, modern dolomite precipitation is occurring and the site is a "natural laboratory" in which to investigate the biogeochemical phenomenon associated with subsurface diagenetic dolomite formation in the context of a salt giant deposit. This location is definitely a worthwhile site to be considered for reoccupation during future Mediterranean drilling campaigns, as it may provide an actualistic model for the origin of massive dolomite deposits associated with other salt giants in the rock record.

Although the recovered core material yielded spectacular results, there have been major scientific advances in the fields of biogeochemistry and salt tectonics/fluid flow in the intervening 42 years, which call for a re-occupation of Site 374. With the approval of the ship-track of the IODP research drilling vessel JOIDES Resolution affirms that, based on proposal pressure, it seems secured that the future navigation path will bring IODP drilling operations into the general area of the Equatorial and North Atlantic in the next few years. The aim of M144/2 was collecting new high-resolutions seismic site survey data for IODP-proposal 857C-FULL.

In the course of M144/2 we collected eleven reflection seismic lines centered around Site 374 during the 3½-day long working program (Fig. 1). These data were processed on board and uploaded to the IODP Site Survey Data Base for proposal 857C-FULL. One Primary Site and 24 potential Alternate Sites were determined from the new material. The IODP Science Evaluation Panel (SEP) positively evaluated 857C-FULL in June 2019. The Environmental Protection and Safety Panel (EPSP) meeting was passed in September 2019 without any relevant problems. The Proponents Response Letter (PRL) has been submitted in November 2019 and will be evaluated during the SEP-meeting in January 2020.

In a joint study with Italian colleagues, we used both our new high-resolution and older deep penetration seismic reflection data (Camerlenghi et al., 2019). Interestingly, the reflection characteristics is different both from the western basins and the Levant Basin (Fig. 2). The different MSC depositional units suggest that the Messinian Ionian Basin was separated by physical thresholds from the Western Mediterranean (Pelagian Sea/Sicily Channel), from the Po Plain/Northern Adriatic Basin (southern Adriatic sill), and the Levant Basin (undefined sill hidden below the Mediterranean Ridge accretionary complex between Crete and the Cyrenaica Peninsula). This likely reflects different hydrological and climatic conditions that affected the basins evaporation and salt precipitation.

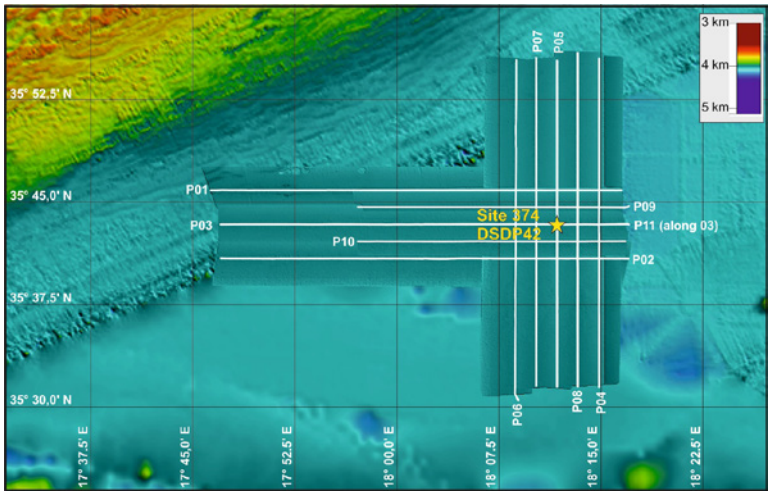

Fig. 1: M144/2 seismic lines. M144/2 multibeam data are plotted over ETOPO1 data.

REFERENCES

Camerlenghi, A, Del Ben A, Hübscher C, Forlin E, Geletti R, Brancatelli G, Micallef A, Saule M, Facchin L Seismic markers of the Messinian salinity crisis in the deep Ionian Basin. Basin Research 2019, doi:10.1111/bre.12392

MSM40 & MSM54

DIRECT OBSERVATIONS OF THE MERIDIONAL OVERTURNING CIRCULATION IN THE SUBPOLAR NORTH ATLANTIC

AUTHORS

GEOMAR Helmholtz Centre for Ocean Research Kiel | Kiel, Germany
J. Karstensen, P. Handmann, M. Visbeck

NOC Southampton | Southampton, UK
M. Oltmanns

The Atlantic Meridional Overturning Circulation (AMOC) is a key component of the global climate system through its transport of heat and freshwater (e. g. Frajka-Williams et al. 2019). The subpolar North Atlantic (SPNA) is a region where the AMOC is actively developed and shaped though mixing and water mass transformation and where large amounts of heat are released to the atmosphere. With contributions from the United States, the United Kingdom, Germany, the Netherlands, Canada, and China, the OSNAP observing system (Fig. 1) comprises an integrated coast-to-coast array of two sections: OSNAP West, extending from the southeastern Labrador shelf to the southwestern tip of Greenland, and OSNAP East, extending from the southeastern tip of Greenland to the Scottish shelf (Lozier et al. 2017). Densely spaced OSNAP mooring arrays, which directly measure the temperature, salinity, and velocity fields, are in place at continental boundaries and on both flanks of the Reykjanes Ridge; additional dynamic height moorings at key locations allow us to estimate geostrophic flows. Glider surveys along topographically complex sections of OSNAP East complement the moored arrays.

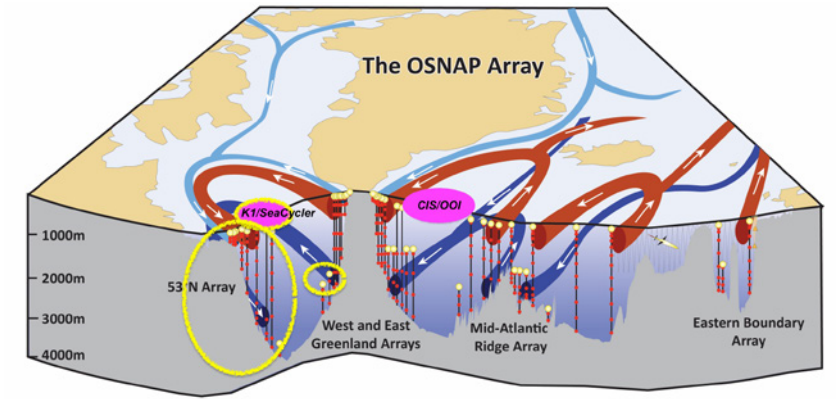

Fig. 1: Sketch of the OSNAP array that is used for a continuous observation of the overturning in the subpolar North Atlantic. Moorings serviced with MSM40 and MSM54 are marked by yellow circles.

The cruises MSM40 (performed on the French NO lAtalante) and MSM54 were key expeditions for retrieving the data used for the first overturning time series estimate for the subpolar North Atlantic. The "overturning in the Subpolar Gyre Program" (OSNAP) is the framework for this remarkable international collaboration. Both cruises serviced the 53°N array at the exit of the Labrador Sea (Fig. 1; Zantop et al. 2017) and the mooring data is used as pillar in the OSNAP West & full array calculations. Moreover, full depth CTD stations along the OSNAP line were performed.

The first synoptic overturning estimate were calculated from MSM40 and MSM54 CTD and (l)ADCP data in combination with UK ships data (Holliday et al. 2018). Using the two hydrographic transbasin sections along the OSNAP Line in the summers of 2014 and 2016 provided a highly spatially resolved views of the SPNA velocity and property fields. Estimates of the AMOC, isopycnal (gyre-scale) transport, and heat and freshwater transport were derived from the ship observations. The overturning circulation, the maximum in northward transport integrated from the surface to seafloor and computed in density space, has a high range, with 20.6 ± 4.7 Sv in June–July 2014 and 10.6 ± 4.3 Sv in May–August 2016. In contrast, the isopycnal (gyre-scale) circulation was lowest in summer 2014: 41.3 ± 8.2 Sv compared to 58.6 ± 7.4 Sv in 2016. The heat transport (0.39 ± 0.08 PW in summer 2014, positive is northward) was highest for the section with the highest AMOC, and the freshwater transport was largest in summer 2016 when the isopycnal circulation was high (-0.25 ± 0.08 Sv). Up to 65 % of the heat and freshwater transport was carried by the isopycnal circulation, with isopycnal property transport highest in the western Labrador Sea and the eastern basins (Iceland Basin to Scotland).

About a year later, the first results of the OSNAP mooring array were presented (Lozier et al., 2019). The first 21 months of array data led to the remarkable finding that the mean and variability of the subpolar Meridional Overturning Circulation is dominated by the overturning east of Greenland. This new view is counter to the contemporary paradigm that deep water formation in the Labrador Sea is the dominant forcing for AMOC variability in the subpolar and subtropical North Atlantic.

The observational studies are closely linked to model studies (e. g. Handmann et al. 2019). The contribution of the data and services financed by Germany are seen as core components by the OSNAP members.

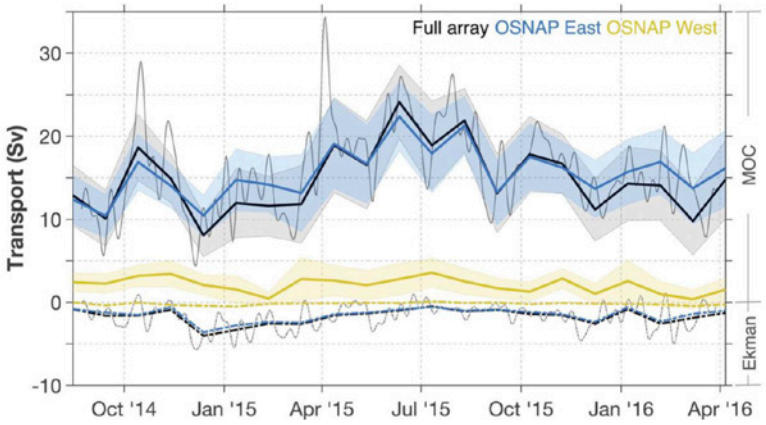

Fig. 2: Overturning transport estimates from the OSNAP array. Black, yellow, and blue lines represent the 30-day mean estimates from the full section, OSNAP West, and OSNAP East, respectively, for Meridional Overturning Circulation (MOC) (solid lines) and Ekman transport (dashed lines). Thin gray lines show the 10-day low- pass filtered daily means for the full OSNAP section. The 53°N Array as part of OSNAP West were installed during MSM40 and recovered during MSM54.

REFERENCES

Frajka-Williams E, Ansorge IJ, Baehr J, Bryden HL, Chidichimo MP, Cunningham SA, Danabasoglu G, Dong S, Donohue KA, Elipot S, Heimbach P, Holliday NP, Hummels R, Jackson LC, Karstensen J, et al. (2019) Atlantic Meridional Overturning Circulation: Observed Transport and Variability. Front. Mar. Sci. 6:260. doi: 10.3389/fmars.2019.00260

Lozier, M.S., F. Li, S. Bacon, F. Bahr, A.S. Bower, S.A. Cunningham, M.F. de Jong, L. de Steur, B. DeYoung, J. Fischer, S.F. Gary, N.J.W. Greenan, N.P. Holliday, A. Houk, L. Houpert, M.E. Inall, W.E. Johns, H.L. Johnson, C. Johnson, J. Karstensen, G. Koman, I.A. LeBras, X. Lin, N. Mackay, D.P. Marshall, H. Mercier, M. Oltmanns, R.S. Pickart, A.L. Ramsey, D. Rayner, F. Straneo, V. Thierry, D.J. Torres, R.G. Williams, C. Wilson, J. Yang, I. Yashayaev and J. Zhao, A Sea Change in Our View of Overturning – First Results from the Overturning in the Subpolar North Atlantic Program, Science, 363, 516–521, February 1, doi: 10.1126/science.aau6592., 2019.

Holliday, N. P., Bacon, S., Cunningham, S. A., Gary, S. F., Karstensen, J., King, B. A., Li, F., & McDonagh, E. L., Subpolar North Atlantic Overturning and gyre-scale circulation in the summer 2014 and 2016. Journal of Geophysical Research: Oceans, 122. https://doi.org/10.1029/2018JC013841., 2018

Handmann, P., Fischer, J., Visbeck, M., Karstensen, J., Biastoch, A., Böning, C., & Patara, L. The deep western boundary current in the Labrador Sea from observations and a high-resolution model. Journal of Geophysical Research: Oceans, 123, 2829–2850. https://doi.org/10.1002/2017JC013702, 2018.

Zantopp, R., J. Fischer, M. Visbeck, and J. Karstensen, From interannual to decadal: 17 years of boundary current transports at the exit of the Labrador Sea, J. Geophys. Res. Oceans, 122, doi:10.1002/2016JC012271, 2017.

Lozier, S., S. Bacon, A.S. Bower, S.A. Cunningham, M.M. Femke de Jong, L. de Steur, B. deYoung, J. Fischer, S.F. Gary, B.W. Greenan, P. Heimbach, N.P. Holliday, L. Houpert, M.E. Inall, W.E. Johns, H.L. Johnson, J. Karstensen, F. Li, X. Lin, N. Mackay, D.P. Marshall, H. Mercier, P.G. Myers, R.S. Pickart, H.R. Pillar, F. Straneo, V. Thierry, R.A. Weller, R.G. Williams, C. Wilson, J. Yang, J. Zhao, and J.D. Zika, Overturning in the Subpolar North Atlantic Program: A New International Ocean Observing System. Bull. Amer. Meteor. Soc., 98, 737–752, doi: 10.1175/BAMS-D-16-0057.1., 2017

MSM43
OBSERVED TRANSPORT DECLINE AT 47°N, WESTERN ATLANTIC

AUTHORS

Institute of Environmental Physics, Universität Bremen | Bremen, Germany
C. Mertens, M. Rhein, A. Roessler

MARUM – Center for Marine Environmental Sciences, Universität Bremen | Bremen, Germany
M. Rhein, A. Roessler

Long-term transport variability in the western Atlantic at 47°N was analysed between 44°W and 31°W, combining moored pressure inverted echo sounders and current meter moorings with lowered acoustic Doppler current profiler and Argo data (Rhein et al., 2019). Correlations with altimetry were used to extend each of the transport time series back to 1993. At the Canadian continental margin the boundary current exports -23.1 ± 1.5 Sv to the south. Nearby, the northward flowing NAC imports 105.9 ± 3.4 Sv into the subpolar gyre. Constrained mainly by topography, about half of that flow recirculates in close proximity to the NAC (-58.8 ± 3.9 Sv). NAC and recirculation are significantly anticorrelated. The flow east of 37°W (-27.8 ± 2.1 Sv) has no permanent regional features and is not correlated to the NAC. The sum of the interior components (19.3 ± 3.3 Sv) shows a significant trend in the time period 1993–2018 of -0.60 Sv/year. This decline is dominated by the significant increase of the southward flow east of 37°W (0.44 Sv/year). The trends of the other individual components are not significant, but the sum of the interior and boundary current transport is -0.71 Sv/year (Fig. 2). The trends are most likely caused by regionally different warming.

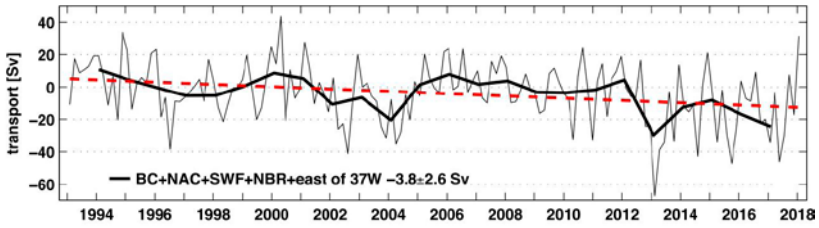

Fig. 1: Bimonthly (thin) and annual (bold) mean top-bottom transport time series (Sv), in the western Atlantic at 47°N between 44°W and 31°W. The red stippled present linear long-term trend. (From Rhein et al., 2019)

REFERENCES

Rhein, M., Mertens, C., and Roessler, A. (2019). Observed transport decline at 47°N, western Atlantic. J. Geophys. Res.: Oceans, 124. doi: 10.1029/2019JC01499

MSM45

HOLOCENE LABRADOR SEA PALEOCEANOGRAPHY DEDUCED FROM MSM 45 SEDIMENT CORES

AUTHORS

Institute of Geosciences, Kiel University | Kiel, Germany
R. Schneider

Max-Planck-Institute for Chemistry | Mainz, Germany
J. Repschläger

Department of Oceanography, Dalhousie University | Halifax, Canada
M. Kienast

During cruise MSM45 we performed a sampling program for Deglacial to Holocene sediment sequences that can be used for the reconstruction of climate variability at high resolution in the Labrador Sea. Sediment coring was complemented by a water-column sampling program for geochemical properties including pteropod distribution mapping and culturing studies. Sampling was executed along the shelf and upper slope of Canada and Greenland and within Hudson Strait in water depths between 200 to 3300 m (Fig. 1)

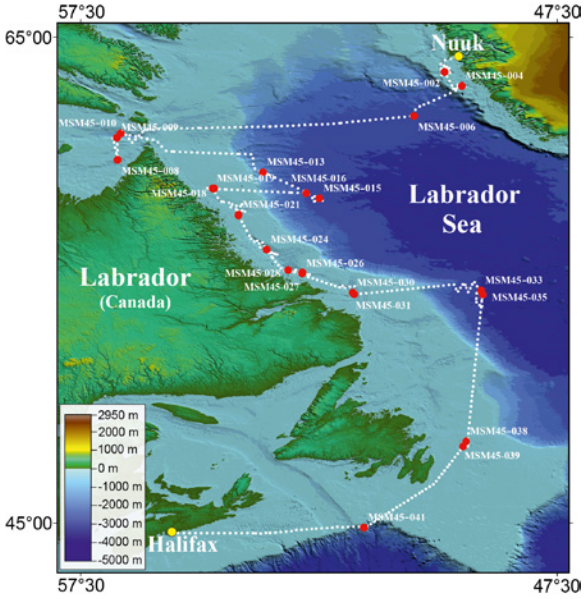

Fig. 1: MSM45 cruise track with water column and geological sampling stations

As it turned out during post-cruise work, perfect locations for high-resolution Deglacial to Holocene climate reconstructions were successfully cored at about 17 shelf locations with 10 to 17 m long piston or gravity cores. Cores taken at intermediate and deep-water sites reach down into the Last Glacial. Particularly, the new shelf core material has enabled us to establish for the first time late Holocene climate records from the western Labrador Current in decadal scale resolution, that infer a strong impact of subsurface ocean warming for the final melt of the Laurentide ice sheet at about 9 to 8 kyrs BP by affecting the grounding line of the last Ice Dome in Hudson Bay (Lochte et al. 2019a). It was found that Labrador Shelf bottom waters experienced an early Holocene warming associated with an intensification of the westward retroflection of the West-Greenland Current (WGC), leading to a decrease in the seasonal sea ice cover. The intensification of the WGC potentially allowed the inflow of these warmer subsurface waters into Hudson Strait and Bay, where they could have helped to accelerate the collapse of the Hudson Bay Ice Saddle, which resulted in a major meltwater plume diluting Labrador Shelf waters down to 200 m depth at 8.5 ka BP (Fig. 2).

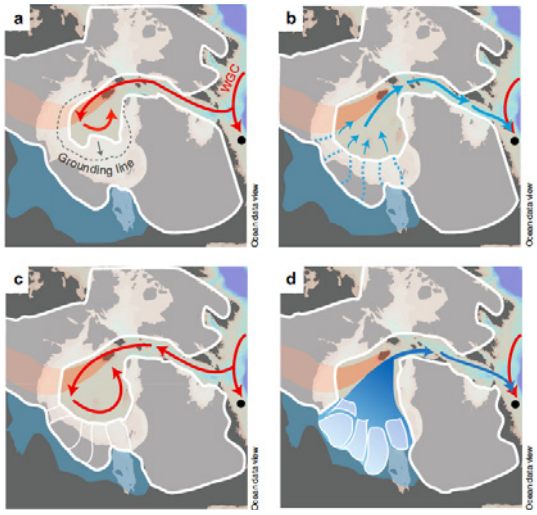

Fig. 2: Schematic areal views of the Hudson Bay Ice Saddle collapse between 8.7–8.4 ka BP. Black dot marks the location of the shelf core. a) Inflowing warmer WGC waters from the (red arrows) caused a retreat of the ice saddle grounding line in Hudson Bay; b and c) As the Hudson Bay Ice Saddle could no longer withstand the hydraulic pressure of Lake Agassiz-Ojibway, drainage of lake waters underneath the ice dam and through Hudson Strait into the Labrador Sea (blue arrows) occurred; d) The final collapse of the Hudson Bay Ice Saddle lead to the discharge of large icebergs and high volumes of freshwater (blue arrows) into the Labrador Sea. (from Lochte et al. 2019a).

Apart from these subsurface warming events, mid to late Holocene Labrador Current (LC) variability was primarily characterized by changes in sea ice cover and SST, likely in response to atmospheric-sea surface coupling, such as different phases of NAO conditions in general (Lochte et al. 2019b). The close connection between LC climate to the NAO variability and LSW water formation could be documented for the last two to

four millenia based on multi-proxy records that will be presented. Based these, the LC appears to be important for the subpolar gyre circulation, hence indirectly affecting LSW formation. As LC freshwater meets the northward flowing North Atlantic Current (NAC) near Flemish Cape, it likely plays a role in regulating NAC temperature and salinity, which partly turns back into the Labrador Sea with its westward retroflection, the IC. Thus, the major meltwater pulse from the Hudson Bay Ice Saddle collapse observed in our record would have freshened and cooled the NAC. This could have led to a cooling of North Atlantic surface waters but would have required a longer time before the freshwater would have reached early Holocene convection sites in the Nordic Seas, prior to the establishment of Labrador Sea convection around 7 ka BP. In turn, an increased sea ice cover and diminished supply of freshwater with the LC during the last 2,100 years would have allowed for a warmer NAC and IC, thereby enhancing central Labrador Sea surface water temperature and or salinity. As increased sea ice cover as well as diminished freshwater supply and reduced current vigor seem to have prevailed during positive modes of the NAO these conditions in the LC may have formed a positive feedback mechanism that further increased Labrador Sea convection during these periods. With these results we could fill an important gap in knowledge as no such records existed for this region before.

REFERENCES

Lochte AA, Repschläger J, Kienast M, Garbe-Schönberg D, Andersen N, Hamann C, Schneider R.R. Labrador Sea freshening at 8.5 ka BP caused by Hudson Bay Ice Saddle collapse. Nature Communications 2019a, 10-586, doi.org/10.1038/s41467-019-08408-6.

Lochte AA., Schneider RR, Repschläger J, Kienast M, Blanz T, Garbe-Schönberg D, Andersen N. Surface and subsurface Labrador Shelf water mass conditions during the last 6,000 years, Climate of the Past Discussions, https://doi.org/10.5194/cp-2019-100, in review, 2019b.

MSM47

THE GRAND BANKS LANDSLIDE REVISITED: RESULTS FROM RV MARIA S. MERIAN CRUISE MSM47

AUTHORS

Christian-Albrechts-Universität zu Kiel | Kiel, Germany
S. Krastel, K. Lindhorst

Leibniz-Institut für Ostseeforschung Warnemünde – IOW | Warnemünde, Germany
P. Feldens

Bedford Institute of Oceanography | Dartmouth (NS), Canada
D.C. Mosher

Dalhousie University | Halifax (NS), Canada
I. Schulten

University of Liverpool | Liverpool, UK
C. Stevenson

Marum, Universität Bremen | Bremen, Germany
A. Kopf

Norwegian Geotechnical Institute | Oslo, Norway
F. Løvholt

And: MSM47-shipboard scientific party

On November 18, 1929, a M7.2 earthquake occurred beneath the Laurentian Channel off the coast of Newfoundland. Nearly simultaneously, 12 undersea trans-Atlantic communication cables were severed and within two hours, a devastating tsunami struck the south coast of Newfoundland, claiming 28 lives. Only in 1952, it was understood that a landslide-generated turbidity current caused the sequential severance of the cables and likely generated the tsunami. The 1929 Grand Banks events were pivotal, as they led to the first unequivocal recognition of a turbidity current and landslide-triggered tsunami. The landslide site was visited numerous times as underwater survey technologies evolved. No major head scarp related to the event was recognized, raising the question, whether a distributed, laterally extensive, shallow submarine mass failure event caused the tsunami.

Hydroacoustic, seismic and core data in the Grand Banks landslide area were collected during Cruise MSM47 in order to investigate the volume of the failed sediments, the type of failure, the geologic/geotechnical processes of failure and the sediment transport pattern of the failed material to the deep sea (Fig. 1) . The analysis of the hydroacoustic and seismic data combined with geotechnical investigations on cores revealed that the failure is more complex than previously thought. Translational surficial sediment failure is widespread at the middle and lower slope. Failed sediments are mainly found beneath up to 25m-high escarpments. The estimated volume of the failure is ~100 km^3. About 60 km^3 of the failed sediments are deposited on the slope while about 40 km^3 quickly disintegrated in turbidity currents; these sediments are transported in submarine channels to the deep sea.

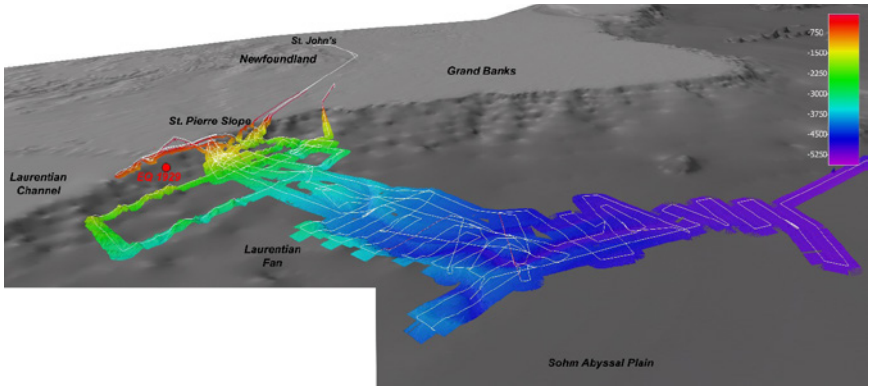

Fig. 1: Bathymetric map including tracks and stations of Cruise MSM47.

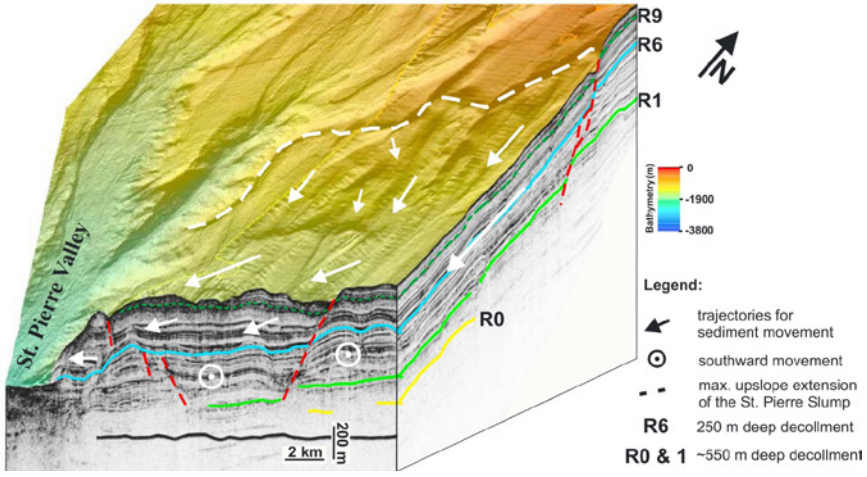

Fig. 2: 3-D image of the St. Pierre Slope covering the upper and middle section of the St. Pierre Slump. Faults are shown as red dashed lines, while white arrows show the interpreted directionally of the slump. St. Pierre Valley toward the west-southwest is incised down to horizon R6. Taken from Schulten et al. (2019).

Numerous oblique low angle faults are found beneath up to 100 m-high escarpments on the upper slope (Fig. 2). These faults reach down to ~ 500 mbsf and show displacements of up to 100 m. They cannot be related to deeper tectonic features because they sole out at various horizons between 300 and 600 mbsf. We interpret the faults as part of a massive complex rotational slump, which was triggered by the 1929 event. The estimated volume of the slump is exceeding 500 km^3; multiple décollements are identified in the seismic data. Both components, the surficial translational failure and the massive slump, contributed to the tsunami generation. Modelling suggest that the slump generated the near-field tsunami component, which impacted the coast of Newfoundland, while the widespread surficial failure caused an ocean-wide tsunami, which was recorded at numerous locations along the coasts of the Atlantic Ocean. Geotechnical investigations show that the slope is currently stable under static conditions but that the slump could be triggered by the 1929 earthquake. The surficial failures may be a direct consequence of the deep-seated slump.

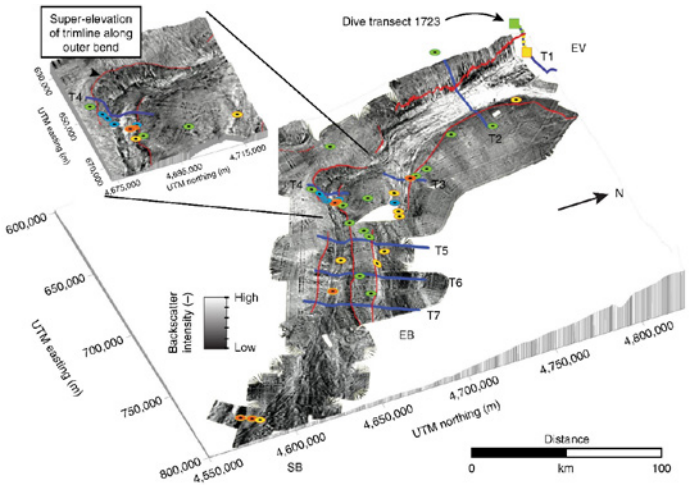

Fig. 3: Acoustic backscatter from Cruise MSM47 across the lower parts of the Eastern Valley channel system with interpretation of erosional trimlines from the 1929 flow. The Eastern Valley (EV) splits into two smaller channels: East Branch (EB) and South Branch (SB). High-intensity backscatter represents rough sandy deposits whilst low-intensity represents smooth mud. Erosional trimlines are inferred from sharp boundaries in backscatter intensity running along the margins of the channels (red lines). Cores show major erosion by the 1929 flow within the channels that extends up to the elevation of the trimlines (gravels – yellow, bypass drapes – blue and bounced – orange circles). Undisturbed sediments occur above the trimline (green circles). Taken from Stevenson et al. (2018).

Sediment coring and hydroacoustic data along the Eastern Valley on the Laurentian Fan allowed to reconstruct the trimline of the 1929 turbidity current (Fig. 3). This information was used to calculate the average bulk sediment concentration of the flow, which was 2.7–5.4 % by volume. To our knowledge, these numbers are the first validated estimates of sediment concentration for giant submarine gravity flows. These values are orders of magnitude higher than directly-measured smaller-volume flows in river deltas and

submarine canyons. The new concentration estimates are a major step towards a quantitative understanding of such large volume flows.

REFERENCES

Schulten I, Mosher DC, Piper DJ, Krastel S (2019) A massive slump on the St. Pierre Slope, a new perspective on the 1929 Grand Banks submarine landslide. Journal of Geophysical Research, 124, 7538–7561, doi:10.1029/2018JB017066

Stevenson CJ, Feldens P, Georgiopoulou A, Schönke M, Krastel S, Piper DJW, Lindhorst K, Mosher DJ (2018) Reconstructing the sediment concentration of a giant submarine gravity flow. Nature Communications, DOI: 10.1038/s41467-018-05042-6

MSM47*

UNDRAINED SHEAR STRENGTH OF SHALLOW MARINE SEDIMENTARY DEPOSITS: FALL CONE EXPERIMENTS ON SEDIMENT CORES COLLECTED OFFSHORE MOROCCO AND CANADA

AUTHORS

Leibniz Institute for Baltic Sea Research Warnemünde | Warnemünde, Germany
P. Feldens

University of Liverpool | Liverpool, UK
C. J. Stevenson

Institute of Geosciences, Christian Albrechts University Kiel | Kiel, Germany
S. Kraste

And: Shipboard Participants of Cruises MSM32 and MSM47

The undrained shear strength of marine sediments is a basic parameter that controls slope stability and resistance of sediments to local erosion. In the first tens of meters of the subsurface, undrained shear strength of marine sediments is often strongly controlled by sediment composition and compaction. However, in the shallow subsurface, local bioturbation impacting the sediment texture can have strong influence on undrained shear strength. In this poster, we showcase a publically available dataset comprising several thousand fall cone experiments on freshly split sediment cores derived from gravity corers and box corers that were collected during cruises MSM32 and MSM47. The dataset covers hemipelagic background sedimentation as well as different debris flow deposits. Radiographies of the sediment cores allow to accurately locate the position of the fall cone experiments in several instances, including bioturbation traces. First results demonstrate the impact of bioturbation traces in different burial depth on undrained shear strength.

MSM49

SEAMOX: THE INFLUENCE OF SEAMOUNTS AND OXYGEN MINIMUM ZONES ON PELAGIC FAUNA IN THE EASTERN TROPICAL ATLANTIC (CRUISE MSM49)

AUTHORS

GEOMAR Helmholtz Centre for Ocean Research Kiel | Kiel, Germany
H.-J. Hoving

Universität Hamburg, Institut für marine Ökosystem- und Fischereiwissenschaften (IMF) | Hamburg, Germany
B. Christiansen

Cruise MSM49 on Maria S. Merian had the objective to map the standing stocks, diversity, distribution, migration and abundance of epi- and mesopelagic fauna around the Archipelago of Cape Verde, under differing hydrographic and bathymetric settings, and to investigate the trophic structure of pelagic fauna. We performed an extensive sampling and observation program in areas with an oxygen minimum zone (OMZ), on Senghor Seamount and its flanks, and in and outside a mesoscale cyclonic eddy. We combined in situ observational technology (towed camera PELAGIOS, UVP) with discrete net sampling (10m2-MOCNESS, 1m2-MOCNESS). Observed and collected fauna included, among others, fishes, cephalopods, krill and other crustaceans, gelatinous fauna, and specimens and data were divided among experts for further analysis.

Total biomass standing stocks of macrozooplankton/micronekton within the upper 1000 m of the water column differed little between stations across the research area; a direct influence of topographic (seamount) and hydrographic (eddy) mesoscale features was not observed. The analysis of abundance and composition from $10m^2$-MOCNESS samples focused on the eddy and the southern stations. Siphonophores were a major component of the macrozooplankton/micronekton community at all stations, particularly dominating the upper 300 m. Other important groups included fish, chaethognaths, copepods, decapods and euphausids. The mesopelagic fish community was dominated by several species of the genus Cyclothone at all stations. Their highest abundance was between 400 and 600 m, i. e. in the layer with lowest oxygen content, during day and night. Indications for diel vertical migrations were not consistent among stations.

Annotating the in situ observations from PELAGIOS showed five distribution patterns of gelatinous zooplankton in relation to the eastern tropical Atlantic OMZ with some 1) taxa avoiding the OMZ, 2) taxa being associated with the OMZ, taxa that occurred 3) below or 4) above the OMZ and 5) taxa that occurred throughout the water column. Comparison

between net sampling and in situ observations showed that gelatinous fauna are undersampled with MOCNESS nets. The pelagic video transects of MSM49 also resulted in the documentation of gelatinous fauna previously unknown from the region, illustrating the need for baseline biological observations in oceanic deep-sea regions. The pelagic video transects of MSM49 formed the foundation data for the Oceanic Biodiversity Observation Database, which is a growing deep-sea biodiversity database at GEOMAR based on cruises in the Atlantic Ocean.

The oceanic foodweb in Cape Verde was reconstructed using stable isotope analysis and revealed that jellies fulfill a range of niches in the pelagic ecosystem of Cape Verde. The ontogenetic change in feeding ecology was investigated for the abundant oceanic squid Sthenoteuthis pteropus using a combination of stomach content analysis and stable isotope analysis. While a dominant food component was lanternfishes, the analysis revealed also cannibalism and likely the consumption of gelatinous fauna. Trace element analysis of Sthenoteuthis pteropus resulted in Cd concentrations that were the second highest reported concentrations for the squid family Ommastrephidae and showed the high bioaccumulation capacity of S. pteropus for heavy metals.

Close communication with land based scientists allowed the detection, location and sampling of a mesoscale cyclonic eddy. Analyzing observations of the fauna inside and outside the eddy showed a clear faunal distinction with larvaceans, pyrosomes, doliolids and radiolarians occurring in higher abundances inside the eddy compared to the reference station. By contrast, the abundance of fishes was markedly lower within the eddy core above 600 m as compared to the reference stations, both at day and night, but was similar below 600 m. Overall MSM49 resulted in a unique and valuable dataset for the region.

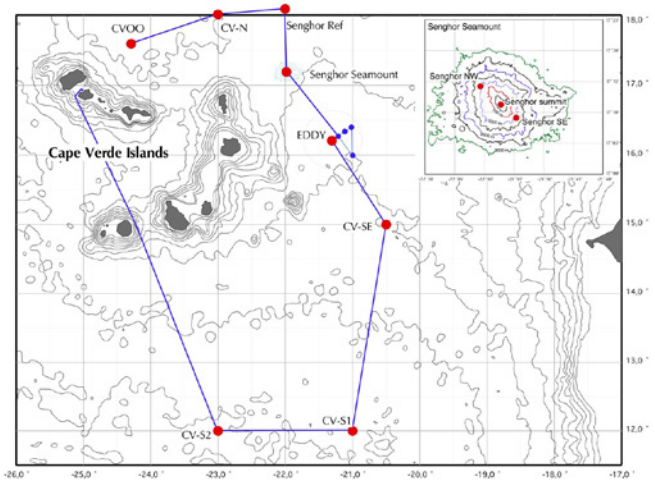

Fig. 1: Cruise track around the Cape Verde Archipelago of cruise MSM49 on RV MARIA S. MERIAN

MSM49*

PELAGIC ECOSYSTEM IMPACTS OF A CYCLONIC EDDY IN THE OPEN TROPICAL ATLANTIC

AUTHORS

GEOMAR Helmholtz Institute for Ocean Research Kiel | Kiel, Germany
H. Hauss, F. Schütte, H. J. T Hoving

Universtiy of Oslo | Oslo, Norway
S. Christiansen

University of British Columbia | Vancouver, Canada
F. Lüskow

Alfred Wegener Institute for Polar and Marine Research | Bremerhaven, Germany
F. Buchholz, C. Buchholz

Universität Hamburg, Institut für marine Ökosystem- und Fischereiwissenschaften (IMF) | Hamburg, Germany
A. Denda, B. Christiansen

The Cape Verde area is a hotspot for mesoscale eddies. In the Eastern Boundary Current System off the west African coast between Mauritania and Senegal, numerous eddies are generated throughout the year and propagate westward. They carry both a coastal anomaly into the open oligotrophic ocean as well as developing their own unique biological, biogeochemical and physical characteristics, depending on their size, rotation, propagation velocity and density structure. Here we report on the pelagic community associated with a productive cyclonic eddy east of the Cape Verde archipelago, which we observed and sampled during cruise MSM49 using a combination of in situ optical (PELAGIOS, UVP5) and acoustic (vmADCP) methods as well as depth-resolved net sampling (MOCNESS). The eddy featured enhanced particle flux and had developed a shallow oxygen minimum zone beneath the mixed layer which, however, did not restrain organisms (e. g. Euphausiacea) from vertically migrating through it. Euphausiids were present at lower diversity but higher abundance (e. g. E. americana and E. pseudogibba) compared to a reference station outside of the eddy. Other taxa that were positively impacted by the eddy included Poeobius sp., Pyrosoma atlanticum, rhizaria, salps and siphonophores.

MSM49*

FEEDING ECOLOGY OF THE ORANGEBACK SQUID STHENOTEUTHIS PTEROPUS IN THE EASTERN TROPICAL ATLANTIC

AUTHORS

GEOMAR Helmholtz Centre for Ocean Research Kiel | Kiel, Germany
V. Merten, J. Javidpour, U. Piatkowski, O. Puebla, H.-J. Hoving

Universität Hamburg, Institut für marine Ökosystem- und Fischereiwissenschaften (IMF) | Hamburg, Germany
B. Christiansen

Leibniz Zentrum für Marine Tropenforschung, Fischökologie und -evolution | Bremen, Germany
O. Puebla

El Colegio de la Frontera Sur | Chetumal, Mexico
F. Buchholz, C. Buchholz, R. Gasca

University of Southern Denmark, Department of Biology | Odense, Denmark
J. Javidpour

Most squids studied to date are characterized by short lifespans, fast growth rates and a single reproductive life cycle after which the individual dies. The orangeback squid Sthenoteuthis pteropus (Fig. 1) is a carnivorous oceanic squid and a dominant species of the epipelagic nekton community in the eastern tropical Atlantic (ETA) including the Cape Verde islands. This study aimed to characterize the role of S. pteropus in the pelagic food web of the ETA by investigating its diet and the dynamics of its feeding habits throughout its ontogeny and migration. Most specimens for this study were caught by hand jigging (n=57) during the cruise MSM49 and combined with specimens from M116 and M119 (nTOTAL=129). To assess the diet, feeding habits and trophic ecology of S. pteropus, stomach content analyses including DNA barcoding were combined with stable isotope analysis (□15N and □13C) of muscle tissue. To trace diet shifts through ontogeny and migration, stable isotope of consecutive gladii samples were measured. The diet analysis showed that S. pteropus mainly feeds on myctophid fishes such as Myctophum asperum, Myctophum nitidulum and Vinciguerria spp., but also on other teleost species, cephalopods (e. g. Enoploteuthidae, Bolitinidae, Ommastrephidae), crustaceans and possibly on gelatinous zooplankton. The squids feeding behavior is highly opportunistic and includes cannibalism which is common among squid species. The stable isotope

analysis of the mantle tissue shows a trophic increase of S. pteropus by one trophic level as the squid grows from a mantle length of 15 cm to 47 cm. The feeding chronologies reconstructed by the isotope analysis of the gladii revealed high intra- and inter-individual variability in the squid's trophic position and foraging area, findings that were not revealed by diet or muscle tissue analysis. This highlights the need to complement different methods to fully understand the variable and complex life history of deep-sea squids involving individual variation and migration.

Fig. 1: The orangeback squid Sthenoteuthis pteropus (photograph taken on MSM49 by Solvin Zankl)

REFERENCES

Merten V, Christiansen B, Javidpour J, Piatkowski U, Puebla O, Gasca R, Hoving HJT Diet and stable isotope analyses reveal the feeding ecology of the orangeback squid Sthenoteuthis pteropus (Steenstrup 1855) (Mollusca, Ommastrephidae) in the eastern tropical Atlantic, PLoS ONE 2017, 12(12): e0189691. https://doi.org/10.1371/journal.pone.0189691

MSM49*

THE VERTICAL DISTRIBUTION AND ABUNDANCE OF GELATINOUS MACROZOOPLANKON IN RELATION TO THE CAPE VERDEAN MESOPELAGIC OXYGEN MINIMUM ZONE

AUTHORS

GEOMAR Helmholtz Centre for Ocean Research Kiel | Kiel, Germany
P. Neitzel, H. Hauss, H.-J. Hoving

Oxygen minimum zones (OMZs) are persistent layers of decreased oxygen concentrations at mesopelagic depths (200–1000 m) that can affect the vertical distribution and migration of pelagic fauna. Gelatinous macrozooplankton are an abundant and ecologically diverse fraction of oceanic pelagic communities that show comparably high resilience towards low oxygen environments. During MSM49 we studied the vertical distribution of gelatinous fauna in the eastern tropical north Atlantic (ETA) close to the Cape Verdean Islands where an oxygen minimum zone is present between 300 and 500 m of depth. We performed horizontal pelagic video transects with the towed camera platform PELAGIOS at intermittent depths in the upper 1000 m of the water-column covering the OMZ as well as the more oxygenated waters located above and below.

From the collected video material we identified and counted the observed fauna and combined their vertical abundance data with CTD and oxygen profiles. As a result, we reconstructed taxon-specific vertical distributions of gelatinous macrozooplankton in relation to the OMZ, prey, temperature and salinity. We observed species that seem to avoid the OMZ (Atolla, Bathochordaeus, Beroe) and species that were associated with the OMZ (Colobonema, Halitrephes, Lilyopsis). We also found vertical distributions of gelatinous fauna that were continuous throughout the oxyclines (Solmissus), suggesting an ecology unaffected by the OMZ presence. These observations include one of the first of its kind in the ETA and we discuss our findings in the context of biodiversity and distribution, as well global change with an ongoing deoxygenation of the oceanic water column.

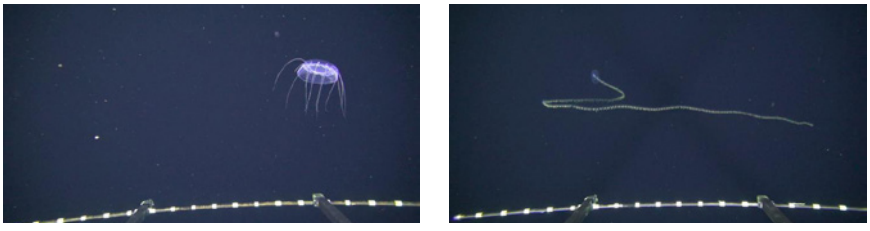

Fig. 1: Examples of fauna that were observed during PELAGIOS video transects in the deep water column of Cape Verde during MSM49. A) Solmissus and B) Praya dubia

MSM50

COASTAL BENTHIC ENVIRONMENTS IN THE NORTH AND BALTIC SEA: EVALUATION OF BENTHIC PROCESSES AND TRANSPORT AT THE SEDIMENT-WATER INTERFACE (KÜNO INTERFACE) – CRUISE MSM050

AUTHORS

Leibniz Institute for Baltic Sea Research Warnemünde | Rostock, Germany
U. Bathmann, M. E. Böttcher, M. Gogina, L. Umlauf, M. L. Zettler

Helmholtz Center Geesthacht, Institute of Coastal Research | Geesthacht, Germany
A. Neumann, D. Pröfrock, T. Sanders

University of Applied Science Hamburg, Faculty of Life Sciences | Hamburg, Germany
G. Witt

Introduction

The fundamental functions of sediments between the coastline and the shelf break are insufficiently synthesized to promote integrating studies along scales. Basic knowledge and integrated comprehension of the system is missing, that is required for an assess¬ment of the spatially resolved benthic ecosystem functions and services that are essential for temporal extrapolations. Thus, the investigation of biogeochemical and physical processes controlling the functional properties of different benthic-pelagic couplings is crucial to assess the sedimentary functions.

The reported expedition was a joint activity of the BMBF-funded projects NOAH (grant no. 03F0742) and SECOS (grant no. 03F0666A) to increase the understanding of biogeochemical, biological and physical processes along the sediment-water interface in the North and Baltic Sea. The core program of the cruise was dedicated to the completion of seasonal data in these regions, with the main focus on the determination of biogeochemical functions, their control mechanism for the relevant benthic habitat types and turbulence measurements of near bottom water layers as well as accumulation of organic pollutants, heavy metals in the sediments.

Methods

At five NOAH stations in the North Sea (Fig.1), sediment samples were taken by MUC and van Veen grab, along with CTD measurements and the use of the IOW benthic chamber lander and dredge. During the passage of Skagerrak and Kattegat, in addition to the classical oceanographic examination, benthic fauna samples were taken at 19 stations for comparison with historical data. A ship-bound current meter recorded physical effects on the

turbulence of finest sediment particles by mini-turbulences. In the Baltic Sea, five SECOS stations were investigated for geological, biological and biogeochemical analysis (pore-water biogeochemistry, associated nutrient fluxes across the sediment-water interface and sediment oxygen consumption) of sediments by using moorings. During the waiting time, microstructure measurements (MSS) of the surrounding water body were performed. Subsequently to biogeochemical analysis, sediment from the pore-water and incubation cores was sieved for taxonomic identification and estimation of benthic macrofauna density.

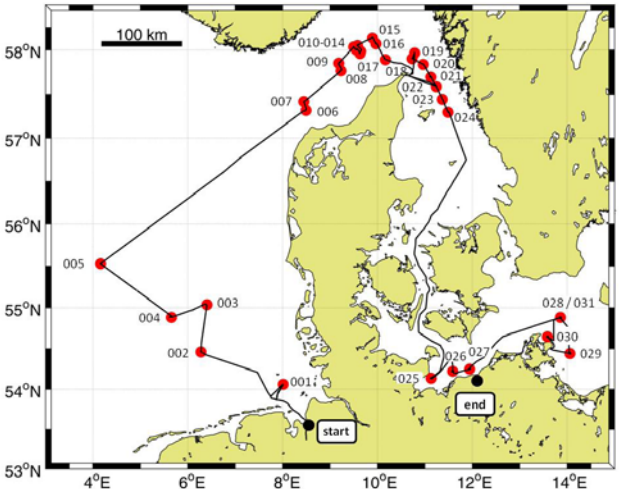

Fig. 1: Track chart of R/V MARIA S. MERIAN Cruise MSM50

Polychlorinated biphenyls (PCBs) and polycyclic aromatic hydrocarbons (PAHs) were determined in the sediment pore water system of North Sea surface sediments and sediment cores. The "ex-situ" SPME passive sampling method was applied.

To obtain data on trace metal distributions and the size and state of agglomeration of TiO_2 NPs in the aquatic environment, we used the hyphenation of inductively coupled plasma-mass spectrometry (ICP-MS) with sedimentation field-flow fractionation (SdFFF). In order to evaluate the potential anthropogenic release of TiO_2 NPs, we analyzed two sediment cores taken at the NOAH-MSM050 stations 10 and 14. Additionally, sediment samples were digested via microwave assisted acid digestion. Concentrations of heavy metals, including Zn, Cd and Pb, were analyzed in the <63µm grain size fraction of the sediment cores, using ICP-MS.

To obtain simultaneous profiles of stratification, turbidity (as a proxy for sediment concentration), and vertical turbulent mixing, we used a MSS90-L turbulence micro-structure profiler. These ship-based measurements were complemented by short-term mooring deployments, yielding a combined data set describing the variability of suspended matter concentrations, mean currents, waves, and mixing parameters.

Results and Discussion

The combined dataset on benthic macrofauna and sediment biogeochemistry was used to determine the dominant factors influencing the vertical distribution of geochemical parameters in the pore-waters of the studied habitats and to find similarities and patterns explaining significant variations of solute fluxes across the sediment-water interface (Gogina et al., 2018; Lipka et al., 2018). The MSM-50 data on benthic fluxes, nutrient concentrations, and N-isotopes in the German Bight represent otherwise scarce observations of nutrient turnover during the winter season and thereby contribute valuable data to the NOAH project.

On the basis of the measurements of 11 PAHs and 5 PCBs, it can be assumed that, on the basis of the substances measured, there is no potential hazard for the organisms living at these measuring points in any of the sediments investigated. The analysis of the sediment depth profiles enabled the reconstruction of recent loads of hydrophobic organic pollutants as well as the determination of the bioavailability and the risk of pollutants in sediment cores for benthic organisms. For the definition of assessment criteria within the framework of the marine protection conventions OSPAR and HELCOM, the data of the sediment cores analyzed in NOAH synthesis will be made available in the ICES database after the scientific publication.

SdFFF-ICP-MS might indicate an increase in the number of TiO_2 NPs in the upper sediment layers. However, up to now no clear statement can be made whether the increase of TiO_2 NPs is caused by anthropogenic inputs or natural effects. Multi-elemental analyses indicate an increase of heavy metal content for distinct sediment fractions. These might be related to anthropogenic heavy metal emissions into the marine environment during the last decades.

Turbulence microstructure observations conducted at stations in the Western Baltic Sea revealed that suspended sediments are confined to a turbulent bottom boundary layer (BBL) of several meters thickness. The dependence of BBL turbulence and resuspension on oscillating near-bottom currents (e. g. , due to upwelling events and internal wave motions) suggests a sediment “pumping” process, resulting in a net upslope transport of fine sediments. Sediment distributions on a transect from the basin towards the coast are in agreement with the type of sediments (characterized by the sediment settling velocity) required for upslope transport under the observed conditions. Fine-grained sediments, once deposited in the Arkona Basin, can thus be transported back onshore.

Conclusions

The results obtained from cruise MSM050 contributed substantially to the overall outcome of the KüNO projects NOAH and SECOS in their first and synthesis phase. By providing scientific knowledge on spatial and temporal patterns of sediment characteristics and functions, the project products NOAH Habitat-Atlas and Baltic Sea Atlas visualize the gained spatial information for use in coastal management processes.

REFERENCES

Gogina M, Lipka M, Woelfel J, Liu B, et al. In search of a field-based relationship between benthic macrofauna and biogeochemistry in a modern brackish coastal sea. Front. Mar. Sci. 2018, 5, 489. doi: 10.3389/fmars.2018.00489.

Lipka M, Woelfel J, Gogina M, Kallmeyer J, et al. Solute reservoirs reflect variability of early diagenetic processes in temperate brackish surface sediments. Frontiers in Marine Science 2018, 5:413: doi: 10.3389/fmars.2018.00413.

MSM50*

NUTRIENT REGENERATION AND BENTHIC FLUXES IN THE COASTAL BALTIC AND NORTH SEA

AUTHORS

Institute of Coastal Research Helmholtz Center Geesthacht | Geesthacht, Germany
A. Neumann, K. Dähnke, T. Sanders

In January 2016, we investigated nutrient fluxes and nitrate stable isotope composition in water samples along a North Sea – Skagerrak – Baltic Sea gradient during the Maria S. Merian cruise MSM 50.

Especially in the North Sea and the Skagerrak region, ^{15}N values of nitrate were unexpectedly high, and sediments were a source of nitrate. This nitrification signal suggests that the biogeochemical fluxes in bottom water resembled an autumn situation rather than the expected winter values. Parallel sediment incubations confirm that the benthic rates of oxygen consumption and nutrient turnover were indeed very similar to respective rates in autumn and that the sediment was a source of recycled nitrate. From the North Sea towards the Baltic Sea, we found, in accordance with previous studies, a depletion in nitrate stable isotope values, which is indicative of different nitrate sources in the respective basins: due to a higher share of nitrogen fixation in the Baltic Sea, the nitrogen stable isotope signal of surface sediments was depleted. This was mirrored in lower nitrate isotope values in the water column above the sediment.

Overall, the data highlight the importance of nitrate regeneration, and flux measurements enable us to unravel seasonal effects of fauna and microbiota.

MSM50*

EXPLORING THE INTERACTIONS BETWEEN BENTHIC MACROFAUNA AND BIOGEOCHEMISTRY IN THE SEDIMENTS OF THE SOUTH-WESTERN BALTIC SEA

AUTHORS

Leibniz Institute for Baltic Sea Research | Rostock, Germany
M. Gogina, M. Lipka, J. Woelfel, M. E. Böttcher, G. Rehder, M. L. Zettler

Porewater chemistry and sediment characteristics, ex situ nutrient fluxes, and structure of macrofauna community were assessed at six sites in the south-western Baltic Sea during different seasons between April 2015 and January 2016. During MSM50 expedition the measurements completing this time series and reflecting the winter conditions were carried out. Analysis of joint dataset revealed that biogenic mixing depth positively corresponded to maximum non-sulfidic depths determined from pore-water geochemistry. It was highest in sands and lowest in muds. From sand to mud, functional characteristics of benthic macrofauna community changed from dominance of suspension-feeders to deposit-feeders; the role of species that penetrate below the oxygenated zone and those having large individual size declined. Simultaneously, benthic solute reservoirs of ammonium, phosphate and silica in the top 10 cm of sediment, and respective diffusive fluxes increased. Derived data suggested the usefulness of bioturbation potential as proxy for variation in porewater reservoirs of biogeochemical components, compared to other available abiotic proxies, abundance or biomass for different functional groups. This can be explained by high scoring of deep-burrowing and bioturbating taxa (particularly large individuals) that have major influence on all oxygen-dependent biogeochemical processes. The effects of macrobenthos on benthic solute reservoirs and total fluxes differed between sediments and seasons, but no clear seasonal patterns could be revealed, reflecting high natural variability, but also occasional anthropogenic influence (e. g. fishery) or impact of storm events that inhibited clear interpretation of field data (Gogina et al., 2018; Lipka et al., 2018). Further investigations, both in deferent study areas and with higher replications, are still needed for precise understanding of biodiversity-environment interactions and ecosystem consequences of changes, which is essential for sustainable governance of marine resources and ecological services.

REFERENCES

Gogina M, Lipka M, Woelfel J, Liu B, Morys C, Böttcher ME, Zettler ML, In search of a field-based relationship between benthic macrofauna and biogeochemistry in a modern brackish coastal sea. Frontiers in Marine Science 2018, 5, 489, doi: 10.3389/fmars.2018.00489.

Lipka M, Woelfel J, Gogina M, Kallmeyer J, Liu B, Morys C, Forster S, Böttcher ME, Solute reservoirs reflect variability of early diagenetic processes in temperate brackish surface sediments. Frontiers in Marine Science 2018, 5, 413, doi: 10.3389/fmars.2018.00413.

MSM52

NEW INSIGHTS INTO SALT TECTONIC PROCESSES IN THE BALTIC SEA SECTOR OF THE NORTH GERMAN BASIN

AUTHORS

Institut for Geophysics, Center for Marine and Climate Research, University of Hamburg | Hamburg, Germany
C. Hübscher, N. Ahlrichs, L. Frahm, E. Seidel

Bundesanstalt für Geowissenschaften und Rohstoffe | Hannover/Berlin, Germany
N. Ahlrichs, V. Damm, V. Noack, M. Schnabel

Helmholtz Centre Potsdam German Research Centre for Geosciences – GFZ | Potsdam, Germany
C. Krawczyk

The Baltic sector of the North German Basin and Tornquist Fan area comprises the dominant tectonic Trans-European Suture Zone. The major aims of RV MARIA S. MERIAN expedition MSM52 was to test two major working hypotheses. These were: 1) Advances and retreats of ice-sheets during the glacially initiated and reactivated faulting of the Post-Permian succession, thereby generating several kilometers long near-vertical faults and small scale anticlines. 2) In contrast to generally accepted textbook models deformation of the Zechstein salt started already during salt deposition as the consequence of the intra-cratonic basin subsidence and resulting salt creep. We took advantage of the fact that, for the first time, the seismic equipment allowed for a gapless imaging of the upper crust from the Zechstein base to the sea floor in water depth of less than 20 meters. The seismic equipment comprised a 2700 m long streamer and eight GI-Guns as the seismic source.

The few 10 meters high and some 100 meters wide anticlines comprise Permian to Quaternary strata, and underlie tunnel valleys. Previous studies indicated a geological nature with an origin during ice advantages, while other publications documented the presence of high-velocity infill in tunnel valleys and resulting velocity pull-ups in seismic sections at various locations. The significant move-out of the reflections and the presence of refracted waves in the MSM52-data allowed the application of different quantitative methods to identify the anticlines as velocity pull-ups. First, the generation of partial-offset sections reveals an offset-dependence in the imaging of the anticlines caused by a local, near surface high-velocity zone. This also explains the observed smoothing of the anticlines with depth in the seismic image. Second, a velocity model gained by a traveltime tomography shows positive

velocity anomalies in the upper strata correlating with tunnel valleys resolved in the reflection seismics. High-frequency reflection seismic data confirms the result by a crisp image of a tunnel valley with a phase-reversed bottom reflection, caused by the velocity inversion at the base of the high-velocity valley fill deposits. Third, a prestack depth migration performed with a velocity model including a high-velocity zone results in a seismic image free of the anticline structure. This study shows on the one hand that the anticlines are no sign of recent salt tectonics in the Baltic Sea but imaging artefacts due to high-velocity infill of tunnel valleys and on the other hand that small velocity variations in the near-surface strata can lead to imaging artefacts and misinterpretation.

The investigation of salt tectonics is not accomplished yet. So far, we discuss the evolution of salt pillows in the Bay of Mecklenburg in the light of thin- and thick-skinned tectonics and differential loading. Stratigraphic interpretation of a 170 km long multichannel seismic line, extending from the Bay of Mecklenburg to northeast of Rügen Island, includes well information of nearby onshore wells. Our analysis reveals that subsidence during Late Triassic to Early Cretaceous at the northeastern basin margin is associated with transtensional dextral strike slip movements at the Tornquist Zone. We reinterpret the Werre and Prerow Fault Zones west of Rügen Island as an inverted, thin-skinned normal fault system. Salt movement in the Bay of Mecklenburg was initiated in the Late Triassic lasting until the Jurassic. A second phase of salt pillow growth occurred during the Coniacian until Tertiary and correlates with uplift of the basin margin. We associate the initiation of the uplift with Late Cretaceous compressional tectonics. Thin-skinned deformation explains salt pillow evolution in the Bay of Mecklenburg. Additionally, we discuss an impact of gravity gliding induced by basin margin tilt on salt pillow evolution. We propose a slow downdip salt flow alongside homogenous updip salt depletion during the Late Cretaceous to Tertiary phase of salt remobilization.

Outlook: Since November 2018 the German Science Foundation funds one PostDoc and one PhD position for three years (DFG grant HU698/25). Under the umbrella of this "BalTec" project, the MSM52 and other seismic reflection data (Fig. 1) are analyzed regarding the general geological evolution of the southern Baltic regrading inversion tectonics, salt tectonics and fluid migration along the Tornquist Zone from Skagerrak to the Polish coast.

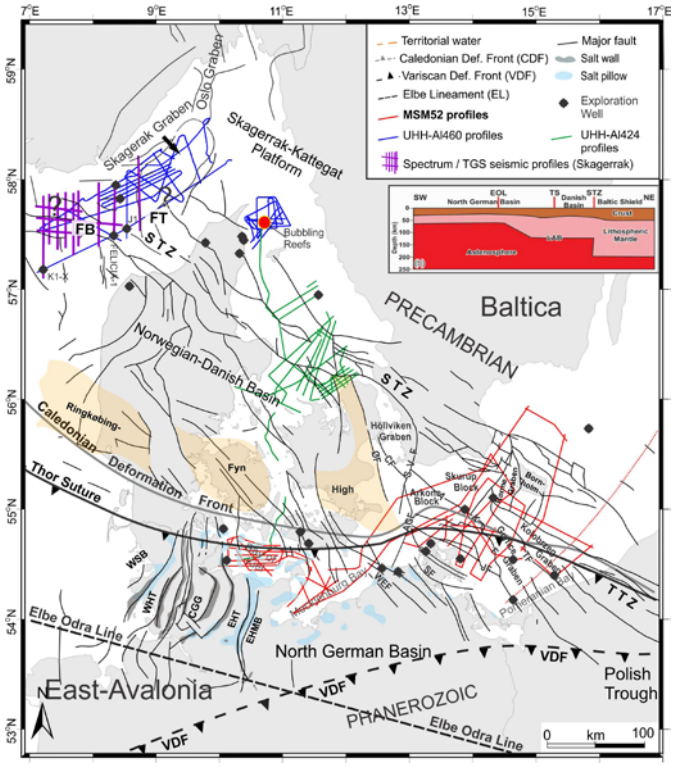

Fig. 1: Study area and seismic base map for BalTec-project. MSM52 profiles in red.

MSM54 & MSM40

PROCESS STUDIES IN THE SUBPOLAR NORTH ATLANTIC

AUTHORS

GEOMAR Helmholtz Centre for Ocean Research Kiel | Kiel, Germany
J. Karstensen, M. Visbeck, P. Handmann

NOC Southampton | Southampton, UK
M. Oltmanns

Intense oceanic uptake of oxygen during 2014–2015 winter convection in the Labrador Sea by Koelling et al. (2017), Measurements of near-surface oxygen (O_2) concentrations and mixed layer depth from the K1 mooring in the central Labrador Sea are used to calculate the change in column-integrated (0–1700 m) O_2 content over the deep convection winter 2014/2015 (MSM40/MSM54). During the mixed layer deepening period, November 2014 to April 2015, the oxygen content increased by 24.3 ± 3.4 mol m^{-2}, 40 % higher than previous results from winters with weaker convection. By estimating the contribution of respiration and lateral transport on the oxygen budget, the cumulative air-sea gas exchange is derived. The O_2 uptake of 29.1 ± 3.8 mol m^{-2}, driven by persistent undersaturation (5 %) and strong atmospheric forcing, is substantially higher than predicted by standard (nonbubble) gas exchange parameterizations, whereas most bubble-resolving parameterizations predict higher uptake, comparable to our results. Generally large but varying mixed layer depths and strong heat and momentum fluxes make the Labrador Sea an ideal test bed for process studies aimed at improving gas exchange parameterizations.

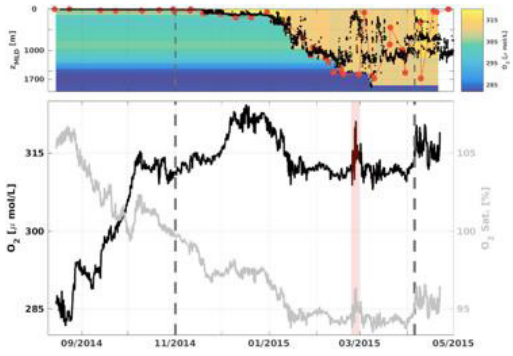

Fig. 1: Koeling et al. (top) Daily mean mixed layer depth, zMLD from mooring data (black dots), instantaneous zMLD from Argo profiles within 100 km of the K1 site (red circles), and contours of $O_2(z, t)$, calculated from equation (1). (bottom) Surface oxygen concentration (black) and saturation (gray). Red shading marks the passing of an eddy, and dashed vertical lines show the start and end times for the analysis of gas exchange.

Mean circulation and EKE distribution in the Labrador Sea Water level of the subpolar North Atlantic by Fischer et al. (2018), A long-term mean flow field for the subpolar North Atlantic region with a horizontal resolution of approximately 25 km is created by gridding Argo-derived velocity vectors using two different topography-following interpolation schemes. The 10-day float displacements in the typical drift depths of 1000 to 1500 m represent the flow in the Labrador Sea Water density range. Both mapping algorithms separate the flow field into potential vorticity (PV) conserving, i. e. , topography-following contribution and a deviating part, which we define as the eddy contribution. To verify the significance of the separation, we compare the mean flow and the eddy kinetic energy (EKE), derived from both mapping algorithms, with those obtained from multiyear mooring observations (serviced by MSM40 and MSM54). The PV-conserving mean flow is characterized by stable boundary currents along all major topographic features including shelf breaks and basin-interior topographic ridges such as the Reykjanes Ridge or the Rockall Plateau. Mid-basin northward advection pathways from the north- eastern Labrador Sea into the Irminger Sea and from the Mid-Atlantic Ridge region into the Iceland Basin are well- resolved. An eastward flow is present across the southern boundary of the subpolar gyre near 52°N, the latitude of the Charlie Gibbs Fracture Zone (CGFZ). The mid-depth EKE field resembles most of the satellite- derived surface EKE field. However, noticeable differences exist along the northward advection pathways in the Irminger Sea and the Iceland Basin, where the deep EKE exceeds the surface EKE field. Further, the ratio between mean flow and the square root of the EKE, the Peclet number, reveals distinct advection-dominated regions as well as basin-interior regimes in which mixing is prevailing.

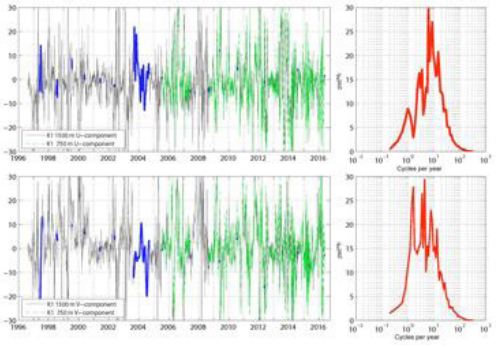

Fig. 2: Fischer et al. (2018) Example of a current time series from the central Labrador Sea at mooring K1. Two depth levels were occupied regularly (750m since 2006, green curve; 1500m since 1996). Gaps (blue lines) are filled by interpolation based on empirical orthogonal functions (Zantopp et al., 2017). High-frequency spectra from 1500m records (right column).

Increased risk of a shutdown of ocean convection posed by warm North Atlantic summers by Oltmanns et al. (2018), A shutdown of ocean convection in the subpolar North Atlantic, triggered by enhanced melting over Greenland, is regarded as a potential

transition point into a fundamentally different climate regime. Noting that a key uncertainty for future convection resides in the relative importance of melting in summer and atmospheric forcing in winter, we investigate the extent to which summer conditions constrain convection with a comprehensive dataset, including hydrographic records that are over a decade in length from the convection regions (MSM40 and MSM54 mooring reinstallation and data calibration). We find that warm and fresh summers, characterized by increased sea surface temperatures, freshwater concentrations and melting, are accompanied by reduced heat and buoyancy losses in winter, which entail a longer persistence of the freshwater near the surface and contribute to delaying convection. By shortening the time span for the convective freshwater export, the identified seasonal dynamics introduce a potentially critical threshold that is crossed when substantial amounts of freshwater from one summer are carried over into the next and accumulate. Warm and fresh summers in the Irminger Sea are followed by particularly short convection periods. We estimate that in the winter 2010–2011, after the warmest and freshest Irminger Sea summer on our record, ~40 % of the surface freshwater was retained.

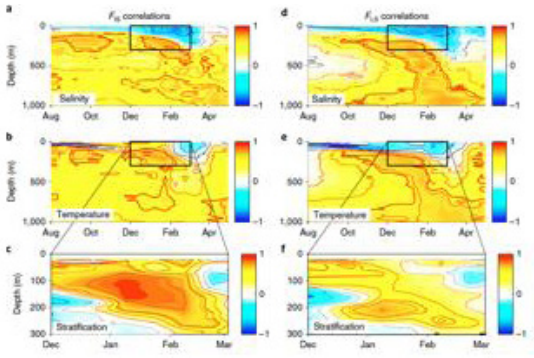

Fig. 3: Oltmanns et al. (2018) Summer constraints on hydrographic evolution in the Labrador Sea. a, b, c, Correlation of salinity (a), temperature (b) and stratification (c) in the Labrador Sea with FIS, where stratification is expressed by means of the vertical potential density gradient. d, e, f, Correlations of the same respective measures, but with FLS. Thick contours delineate the 95 % confidence level and thin contours represent isolines at intervals of 0.2. The underlying hydrographic time series were obtained from the mooring and Argo float observations

From interannual to decadal: 17 years of boundary current transports at the exit of the Labrador Sea by Zantopp et al. (2017), Over the past 17 years, the western boundary current system of the Labrador Sea has been closely observed by maintaining the 53°N Array (moorings and shipboard station data; including MSM40 & MSM54) measuring the top-to-bottom flow field offshore from the Labrador shelf break. Volume transports for the North Atlantic Deep Water (NADW) components were calculated using different methods, including gap filling procedures for deployment periods with suboptimal instrument coverage. On average the Deep Western Boundary Current (DWBC) carries 30.2 6 6.6 Sv of NADW southward, which are almost equally partitioned between Labrador Sea Water (LSW, 14.9 6 3.9 Sv) and Lower North Atlantic Deep Water

(LNADW, 15.3 6 3.8 Sv). The transport variability ranges from days to decades, with the most prominent multiyear fluctuations at interannual to near decadal time scales (65 Sv) in the LNADW overflow water mass. These long-term fluctuations appear to be in phase with the NAO-modulated wind fluctuations. The boundary current system off Labrador occurs as a conglomerate of nearly independent components, namely, the shallow Labrador Current, the weakly sheared LSW range, and the deep baroclinic, bottom-intensified current core of the LNADW, all of which are part of the cyclonic Labrador Sea circulation. This structure is relatively stable over time, and the 120 km wide boundary current is constrained seaward by a weak counterflow which reduces the deep water export by 10–15 %.

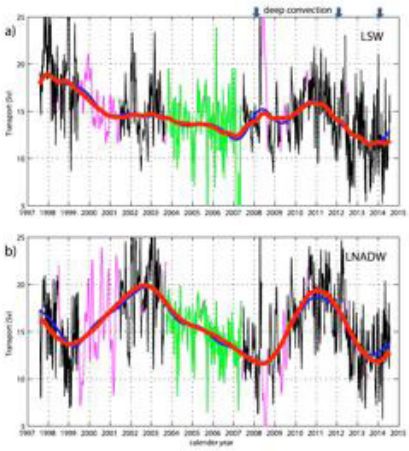

Fig. 4: Zantopp et al. (2017) Export from the Labrador Sea at 5-day resolution and without gaps; black lines are for periods of full array coverage; green lines for periods with reduced coverage but with central mooring K9 in place, and magenta lines for gaps filled by SSA (EOF) modes. The low frequency variation is dominated by a pair of SSA modes at quasi-decadal time scales.

The Deep Western Boundary Current in the Labrador Sea From Observations and a High-Resolution Model by Handmann et al. (2018) Long-term observations from a 17 year long mooring array at the exit of the Labrador Sea at 53°N are compared to the output of a high-resolution model (VIKING20). Both are analyzed to define robust integral properties on basin and regional scale, which can be determined and evaluated equally well. While both, the observations and the model, show a narrow DWBC cyclonically engulfing the Labrador Sea, the model's boundary current system is more barotropic than in the observations and spectral analysis indicates stronger monthly to interannual transport variability. Compared to the model, the observations show a stronger density gradient, hence a stronger baroclinicity, from center to boundary. Despite this, the observed temporal evolution of the temperature in the central Labrador Sea is reproduced. The model results yield a mean export of North Atlantic Deep Water (NADW) (33.0+-5.7 Sv), which is comparable tothe observed transport (31.2+-5.5 Sv) at 538N. The results also include a comparable spatial pattern and March mixed layer depth in the

central Labrador Sea (maximum depth approx. 2,000 m). During periods containing enhanced deep convection (1990s) our analyses show increased correlation between LSW and LNADW model transport at 538N. Our results indicate that the transport variability in LSW and LNADW at 538N is a result of a complex modulation of wind stress and buoyancy forcing on regional and basin wide scale.

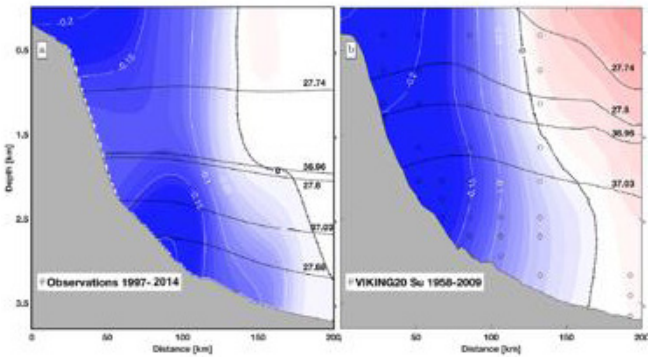

Fig. 5: Handmann et al; Mean velocity field along the 53°N section, computed from (a) LADCP and mooring data (1997–2014); (b) the horizontally and vertically subsampled model output (1958–2009). The mean velocity fields are superimposed by isotachs in m s^{-1} (white) and sigma2 and sigma 0 mean isopycnals. Additionally the 0 isotach is marked in dotted black. Blue velocities are directed to the southeast and red velocities are directed to the northwest.

REFERENCES

Fischer, J., Karstensen, J., Oltmanns, M., and Schmidtko, S.: Mean circulation and EKE distribution in the Labrador Sea Water level of the subpolar North Atlantic, Ocean Sci., 14, 1167–1183, https://doi.org/10.5194/os-14-1167-2018, 2018.

Handmann, P., Fischer, J., Visbeck, M., Karstensen, J., Biastoch, A., Böning, C., & Patara, L. The deep western boundary current in the Labrador Sea from observations and a high-resolution model. Journal of Geophysical Research: Oceans, 123, 2829–2850. https://doi.org/10.1002/2017JC013702, 2018.

Oltmanns, M., J. Karstensen, J. Fischer. Increased risk of a shutdown of ocean convection posed by warm North Atlantic summers. Nature Climate Change, http://dx.doi.org/10.1038/s41558-018-0105-1, 2018.

Koelling, J., Wallace, D. W. R., Send, U. and Karstensen, J., Intense oceanic uptake of oxygen during 2014–15 winter convection in the Labrador Sea, Geophys. Res. Lett., doi:10.1002/2017GL073933, 2017.

Zantopp, R., J. Fischer, M. Visbeck, and J. Karstensen, From interannual to decadal: 17 years of boundary current transports at the exit of the Labrador Sea, J. Geophys. Res. Oceans, 122, doi:10.1002/2016JC012271, 2017.

MSM55

MARIA S. MERIAN CRUISE MSM55 – HABITAT CHARACTERISTICS AND CARBONATE CYCLING OF MACROPHYTE-SUPPORTED POLAR CARBONATE FACTORIES (SVALBARD)

AUTHORS

Marine Research Department | Wilhelmshaven, Germany
M. Wisshak

In June 2016, the RV Maria S. Merian expedition MSM55 (acronym ARCA) led a team of 14 scientists (chiefly from SENCKENBERG and GEOMAR), 2 technicians, the 3-persons JAGO team, and two journalists, into the polar waters of the Svalbard Archipelago for studying two contrasting sites of intense biogenic carbonate production. Specifically, these cold-water "carbonate factories" were the rhodolith beds in Mosselbukta in northern Spitsbergen and the extensive biogenic carbonate sediments accumulating in the strong hydrodynamic regime at Bjørnøy-Banken near the southern delineation of the archipelago.

The habitat characteristics and biosedimentary dynamics of these carbonate factories were studied along bathymetrical gradients from the intertidal to aphotic depths, following a holistic approach. The scientific disciplines and methodological tool-kit comprised hydroacoustic habitat mapping (multibeam-echosounder and sidescan-sonar surveys), visual habitat mapping (research submersible and drop-camera surveys), hydrographic investigations including assessment of the aqueous carbonate system (CTD and water samples), epibenthos inventory (beam-trawls and excursions to shore), recording of short-term environmental fluctuations and benthic community dynamics (camera-lander), classical carbonate facies (Shipek-grabs and excursions to shore), and an evaluation of carbonate (re)cycling, including budgeting calcification versus bioerosion (recovery of a 10-year settlement experiment). The vulnerability to past and future climate change, i. e. ocean acidification and warming, was studied by means of applying and developing geochemical proxies encoded in the skeletons of calcifiers (e. g., coralline algae, balanids, bivalves), and via on-board acidification and temperature-stress experiments. Despite of a two-day delay already before the start of the cruise (due to repair of MSM's A-frame) all of the proposed target stations were successfully covered, providing sufficient samples and hydroacoustic/environmental data for tackling the ten scientific goals outlined in the proposal and cruise report.

To this date (November 2019), the results of our multidisciplinary analyses were funnelled into a total of nine peer-reviewed ISI publications (5 published and 4 in review) and half a dozen of additional papers that are currently in preparation. An

add-on project entitled "Patterns and Pace of Polar Bioerosion" (DFG Wi 3754/3-1) was proposed and approved. Half of the scientific objectives have been successfully concluded and good progress in being made in the other half. Key results include a detailed portrait of the seasonal as well as short-term environmental fluctuations and epibenthos dynamics (filter-feeding activity and motion tracking) at the two studied polar carbonate factories (Wisshak et al. 2019, Wisshak & Neumann in review), the first inventory of Arctic microbioerosion traces (Meyer et al. in review), including a new ichnospecies indicative for polar environments (Wisshak et al. 2018), as well as geochemical proxy development and application in brachiopods (Bajnai et al. 2018), the calcareous rhodophytes Lithothamnion glaciale (Hofmann & Heesch 2018, Teichert et al. in review) and Clathromorphum compactum (Hetzinger et al. 2019), the latter yielding a +200 year record of an alarming decline in sea ice cover in N-Spitzbergen. In addition, a likewise alarming analysis of microplastics was undertaken, which revealed accumulation of microplastics in the Mosselbukta rhodolith beds (Löder et al. in review). In respect to public outreach in prime print media, the cruise and its scientific background were portrayed in the feature article "Karbonatfabriken im Polarmeer" in Natur-Forschung-Museum as well as in the article "Tauchfahrt ins Archiv der Arktis" in the magazine GEO.

REFERENCES

Bajnai D, Fiebig J, Tomašových A, Milner SG, Rollion-Bard C, Raddatz J, Löffler N, Primo-Ramos C & Brand W (2018). Assessing kinetic fractionation in brachiopod calcite using clumped isotopes. Scientific Reports 8: article 533. DOI: 10.1038/s41598-017-17353-7.

Hetzinger S, Halfar J, Zajacz Z, Wisshak M (2019) Early start of 20th-century Arctic sea-ice decline recorded in Svalbard coralline algae. Geology 47:963–967. DOI: 10.1130/G46507.1

Hofmann LC & Heesch S (2018) Latitudinal trends in stable isotope signatures and carbon-concentrating mechanisms of northeast Atlantic rhodoliths. Biogeosciences 15:6139-6149. DOI: 10.5194/bg-15-6139-2018

Löder MGJ, Teichert S, Pyko I, Mordek M, Schulbert C, Wisshak M, Laforsch C (in review) Arctic rhodolith beds – a biodiverse ecosystem endangered by microplastics? Nature Communications.

Meyer N, Wisshak M, Freiwald A (in review) Ichnodiversity and bathymetric range of microbioerosion traces in polar balanids of Svalbard. Polar Research.

Teichert S, Voigt N, Wisshak M (in review) Do skeletal Mg/Ca ratios of Arctic rhodoliths reflect atmospheric CO_2 concentrations? Polar Biology.

Wisshak M, Meyer N, Radtke G & Golubic S (2018) Saccomorpha guttulata – a new marine fungal microbioerosion trace fossil from cool- to cold-water settings. Paläontologische Zeitschrift 92:525–533. DOI: 10.1007/s12542-018-0407-7

Wisshak M, Neumann C (in review) Dead Urchin Walking – resilience of an Arctic Strongylocentrotus droebachiensis with presumably fatal predation damage. Polar Biology.

Wisshak M, Neumann H, Rüggeberg A, Büscher JV, Linke P, Raddatz J (2019) Epibenthos dynamics and environmental fluctuations in two contrasting polar carbonate factories (Mosselbukta and Bjørnøy-Banken, Svalbard). Frontiers in Marine Science 6: article 667. DOI: 10.3389/fmars.2019.00667

MSM55*

ARCTIC RHODOLITH BEDS – A BIODIVERSE ECOSYSTEM ENDANGERED BY MICROPLASTICS?

AUTHORS

Fachgruppe Paläoumwelt, GeoZentrum Nordbayern, Friedrich-Alexander-Universität Erlangen-Nürnberg (FAU) | Erlangen, Germany
S. Teichert*, I. Pyko*, C. Schulbert

Department of Animal Ecology I and BayCEER, University of Bayreuth | Bayreuth, Germany
M. G. J. Löder*, M. Mordek, C. Laforsch

Marine Research Department, Senckenberg am Meer | Wilhelmshaven, Germany
M. Wisshak

* Equal author contribution

Microplastic (MP) particles have been reported to occur in the Arctic environment. However, the impact on the ecosystem and organism level remains widely unclear. Along the remote coast of Svalbard, large areas of the seafloor are covered by rhodolith beds. Rhodoliths consist of rigid calcite nodules formed by coralline red algae of the species Lithothamnion glaciale. The rhodoliths are gouged by boring bivalves of the species Hiatella arctica, thus resulting in hollow rhodoliths. The interaction of these two ecosystem engineers increases the local biodiversity significantly, because the hollow rhodoliths are inhabited by a great variety of organisms. Using samples from two different water depths (27 m and 40 m), we show a ubiquitous MP contamination within H. arctica. In 12 bivalves, originating from six rhodoliths localized using micro-computed tomography, we found 516 particles of eight different polymer types. The number of ingested particles correlated with bivalve size. Polymer composition and abundance differed with water depth according to polymer density. Long-term consequences are yet unclear, but ingested MPs may compromise the vitality of the bivalves, which need approx. 20 years to gouge one rhodolith. Therefore, a deterioration of, e. g., the bivalve's drilling capacity and thereby its functioning as an ecosystem engineer would imply lasting consequences for the local biodiversity.

MSM55*

EARLY START OF 20TH-CENTURY ARCTIC SEA-ICE DECLINE RECORDED IN SVALBARD CORALLINE ALGAE

AUTHORS

Institut für Geologie, Universität Hamburg | Hamburg, Germany
S. Hetzinger (Corresponding author)

CPS-Department, University of Toronto Mississauga | Mississauga (ON), Canada
J. Halfar

Department of Earth Sciences, University of Toronto | Toronto (ON), Canada
Z. Zajacz

Senckenberg am Meer, Marine Research Department | Wilhelmshaven, Germany
M. Wisshak

The fast decline of Arctic sea-ice is a leading indicator of ongoing global climate change and is receiving substantial public and scientific attention. Projections suggest that Arctic summer sea-ice may virtually disappear within the course of the next fifty or even thirty years with accelerating Arctic warming, which is approximately twice as large as the global average. However, limited observational records and lack of annual-resolution marine sea-ice proxies hamper the assessment of long-term changes in sea-ice, leading to large uncertainties in predictions of its future evolution under global warming. Crustose coralline algae of the species Clathromorphum compactum can reach multi-century lifespans, form annual growth bands, and are widespread and abundant throughout the Arctic growing on the shallow seafloor. By analyzing geochemical signals and annual growth increments encoded in the algaes' high-Mg calcite skeletons, they can provide annually resolved reconstructions of past Arctic sea-ice variability.

Here, we use long-lived encrusting coralline algae that strongly depend on light availability as a new in situ proxy to reconstruct past variability in the duration of seasonal sea-ice cover off northern Spitsbergen, Svalbard (79.9°N, 15.9°E, Figure 1). Coralline algal samples were collected during R/V Maria S. Merian cruise 55 in 2016. Our data represent the northernmost annual-resolution marine sea-ice reconstruction to date, extending to the early 19th century (Figure 2), significantly beyond satellite-based sea-ice measurements beginning in the late 1970s. Algal records show that the decreasing trend in sea-ice cover in the high Arctic has already started at the beginning of the 20th century (Hetzinger et al. 2019), earlier than previously reported from sea-ice reconstructions based on terrestrial archives. Our data further suggest that, although sea-ice varies on

multidecadal timescales, lowest sea-ice values within the last 200 years occurred at the end of the 20th century.

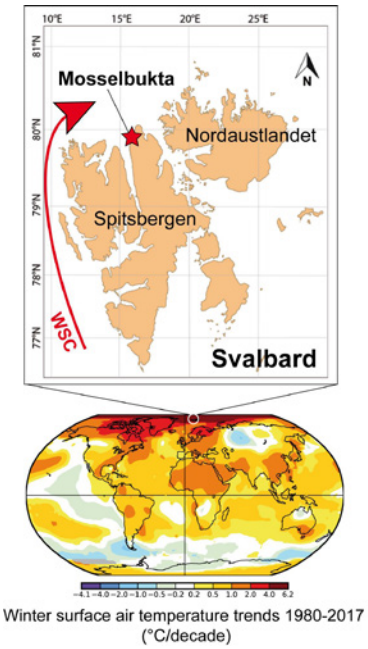

Fig. 1: Study area and Arctic warming trends. Upper plot: Map of Svalbard archipelago in the arctic North Atlantic with location of Mosselbukta study site in northern Spitsbergen (red asterisk), where long-lived encrusting coralline algal buildups were collected in June 2016. Red arrow indicates approximate path of West Spitsbergen Current (WSC). Lower plot: Global winter surface air temperature trends since C.E. 1980 (linear trends in °C/decade for December–February). Location of Svalbard archipelago (white open circle) is shown. Data source: http://data.giss.nasa.gov/gistemp. Modified from Hetzinger et al. (2019).

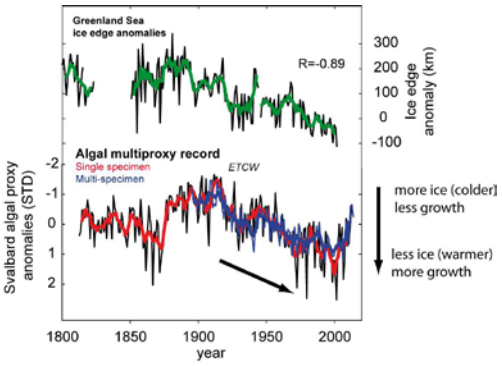

Fig. 2: Sea-ice proxy reconstructions from the Svalbard algal multiproxy record, shown as single-specimen (red; time span covered by the proxy: 1813–2015) and multi-specimen records (blue; 1895–2015), together with the ETCW (early 20th-century warming in the Arctic). Black thick arrow depicts declining trend in Svalbard sea-ice since the early 20th-century. The algal sea-ice reconstruction shows high correspondence to historical observations of the sea-ice edge position from the Greenland Sea (green). Correlation coefficient (R) for 11-year running mean. Modified from Hetzinger et al. (2019).

REFERENCES

Hetzinger, S., Halfar, J., Zajacz, Z., Wisshak, M., (2019), Early start of 20th-century Arctic sea-ice decline recorded in Svalbard coralline algae, Geology, v. 47(10), pp. 963–967, doi:10.1130/G46507.1

MSM56

DRILLING GAS HYDRATES ON THE CONTINENTAL MARGIN OF WESTERN SVALBARD, ARCTIC OCEAN

AUTHORS

Alfred-Wegener-Institut Helmholtz Zentrum für Polar- und Meeresforschung | Bremerhaven, Germany
B. P. Koch, U. John, C. Burau, J. Geuer, M. Hoppema, M. Iversen, C. Konrad, N. Kühne, A. Mackensen, M. Seifert, H. van der Jagt, S. Wohlrab

University of Applied Sciences | Bremerhaven, Germany
B. P. Koch

Max-Planck-Institut für Marine Mikrobiologie | Bremen, Germany
R. Amann, J. Wulf

Norwegian Polar Institute, Fram Centre | Tromsø, Norway
P. Assmy, M. Fernández-Méndez

Helmholtz-Zentrum für Ozeanforschung | Kiel, Germany
L. Bach

University of Oslo | Oslo, Norway
B. Edvardsen

Institut für Chemie und Biologie des Meeres der Universität Oldenburg | Oldenburg, Germany
A. Friedrichs, K. Schwalfenberg, O. Zielinski

University of Bremen | Bremen, Germany
O. Huhn

Zentrum für Marine Umweltwissenschaften der Universität Bremen | Bremen, Germany
M. Iversen, H. van der Jagt

Helmholtz-Zentrum für Umweltforschung Leipzig | Leipzig, Germany
O. J. Lechtenfeld

Virginia Commonwealth University | Richmond (VA), USA
11 S. L. McCallister,

University of Helsinki | Helsinki, Finland
12 E. Nystedt

Helmholtz Zentrum München | München, Germany
13 P. Schmitt-Kopplin

Technical University of Denmark | Copenhagen, Denmark
14 C. Stedmon, U. Wünsch

Netherlands Institute of Ecology | Wageningen, Netherlands
15 D. van de Waal

Global change causes fundamental environmental changes in the Arctic. Increasing temperatures result in melting of the Greenland ice sheet and increased freshwater discharge. Currently, the average net loss of ice on Greenland exceeds 200 Gigatons per year contributing to a sea level rise of more than 0.5 mm per year. The cruise MSM56 hosted 22 participating scientists from Germany, Norway, the Netherlands, Denmark, Sweden, Finland and the United States and covered scientific expertise in (micro-) biology, chemistry, and oceanography. Our study aimed at (i) changes of the phyto- and bacterioplankton community along salinity gradients in Arctic fjords and (ii) the impact of changes in freshwater input on biogeochemical fluxes and chemical modification of organic substrates and metabolites. Community composition is an important driver of particulate and dissolved matter partitioning and for the bioavailability of organic matter to grazers and microbes. Hence, carbon flux in the water column depends on primary production and respiration from, both, microbes and vertically migrating zooplankton flux feeders. We studied three Fjord systems (Kongsfjord, Svalbard; Scoresby Sund, Greenland and Arnarfjörður, Iceland), which differed in their extent of available scientific information, their size, geomorphology, glacier volume, extent of freshwater input, and their biogeochemical settings. The Scoresby Sound is world's largest fjord and was the main study area of our expedition. At the inner end of the Scoresby Sound (Nordvestfjord), the massive Daugaard-Jensen Glacier drains about 4% of the Greenland ice sheet. One of the few well-documented expeditions in the Scoresby Sound was carried out with the German research vessel Polarstern in September 1990. Compared to our cruise the salinity at depth of the fjord was identical but the temperature showed an increase of almost +0.5°C after 26 years. The higher temperature is attributed to the inflow of warmer water from the East Greenland Sea. In addition to direct measurements of hydrography, biogeochemical parameters and sediment trap fluxes, we derived net community production (NCP) and full water column particulate

organic carbon (POC) fluxes, and estimated carbon remineralization from vertical flux attenuation. While the narrow Nordvestfjord is influenced by subglacial and surface meltwater discharge, these meltwater effects on the outer fjord part of Scoresby Sund are weakened due to its enormous width. We found that subglacial and surface meltwater discharge to Nordvestfjord significantly limited NCP to 32–36 mmol C m^{-2} d^{-1} compared to the outer fjord part of Scoresby Sund (58–82 mmol C m^{-2} d^{-1}) by inhibiting the resupply of nutrients to the surface and by shadowing of silts contained in the meltwater. The POC flux close to the glacier fronts was elevated due to silt-ballasting of settling particles that increases the sinking velocity and thereby reduces the time for remineralization processes within the water column. By contrast, the outer fjord part of Scoresby Sund showed stronger attenuation of particles due to horizontal advection and, hence, more intense remineralization within the water column. Our results imply that glacially influenced parts of Greenland's fjords can be considered as hotspots of carbon export to depth. In a warming climate, this export is likely to be enhanced during glacial melting. Additionally, entrainment of increasingly warmer Atlantic Water might support a higher productivity in fjord systems. It therefore seems that future ice-free fjord systems with high input of glacial meltwater may become increasingly important for Arctic carbon sequestration.

MSM57

DRILLING GAS HYDRATES ON THE CONTINENTAL MARGIN OF WESTERN SVALBARD, ARCTIC OCEAN

AUTHORS

MARUM – Center for Marine Environmental Sciences and Department of Geosciences, University of Bremen | Bremen, GERMANY
T. Pape, G. Bohrmann, T. Freudenthal, P. Wintersteller

GEOMAR – Helmholtz Centre for Ocean Research Kiel | Kiel, GERMANY
M. Riedel, K. Wallmann, C. Berndt

CAGE – Centre for Arctic Gas Hydrate, Environment and Climate, Department of Geosciences, UiT - The Arctic University of Norway | Tromsø, NORWAY
WL. Hong, S. Bünz, G. Panieri, A. Lepland

CEOAS, Oregon State University | Corvallis (OR), USA
M. Torres

The main objective of cruise MSM57/1+2 was to investigate gas hydrate systems and their dynamics at the western continental margin of Svalbard. Based on seismic data collected during previous cruises, two research areas (Nos. 1 and 2; Figure 1) were selected for sediment core drilling with the seafloor drill rig MARUM-MeBo70 (Freudenthal & Wefer, 2013). Additional cores of shallow sediment were retrieved by gravity coring, while in situ sediment temperatures were determined with a temperature lance. Furthermore, hydroacoustic surveys have been conducted with the hull-mounted KONGSBERG EM122 and EM1002 multibeam echosounder systems. Here we report on the activities in the indi–vidual research areas and present results as well as interpretations of data obtained.

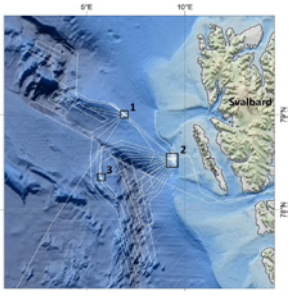

Fig. 1: Track lines of MARIA S. MERIAN cruise MSM57 with stations visited with the MARUM-MeBo70 seafloor drill rig in three areas: 1 = Vestnesa Ridge, 2 = upper continental margin of Svalbard off Prins Karls Foreland, 3 = Svyatogor Ridge.

Vestnesa Ridge (Research Area 1) is an elongated sediment drift that hosts an active gas and gas hydrate system. Along its crest line several pockmarks occur above seismic chimney structures in the subsurface with some of them showing active seafloor gas seepage. In order to determine the distribution of gas hydrates inside and outside of chimney structures four MeBo drillings down to 62.5 meters below seafloor (mbsf) were conducted at the so-called Lunde pockmark at ~1200 meters below sea level (mbsl) (Figure 2).

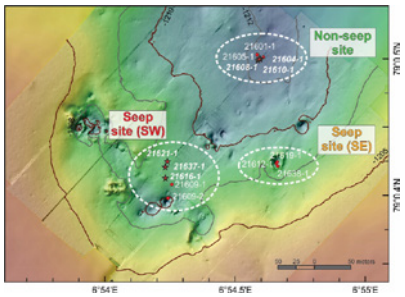

Fig. 2: Micro-Bathymetric map of Lunde pockmark showing positions of MeBo cores (red stars) gravity cores (red dots) and at the non-seep site and the two seep sites. Figure modified after Pape et al. (accepted).

Results from the drillings revealed that gas hydrates and seafloor gas seepage are present where a fracture net–work beneath the pockmark focusses migration of thermo–genic hydrocarbons. Thermo–genic hydrocarbons bound in shallow hydrates clearly differ in hydrocarbon ratios (C_1/C_{2+}) and stable isotopic compositions (δ^2H-CH_4, δ^{13}C-CH_4) from microbial hydrocarbons that were collected at the 'Non-seep site' and a nearby reference station (Pape et al., accepted; Figure 3).

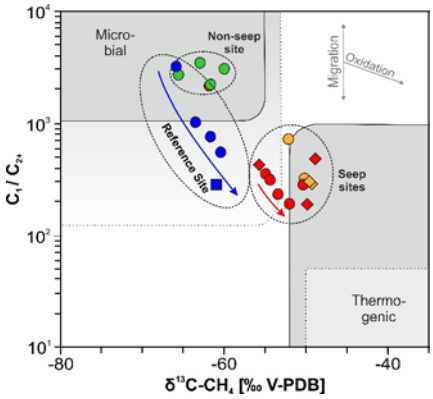

Fig. 3: Molecular composition of light hydrocarbons (expressed as $C_1/_{C2+}$) vs. stable carbon isotopic composition of methane (δ13C-CH4) in hydrate-bound gas (diamonds) and in void gas (circles) prepared from MeBo cores as well as in gas from a MeBo pressure core (square). Most hydrate samples plot within the field representative for thermogenic hydrocarbons. Direction of arrows close to samples from the reference site and seep site indicates increasing sediment depth. Figure modified after Pape et al. (accepted).

U/Th-dating of authigenic seep carbonates sampled from the seabed and from the MeBo cores taken from inside the pockmark revealed three gas emission episodes during the penultimate glacial maximum, during an interstadial in the last glacial, and in the aftermath of the last glacial maximum, respectively (Himmler et al., 2019). It is inferred that glacial tectonics induced by ice sheet fluctuations on Svalbard mainly controlled methane release from the pockmarks at Vestnesa Ridge (Figure 4).

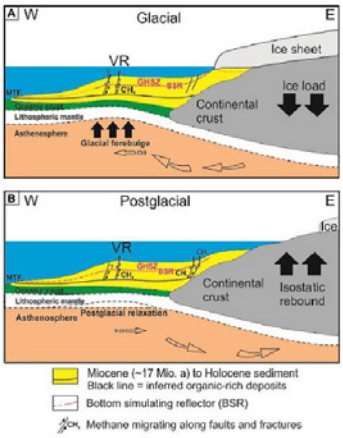

Fig. 4: Sketch illustrating the impact of glacial tectonics on the fluid system of Vestnesa Ridge (VR). (A) During growth of the Svalbard ice-sheet, horizontal mass transfer within the asthenosphere (open arrows) facilitated migration of glacial forebulge underneath VR; sediment compaction (black arrows) caused reservoir overpressure and migration of deep-sourced fluids through the gas hydrate stability zone (GHSZ). (B) Post-glacial relaxation resulted in isostatic adjustment (black arrows) and fault re-activation, providing fluid migration pathways. BSR = bottom simulating reflector; MTF = Molly Transform Fault. Figure adopted from Himmler et al. (2019).

Several MeBo drillings were performed at the upper continental slope of western Svalbard (Research Area 2). In a previous study hydrate decomposition due to a potential water temperature increase by ~1° C during the past three decades was used to explain the presence of numerous gas emission sites at ~400 mbsl close to the top of the GHSZ. In

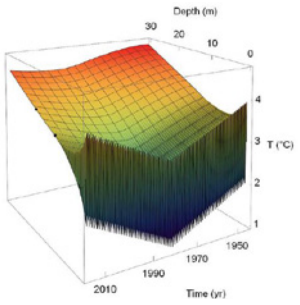

Fig. 5: Results of thermal modeling for MeBo drill site GeoB21632 at ~390 mbsl visited during MSM57. Solid black dots indicate the two measurements obtained in August 2016. Figure adopted from Riedel et al. (2017).

order to investigate dynamics of potential hydrate in the depth interval between ~300 and 500 mbsl, MeBo drills and sediment temperature mea–surements down to 28 mbsf were conducted at five sites and amended by heat flow measurements. Gas hydrates have not been found in this area neither before cruise MSM57 nor during the MeBo drillings. Combined modeling of temperature data, pore-fluid data, and thermal conductivities in order to evaluate the dynamics of the GHSZ during the past 70 years showed that gas hydrate is not stable at sites shallower than 390 mbsl (Figure 5; Riedel et al. 2017). Remarkably, pore water freshening indicative for dissociating hydrates has been observed for all MeBo cores from this area (Wallmann et al., 2018). Modeling of pore water data considering past sea levels indicated that freshening began around 8 ka BP when the rate of isostatic uplift outpaced eustatic sea-level rise. It was concluded that retreat of the Barents Sea ice sheet led to offshore gas hydrate dissociation.

At Svyatogor Ridge (Research Area 3, Figure 1), 22 stations with the temperature lance were carried out and three gravity cores were taken. Data analysis and evaluation has not been completed yet.

REFERENCES

Bohrmann G. et al., 2017. R/V MARIA S. MERIAN Cruise Report MSM57, Gas Hydrate Dynamics at the Continental Margin of Svalbard, Reykjavik – Longyearbyen – Reykjavik, 29 July – 07 September 2016., Berichte, MARUM - Zentrum für Marine Umweltwissenschaften, Fachbereich Geowissenschaften, Universität Bremen, Bremen, p. 204. http://nbn-resolving.de/urn:nbn:de:gbv:46-00105895-15

Freudenthal T, Wefer G, 2013. Drilling cores on the sea floor with the remote-controlled sea floor drilling rig MeBo. Geoscientific Instrumentation Methods and Data Systems 2, 329-337. doi: 10.5194/gi-2-329-2013

Himmler T, Sahy D, Martma T, Bohrmann G, Plaza-Faverola A, Bünz S, Condon DJ, Knies J, Lepland A, 2019. A 160,000-year-old history of tectonically controlled methane seepage in the Arctic. Science Advances 5, eaaw1450. doi: 10.1126/sciadv.aaw1450

Pape T., Bünz S, Hong WL, Torres ME, Riedel M, Panieri G, Lepland A, Hsu CW, Wintersteller P, Wallmann K, Schmidt C, Yao H, Bohrmann G., accepted. Origin and transformation of light hydrocarbons ascending at an active pockmark on Vestnesa Ridge, Arctic Ocean. Journal of Geophysical Research – Solid Earth. doi: 10.1029/2018JB016679

Riedel M, Wallmann K, Berndt C, Pape T, Freudenthal T, Bergenthal M, Bünz S, Bohrmann G, 2018. In situ temperature measurements at the Svalbard continental margin: Implications for gas hydrate dynamics. Geochemistry, Geophysics, Geosystems 19, 1165-1177. doi: 10.1002/2017GC007288

Wallmann K, Riedel M, Hong WL, Patton H, Hubbard A, Pape T, Hsu CW, Schmidt C, Johnson, JE, Torres ME, Andreassen K, Berndt C, Bohrmann G, 2018. Gas hydrate dissociation off Svalbard induced by isostatic rebound rather than global warming. Nature Communications 9, 83. doi:10.1038/s41467-017-02550-9.

MSM58/1

NEW INSIGHTS INTO AMOC VARIABILITY FROM THE CENTRAL NORTH ATLANTIC USING OLD AND NEW PROXIES – FIRST RESULTS FROM THE NAGAF CRUISE

AUTHORS

Max-Planck-Institut für Chemie | Mainz, Germany
J. Repschläger, A. Jentzen, K-P. Jochum, R. Schiebel, H. Vonhof, G. Haug

Christian-Albrechts-Universität zu Kiel | Kiel, Germany
R. Schneider, T. Blanz, C. Eich, D. Garbe-Schönber, N. Keul, J. Kiefer

Universität Heidelberg | Heidelberg, Germany
P. Blaser, J. Lippold, F. Pöppelmeier

GEOMAR Helmholtz-Zentrum für Ozeanforschung Kiel | Kiel, Germany
D. Nürnberg

Laboratoire de Géologie de Lyon | Lyon, France
S. Pichat

University of California | Davis (CA), USA
H. Spero

The subtropical Gyre (STG) in the central North Atlantic is a key region to investigate past changes in ocean circulation. It acts as an area of heat storage during weak phases of the Atlantic Meridional Overturning Circulation (AMOC), and the northward release of the warm waters plays a major role in the resumption of AMOC. The position of the northern boundary of the STG that is characterized by the Azores Front (AF) is strongly coupled to the position of the westerly wind belt. The AF is known to have changed over time (Repschläger et al., 2015; 2017; Schiebel et al., 2002) and especially during cold Heinrich Stadials (HS) it is supposed to be shifted towards the south due to large amounts of meltwater that enter the subpolar North Atlantic. Yet, the exact southernmost position of the AF during HS and the role of the STG as a warm water reservoir on glacial-interglacial timescales is still unknown. With its strong influence on upper ocean heat distribution and hydrographic fronts the research area has a major influence on the continental climate of Europe and Africa. Furthermore, the subtropical oligotrophic gyre is supposed to be stable in nutrient utilization over past glacial-interglacial cycles and thus can be used to evaluate the background nutrient inventory of the global ocean. At

depths the central North Atlantic is governed by the deepwater return flow of the AMOC. Despite decades of research main questions on the glacial and interglacial distribution of North Atlantic Deep Water (NADW) versus Antarctic Bottom Water (AABW) are still unanswered.

The aim of cruise MSM58/1 was to investigate the interaction between the heat storage in the subtropical Gyre (STG) region of the central North Atlantic, and Atlantic deepwater distribution over glacial and interglacial time scales. Additionally, changes in nutrient assimilation in the oligotrophic STG are used to address the global background value of glacial to interglacial changes in nitrogen utilization. Cruise MSM58/1 was carried out in 2016 with a program to sample water column and sediments along a transect from 41°N to 32°N along the Mid Atlantic Ridge (MAR of the Atlantic) and on transects into the eastern and western deep Atlantic basins. The first three years after the cruise were used for proxy calibrations, core top studies and first downcore time series and age model set up of four major cores along the N-S transect. Despite the original proposal, long Holocene sections more than 50 cm could not be obtained by coring. The lack of high-resolution Holocene and deglacial sediment sequences led us to shift our project focus to longer time scales including MIS 5e as an analogue for future climate warming scenarios.

Here we present first results of samples analyses obtained at cruise MSM58/1. The results from onboard studies on living foraminifera indicate the dependence of the reproduction cycle of foraminifera on the earth' magnetic field. Water sample and core top analyses of stable oxygen isotope analyses, trace element analyses, nitrogen isotope analyses were used for new proxy development including the testing of femtosecond laser ablation techniques on foraminifera (Jochum et al., 2019), and habitat studies on O. universa using different microscale analyses techniques (NanoSIMS, laser ablation ICP-MS, stable isotope measurements on shell fragments) and nitrogen isotope analyses. Additionally, box core samples were used to set up new cleaning and measurement routines for combined Mg/Ca and Na/Ca measurements on small sample sizes, that even allow single foraminifera measurements by wet chemistry. Core top ^{14}C AMS dating on planktic foraminifera, benthic foraminifera $\delta^{13}C$ and $\delta^{18}O$ analyses, as well as εNd analyses were carried out to investigate deep water properties at the coring sites under modern conditions and a feasibility study for the use of $^{231}Pa/^{230}Th$ on was carried out.

Core top ages are oldest in the shallower sites and are in average younger in the western Atlantic basin than in the eastern Atlantic Basin. This age pattern can be explained with strong deepwater currents at the shallower sites, and lower sedimentation rates in the eastern Atlantic basin. εNd analyses indicate a strong potential of this proxy for downcore reconstructions of deepwater current changes. Results from benthic $\delta^{13}C$ measurements on core top samples were included into a new global compilation of benthic $\delta^{13}C$ in the modern ocean (Schmittner et al.,

2017), that proposes a new calibration between $\delta^{13}C$ of dissolved organic carbon and $\delta^{13}C$ from foraminifera shells, which can be used as reference for modern deep ocean conditions.

First downcore analyses were carried out on four sediment cores and included 1) XRF sediment core scanning, 2) 14C AMS dating, 3) planktic foraminifera assemblage counts 4) stable isotope ($\delta^{18}O$ and $\delta^{13}C$) measurements of benthic and planktic foraminifera, 5) trace element analyses (Mg/Ca, Na/Ca, Ba/Ca) on planktic foraminifera, and 6) alkenone analyses. The North South transect study indicates that the Azores Front is displaced southward during cold Heinrich Stadials at least down to 32° N. Preliminary results from deepwater stable isotope reconstructions indicate increasing deepwater ventilation, potentially associated with increasing AMOC strength, over MIS 5 in the subpolar North Atlantic. Surface heat storage patterns during MIS 5 corroborate previous results from the topical Atlantic (Weldeab et al., 2007). Furthermore, a strong imprint of changing dust sources is reconstructed for glacial and deglacial cold events. Additionally, first results from nitrogen isotope analyses from the oligotrophic North Atlantic across the last glacial cycle will be shown.

REFERENCES

Jochum, K. P., A. Jentzen, R. Schiebel, B. Stoll, U. Weis, J. Leitner, J. Repschläger, D. Nürnberg, and G. H. Haug (2019), High-Resolution Mg/Ca Measurements of Foraminifer Shells Using Femtosecond LA-ICP-MS for Paleoclimate Proxy Development, Geochemistry, Geophysics, Geosystems, 20(4), 2053-2063, 10.1029/2018GC008091.

Repschläger, Weinelt, Kinkel, Andersen, Garbe-Schönberg, & Schwab. (2015). Response of the subtropical North Atlantic surface hydrography on deglacial and Holocene AMOC changes. Paleoceanography, 30. 10.1002/2014pa002637

Repschläger, Weinelt, Andersen, Garbe-Schönberg, & Schneider. (2015). Northern source for Deglacial and Holocene deepwater composition changes in the Eastern North Atlantic Basin. Earth and Planetary Science Letters, 425(0), 256-267. http://dx.doi.org/10.1016/j.epsl.2015.05.009

Repschläger, Garbe-Schönberg, Weinelt, & Schneider. (2017). Holocene evolution of the North Atlantic subsurface transport. Clim. Past, 13(4), 333-344. 10.5194/cp-13-333-2017

Schiebel, Schmuker, Alves, & Hemleben. (2002). Tracking the Recent and late Pleistocene Azores front by the distribution of planktic foraminifers. Journal of Marine Systems, 37(1–3), 213–227.

Schiebel, Waniek, Zeltner, & Alves. (2002). Impact of the Azores Front on the distribution of planktic foraminifers, shelled gastropods, and coccolithophorids. Deep Sea Research Part II: Topical Studies in Oceanography, 49(19), 4035-4050.

Schmittner, A., et al. (2017), Calibration of the carbon isotope composition ($\delta^{13}C$) of benthic foraminifera, Paleoceanography, 32(6), 512-530, 10.1002/2016PA003072.

Weldeab, Lea, Schneider, & Andersen. (2007). 155,000 Years of West African Monsoon and Ocean Thermal Evolution. Science, 316(5829), 1303-1307. 10.1126/science.1140461

MSM58/2*

MAX-DOAS MEASUREMENTS OF OUTFLOW FROM VOLATILE ORGANIC COMPOUND IN THE ATLANTIC OCEAN

AUTHORS

Institute of Environmental Physics (IUP-UB), University of Bremen| Bremen, Germany
L. K. Behrens, A. Hilboll, A. Richter1, E. Peters*, L. M. A. Alvarado, A. B. Kalisz Hedegaard, F.Wittrock, J. P. Burrows, M. Vrekoussis

MARUM – Center for Marine Environmental Sciences, University of Bremen | Bremen, Germany
A. Hilboll

DLR – Institute of Atmospheric Physics, German Aerospace Center | Oberpfaffenhofen, Germany
A. B. Kalisz Hedegaard

Energy, Environment and Water Research Center (EEWRC), The Cyprus Institute | Nicosia, Cyprus
M. Vrekoussis

*now at: DLR – Institute for protection of maritime infrastructures, German Aerospace Center | Bremerhaven, Germany

Enhanced levels of atmospheric key pollutants can regularly be identified over remote ocean areas such as the Atlantic Ocean in global trace gas maps retrieved from ultraviolet and visible satellite measurements. To validate these results, ship-based measurements of trace gases were conducted during the DFG project Continental Outflow of Pollutants towards the MArine tRoposphere (COPMAR). The spatial gradients and the ambient levels of atmospheric key species are of particular interest.

For the COPMAR project, a Multi-AXis Differential Optical Absorption Spectrometer (MAX-DOAS) was installed on board the research vessel Maria S. Merian for the cruise MSM58/2. This cruise took place in October 2016 and went from Ponta Delgada (Azores) to Cape Town (South Africa), crossing between Cape Verde and the African continent. The MAX-DOAS instrument was continuously scanning the horizon looking towards the African continent while the ship sailed at nearly constant speed during the whole cruise.

The temporal variability and the spatial gradients of tropospheric formaldehyde (HCHO) and glyoxal (CHOCHO) along the cruise track are investigated. Both trace gases are

regularly observed from satellites over the Atlantic Ocean, but given their short atmospheric lifetime their origin is unclear.

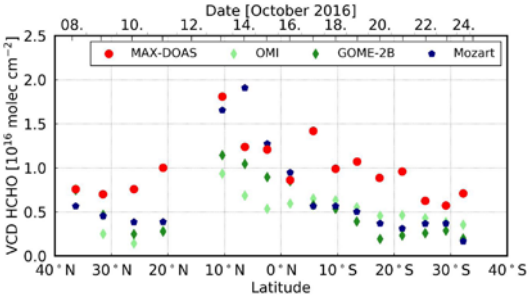

Fig. 1: Daily mean HCHO vertical column densities over the course of the cruise. Enhanced HCHO values can be observed in the area of expected outflow and agree with satellite observations and model simulations.

The observed MAX-DOAS spatial gradient of HCHO and CHOCHO confirmed the latitudinal pattern which is retrieved from satellite measurements and simulated with the MOZART-4 global chemistry transport model. The detected continental pollution outflow is at elevated atmospheric layers suggesting convection and subsequent advection of air masses which reach the geolocation of the vessel after several days. Possible sources of the pollutants are biogenic emissions or biomass burning according to FLEXible PARTicle dispersion model (FLEXPART) emission sensitivities.

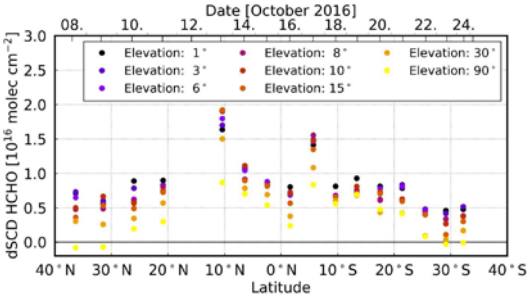

Fig. 2: Daily mean HCHO differential slant column densities over the course of the cruise. Enhanced values in the areas of expected outflow show a different scan angle dependency indicating an elevated HCHO layer.

MSM60/1

STUDIES IN THE SOUTH ATLANTIC ALONG THE SAMOC/SAMBA LINE DURING "MYSCIENCE CRUISE" MARIA S MERIAN MSM60

AUTHORS

GEOMAR Helmholtz Centre for Ocean Research Kiel | Kiel, Germany
J. Karstensen, T. Tanhua

Ecole Normal Superior | Paris, France
S. Speich

Introduction

Oceanic exchange pathways south of Africa and South America drive water mass interactions between the Indian, Pacific, and Atlantic oceans. The Agulhas Current, which flows westward around the southern coast of South Africa, contributes strongly to the upper limb of the Meridional Overturning Circulation (MOC) northward/warm water flow in the Atlantic Ocean. The frequent shedding of Agulhas rings into the eastern South Atlantic is a major source of salinity to the Atlantic. The path of deep waters to the Southern Ocean and the Indian Ocean is presumably partitioned between flows along the western boundary and within the Agulhas Undercurrent. In addition, intense mixing in the Cape Basin and the Brazil/Malvinas Confluence induce significant short-circuits in the MOC. The latitude 34.5°S, the SAMBA/SAMOC line, in the South Atlantic has been identified most crucial to any examination of how interocean exchange influences the MOC.

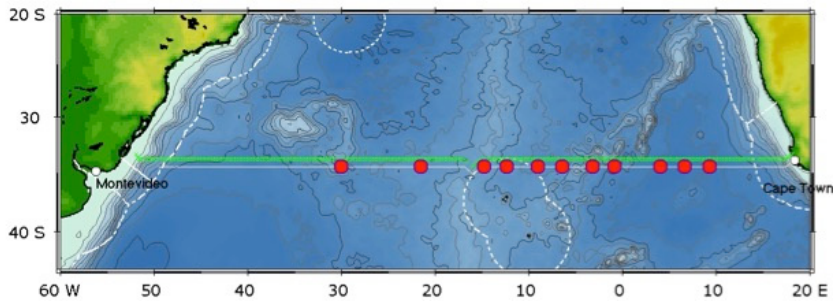

Fig. 1: RV Maria S Merian MSM60 Cape Town/RZA to Montevideo/Uruguay. Green crosses indicate CTD/Bottle/lADCP/UVP casts, red dots indicate Argo float deployments, underway data track (ADCP, TSG) are shown with latitude offset for clarity. The EEZ regions are indicated by broken lines.

The aim of the MARIA S. MERIAN MSM60 expedition was to survey for the first time a transbasin section along the SAMBA/SAMOC line. Frequent repeats of partial occupations

of the SAMBA/SAMOC line have been done from both sides of the Atlantic Ocean (off South Africa and off Brazil/Uruguay) and transbasin sections only close to 30°S and at 24°S. Ship-based hydrography is the only method for obtaining high-quality, high spatial and vertical resolution measurements of concurrent physical, chemical, and biological parameters over the full ocean water column. Ship-based hydrography is essential for documenting decadal physical and chemical ocean changes throughout the water column, especially for the deep ocean below 2 km (below the measurements of Argo or XBTs).

The MSM60 science program included the following specific objectives: reduce uncertainties in global freshwater, heat, and sea-level budgets; determine the distributions and controls of natural and anthropogenic carbon (both organic and inorganic); determine ocean ventilation and circulation pathways and rates using chemical tracers; determine the variability and controls in water mass properties and ventilation; determine the significance of a wide range of biogeochemically and ecologically important properties in the ocean interior; and augment the historical database of full water column observations necessary for the study of long-timescale changes.

MyScience cruise: The execution of the cruise was motivated by the EU H2020 project AtlantOS which also aimed for an intensification of South Atlantic Ocean Observing. All SAMBA/SAMOC PIs from Argentina, South Africa, Brazil, USA and France provided material and staff for the cruise. Students at masters and PhD level joined the cruise and applied known techniques and learned new. The "Partnership for Observation of the Global Oceans" (POGO) provided cruise and analysis support. It is a group of graduating students that make use of the MSM60 data in their thesis and at this stage no peer reviewed scientific publication has been published from the cruise but many publications are in preparation.

Sub-mesoscale mediated deep carbon export associated with a cyclonic eddy by Rogge at al. (in prep) The biological carbon pump (BCP) regulates atmospheric carbon dioxide concentrations via its transport of particulate organic carbon to the deep ocean, while the depth of export regulates the time scale of carbon removal from the atmosphere. The region-specific efficiency of the BCP is determined by velocity and turnover of settling organic matter. Mesoscale cyclonic eddies often have high POC export, but detailed descriptions of the influence of physical factors on deep export dynamics, qare still rare. Here we used in situ optics and acoustics to show that internal waves propagating along the eddy boundary drive organic particle production, which is then concentrated into a wine glass shape by the vorticity field, accelerating aggregation and repackaging of the export flux (EF), thus incrasing EF 3-fold. Fertilization was visible as a shallowing and increase of the deep fluorescence maximum at the eddy perimeter not detectable by remote sensing. Nutrient intrusions were triggered through mixing via horizontal shear driven by the vertical propagation of near-inertial gravity waves (NIW) in the positive, anticyclonic vorticity field of the eddy perimeter. While flux attenuation depleted small particles (0.08–0.51 mm) to ambient concentrations within the upper 1000 m, below this depth, larger

particles > 0.51 mm were concentrated towards the eddy core. Following the anticyclonic vorticity pattern into a characteristic wine glass shape below 1000 m, particle aggregation and densification was promoted by horizontal vorticity shear, resulting in potentially high sinking velocities. We infer that this, in combination with low microbial activity in bathypelagic depths, increased carbon export to 3-fold down to 3000 m and further 2-fold down to 4000 m, as estimated based on the particle size distribution. We conclude that both vertical mixing (increasing production) and particle concentration (increasing sinking rates) at the vorticity boundary occur spatially at the region of maximum rotation and minimum vorticity of a mesoscale eddy, promoting carbon export. This is not necessarily linked to central shoaling (cyclones) or deepening (anticyclones) of the eddy nutricline. Considering the limited ability of remote sensing to detect deep primary production, and the high coverage of eddy vorticity fields (e. g., 1/6–1/3 of the world ocean), we suggest that estimates of both productivity and of deep carbon export in oligotrophic oceans could be significantly underestimated.

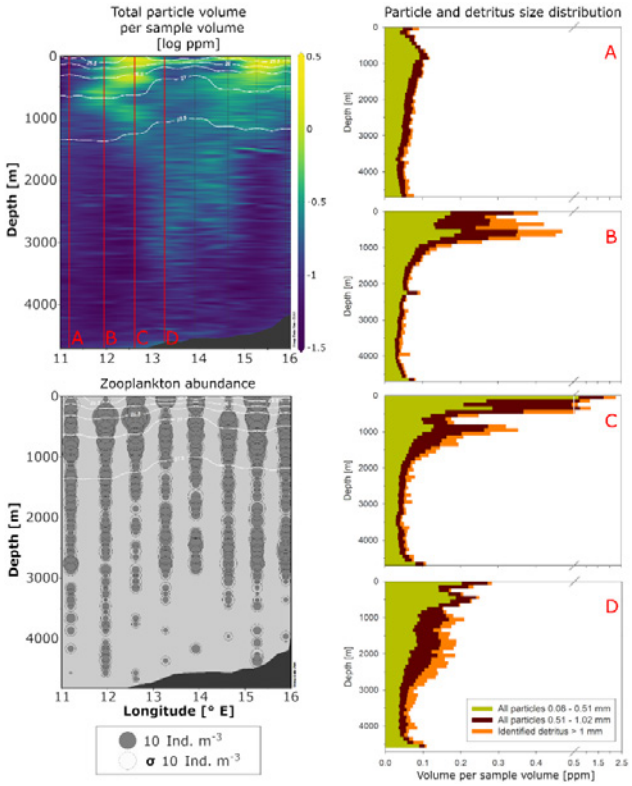

Fig. 2: Rogge et al (in prep) Distribution of aggregates as well as living particulate material. Total particle volume per sample volume calculation include total particulate material with an ESD between 0.08 and 1 mm, as well as identified aggregates and fecal pellets > 1mm. Particle and aggregates size distribution is based on averaged 100 m depth bins of size classes in different zones of the cyclonic eddy: Profile A represents area outside of the eddy, B and C the eddy perimeter and D the eddy core. Distribution of identified Zooplankton shows high concentration of grazers within areas of high particle abundance, i. e. at the eddy perimeter. White lines indicate isopycnals in kg m^{-3} (ρ–1000 kg m^{-3}).

Particle and Zooplankton Distribution through a Cyclonic Eddy in the Atlantic Determined via Underwater Vision Profiling by Prondzinsky (2018) Throughout Earth's oceans, organic matter is exported to the deep sea through the biological carbon pump. So far, the deployment of sediment trap moorings has been used as the main method to assess and quantify the export of this material to the deep. However, the use of stationary monitoring systems limits the description and quantification of processes that take place throughout the entire water column. These processes include, but are not limited to the grazing activity of zooplankton species or the aggregation patterns of marine snow. Here an Underwater Vision Profiler (UVP5 HD) was used to capture particles and organisms at a high vertical resolution to describe their distribution in the South Atlantic Ocean. The online software tool 'Ecotaxa' was then used to taxonomically classify and distinguish the organisms and aggregates captured by the UVP. The resulting zooplankton community compositions and the distribution of inanimate aggregates of organic matter served as the basis to describe the effect that physical mesoscale features have on biological processes in the ocean. We show that one of those features, a cyclonic eddy in the east of the ocean basin, locally increases the abundance of particles and enhances the export of carbon to the deep sea.

REFERENCES

Ditzinger, G.X., (2017) On the Effective Planetary Vorticity in selected Eddies in the Atlantic Ocean, BSc thesis, CAU Kiel

Losch J., (2019) Redfield stoichiometry along the South Atlantic SAMOC-SAMBA line (34.5°S), BSc thesis, CAU Kiel

Manta, G., et al. (in prep)

Prondzinsky P.A., (2018) Particle and Zooplankton Distribution through a Cyclonic Eddy in the Atlantic Determined via Underwater Vision Profiling; Master thesis University Bremen, Bremen

Reckling, K. (2017) Meridional Ekman transport across the SAMOC/SAMBA line in boreal winter 2017, science project, University Oldenburg, Oldenburg

Rogge, Andreas (2019): Microbial processes and element cycling from micro- to meso-scale: from single cells and aggregates to the whole water column perspective. http://nbn-resolving.de/urn:nbn:de:gbv:46-00107425-12. urn:nbn:de:gbv:46-00107425-12.

Rogge, A., et al. (in prep) Sub-mesoscale mediated deep carbon export associated with a cyclonic eddy

MSM63

MARIA S. MERIAN CRUISE MSM63: PIPE STRUCTURES AND POCKMARKS IN THE NORTH SEA

AUTHORS

GEOMAR Helmholtz Centre for Ocean Research Kiel | Kiel, Germany
C. Berndt, J. Elger

And: Shipboard Scientific Party

The location and potential intensity of any possible CO_2 leakage at the seafloor are critically dependent on the distribution and permeability of fluid pathways in the sediment overburden overlying any putative storage reservoir. Evaluation of seismic reflection data, as part of a European Union funded project (STEMM-CCS), has revealed structures crosscutting the overburden within the North Sea and Norwegian Sea. These seismically-imaged pipes and chimneys are considered to be possible pathways for fluid flow. Natural fluids from deeper strata have migrated through these structures at some point in geological time. If CO_2 leaking from sub-seafloor storage reservoirs reaches the base of these structures, and if their permeability is sufficiently high, they could act as CO_2 leakage pathways towards the seafloor and overlying water column. To provide a reliable prediction of potential seafloor seep sites, the hydraulic continuity, and especially the permeability of these pathways, needs to be better constrained and quantified. We present results from MSM63 to the Scanner pockmark field in the North Sea. These pockmarks were known to be the locations of vigorous methane venting, were associated with bright spots at shallow depth, and had chimney structures imaged on 3D seismic reflection data to depths of several hundred meters. This cruise aimed to collect data that could be used to constrain the geometry and internal structures of fluid flow "chimney" structures with the eventual aim of determining the current permeability of the sub-surface. Understanding the flow of methane from different depths in the sub-surface will facilitate an understanding of possible pathways of CO_2.

In April-May 2017, Maria S. Merian cruise no. 63 (funded by STEMM-CCS) collected multi-beam bathymetry and sub-bottom profiler data as well seismic reflection data using GI guns. The shots were recorded using a GeoEel streamer and 18 Ocean bottom seismometers (OBS) around the Scanner pockmark. Electromagnetic surveying was also completed to determine electrical resistivity variations in the sub-surface using a source towed close to the seabed. The controlled-source electromagnetic system consists of two receivers measuring the full vector electric field that were towed behind the source, and 14 ocean bottom electric field instruments each with two orthogonal horizontal electrodes, some of which were equipped also with a new set of vertical electrodes.

The Scanner pockmark is a composite feature involving two overlapping seabed pockmarks, each a few hundred meters in diameter, lying in ~155 m water depth (Figure 1). It is a site of active and persistent methane gas venting. Preliminary analysis of 2D seismic reflection profiles shows the overall shape of the sedimentary succession underneath the Scanner pockmark. Between the seafloor and the well-stratified sediments of the Nordland formation (200–350 ms TWT) clear indications for several stages of deposition and erosion are visible. A characteristic tunnel valley with steep flanks and several phases of deposition and erosion is located SW of the Scanner pockmark. New high-resolution seismic reflection data provide higher resolution and quality than the existing 3D industry seismic data for the upper 500 ms TWT, and indicates the presence of gas at several different levels and complex areas of gas blanking. The new data reveal a complex fluid migration system in the subsurface, which comprises fluids that rise from several hundred meters depth as well as fluids that are sourced from the shallow most postglacial sediments resulting in a multitude of fluid pathways and seep sites at the sea floor.

Unfortunately, the drilling campaign using British Geological Service's (BGS) RockDrill2 (RD2) drill rig could not be accomplished during MSM63 because of problems with the vessel. The drilling campaign with BGS's RD2 was finally put in place during cruise Maria S. Merian no. 78.

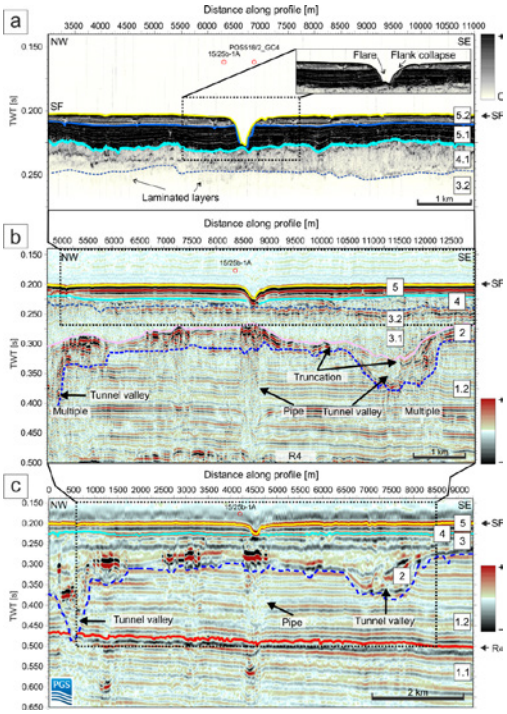

Fig. 1: Parasound (top) and 3D seismic data from the Scanner Pockmark area showing the fluid pathways that link up to pockmarks at the Seafloor.

MSM64

BASIN-WIDE CHANGES OF LABRADOR SEA WATER OBSERVED AT 47°/48°N IN THE NORTH ATLANTIC – INSIGHTS FROM MARIA S. MERIAN CRUISES MSM42, MSM53, AND MSM64

AUTHORS

University of Bremen, Institute of Environmental Physics (IUP) | Bremen, Germany
D. Kieke, M. Rhein, R. Steinfeldt

University of Bremen, MARUM – Center for Marine Environmental Sciences | Bremen, Germany
D. Kieke, M. Rhein, R. Steinfeldt

Federal Maritime and Hydrographic Agency (BSH) | Hamburg, Germany
B. Klein, M. Moritz, K. Jochumsen, H. Klein, M. Köllner

The ship-based repeat hydrography program conducted along 47°/48°N covers the southern subpolar North Atlantic from the Grand Banks in the west to the European shelf break in the east. The hydrographic line crosses the swift western and eastern boundary currents as well as the North Atlantic Current and its various recirculating branches. Hydrographic observations from this line are merged with data from the historic repeat lines located in the vicinity of 47°/48°N. This data set allows to gain insight into decadal changes regarding the spreading, characteristics, and spatio-temporal property changes of the water masses forming the deep and cold branch of the Atlantic Meridional Overturning Circulation. With focus on Labrador Sea Water (LSW) we report on hydrographic data collected from ship surveys and Argo profilers complemented with tracer observations and discuss basin-wide changes observed at 47°/48°N. Recent observations in the source region of LSW showed that winter time buoyancy forcing over the Labrador Sea increased since winter 2013/14, when the North Atlantic Oscillation went back into a positive state. Resulting from intensified deep convection the coldest and freshest LSW observed since years formed since then. LSW propagates along three major pathways away from the formation region: a northeastward branch spreads into the Irminger Sea, an eastward branch crosses the Mid-Atlantic Ridge near 50°N, and a southward branch transfers LSW as part of the Deep Western Boundary Current into the subtropics. The repeat hydrography program conducted with RV MARIA S. MERIAN along 47°/48°N serves to study the emergence of these signatures in a region, where the subpolar regime encounters the subtropical regime. Via interior pathways this renewed LSW invades the interior of the western and eastern deep basins of the North Atlantic, thus carrying increased contents of oxygen and anthropogenic tracers and thereby increasingly ventilating these regions again. In this presentation we discuss the

formation history of LSW over the recent two decades and the respective manifestation of the new LSW class formed since 2013/2014 at the western and eastern boundaries and in the deep basins of the southern subpolar North Atlantic.

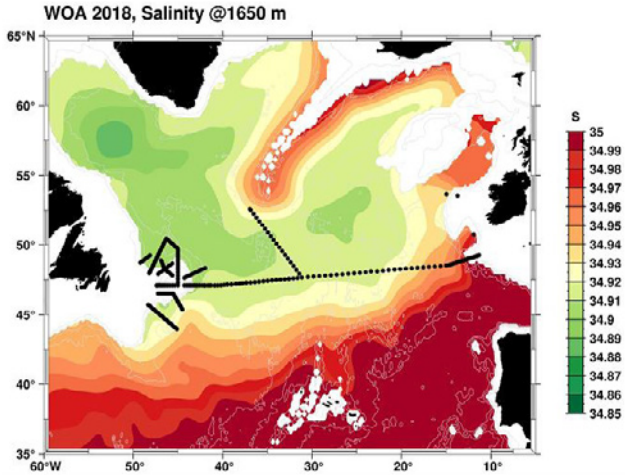

Fig. 1: Location of CTD stations conducted during MARIA S. MERIAN cruises MSM42, MSM53, and MSM64 (2014–2016) superimposed on the climatological salinity distribution at the Labrador Sea Water (LSW) level, 1650m. Salinity data was obtained from the World Ocean Atlas 2018, NOAA/NODC.

MSM65

GREENHAB II – DO HARMFUL ALGAE HAVE A NORTHERN LIMIT?

AUTHORS

Institute for Chemistry and Biology of the Marine Environment (ICBM), University of Oldenburg | Oldenburg, Germany
O. Zielinski

Woods Hole Oceanographic Institution (WHOI), Biology Department | Woods Hole (MA), USA
D. M. Anderson

GEMA Center for Genomics, Ecology & Environment, Universidad Mayor | Santiago,Chile
N. Trefault

Alfred Wegener Institute-Helmholtz Zentrum für Polar- und Meeresforschung | Bremerhaven, Germany
U.Tillmann

German Research Center for Artificial Intelligence (DFKI) | Oldenburg, Germany
O. Zielinski

The "GreenHAB II" expedition investigated the fjords of West Greenland as well as along a latitudinal transect at the West Greenland coast to explore the interactions between hydrography, bio-optics (light regime), biogeochemistry, and plankton composition and metagenomics with special attention on harmful algae and their toxin composition. These fjords differ in their ice cover, glacial melt-water runoffs, and history. In total, 50 stations were conducted, with 50 CTD water sampler casts, 63 plankton net tows, 43 bio-optical-package profiles, 43 Secchi disk readings, 39 hyperspectral radiometric profiles, 26 Van Veen grabs, 12 MUC (multi-corer), and 22 vibro-corer operations. 8 surface drifters were successfully deployed, and one mooring was successfully recovered (SeaCycler). Underway, 2750 nautical miles of FerryBox and radiometric reflectance data were sampled. Changing environmental conditions in Greenland (i. a. due to climate change, higher water temperature, etc.) makes this area of high interest as it can have changes of HAB composition and its geographical occurrence. Three main topics were investigated during the MSM65 cruise: (A) Northern limitation of dinoflagellate HAB species, (B) Arctic HAB diatoms going North, and (C) HAB hatcheries. Various hypothesizes were tested for an overall overview combining all single disciplines of the observed area.

With this contribution we present the actual situation in West Greenland during the MSM65 expedition, combining hydrography and light regime with occurrence of harmful algae, their toxin profiles and cyst appearance. Investigations will be compared with previous cruises (e. g. MSM21/2, Cembella et al, 2016) as well as other investigations in the Greenland area (see e. g. Meire et al, 2015, 2017; Murray et al, 2015, Richlen et al, 2016).

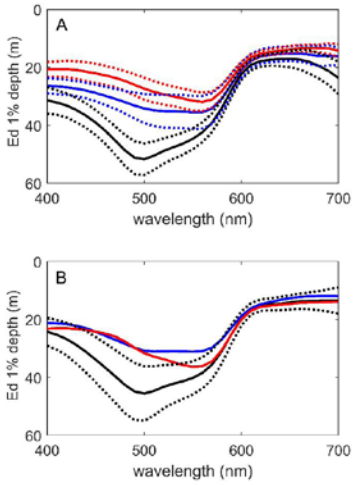

Fig. 1: Spectral types of 1 % downwelling irradiance (Ed) in the (A) Vaigat-Disko Bay and (B) Godthabsfjord (Mascarenhas & Zielinski, 2019).

Results in a nutshell: Light availability was investigated at almost each station. Exemplarily 1 % penetration depth for downwelling irradiance (Ed) in the Vaigat-Disko Bay and the Godthabsfjord is shown in Figure 1. Results of our investigations provide evidence of near-surface bio-optical variability being highly influenced by regional hydrography and the efficiency of machine learning tools such as cluster analysis in identifying bio-optical domains driven by regional hydrography. With increasing meltwater influx in coastal ecosystems around Greenland, monitoring changes in regional hydrography is essential to account for local forcing factors that drive bio-optical variability.

Microplankton groups detected during MSM65 include flagellates, dinoflagellates, diatoms and ciliates. Phycotoxins were found across the entire cruise transect, with spirolides being the most abundant toxin group with total spirolide abundance up to 1650 ng per net tow in the Disko Bay. Spirolides were most abundant in Godthåbsfjord and Disko Bay. Furthermore, we found a new specie (Figure 2) in the central Labrador Sea (1st station, SeaCycler Recovery), described here as Azadinium perforatum sp. nov. More details will be given in Tillmann et al, 2019 (accepted).

Regarding the metagenomic approach similar diversity trends among size fractions were found at the Disko Bay in summer 2012 (Elfernik et al., 2017). Taxonomic affiliations show that most of the sequences were assigned to the phylum Dinoflagellata, followed by Haptophyta and Ochrophyta across all samples. The proportion of Haptophyta decreased, and Dinoflagellata and Ochrophyta increased with increasing size fractions. Here, a different trend was observed compared to the previous report for the area (Elfernik et al., 2017).

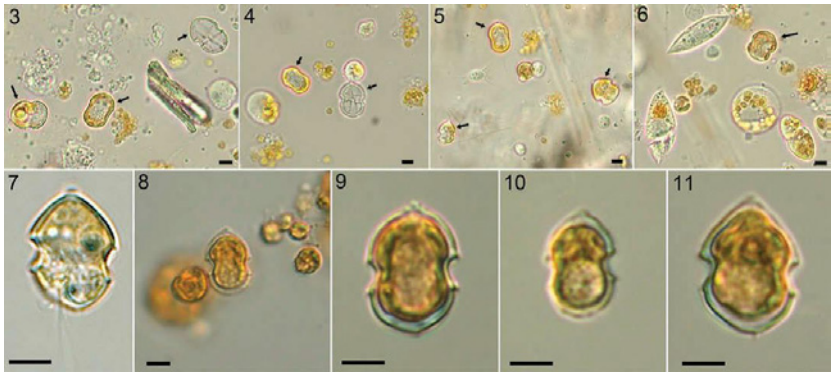

Fig. 2: Records of Amphidomataceae from the central Labrador Sea (station 1). 3–7. Living samples with Amphidomatacean cells or empty thecae (both are designated by arrows). Scale bars = 5 µm. 8–11. Amphidomatacean cells in Lugol-fixed Utermöhl samples. Scale bars = 5 µm (Tillmann et al, accepted).

The dominant species of dinoflagellate cysts observed in western Greenland sediments were Scrippsiella spp., Protoceratium reticulatum, Alexandrium catenella, Gonyaulax spinifera, and Alexandrium ostenfeldii (cysts were most abundant at latitudes 64–69°N (Figure 3), but were observed at nearly all of the sites sampled from latitudes 64°N to as far north as 75°N (Figure 4) – now the northernmost location at which A. catenella has been found (Natsuike et al, 2013).

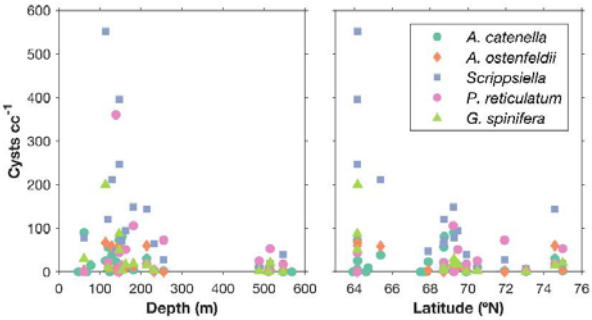

Fig. 3: Cyst abundances of the dominant species of dinoflagellates in surface sediments shown in relation to depth and latitude.

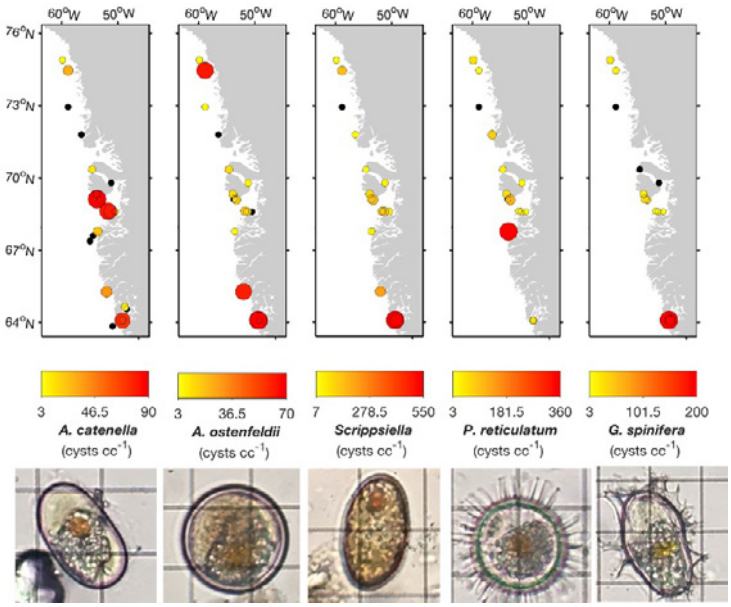

Fig. 4: Cyst abundances of the dominant species of dinoflagellates in surface sediments shown in relation to depth and latitude.

REFERENCES

Cembella A, et al. ARCHEMHAB: Interactions and feedback mechanisms between hydrography, geochemical signatures and microbial ecology, with a focus on HAB species diversity, biogeography and dynamics – Cruise No. MSM 21/3 – July 25 – August 10, 2012 – Nuuk (Greenland) – Reykjavik (Iceland), 2016, 49pp.

Elferink S, Neuhaus S, Wohlrab S, Toebe K, Voß D, Gottschling M, John, U. Molecular diversity patterns among various phytoplankton size-fractions in West Greenland in late summer. Deep-Sea Research Part I, 2017,121,54–69.

Mascarenhas V J, Zielinski O. Hydrography-Driven Optical Domains in the Vaigat-Disko Bay and Godthabsfjord: Effects of Glacial Meltwater Discharge. Frontiers in Marine Science 2019, 6:335. DOI: 10.3389/fmars.2019.00335

Meire L, Søgaard D H, Mortensen J, Meysman F J R, Soetaert K, Arendt K E, Juul-Pedersen T, Blicher M E, Rysgaard S. Glacial meltwater and primary production are drivers of strong CO_2 uptake in fjord and coastal waters adjacent to the Greenland Ice Sheet. Biogeosciences, 2015, 12, 2347–2363, doi:10.5194/bg-12-2347-2015

Meire L, Mortensen J, Meire P, Juul-Pedersen T, Sejr M K, Rysgaard S, et al. Marine-terminating glaciers sustain high productivity in Greenland fjords. Glob. Change Biol. 23, 2017, 5344–5357. doi: 10.1111/gcb13801

Murray, C., Markager, S., Stedmon, C. A., Juul-Pedersen, T., Sejr, M. K., Bruhn, A. The influence of glacial melt water on bio-optical properties in two contrasting Greenlandic fjords. Estuar. Coast. Shelf Sci. 163, 2015, 72–83, doi: 10.1016/j.ecss.2015.05.041

Natsuike M, Nagai S, Matsuno K, Saito R, Tsukazaki C, Yamaguchi A, Imai I. Abundance and distribution of toxic Alexandrium tamarense resting cysts in the sediments of the Chukchi Sea and the eastern Bering Sea. Harmful Algae 27, 2013, 52–59.

Richlen M L, Zielinski O, Holinde L, Tillmann U, Cembella A, Lyu Y, Anderson D M. Distribution of Alexandrium fundyense (Dinophyceae) cysts in Greenland and Iceland, with an emphasis on viability and growth in the Arctic. Marine Ecology Progress Series 547, 2016, 33–46.

Tillmann U, Wietkamp S, Krock B, Tillmann A, Voss D, Gu H. Amphidomataceae (Dinophyceae) in the western Greenland area, including description of Azadinium perforatum sp. nov. PHYCOLOGIA, 2019. Accepted [UPHY #1670013]

MSM67

VOLCANIC BREAKUP OF THE NE GREENLAND CONTINENTAL MARGIN

AUTHORS

BGR – Federal Institute for Geosciences and Natural Resources | Hannover, Germany
D. Franke, P. Klitzke, U. Barckhausen, K. Berglar , V. Damm, A. Ehrhardt, M. Engels, M. Schnabel

GEOMAR – Helmholtz Centre for Ocean Research | Kiel, Germany
C. Berndt, A. Dannowski

GEUS – Geological Survey of Denmark and Greenland | Copenhagen, Denmark
T. Funck

AWI – Alfred-Wegener-Institute | Bremerhaven, Germany
W. Geissler

Department of Geoscience, Aarhus University | Aarhus, Denmark
P. Trinhammer

Applied Geophysics, Christian-Albrechts-Universität zu Kiel | Kiel, Germany
M. Thorwart

During MSM67 new marine geophysical data was acquired across the partly ice-covered northern East Greenland continental margin which highlight a complex interaction between tectonic and magmatic events. Post-Caledonian reactivation to form the North Atlantic rift systems essentially followed pre-existing orogenic crustal structures, while eventual breakup reflected a change in stress field and exploitation of a deeper-seated, lithospheric-scale shear fabrics (Schiffer et al., in press). Breakup-related lava flows are imaged in reflection seismic data as seaward dipping reflectors (SDRs). These exhibit considerable variation in structural style and architecture along the 600 km-long continental slope between the West Jan Mayen Fracture Zone and the Greenland Fracture Zone (Franke et al., 2019). Generally, SDRs are found to decrease in size towards the north and south from a central point at 75°N. The most prominent SDRs are present 300 km along of the margin, between 74°N and 75.8°N. South of 74°N, a single, small SDR wedge is imaged that further decreases in size towards the West Jan Mayen Fracture Zone. Around the West Jan Mayen Fracture Zone, SDRs are indistinct or absent. From the

architecture and tectono-magmatic style of the SDRs, it is shown that the NE Greenland margin is broadly segmented into three segments that broke up in a consecutive way. The segment boundaries, however, did not develop into oceanic fracture zones, except the East Jan Mayen Fracture Zone.

We interpret the transition between oceanic and magmatically overprinted continental crust at the continental slope, in the vicinity of the SDR wedges. From magnetic modelling we propose that SDRs and lava flows are causing magnetic anomalies at the continental slope. The magnetic anomaly pattern associated with the SDRs, then is used to deduce a relative timing of the emplacement of the volcanic wedges. The inner SDRs in the northern margin segment (75°N–75.8°N) have been emplaced before the negative polarity chon C24r time and thus before volcanic rifting took place in the central and southern margin segment. The SDRs in the central margin segment (74°N–75°N) initiated during the negative polarity chon C24r time but the major portion of the inner SDRs corresponds to the normal C24n magnetic chron (54.0–52.6 Ma). The deposition of a separate, seaward SDR wedge may even have lasted until chron C23n (51.8–50.6 Ma). The different magnetic anomalies associated with the two SDR wedges suggest two phases of volcanism resulting in the two wedges that were likely emplaced with a time lag. Finally, the small SDR wedge in the southern segment (73°N–74°N) coincide broadly with negative magnetic anomaly C23r (52.6–51.8 Ma).

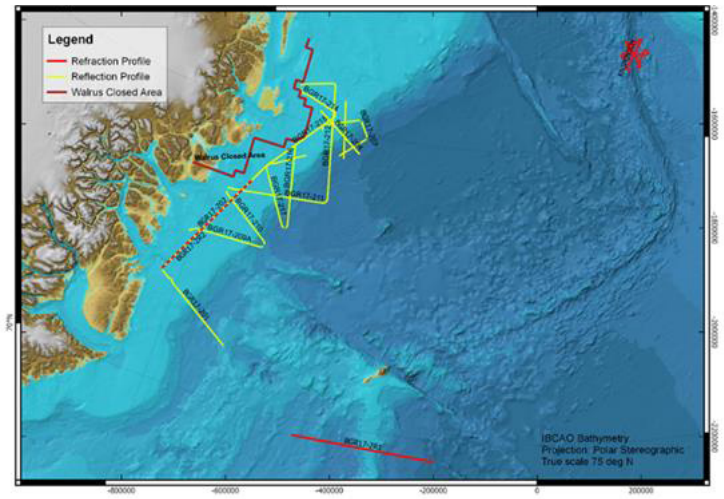

Fig. 1: Survey lines of MSM67: Yellow lines are MCS profiles with gravity, magnetic, para-sound and bathymetry; red lines are refraction seismic lines; the near coastal purple line marks the Walrus closed area.

The remnant magnetization of the individual lava flows is used to deduce a relative timing of the emplacement of the volcanic wedges. We find that the SDRs have been emplaced over a period of 2–4 Ma progressively from north to south and from landward

to seaward. The new data indicate a major late Eocene magmatic phase around the landward termination of the West Jan Mayen Fracture Zone. This post-40 Ma volcanism likely was associated with the progressive separation of the Jan Mayen microcontinent from East Greenland. The break-up of the Greenland Sea started at several isolated seafloor spreading cells whose locations was controlled by rift structures leading to the present-day segmentation of the margin. The original rift basins were subsequently connected by steady-state seafloor spreading that propagated southwards, from the Greenland Fracture Zone to the Jan Mayen Fracture Zone.

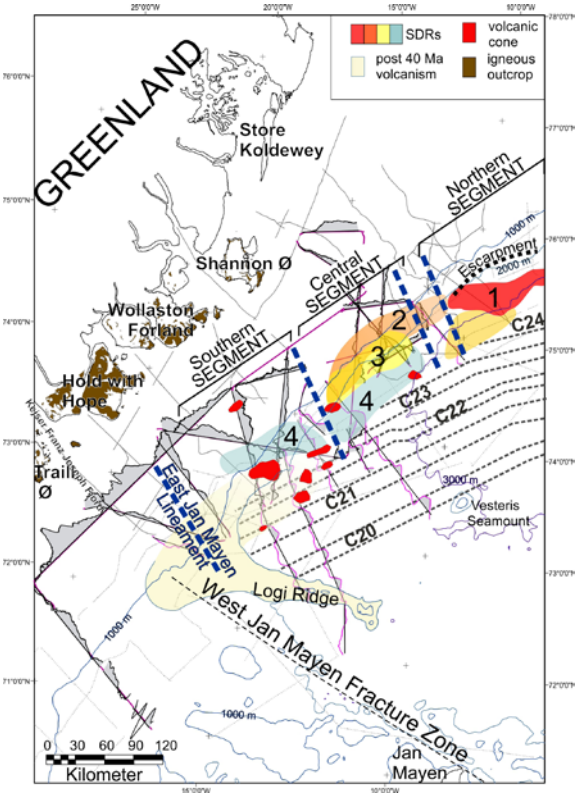

Fig. 2: Location of the different SDR wedges according to their time of emplacement (red (1) through orange (2, 3) and blue (4)) and inferred rift segment boundaries (blue dashed lines) shown on the bathymetric map. The East Jan Mayen Lineament is the onshore prolongation of the East Jan Mayen Fracture Zone. Younger volcanism (post-middle Eocene; minimum extent estimate) and volcanic cones are shown in yellow and light red, respectively. Magnetic anomalies shown as wiggles along survey lines with positive anomalies shaded in grey. All newly acquired profiles are pure black, other lines from cruise BGR75 and from GEODAS database are shown with a purple anomaly outline. Dashed white lines show interpreted seafloor spreading anomalies. Onshore igneous outcrops according to Horni et al. [2017].

Breakup took place with punctual seafloor spreading, but the earliest steady-state oceanic crust formation reveals a clear, north to south-directed propagation (Gernigon et al., in press). Each tectono-magmatic phase overprinted the areas that were previously rifted,

resulting in tectonic deformation. Major volcanism during breakup time occurred distal from the locus of rift initiation and initial oceanic crust accretion and extension did not propagate away from a newly formed LIP (Peace et al., 2019).

REFERENCES

Franke, D., Klitzke, P., Barckhausen, U., Berglar, K., Berndt, C., Damm, V., Dannowski, A., Ehrhardt, A., Engels, M., Funck, T., Geissler, W., Schnabel, M., Thorwart, M., and Trinhammer, P., Polyphase magmatism during the formation of the northern East Greenland continental margin. Tectonics 2019. doi: 10.1029/2019TC005552.

Gernigon, L., Franke, D., Geoffroy, L., Schiffer, C., Foulger, G., Stoker M., Crustal fragmentation, magmatism, and the diachronous breakup of the Norwegian-Greenland Sea, Earth-Science Reviews (in press), doi: j.earscirev.2019.04.011.

Horni, J. Á., J. R. Hopper, A. Blischke, W. H. Geisler, M. Stewart, K. McDermott, M. Judge, Ö. Erlendsson, and U. Árrting, Regional distribution of volcanism within the North Atlantic Igneous Province, in Geological Society Special Publication 2017, pp. 105–125, doi: 10.1144/sp447.18.

Peace, A.L., Phethean, J.J.J., Franke, D., Foulger, G.R., Schiffer, C., Welford, J.K., McHone, G., Rocchi, S., Schnabel, M., and Doré, A.G., A review of Pangaea dispersal and Large Igneous Provinces – In search of a causative mechanism: Earth-Science Reviews 2019, p. 102902, doi: 10.1016/j.earscirev.2019.102902.

Schiffer, C., Doré, A.G., Foulger, G.R., Franke, D., Geoffroy, L., Gernigon, L., Holdsworth, B., Kusznir, N., Lundin, E., McCaffrey, K., Peace, A., Petersen, K.D., Phillips, T., Stephenson, R., Stoker, M.S., and Welford, K., 2019, Structural inheritance in the North Atlantic, Earth-Science Reviews (in press), p. 102975, doi: 10.1016/j.earscirev.2019.102975.

MSM68

KNIPAS – EXPLORING ACTIVE SEAFLOOR SPREADING AT SEGMENT-SCALE | PRELIMINARY RESULTS FROM A PASSIVE SEISMIC EXPERIMENT ON KNIPOVICH RIDGE

AUTHORS

Alfred-Wegener-Institute, Helmholtz Centre for Polar and Marine Research | Bremerhaven, Germany
V. Schlindwein, M. Meier, J.-R. Scholz, D. Essing, J. Geils

Institute of Earth and Environmental Sciences, University of Potsdam | Potsdam, Germany
F. Krüger, G. Kulikova, H. Lilienkamp

Institute of Geophysics, Polish Academy of Sciences | Warsaw, Poland
W. Czuba, D. Wojcik, T. Janik

KNIPAS constitutes one of the largest ocean bottom seismometer (OBS) experiments conducted on mid-ocean ridges. A network of 26 OBS distributed over a distance of 160 km along the ultraslow spreading Knipovich Ridge recorded its earthquake activity for a period of up to 13 months (Fig. 1). The instruments stem from the DEPAS pool (27 instruments at 23 locations) and the Polish Academy of Sciences (3 locations) and were deployed during two cruises of RV Polarstern and Horyzont II as a collaborative effort between AWI, the University of Potsdam and the Institute of Geophysics, Polish Academy of Sciences. MSM68 on RV Maria S. Merian successfully recovered all 27 DEPAS OBS in October 2017 and conducted comprehensive high-resolution mapping of the ridge topography.

The key scientific aim of KNIPAS is to understand how the little amounts of melts present at the slowest spreading mid-ocean ridges on Earth are steered towards isolated but pronounced volcanic centres and rise there through a thick lithosphere. In addition, KNIPAS investigates how a strongly oblique mid-ocean ridge is segmented and what kind of active spreading processes operate in magma controlled and in magma-starved segments to produce the anomalous oceanic lithosphere of ultraslow spreading ridges.

Since the recovery of the OBS we conducted laborious processing to determine the clock drift of the OBS recorders, the orientation of the seismometers at the seafloor and to identify, extract and pick the P- and S-phases of about 20.000 local earthquakes. 2D refraction seismic profiles of Logachev seamount gave preliminary seismic velocity profiles. A preliminary location of the 1000 best recorded earthquakes (Fig. 1) clearly

indicates an undulating base of the mechanical lithosphere, with different maximum earthquake depths in different spreading segments. Deep earthquakes are in particular seen where oblique axial volcanic ridges meet the flanks of the rift valley. Logachev Seamount shows a prominent seismic gap, indicating potentially a region of melt. Two seismic swarms were recorded at Logachev Seamount that may testify to ongoing magmatic activity and open interesting research opportunities. We expect that the seismicity pattern, the amount of high-quality local and teleseismic events recorded by the network will support a comprehensive analysis of spreading processes and lithospheric structure as the project proceeds.

A problem for the KNIPAS OBS network that was not anticipated were strong ocean bottom currents that seriously affected the records (Fig. 2). The currents reach velocities of up to 20 cm/sec and lead to Karman vortex shedding and strumming at the head buoy and the flag pole of the OBS. This produced pronounced harmonic tremor signals on all seismometer channels in a frequency band of about 1–10 Hz obscuring earthquake arrivals in times of strong tremor. We extracted the fundamental frequency of the tremor in the entire network for the duration of the survey and reconstructed ocean bottom current velocities and their variation in time and space. Measures have been taken to avoid this problem in future surveys.

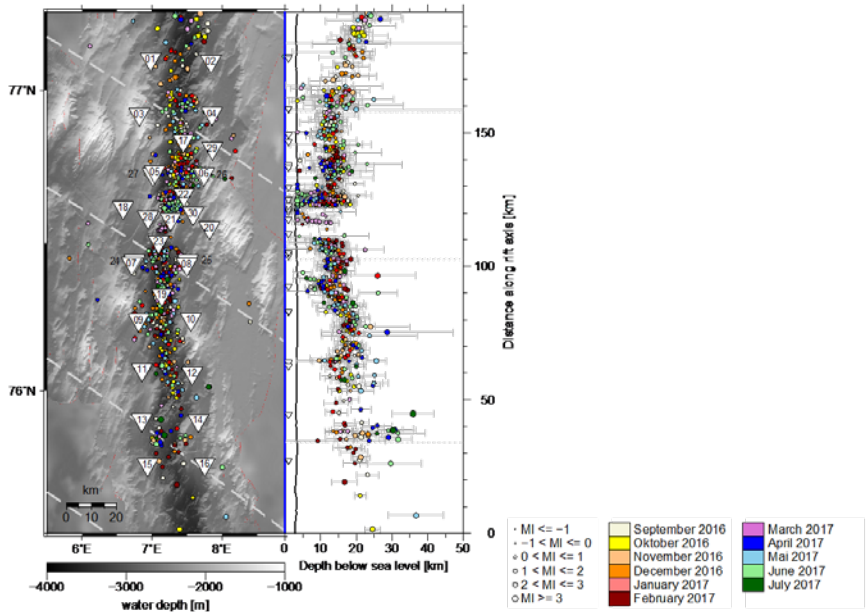

Fig. 1: Preliminary location of the hypocentres of the 1000 best recorded earthquakes of the KNIPAS data set. Numbered triangles refer to ocean bottom seismometer positions.

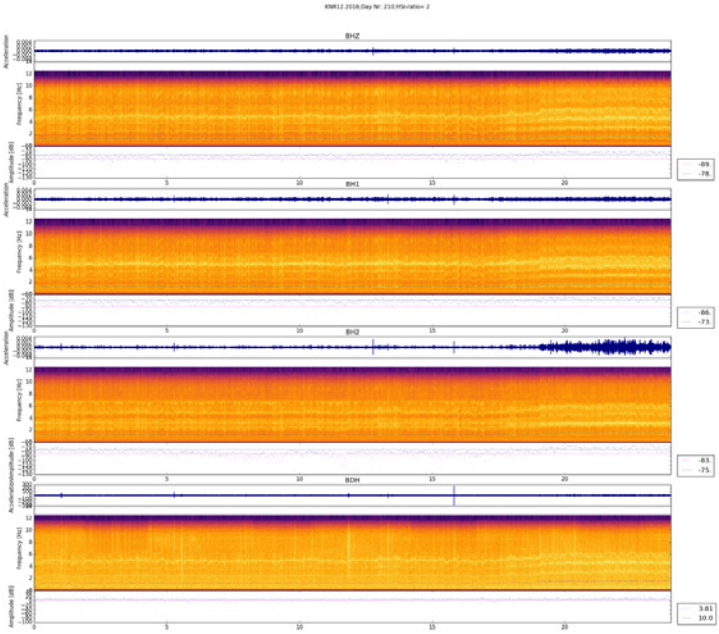

Fig. 2: Spectrograms of 24 hours of data from station KNR12 showing the 4 OBS channels. The harmonic tremor signal caused by currents acting on the OBS is clearly visible. An increase in tremor amplitude is particularly evident on channel BH2 around 20:00 connected also with different frequencies that may point to an additional vibrating source. Dots and panels with dots indicate the performance of the tremor detection algorithm in finding the fundamental frequency of harmonic tremor signals.

MSM68/2*

REFERENCE DATA FOR THE ATMOSPHERE AND OCEAN FROM THE ATLANTIC: NEW OPPORTUNITIES FROM EXPEDITION MSM68/2

AUTHORS

Max-Planck-Institute for Meteorology | Hamburg, Germany
Stephanie Fiedler*

* Now at: University of Cologne, Institute for Geophysics and Meteorology, Cologne

We used the North Atlantic expedition MSM68/2 with RV MARIA S. MERIAN from Emden to Mindelo, Cape Verde, for measurements in the atmosphere and ocean to extend the record of reference data in regions, where the observational network is sparse. We document some of our research instruments on board with the image gallery in Figure 1, ranging from a novel cloud observatory on the pile deck to well-established ocean measurements.

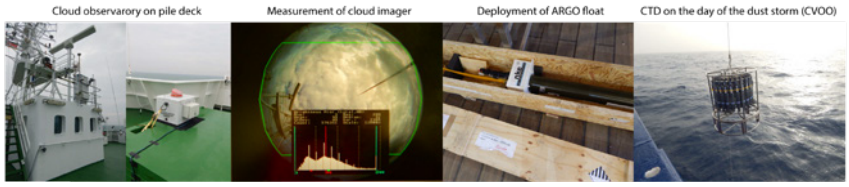

Fig.1: Some of the used instruments aboard RV MARIA S. MERIAN during MSM 68/2.

Despite the rather short duration of the expedition with just ten days at sea, the multi-disciplinary team of MSM68/2 had a number of successes helping to shape and advance their scientific research. These are:

(1) the opportunity to observe and subsequently study an impressive desert-dust storm from North Africa with the measurements from MSM 68/2 (Fiedler, 2018) and high-resolution model simulations. The simulations and in-depth analysis of the development of the dust outbreak is a major part of a new PhD student project at the Desert Research Institute, USA, in collaboration with S. Fiedler.

(2) the deployment, operation and prototype analysis of the new 'Pinocchio' cloud imager during MSM 68/2. The instrument is installed on the pile deck records images since our expedition such that we have now a dataset of a few years available for the further

development of the retrieval software and more comprehensive analyses for a novel Marine Cloud Statistics (MCloudS). This work will be continued as undergraduate student project at the University of Cologne supervised by S. Fiedler,

(3) the surprisingly many sightings of marine mammals for extending the regional database of PLOCAN despite poor observational conditions by S. Neves,

(4) the innovative underway measurements of seawater alkalinity and subsequent analyses shaping the PhD project of K. Seelmann from GEOMAR, and

(5) the unique measurements of sunlight spectra with a new MAX-DOAS instrument that is part of research for obtaining the PhD degree of S. Donner and contributes to a larger database at the Max-Planck-Institute for Chemistry.

We further extended the observational records of aerosol optical properties for the Maritime Aerosol Network (MAN) of NASA's AeroNet program, graphically displayed in Figure 2, of rainfall for the OceanRAIN network of the University of Hamburg, of ocean measurements for the global Argo program by deploying a new float for BSH, and for the Cape Verde Ocean Observatory by performing a CTD, as well as of bathymetry data for GEOMAR. Two years after the expedition, we have used the new data in PhD research theses, wrote first journal publications on the results, and published a comprehensive book on the scientific work of MSM 68/2 in the report series of the Max-Planck-Institute for Meteorology (Fiedler, 2018). Scientifically using the collected data is ongoing work by the scientific team members of MSM 68/2 and others.

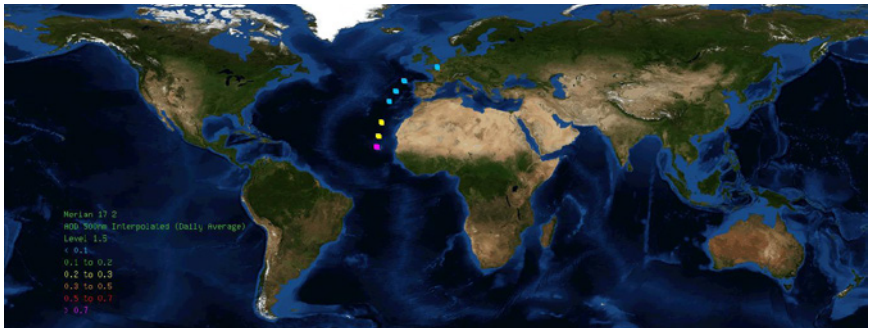

Fig. 2: Measurements of the aerosol optical depth from MSM 68/2. Larger values (yellow and pink) mark the occurrence of dust aerosols from North Africa.

REFERENCES

Fiedler, S., 2018. Expedition to the North Atlantic with RV MARIA S. MERIAN. Berichte zur Erdsystemforschung, 211, doi: 10.17617/2.3006588. https://pure.mpg.de/rest/items/item_3006588_7/component/file_3006589/content

MSM69

STRUCTURE OF OCEANIC LITHOSPHERE AS A FUNCTION OF GEOLOGICAL TIME: EVIDENCE FOR CRUSTAL AGEING AND EPISODICITIES OF CRUSTAL ACCRETION

AUTHORS

GEOMAR Helmholtz Zentrum für Ozeanforschung | Kiel, Germany
I. Grevemeyer, K. Growe, C. Papenberg, L. Gómez de La Peña

Institut de Physique du Globe de Paris, Universite de Paris | Paris, France
S. Singh, V. Vaddineni

Fachbereich Geowissenschaften, Universität Bremen | Bremen, Germany
H. Villinger, N. Kaul

The oceanic lithosphere is created by seafloor spreading at mid-ocean ridges and covers approximately 57 % of the Earth surface. Properties of the oceanic crust – like its thickness and lower crustal velocity – are inherently related to the formation of the plate and can be used to infer periodicities in crustal accretion when moving away from the spreading ridge. After its formation the shallow lithosphere or crust is affected by hydrothermal circulation in the uppermost permeable crust over tens of millions of years. In turn, heat is removed from the lithosphere by circulating seawater and mineral precipitation modifies and seals open void spaces, affecting the heat loss, seismic velocity, and composition of the crust. In addition, the lithosphere cools and thickens with age, resulting in the well-known subsidence of the seabed, decreasing heat flow, geoid height, and increasing seismic velocities in the uppermost mantle. While the formation of crust and lithosphere at the spreading ridges is reasonably well studied, little is known about how crustal accretion changed over time and how crust and lithosphere change when being carried away from the underlying heat source. Understanding how lithosphere evolves with age is thus a major challenge in Earth sciences. In the equatorial Atlantic, MSM69 provided seismic data from an 1100 km long transect, call P01, surveying age-dependent features of the lithosphere, revealing crustal structure and mantle properties, including major lithospheric boundaries like Moho and decaying heat flow; 71 OBS were deployed along the seismic transect.

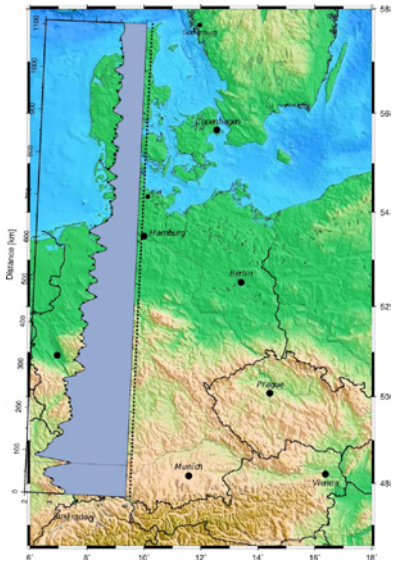

Fig. 1: The 1100 km long transect shot during MSM69 superimposed on Germany.

Crustal structure revealed along P01 is on average approximately 5.5 km thick and is therefore much thinner than the 7 km reported by White et al. (1992) for the Atlantic Ocean. However, crustal thickness shows considerable variations, being with 4–5 km thinnest at 800 to 1000 km away from the ridge crest and with 7 to 9 km thickest at 550 to 700 km from the axis. Further, lower crustal velocity is lowest at the ridge axis, increasing with distance and probably age from <6.8 km/s to ~7 km/s roughly 300 km away from the axis. Most interestingly, the domain if the thickest crust provides reasonably slow lower crustal velocity, suggesting that variations in crustal thickness might be controlled by mantle heterogeneities rather than being related to variations of mantle temperature. In addition, upper crustal velocity increases with age, indicating hydrothermal sealing of open void space. Heat flow anomalies support a vigorous hydrothermal circulation system along the entire transect, revealing strong heat flow variations at all lithospheric ages.

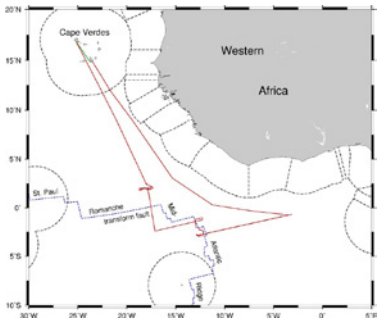

Fig. 2: Track chart of MSM69

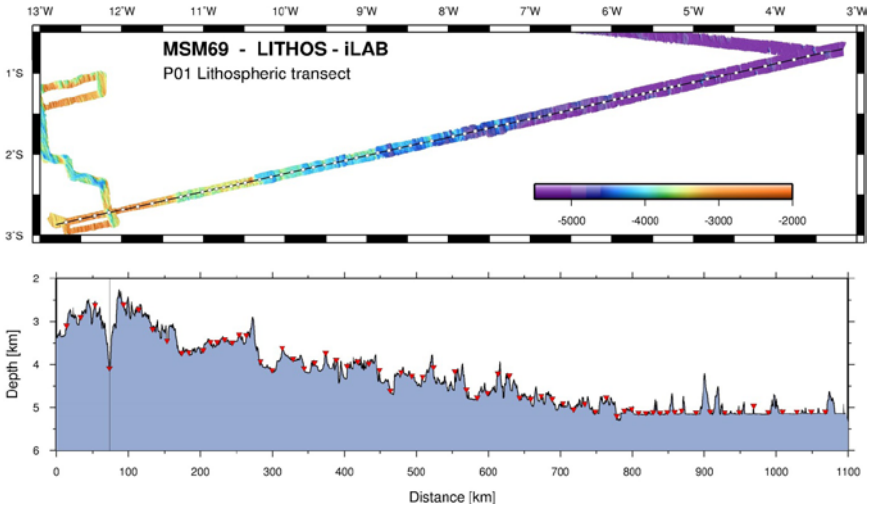

Fig. 3: Bathymetirc map and bathymetric profile with OBS of profile P01

The structure of large-offset transform faults and fracture zones associated with the Mid-Atlantic Ridge studied before the 1990s exhibits anomalous crustal structures that fall well outside the range typically observed for normal oceanic crust, both in thickness and internal structure. The geological nature of the seismically anomalous crust and how this crust forms, are still a matter of debate. One interpretation is that the crust within North Atlantic fracture zones consists of a thin, intensely fractured, and hydrothermally altered basaltic section overlying ultramafics that are extensively serpentinized in places. (Detrick et al., 1993). For nearly three decades, transform faults and fracture zones garnered little attention. However, during MSM69 we surveyed the St. Paul fracture zone near 18°W; 14 ocean-bottom-seismometers and hydrophones sampled seismic shots fired along a 140 km long seismic profile, running within the ~10 km wide valley of the fracture zone, that separates 40 Ma crust in the south with 70 Ma crust in the north. Seismic refraction and wide-angle data provided both first arrival refracted P-waves and wide-angle reflections. Furthermore, a clear Pn refraction branch with the apparent velocity of ~8 km/s has been observed. Joint refraction and reflection tomographic inversion of P-wave travel times supports a seismic structure, which is heterogeneous, but shares common features with 4–5 km thick normal oceanic crust, supporting a magmatic origin of the crust. Both the observed reflections from the crust-mantle boundary and upper mantle P-wave speed of ~8 km/s provide little evidence for large quantities of serpentinites being distributed through the crust and upper mantle.

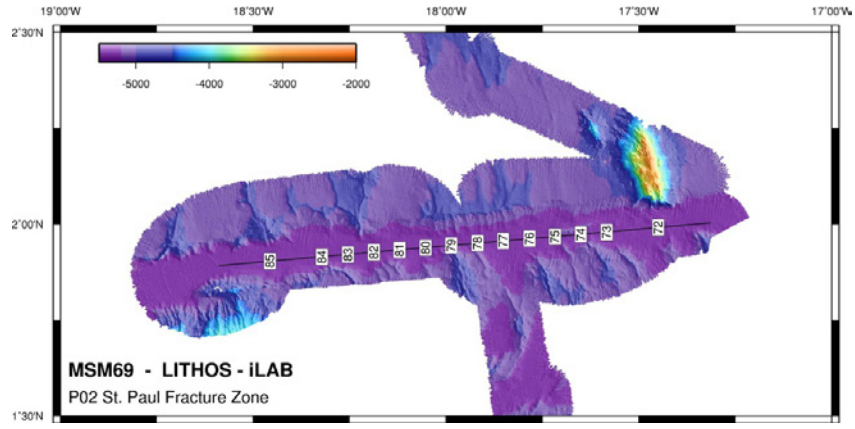

Fig. 4: Seismic profile P02 shot along the St. Paul Fracture Zone

REFERENCES

Detrick, R S, White, R S, and Purdy, G M, Crustal structure of North Atlantic Fracture Zones, Rev. Geophys. 1993, 31(4), 439–458, doi:10.1029/93RG01952.

White R S., McKenzie D, O'Nions R K, Oceanic crustal thickness from seismic measurements and rare earth element inversions, J. Geophys. Res. 1992, 97, 19,683–19,715.

MSM69*

STRUCTURE OF JUVENILE AND MATURE OCEANIC LITHOSPHERE ALONG | AN 1100 KM LONG SEISMIC TRANSECT IN THE EQUATORIAL ATLANTIC OCEAN

AUTHORS

GEOMAR Helmholtz Zentrum für Ozeanforschung | Kiel, Germany
I. Grevemeyer, C. Papenberg, L. Gómez de La Peña

Institut de Physique du Globe de Paris, Universite de Paris | Paris, France
S. Singh, V. Vaddineni, P. Audhkhasi

The velocity structure of the oceanic crust formed by seafloor spreading at mid-ocean ridges is inherently associated with mantle melting. The amount of melt produced by adiabatic decompression of the mantle and the composition of the resultant igneous crust depend on the temperature, composition, and water content of the mantle source (e. g., Korenaga et al., 2002). Normal oceanic crust with a thickness of 6–7 km and Mid-Ocean Ridge Basalt (MORB) like composition is the result of decompressional melting of a mantle source composed of dry pyrolite with a mantle temperature of ~1300°C. Thus, crustal formation occurs as passive response to seafloor spreading (i. e., passive upwelling). Higher mantle temperatures or compositional anomalies may cause buoyant upwelling of the mantle (i. e. active upwelling). The combination of active upwelling and higher mantle temperatures, or the presence of a more fertile mantle source, will produce larger amounts of melting and, likely, a thicker crust. If formed by melting of a pyrolytic mantle, thicker crust is associated with fast lower crustal velocity.

The formation of crust and lithosphere at spreading ridges is reasonably well studied, however, little is known about how crustal accretion changed over time and how crust and lithosphere change when carried away from the underlying heat source. Understanding how lithosphere evolves with age is thus a major challenge in Earth sciences. In November and December of 2017, we acquired in a joint German and French effort an 1100-km-long transect in the equatorial Atlantic Ocean aboard the German research vessel MARIA S. MERIAN (MSM69). The profiles runs from 12.8°W/2.8°S, for 75 km on the South American plate, crosses the Mid-Atlantic Ridge and terminates at 3.2°W/0.7°S, roughly covering zero-age to approximately 50 Myr old lithosphere of the African plate. The seismic refraction and wide-angle transect was covered with 71 Ocean-Bottom-Seismometers and hydrophones spaced at 10 to 20 km intervals. The profile was shot at an increased interval of 210 s to decrease the shot-induced-level, improving signal-noise-ratio and providing an average shot spacing of 410 m.

We used a joint reflection and refraction tomography (Korenaga et al., 2000), revealing the crustal and mantle P-wave velocity structure and the geometry of the crust/mantle boundary and, in turn, crustal thickness.

Along the transect, seismic tomography indicates an average crustal thickness of 5.5 km. Thus, crust is much thinner than found elsewhere in the North Atlantic where crust is reported to be in the order of 7 km (White et al., 1992). However, crustal thickness reveals considerable variations along P01, being with 4–5 km thinnest at the eastern end of the corridor, about 800 to 1000 km away from the ridge crest, and with 7 to 9 km thickest at 550 to 700 km from the axis.

Further, seismic velocity indicates age-dependent features, including a lower crustal velocity that is lowest at the ridge axis, increasing with distance and probably age from <6.8 km/s to ~7 km/s roughly 300 km away from the axis. Most interestingly, the domain if the thickest crust provides reasonably slow lower crustal velocity, suggesting that variations in crustal thickness might be controlled by mantle heterogeneities rather than being related to variations of mantle temperature. Mantle velocity increases with distance to the ridge axis from <7.7 km/s at the crest to >8.0 km/s as lithosphere ages.

REFERENCES

Korenaga, J, Holbrook, W S, Kent, G M, Kelemen, P B, Detrick, R S, Larsen, H-C, Hopper, J R, and Dahl-Jensen T, Crustal structure of the southeast Greenland margin from joint refraction and reflection seismic tomography, J. Geophys. Res. 2000, 105, 21 591–21 614.

Korenaga, J, Kelemen, P B and Holbrook, W S, Methods of resolving the origin of large igneous provinces from crustal seismology, J. Geophys. Res. 2002, 107, 2178, doi:10.1029/2001JB001030.

White R S., McKenzie D, O'Nions R K, Oceanic crustal thickness from seismic measurements and rare earth element inversions, J. Geophys. Res. 1992, 97, 19,683–19,715.

MSM69*

AMBIENT NOISE CORRELATION FUNCTIONS AT THE MID-ATLANTIC RIDGE: CONSTRAINTS FROM 10 DAYS OF OCEAN-BOTTOM-HYDROPHONE DATA

AUTHORS

GEOMAR Helmholtz Zentrum für Ozeanforschung | Kiel, Germany
I. Grevemeyer, D. Lange, C. Papenberg

Institut de Physique du Globe de Paris, Universite de Paris | Paris, France
S. Singh

Seismic observations based on cross-correlations between pairs of stations have confirmed the theory that cross-correlation of diffusive wave fields, e. g., ambient noise or scattered coda waves, can provide an estimate of the Green's function between stations and thus can be used to yield constraints on the structure of the Earth's interior using surface waves. In general, the emergence of the Green's function is efficient only after sucient averaging that is provided by random spatial distribution of the noise when considering long time-series (Shapiro and Campillo, 2004; Stehly et al., 2007). Here, however, we use only 10 days of ambient noise correlation functions obtained during the cruise MSM69 of RV MARIA S. MERIAN at the equatorial Mid-Atlantic Ridge to show that Green's functions may emerge after a few hours using Welch's method (Seats et al., 2012).

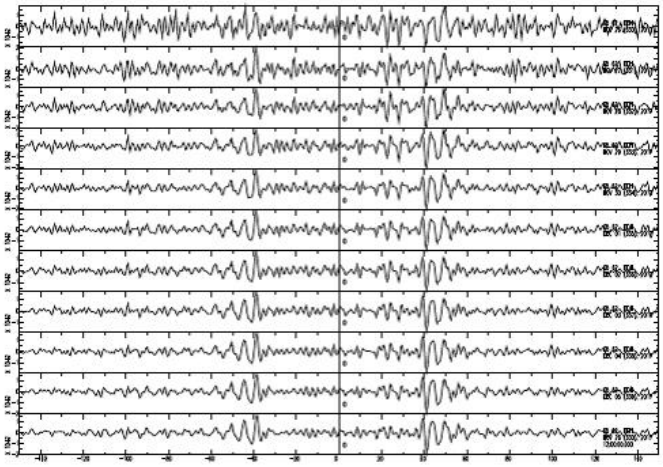

Fig. 1: Waveform example of cross-correlation functions obtained using Welch's method, dividing ambient noise records into 1 h long overlapping time windows (overlap of 20 %); all traces are hydrophone data. Bottom trace – sum of daily traces; upper ten traces are daily stacks.

The Green's function is band-limited in the frequncy domain of secondary microseisms (periods of ~2 s to 9 s), representing a kind of wave guide or Scholte wave. Group and phase velocity derived from the observed cross-correlated wave trains indicate a strong dependence on the water depth and average water velocity. However, cross-correlation functions also contain structural information reflecting the structure of the oceanic crust and the uppermost mantle. Unfortunately, uncertainties of group and phase velocity are still too large to yield clear signals, for example, reflecting crustal ageing. Longer time-series of a few weeks or months may provide robust estimates and perhaps longer period signals from primary microseisms, carrying structural information from the upper mantle.

REFERENCES

Stehly, L, Campillo M, and Shapiro N M, Traveltime measurements from noise correlation: stability and detection of instrumental time-shifts, Geophys. J. Int. 2007, 171, 223–230, doi:10.1111/j.1365-246X.2007.03492.x

Shapiro, N M , and Campilo M, Emergence of broadband Rayleigh waves from correlations of the ambient noise, Geophys. Res. Lett. 2004, 31, L07614, doi:10.1029/2004GL019491.

Seats, K J, Lawrence J F, and Prieto G A, Improved ambient noise correlation functions using Welch's method, Geophys.J. Int. 2012, 188, 513–523, doi:10.1111/j.1365-246X.2011.05263.x

MSM81*

ONSET AND MODIFICATIONS IN INTENSITY AND PATHWAYS OF WATER MASS EXCHANGE BETWEEN THE SOUTHEAST PACIFIC AND THE SOUTH ATLANTIC WITH FOCUS ON THE FALKLAND PLATEAU

AUTHORS

Alfred-Wegener-Institut Helmholtz-Zentrum für Polar- und Meeresforschung | Bremerhaven, Germany
B. Najjarifarizhendi, G. Uenzelmann-Neben

MARUM, Universität Bremen | Bremen, Germany
T. Westerhold

The opening of Drake Passage and the Scotia Sea enabled the exchange of water masses between the southern Pacific and the South Atlantic. In this way heat and energy could be transferred between the two oceans. Together with the opening of the Tasman Gateway this allowed the establishment of the Antarctic Circumpolar Current (ACC) thermally isolating Antarctica, which has been considered as one of the major causes for the onset of widespread glaciation. Both tectonic movements within Drake Passage and the Scotia Sea as well as modifications in climate have led to changes in intensity and pathway of the ACC and the water masses flowing within it. The onset of the ACC and those changes have been documented in sedimentary structures deposited on the Falkland Plateau. A study of the sediment drifts shaped by Circumpolar Deepwater, Weddell Sea Deepwater and Antarctic Bottomwater will provide information on modifications of the circulation resulting from tectonic movements and changes in climate. A grid of high-resolution seismic data collected during expedition MSM 81 with RV Maria S Merian will allow the deciphering of the sediment drifts structures as well as their modification and reshaping and the identification and relocation of depot centres.

Additionally, the data will form the base for a site survey package for IODP proposal 862 set on studying the earliest phase of water mass exchange via Drake Passage.

SO237*

DISCOVERY OF WIDELY AVAILABLE ABYSSAL BEDROCK REVEALS OVERLOOKED HABITAT TYPE AND NEW ANGLES TO STUDY DEEP-SEA BIODIVERSITY

AUTHORS

Senckenberg Research Institute and Natural History Museum, Department Marine Zoology, Section Crustacea | Frankfurt am Main, Germany
T. Riehl (Corresponding author), A. Brandt

Goethe-University of Frankfurt, Institute for Ecology, Evolution and Diversity | Frankfurt am Main, Germany
T. Riehl (Corresponding author), A. Brandt

GEOMAR Helmholtz Centre for Ocean Research Kiel | Kiel, Germany
A.-C. Wölfl, N. Augustin, C. Devey

Senckenberg am Meer, German Centre for Marine Biodiversity Research (DZMB) | Wilhelmshaven, Germany
P. Martínez Arbizu

The assumption of a generally homogeneous, sedimented abyssal seafloor (Divins 2003; Glasby 2007; Smith et al. 2008; Thistle 2003) is at odds with the fact that the faunal diversity in some abyssal regions exceeds that of shallow-water environments (e. g. McClain and Schlacher 2015; Sanders 1968; Snelgrove and Smith 2002).

Habitat heterogeneity and species diversity are often linked; on the deep seafloor, sediment variability and hard-substrate availability influence geographic patterns of species richness and turnover (Levin et al. 2001; Levin and Dayton 2009). A correlation between habitat heterogeneity and species diversity also begins to emerge in the abyss (see, e. g., Cordes et al. 2010; Durden et al. 2015; Levin et al. 2010; Simon-Lledó et al. 2018; Stein et al. 2014; Vanreusel et al. 2010).

Here we show, using a ground-truthed analysis of multibeam sonar data, that the deep seafloor may be much rockier than previously assumed. Data collected during RV Sonne cruise SO237 from a trans-Atlantic corridor along the Vema Fracture Zone (VFZ) (Devey et al. 2018; Devey 2015), covering crustal ages from 0–100 million years, show rock exposures occurring at all crustal ages (Fig. 1). Extrapolating to the whole Atlantic, over 260,000 km^2 of rock habitats potentially occur along Atlantic fracture zones alone, significantly increasing our knowledge about abyssal habitat heterogeneity.

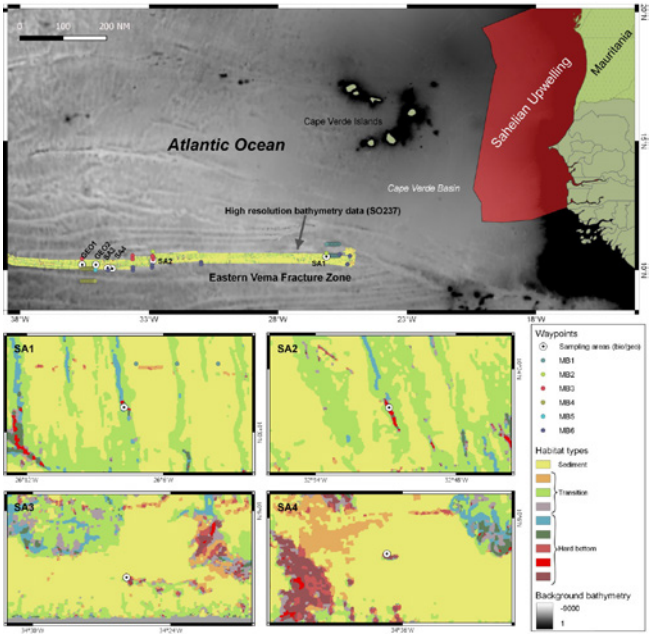

Fig. 1: Overview map of BEDROCK stations (top) and habitat characterization (below) of the biological sampling areas (SA). The grey topography is based upon the GEBCO dataset. The colored seafloor represents the area surveyed during SO237 with high-resolution bathymetric data and habitat characterization (below). The color scheme indicates the type of seafloor. Biological sampling areas represent insular rock habitats surrounded by sediment plains. They were chosen for their isolated location from other such habitats and distance from each other (10 NM, 50 NM, and 500 NM apart).

This higher-than-expected habitat heterogeneity implies that future abyssal benthic sampling campaigns need to be considerably more sophisticated than at present to capture the full deep-sea habitat heterogeneity and biodiversity.

The proposed campaign BEDROCK (BEnthos Diversity and habitat structure caused by abyssal hard ROCK) targets these rock habitats using an innovative sampling design to test the following hypotheses:

(H1) the heterogeneous abyssal sea causes restricted distributions and connectivity, and high turnover in the benthos;

(H2) species turnover and environmental gradients caused by hard rock are positively correlated;

(H3) connectivity between populations inhabiting supposedly isolated habitats (e. g., seamounts) is provided by hard-rock patches in the abyss;

(H4) seafloor geological processes impact biological diversity on the local as well as regional scale.

BEDROCK aims at unravelling the effects of the widely distributed rock patches on the community composition and evolution of the abyssal benthos. The innovative biological sampling strategies, involving ROV benthos sampling and photographic surveys, allow studying the abyssal hard-rock fauna and the topology effects on adjacent sediment variability and biodiversity. For sustainable ocean governance, such as the designation of marine protected areas, or impact assessments connected to deep-sea mining, abyssal bedrock and its role in the deep-sea ecosystem require consideration. This study comprises a baseline for the development of multibeam remote sensing strategies for habitat and biodiversity assessments in abyssal depths.

REFERENCES

Cordes EE, Cunha MR, Galéron J, et al. (2010) The influence of geological, geochemical, and biogenic habitat heterogeneity on seep biodiversity. Mar Ecol 31:51–65. doi: 10.1111/j.1439-0485.2009.00334.x

Devey CW (2015) RV SONNE Fahrtbericht / Cruise Report SO237 Vema-TRANSIT. Geomar Rep 23:130. doi: 10.3289/GEOMAR_REP_NS_23_2015

Devey CW, Augustin N, Brandt A, et al. (2018) Habitat characterization of the Vema Fracture Zone and Puerto Rico Trench. Deep Sea Res Part II Top Stud Oceanogr. doi: 10.1016/j.dsr2.2018.02.003

Divins DL (2003) Total sediment thickness of the world's oceans and marginal seas. In: NOAA Natl. Geophys. Data Cent. Boulder CO. http://www.citeulike.org/group/11419/article/11348784. Accessed 4 Apr 2017

Durden JM, Bett BJ, Jones DOB, et al. (2015) Abyssal hills – hidden source of increased habitat heterogeneity, benthic megafaunal biomass and diversity in the deep sea. Prog Oceanogr 137, Part A:209–218. doi: 10.1016/j.pocean.2015.06.006

Glasby GP (2007) Broad region of no sediment in the southwest Pacific Basin: comment and reply comment. Geology 35:e132–e132.

Levin LA, Dayton PK (2009) Ecological theory and continental margins: where shallow meets deep. Trends Ecol Evol 24:606–617.

Levin LA, Etter RJ, Rex MA, et al. (2001) Environmental influences on regional deep-sea species diversity. Annu Rev Ecol Syst 32:51–93. doi: 10.1146/annurev.ecolsys.32.081501.114002

Levin LA, Sibuet M, Gooday AJ, et al. (2010) The roles of habitat heterogeneity in generating and maintaining biodiversity on continental margins: an introduction. Mar

Ecol 31:1–5. doi: 10.1111/j.1439-0485.2009.00358.x

McClain CR, Schlacher TA (2015) On some hypotheses of diversity of animal life at great depths on the sea floor. Mar Ecol 1–24. doi: 10.1111/maec.12288

Sanders HL (1968) Marine benthic diversity: a comparative study. Am Nat 243–282.

Simon-Lledó E, Bett BJ, Huvenne VAI, et al. (2018) Megafaunal variation in the abyssal landscape of the Clarion Clipperton Zone. Prog Oceanogr. doi: 10.1016/j.pocean.2018.11.003

Smith CR, De Leo FC, Bernardino AF, et al. (2008) Abyssal food limitation, ecosystem structure and climate change. Trends Ecol Evol 23:518–528.

Snelgrove PVR, Smith CR (2002) A riot of species in an environmental calm: the paradox of the species-rich deep-sea floor. Oceanogr Mar Biol Annu Rev 40:311–342.

Stein A, Gerstner K, Kreft H (2014) Environmental heterogeneity as a universal driver of species richness across taxa, biomes and spatial scales. Ecol Lett 17:866–880.

Thistle D (2003) The deep-sea floor: an overview. Ecosyst World 5–38.

Vanreusel A, Fonseca G, Danovaro R, et al. (2010) The contribution of deep-sea macrohabitat heterogeneity to global nematode diversity. Mar Ecol 31:6–20. doi: 10.1111/j.1439-0485.2009.00352.x

SO253

GEOCHEMICAL AND ECOLOGICAL IMPACTS OF HYDROTHERMAL PROCESSES AT THE KERMADEC INTRAOCEANIC ARC (SW PACIFIC, CRUISE SO253)

AUTHORS

Jacobs University Bremen; University of Bremen; University of Münster; University of Oldenburg; University of Hamburg; Max Planck Institute for Marine Microbiology in Bremen | Bremen, Germany

Andrea Koschinsky and project partners of SO253

Hydrothermal systems along volcanic island arcs are different to those at mid-ocean ridges because of their mostly shallow water depth and strong magmatic input into their fluids. Their hydrothermal plumes often reach up into the photic zone.

During the R/V Sonne cruise SO253 at the Kermadec intraoceanic arc, four different hydrothermally active working areas between 250 and 1600 m water depth - Macauley, Haungaroa, Brothers and Rumble III - were studied for their geological, geochemical as well as biological diversity. One specific focus was on the role of hydrothermal vents at volcanic arcs for the global elemental budget of the ocean and for local chemical and biological processes in the water column and at the seafloor. Hydrothermal fluids at low-temperature diffuse vent sites and from high-temperature black smokers, rocks, sulfide mineralisations, Fe-Mn precipitates, hydrothermal plumes within the water column as well as diverse biota were sampled. The research results of the team of project partners are summarized in the following.

Data from sampled hot fluids clearly show that the geochemical fluid composition is very variable but basically divides into two types: one that indicates distinct magmatic input (Macauley, Brothers Cone) and another that shows evidence for intense water-rock interaction under hot, acidic conditions (Haungaroa, Brothers NW Caldera Wall) (Kleint et al., 2019). Results from the plume surveys show that especially Fe and Zn appear to be very stable in the laterally dispersing plume, possibly due to organic complexation. At the shallowest sampling site, Macauley (~ 300 m water depth), such trace metals even reach the photic zone, where they can act as micronutrients or potential toxins to marine organisms.

To evaluate the extent of mass transfer between hydrothermal fluids and the volcanic basement rock, the overall geochemical composition of the volcanic rocks and hydrothermal precipitates was characterized. Additionally, dissolved volatiles were analyzed, in order to determine the influence of volcanic gases on the hydrothermal

systems. High concentrations of CO_2 together with volatile sulfur species confirm that fluids from Macauley and Brothers Cone have taken up magmatic volatiles. Such data was embedded in thermodynamic reaction path models and fluid-seawater mixture models, which were able to simulate both the fluid composition and the minerals at these vents. The modelling has shown that the mobilization of metals, such as Al, Cu, Fe and Zn is enhanced by the presence of sulfuric gases. Furthermore, the models were able to predict the presence of extremely hydrothermally leached rocks. Exactly these rocks were recovered and analyzed at the hydrothermal field at Macauley volcano.

The $^{3}He/^{4}He$ ratios at the volcanoes vary between 5.8 and 6.5 Ra (atmospheric ratio). The maximum observed $\delta^{3}He$ (excess ^{3}He, of primordial origin) at the non-buoyant plume level are for Rumble III 90 %, Haungaroa 83 %, Macauley Cone site 144 %, Macauley Caldera site 16 %, Brothers Cone site 56 %, Brothers NW Caldera site 94 %. While the systems at Brothers and Macauley Caldera appear to be relatively stable since the late 1990s/early 2000s, the $\delta^{3}He$ at Macauley Cone has increased significantly since the observations during the NZASRoF expedition in 2005. This site also showed the highest recorded δ3He of 445 % in a weakly diluted sample (pH = 5.0) from rising plume, less than 1m above the vent.

In accordance with differences in the chemical composition, hydrothermal fluids discharging at each vent site studied are characterized by a distinct sulfur isotopic composition. Combined $\delta^{34}S$ and $\Delta^{33}S$ results for dissolved sulfide indicate SO_2 disproportionation and, thus, a distinct contribution of magmatic sulfur to the hydrothermal fluids at some sites Other vent sites resemble a sulfur isotopic composition typical for black smoker fluids. The latter indicate thermochemical reduction of seawater sulfate and fluid interaction with the oceanic crustal rocks as prominent sulfur sources. Yet, highly variable δ34S values in the vent fauna indicate sulfur cycling presumably by chemosynthetic symbionts.

The analysis of short-lived radium (Ra) isotopes in fluids and plumes revealed that they can serve as important new tools to study horizontal and vertical plume dispersion dynamics, as these radioactive isotopes can be used as chronometers (Neuholz et al., 2019). Using short-lived Ra isotopes, it was further possible to present an approach to calculate the flux of hydrothermal fluids discharging from the NW Caldera Wall at Brothers volcano.

Dissolved organic matter (DOM) compositions clearly reflect the imprint of thermal degradation occurring during hydrothermal circulation. Thereby variability between samples is predominantly controlled by the degree of dilution of the actual hydrothermal fluid. Samples with high hot hydrothermal fluid contribution exhibit on average a lower molecular mass, O/C and H/C ratio of the DOM compounds. Moreover, a lower total number of compounds is detected, which is in line with previous thermal degradation experiments. Incubation experiments clearly showed an increased bacterial growth in

incubations with bulk thermally degraded DOM, while others containing only the extractable DOM fraction (SPE-DOM) showed no additional growth compared to the control incubations (Hansen et al., 2019). Detailed characterization of the SPE-DOM fraction revealed that no compositional changes occurred during the incubation related to microbial growth. These results indicate that thermal degradation of DOM results in significant fractions of it becoming accessible to microbial utilization, however, it is an unextractable fraction that becomes available while the extractable fraction remains recalcitrant.

The microbial community structure and its chemosynthetic capacity was assessed through incubation experiments. Consumption to CO_2 fixation ratios from Haungaroa volcanic ash sediment incubations indicated that sulfide oxidation likely fuelled autotrophic CO_2 fixation. Transcript analyses with the sulfide-supplemented sediment slurries demonstrated that Sulfurovum prevailed in the experiments, as was also the case in the natural environment (Böhnke et al., 2019). Hence, these incubation experiments appeared to simulate environmental conditions well, indicating that probably Sulfurovum catalyzed sulfide oxidation drives biomass synthesis in the volcanic ash sediments. In contrast, the Brothers hydrothermal fluid incubations exhibited highest autotrophic CO_2 fixation if they were supplemented with iron or hydrogen.

Chemosynthetic hydrothermal vent symbioses included three mussel species: Gigantidas gladius had a wide distribution range from Macauley to Rumble III in shallow to intermediate water depths. Vulcanidas insolatus was limited to shallow waters in Macauley Cone, while Bathymodiolus manusensis occurred only in intermediate and greater water depths at Haungaroa and Brothers. Each of these mussel species is associated with species-specific endosymbiotic sulfur-oxidizing SUP05 bacteria in their gills. Stable carbon isotope signatures of mussel tissues from all three host species ranged in the so called "30‰ group" of vent mussels that live in symbiosis with sulfur-oxidizing bacteria indicating that all three Kermadec species primarily rely on chemosynthetic primary production of their symbionts. G. gladius and B. manusensis additionally regularly harbored spirochetes in their gills. Similar bacteria have not been observed in other vent and seep mussels, and preliminary metagenomic data suggest these spirochetes are heterotrophic and host-specific intracellular parasites.

Whereas the microbial communities at some vent sites had already been characterized before (e. g. Brothers), others (Haungaroa, Rumble III) have been visited for the first time for targeted microbial sampling. A comparative 16S rRNA gene diversity analysis of plume samples revealed a high proportion of SUP05-clade bacteria in plumes at Brothers and Macauley volcano, verified by fluorescence in situ hybridization. However, the high abundance of this group in iron rich plumes of the NW caldera at Brothers volcano and of a distinct subgroup in plume at Macauley was striking. Targeted re-assembly of metagenomes from both sites revealed 6 SUP05 bins. Their analysis revealed the already known metabolic traits.

REFERENCES

Kleint et al. (2019): Geochemical characterization of highly diverse hydrothermal fluids from volcanic vent systems of the Kermadec intraoceanic arc. Chemical Geology 528. doi: 10.1016/j.chemgeo.2019.119289

Neuholz et al. (2019): Near-field hydrothermal plume dynamics at Brothers Volcano (Kermadec Arc): A short-lived radium isotope study. Chemical Geology. doi: 10.1016/j.chemgeo.2019.119379

Hansen et al. (2019): Biodegradability of hydrothermally altered deep-sea dissolved organic matter. Marine Chemistry 217. doi: 10.1016/j.marchem.2019.103706

Böhnke et al. (2019): Parameters Governing the Community Structure and Element Turnover in Kermadec Volcanic Ash and Hydrothermal Fluids as Monitored by Inorganic Electron Donor Consumption, Autotrophic CO_2 Fixation and 16S Tags of the Transcriptome in Incubation Experiments. Frontiers in Microbiology. 10:2296. doi: 10.3389/fmicb.2019.02296

SO253*

GEOCHEMICAL CHARACTERIZATION OF HIGHLY DIVERSE HYDROTHERMAL FLUIDS FROM THE KERMADEC INTRAOCEANIC ARC AND THEIR CORRESPONDING TRACE METAL FLUXES INTO THE WATER COLUMN

AUTHORS

Department of Physics and Earth Sciences, Jacobs University Bremen gGmbH | Bremen, Germany
C. Kleint, A. Koschinsky

MARUM , University of Bremen | Bremen, Germany
C. Kleint, W. Bach, A. Diehl, A. Koschinsky

Department for Geosciences, University of Bremen | Bremen, Germany
W. Bach, A. Diehl

Department of Marine Sciences, GNS Science | Lower Hutt, New Zealand
C. de Ronde, V. Stucker

Marine Environmental Studies Laboratory, IAEA – Nuclear Applications | Monaco, Principality of Monaco
S. G. Sander

Department of Chemistry, University of Otago | Dunedin, New Zealand
S. G. Sander, R. Zitoun

Department for Geology and Palaeontology, University of Münster | Münster, Germany
H. Strauss

Royal Netherlands Institute for Sea Research (Royal NIOZ) | Den Burg, Texel, Netherlands
R. Middag, P. Laan

Compared to mid-ocean ridges, hydrothermal vent systems at intraoceanic arcs are located in shallower water depth. Therefore, their hydrothermal plumes may reach surface waters and directly supply essential micronutrients into the photic zone, such as Fe and Zn, which are usually strongly depleted in surface waters.

During the R/V Sonne cruise SO253 in 2016/2017, hydrothermal fluids and corresponding plumes in the water column were sampled at four active volcanoes along the Kermadec intraoceanic arc: Macauley, Haungaroa, Brothers and Rumble III (Figure 1a). Water depths ranged between 300 m and 1700 m. Samples were taken from diffuse-flow sites as well as from white and black smokers – rich in metals and gases – with discharge temperatures as high as 311°C (Figure 1b and c). Their fluid composition is very variable but basically divides into two types: one that indicates distinct magmatic input and another that shows evidence for intense water-rock interaction under hot, acidic conditions.

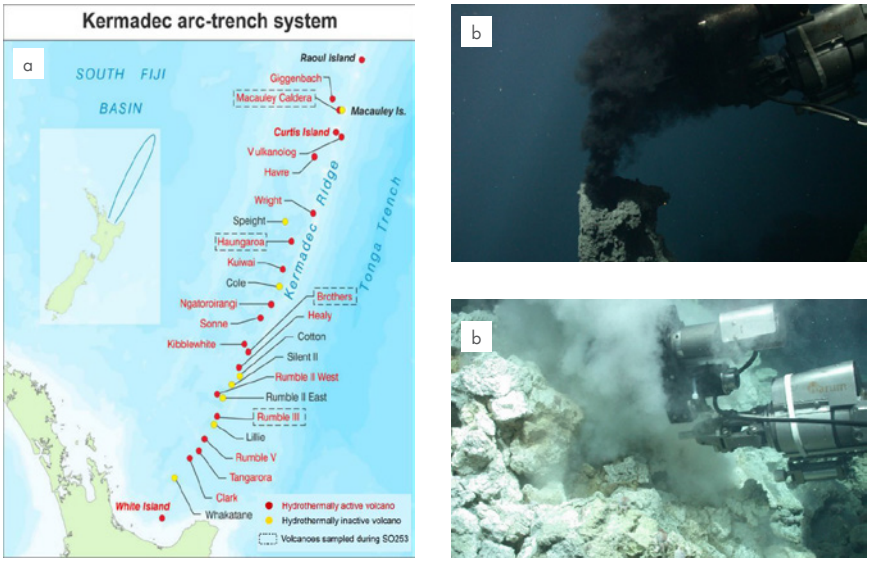

Fig. 1: a) Map showing the active and inactive hydrothermal sites along the Kermadec arc with the working areas of research cruise SO253 (Macauley, Haungaroa, Brothers and Rumble III) highlighted by dashed boxes (Kleint et al., 2019). b): Sampled black smoker at Brothers NW Caldera Wall; c) a sampled white smoker at Macauley. Copyright: Marum, University of Bremen.

Fluid samples from Macauley, the shallowest sampling site (~ 300 m), had Fe concentrations as high as 1.7 mM, Al concentrations up to 122 µM and H_2S up to 10 mM at a pH of only 1.2. At Brothers, the deepest sampling site (down to 1600 m), we identified two different fluid types: 1) A magmatically-influenced type at the Upper and Lower Cone with highest temperatures of 115°C, up to 95.6 mM Mg (the highest Mg concentration measured in fluids from intraoceanic arc systems so far), elevated SO_4^{2-} (76.9 mM), high H_2S (5.0 mM), but Fe concentrations of only 15 µM and 2) A fluid with low Mg (5.4 mM), low H_2S (1.1 mM), temperatures reaching 311°C and high Fe contents (12.4 mM) at the Upper Caldera and NW Caldera Wall, typical of a black smoker fluid. Chloride concentrations in all fluids were similar, or highly enriched when compared to seawater (e. g. up to 787 mM, brine fluids), with also one low-chlorinity vapour-phase

fluid sample recovered, indicating that phase separation is occurring at Brothers. Unusual highly elevated Mg concentrations in fluids from the Brothers Lower Cone (95.6 mM, compared to 53.2 mM in ambient seawater) combined with highly elevated concentrations of SO_4^{2-} (76.9 mM, compared to 29.0 mM in ambient seawater) indicate dissolution of Mg- and SO_4^{2-} bearing minerals in the subsurface, such as caminite (Kleint et al., 2019).

Plume surveys at the shallowest sampling site Macauley (~ 300 m) indicated strong plume signals for dissolved Fe, Mn, Cu and Zn (up to 1.2 µM, 1 µM, 160 nM, 150 nM, respectively) close to the source in 300 m water depth. With distance from the vent, the metal concentrations decrease, as to be expected, however, Zn/Fe ratios increase (from 0.12 close to the source to ~ 2.3 in a few km distance).

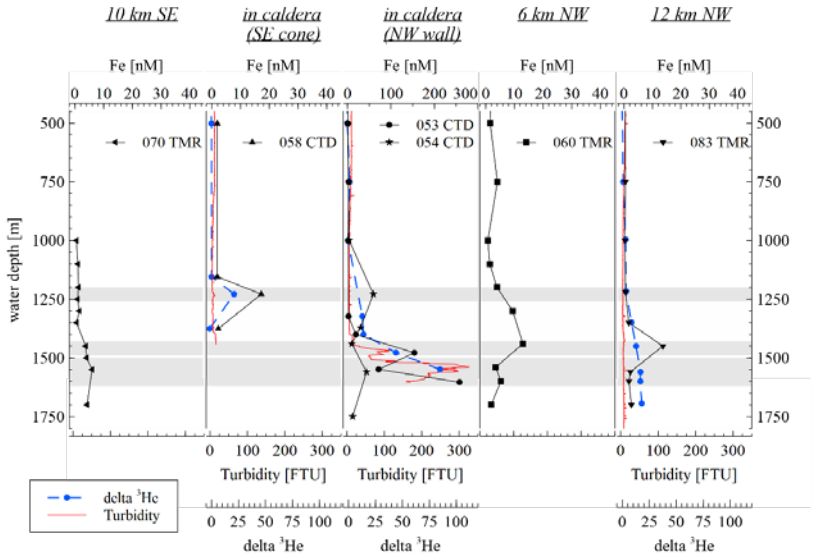

Fig. 2: Dissolved Fe concentrations for different CTD casts over the Brothers volcano together with delta 3He and turbidity data. No helium and turbidity data are available for TMR casts (070 TMR and 060 TMR). Turbidity and helium data shown for 083 TMR were taken from an equivalent CTD cast (082 CTD) at the same position. The grey areas indicate plume depths. From: Neuholz et al., submitted to Frontiers in Marine Science.

It is known that hydrothemal Fe is stabilized in its dissolved form by organic and inorganic ligands or in nanoparticular form and may thereby be transported over long distances, contributing to the global oceanic Fe cycle. At Macauley, the persistence of a distinct Zn plume signal with distance from the source may be due to higher solubility of Zn and possible additional stabilization through organic complexes. likely. Similar trends for Fe and Zn were also observed at Brothers Volcano, where multiple plume depths could be characerized (Figure 2) and traced over 12 km. As Brothers Volcano is located in a deeper water depth (~1600 m) compared to Macauley (~300 m), a transport of hydrothermally derived trace metals from Brothers into the photic zone is not very Our

data show how highly diverse and variable island arc systems can be with respect to their fluid chemistry, both spatially and temporally. The higher range in fluid chemistry together with shallower water depth implies that the fluids from intraoceanic arcs may contribute a significant fraction of dissolved metals (especially for Fe and Zn) not only to the global oceanic biogeochemical cycle but also into the photic zone, the area of highest bioproductivity (as seen for Macauley).

REFERENCES

Kleint et al. (2019): Geochemical characterization of highly diverse hydrothermal fluids from volcanic vent systems of the Kermadec intraoceanic arc. Chemical Geology 528. doi: 10.1016/j.chemgeo.2019.119289

Neuholz et al. (2019): Near-field hydrothermal plume dynamics at Brothers Volcano (Kermadec Arc): A short-lived radium isotope study. Chemical Geology. doi: 10.1016/j.chemgeo.2019.119379

SO253*

MAGMATIC DEGASSING AND PHASE SEPARATION ARE THE MAIN PROCESSES SHAPING THE COMPOSITION OF HYDROTHERMAL FLUIDS IN THE SOUTH KERMADEC ARC

AUTHORS

Faculty of Geosciences, University of Bremen | Bremen, Germany
A. Diehl, W. Bach

MARUM Center for Marine Environmental Sciences, University of Bremen | Bremen, Germany
A. Diehl, C. Kleint, A. Koschinsky, W. Bach

GNS Science | New Zealand
C.E.J. deRonde, V. Stucker

Woods Hole Oceanographic Institute | Woods Hole (MA), USA
S. E. Humphris, J. S. Seewald

Jacobs University Bremen | Bremen, Germany
C. Kleint, A. Koschinsky

University Münster | Münster, Germany
H. Strauss

During cruise SO253 three hydrothermally active volcanoes along the south Kermadec arc have been sampled for volcanic rocks, high-temperature hydrothermal fluids and hydrothermal precipitates. The three volcanoes Brothers, Haungaroa and Macauley (Figure 1) are great examples to illustrate the diversity of arc hydrothermal fluids and different subsurface processes affecting their compositions and mineralization in these arc environments.

Brothers volcano hosts the two hydrothermal endmember types of high-temperature hydrothermal fluids found along arcs (seawater-dominated and acid-sulfate type), in close proximity. Vent fluids have been sampled by us during two expeditions (SO253, German and TN350, US) using isobaric gas tight samplers (Seewald et al. 2001). The systematics of these components show that the two hydrothermal systems at Brothers volcano (NW Caldera and Cone sites) vent fluids with strongly different chemical compositions. At northwest Caldera, fluids are relatively rich in H_2, CH_4, CO_2 and H_2S. The Cone sites are extremely poor in H_2 and CH_4, but extremely rich in CO_2 and H_2S.

For the NW caldera a clear correlation between Cl and dissolved volatiles (best for CO_2) shows a trend of phase separation as a result of rising fluids undergoing boiling (Fig. 1). Furthermore, H_2 activities for most fluids do not match the most common buffer reactions that usually control the H_2 concentrations in hydrothermal reaction zones (Fig. 2). This mismatch can most plausibly be attributed to the influence of phase separation, which changes the gas concentrations in the rising fluids. found to be considerably below the boiling curve. Microthermometric investigations of fluid inclusions of samples from the NW Caldera confirm the impression gained from vent fluid compositions and give a broader range of salinities and temperatures than the fluid samples do. Inclusions record a wider spectrum of salinities, from nearly 0 to about 8 wt. % NaCl eq. and temperatures of 220 to 352°C (i. e. the boiling temperature at the ambient pressure of the vent sites). Most saline fluid inclusions may be produced by the mobilization of sequestered brines that are mobilized after the Caldera collapsed (deRonde et al. 2019). These findings suggest that most of the fluids at the NW Caldera are presently boiling at depth within the Caldera wall and mixing with seawater must occur at shallower depths.

Volatile concentrations at the Cone sites of Brothers volcano tell a story of magmatic degassing. Concentrations of CO_2 and H_2S do neither correlate with Mg (as tracer for seawater mixing), nor with Cl (as tracer for phase separation, cf. Figure 3). The resulting conclusion is that these species are directly produced by the degassing of volatiles from a magmatic source. Thermodynamic reaction path model show that the contribution of CO_2 and SO_2 to the reaction zone can explain a broad spectrum of the chemical properties of the Cone fluids (especially the Upper Cone). Adding SO_2 to the reaction zone makes the fluid become extremely acidic (pH<<2), rich in SO_4 and Mg (Fig. 3). High Al and Zn concentrations found in these fluids (Kleint et al. 2019) are predicted by the model. These hydrothermal systems are hence directly linked to the export of metals into the ocean.

The rare earth elements (REE) data of the fluids (Kleint et al., 2019) could also be explained using thermodynamic reaction path models (Fig. 4). The flat REE pattern typical for acid-sulfate type fluids is a consequence of element speciation and their resulting solubilities. The acidic and more oxidizing conditions in acid-sulfate type fluids lead to a predominance of sulfate-complexed or free REE. Under these conditions all REE show a similar solubility behavior. This speciation results in the typical unfractionated – and hence flat – REE patterns for acid-sulfate type hydrothermal fluids found at Brothers Cones and Macauley. In the seawater-dominated systems of NW Caldera at Brothers volcano und Huangaroa, the light REE are clearly Cl-complexed, whereas heavy REE tend to be sulfate- or hydroxy-complexed. Eu stands out by being exclusively chloro-complexed due to the exceptional stability of the $[EuCl_4]^{2-}$ complex in these fluids. This behavior leads to enrichments in light REE and depletions in heavy REE and the pronounced Eu anomaly for black-smoker type (seawater-dominated) systems found at Brothers NW Caldera and Haungaroa volcano (Fig. 4).

Overall our investigations demonstrate that the degassing of magmatic volatiles and phase separation processes in intraoceanic arc hydrothermal systems create a chemical diversity in

hydrothermal fluids that is not displayed by hydrothermal systems hosted in mid-ocean ridge settings. Besides water-rock reactions, phase separation and magma degassing both exert a primary control on vent fluid composition. The latter dominates compositions of vent systems hosted in resurgent domes at Brothers and Macauley volcanoes. Tectonically controlled settings (here: NW Caldera) lack this magmatic degassive influx. For estimates of the global relevance of these arc hydrothermal systems in global element budgets between the ocean and the lithosphere an improved understanding of the relative frequency of the two types of systems is required.

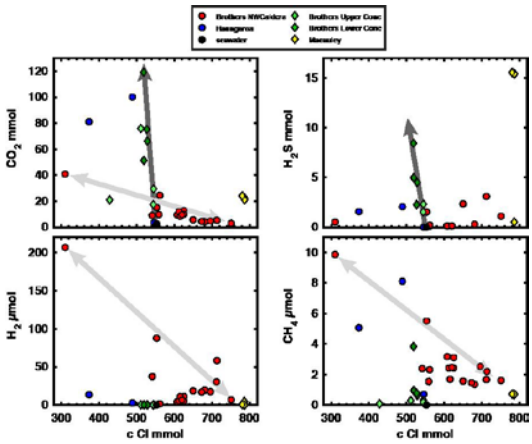

Fig. 1: Covariation of volatiles and Cl for the vent fluids. Negative slopes indicate enrichment or depletion due to phase separation (indicated by the light grey arrows). The dark grey arrows show the trend for the Cone sites. Major changes in H_2S and CO_2 that barely affect Cl hints to the addition of magmatic volatiles.

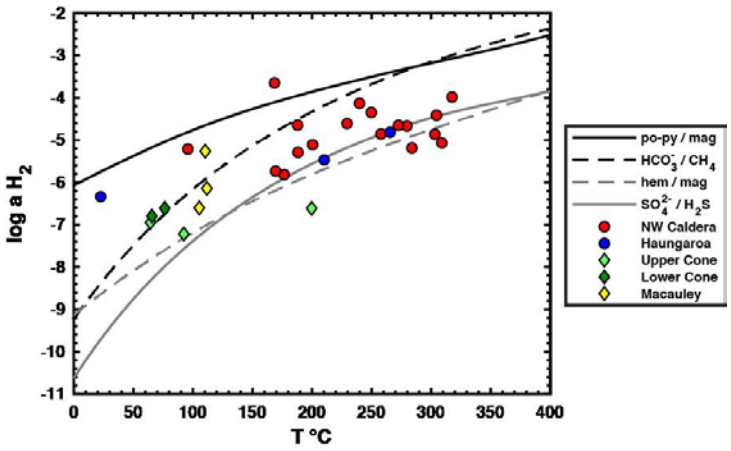

Fig. 2: H_2 activity in hydrothermal fluids plotted with equilibrium activities of potential subsurface buffer reactions that often control H_2 activities. Some vent fluids from Haungaroa Brothers NW caldera plot along the equilibrium activity of the sulfate/sulfide reaction. Acid sulfate-type fluids and most other fluids rather scatter around the different equilibrium activities suggesting that redox in these systems is not fully buffered by water-rock reactions

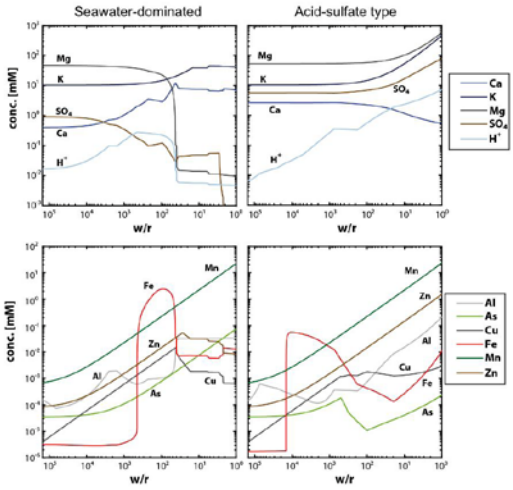

Fig. 3: Modelled fluid chemistry in the reaction zone for fluids with- and without contribution of magmatic volatiles (SO_2). Seawater-dominated systems are depleted in SO_4 and Mg and are moderately acidic, whereas volatile-influenced systems develop high concentrations of Mg and SO_4 and are extremely acidic. Note how acid sulfate type fluids effectively mobilize Al and Zn at low water-rock ratios.

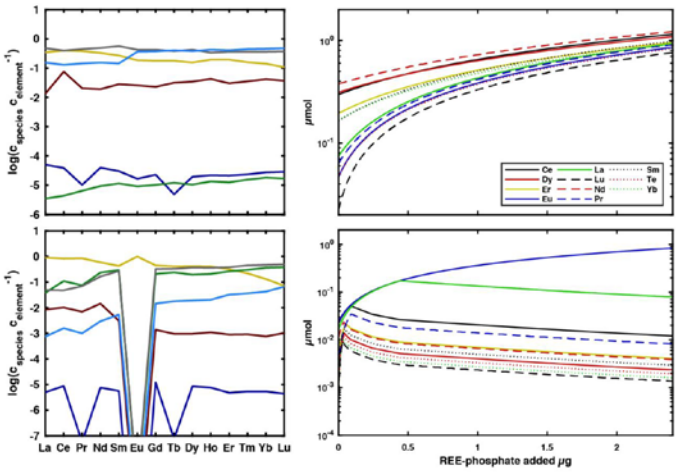

Fig. 4: REE speciation and solubility of seawater-dominated and acid-sulfate type fluids. The fluid chemistry controlls the speciation of REE which in turns controlls their solubility. This shows that REE patterns can indeed be used as indicators for a contribution of magmatic volatiles (especially SO_2)

REFERENCES

Kleint C, Bach, B, Diehl A, Fröhberg N, Garbe-Schönberg D, Hartmann J F, de Ronde C E J, Sander S G, Strauss H, Stucker V K, Thal J, Zitoun R, Koschinsky A, Geochemical characterization of highly diverse hydrothermal fluids from volcanic vent systems of the Kermadec intraoceanic arc, Chemical Geology 528 (2019) 119289, doi: 10.1016/j.chemgeo.2019.119289.

SO253*

CHEMOSYNTHETIC BIVALVE SYMBIOSES FROM HYDROTHERMAL VENTS IN THE KERMADEC ARC

AUTHORS

Max Planck Institute for Marine Microbiology | Bremen, Germany
C. Borowski, M. Ücker, N. Leisch

Institute for Geology and Paleontology, Westfälische Wilhelms-Universität | Münster, Germany
H. Strauß

Kermadec Arc hydrothermal vents occur in a wide depth range between 300 m to > 1500 m, and bathymodioline mussels living in symbiosis with chemosynthetic bacteria are dominant fauna at these vents. Little is known about species compositions and the nature of mussel symbioses in different water depths and along the volcanic arc.

We collected three mussel species at the four submarine volcanoes Macauley, Haungaroa, Brothers and Rumble III along 660 km of the Kermadec arc: Gigantidas gladius had a wide distribution range from Macauley to Rumble III in shallow to intermediate water depths (300–700 m). Vulcanidas insolatus was limited to shallow waters (300 m) at the Macauley Cone volcano, while Bathymodiolus manusensis occurred only in intermediate and greater water depths (700–1500 m) at Haungaroa and Brothers. Each of these mussel species is associated with species-specific endosymbiotic sulfur-oxidizing SUP05 bacteria in their gills. G. gladius and B. manusensis additionally regularly harbored spirochetes in their gill cells. Similar bacteria have not been observed in other vent and seep mussels, and preliminary metagenomic data suggest these spirochetes are heterotrophic and host-specific intracellular parasites.

Stable carbon isotope signatures of mussel tissues from all three host species ranged in the so called "30‰ group" of vent mussels that live in symbiosis with sulfur-oxidizing bacteria. This indicated all three Kermadec species primarily rely on chemosynthetic primary production of their symbionts, and phototrophically produced carbon does not play a significant role in their nutrition even in shallow water depths. Sulfur isotopic signatures in tissues matched those of the hydrothermal fluids or were even more depleted in 34S suggesting sulfur cycling by the bacteria.

SO253*

VARIABILITY OF DISSOLVED ORGANIC MATTER IN SELECTED HYDROTHERMAL VENTS FROM THE KERMADEC ARC

AUTHORS

Institute for Chemistry and Biology of the Marine Environment (ICBM), Carl von Ossietzky University of Oldenburg | Oldenburg, Germany
C. Oster, C. T. Hansen, T. Dittmar

MARUM – Center for Marine Environmental Sciences Bremen, Germany
C. Oster, C. T. Hansen

Helmholtz Institute for Functional Marine Biodiversity at the University of Oldenburg (HIFMB) | Oldenbrug, Germany
T. Dittmar

Marine dissolved organic matter (DOM) constitutes a major reservoir of reduced carbon in the world's oceans and it is of key importance for the global carbon cycle and marine heterotroph life (Dittmar and Stubbins, 2014; Hansell et al., 2009). While DOM represents a highly complex mixture of hundreds of thousands of different molecular compounds, a major fraction of the DOM that accumulated in the deep ocean today appears to resist degradation in context of thermohaline circulation and by heterotroph microorganisms (Carlson and Hansell, 2015; Jiao et al., 2010; Zark et al., 2017). Recent studies showed that thermal degradation within hydrothermal systems can be a major think for this recalcitrant DOM fraction, effectively controlling the long-term stability of the marine DOM budget (Hawkes et al., 2015). Experiments could further demonstrate that the subjection to elevated temperatures results in a major compositional modification of DOM, even returning fractions of it accessible to marine microbes (Hansen et al., 2019; Hawkes et al., 2016). In addition, hydrothermal DOM involving organic complexation is likely a key mechanism in supplying essential trace elements to marine life in the open ocean (Sander and Koschinsky, 2011). Despite this significance, very few studies exist that characterize natural hydrothermal vent derived DOM on a molecular level (Rossel et al., 2017).

This study covers a unique sample set of hydrothermal vent fluids from the Kermadec Arc acquired during an RV Sonne expedition in 2017 (SO253). The Tonga-Kermadec Arc trench-ridge system is associated with the subduction of the Pacific plate under the Australian plate which gives rise to strong magmatic and hydrothermal activity in the region (de Ronde and Stucker, 2015). Hydrothermal vent fields associated with the four active volcanoes Macauley, Haungaroa, Brothers and Rumble III were sampled for

diffuse and focused fluids utilizing the remotely operated vehicle (ROV) MARUM QUEST 4000. Sub-samples were taken for quantification of dissolved organic carbon (DOC) and for a solid-phase extraction procedure that enabled a detailed characterization of this SPE-DOM fraction on molecular level via Fourier-Transform Ion Cyclotron Resonance Mass Spectrometry (FT-ICR-MS). The DOM related data was then investigated in context of additional physical and chemical fluid characteristics to evaluate how DOM composition varies with variable hydrothermal fluid contribution and between the different sites along the Kermadec Arc.

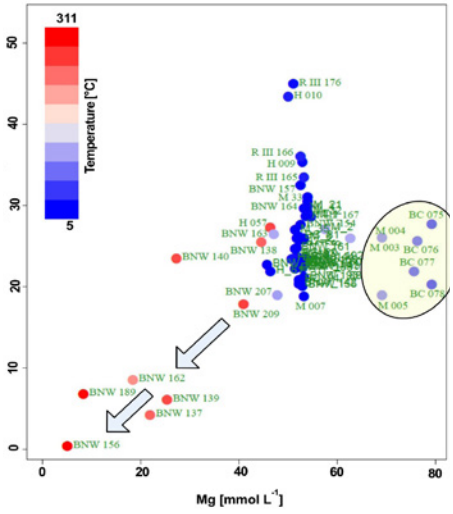

Fig. 1: Variability of fluid samples with respect to SPE-DOC in relation to Magnesium content and measured in-situ fluid temperature (BNW – Brothers North West Caldera, BC – Brothers Cone, M – Macauley, H – Haungaroa, R – Rumble III).

While bulk DOC concentrations are highly variable (14.4–450 µmol L^{-1}), especially at the shallow Macauley and Rumble III site, a major fraction of this variability is likely due to very labile unextractable compounds that are not further characterizable by FT-ICR-MS. Looking at the variability of the solid-phase extractable fraction (SPE-DOM), which is also much less prone to contamination, provided first clues on the key differences between the different sites. Magnesium concentrations were used as an indicator for the degree of hydrothermal contribution to the fluid sample. Most of the samples reveal to be highly diluted with ambient seawater, exhibiting Mg concentrations close to 53 mmol L^{-1}. But in agreement with an expected thermal degradation of SPE-DOM within hydrothermal systems, hot fluids from the North West Caldera of Brothers follow a correlation between decreasing Mg and SPE-DOC concentrations. In contrast, SPE-DOC concentrations in multiple samples from the Macauley and Brothers Lower Cone sites, characterized by elevated Mg concentrations at elevated temperatures, appeared to be undistinguishable from less hydrothermally influenced samples from the same sites (Fig. 1).

Detailed molecular characterization of SPE-DOM via FT-ICR-MS revealed a highly variable DOM composition within the samples from the Kermadec Arc. Multivariate statistics were used to further separate the samples into different groups that shared certain characteristics. One group of samples from Brothers North West Caldera and Upper Cone site as well as Haungaroa followed a more typical pattern of decreasing SPE-DOC concentrations with decreasing Mg. This group was characterized by a lower total number of molecular formulae detected in the sample with increasing hydrothermal contribution. Moreover, the compounds in these samples had a lower average mass, lower O/C and H/C ratios and showed a higher average degree of unsaturation. In contrast the Brothers Lower Cone and Macauley samples with elevated Mg concentrations exhibited reduced H/C ratios with increasing hydrothermal contribution, which might be related to phase separation affecting these fluids (Kleint et al., 2019). Overall the investigation confirms that thermal degradation results in high molecular weight compounds being successively reduced to low molecular weight compounds and that oxygen-containing functional groups are preferentially removed in the process. The variability of DOM composition between the different sites is also predominantly controlled by the degree of dilution of the sample.

REFERENCES

Carlson, C.A., Hansell, D.A., 2015. Biogeochemistry of Marine Dissolved Organic Matter, 2nd ed, Biogeochemistry of Marine Dissolved Organic Matter. Elsevier.

de Ronde, C.E.J., Stucker, V.K., 2015. Seafloor Hydrothermal Venting at Volcanic Arcs and Backarcs, in: The Encyclopedia of Volcanoes. Elsevier, pp. 823–849.

Dittmar, T., Stubbins, A., 2014. Dissolved Organic Matter in Aquatic Systems, in: Treatise on Geochemistry. Elsevier, pp. 125–156.

Hansell, D.A., Carlson, C.A., Repeta, D.J., Schlitzer, R., 2009. Dissolved Organic Matter in the Ocean A Controversy Stimulates New Insights. Oceanography 22, 202–211.

Hansen, C.T., Niggemann, J., Giebel, H.A., Simon, M., Bach, W., Dittmar, T., 2019. Biodegradability of hydrothermally altered deep-sea dissolved organic matter. Mar. Chem. 217, 103706.

Hawkes, J.A., Hansen, C.T., Goldhammer, T., Bach, W., Dittmar, T., 2016. Molecular alteration of marine dissolved organic matter under experimental hydrothermal conditions. Geochim. Cosmochim. Acta 175, 68–85.

Hawkes, J.A., Rossel, P.E., Stubbins, A., Butterfield, D., Connelly, D.P., Achterberg, E.P., Koschinsky, A., Chavagnac, V., Hansen, C.T., Bach, W., Dittmar, T., 2015. Efficient removal of recalcitrant deep-ocean dissolved organic matter during hydrothermal circulation. Nat. Geosci. 8, 856–860.

Jiao, N., Herndl, G.J., Hansell, D.A., Benner, R., Kattner, G., Wilhelm, S.W., Kirchman, D.L., Weinbauer, M.G., Luo, T., Chen, F., Azam, F., 2010. Microbial production of recalcitrant dissolved organic matter: Long-term carbon storage in the global ocean. Nat. Rev. Microbiol. 8, 593–599.

Kleint, C., Bach, W., Diehl, A., Fröhberg, N., Garbe-Schönberg, D., Hartmann, J.F., de Ronde, C.E.J., Sander, S.G., Strauss, H., Stucker, V.K., Thal, J., Zitoun, R., Koschinsky, A., 2019. Geochemical characterization of highly diverse hydrothermal fluids from volcanic vent systems of the Kermadec intraoceanic arc. Chem. Geol. 528, 119289.

Rossel, P.E., Stubbins, A., Rebling, T., Koschinsky, A., Hawkes, J.A., Dittmar, T., 2017. Thermally altered marine dissolved organic matter in hydrothermal fluids. Org. Geochem. 110, 73–86.

Sander, S.G., Koschinsky, A., 2011. Metal flux from hydrothermal vents increased by organic complexation. Nat. Geosci. 4, 145–150.

Zark, M., Christoffers, J., Dittmar, T., 2017. Molecular properties of deep-sea dissolved organic matter are predictable by the central limit theorem: Evidence from tandem FT-ICR-MS. Mar. Chem. 191, 9–15.

SO253*

MICROBIAL ECOLOGY OF PLUME COMMUNITIES AT THE KERMADEC INTRAOCEANIC ARC

AUTHORS

Max Planck Institute for Marine Microbiology | Bremen, Germany
B. Dede, R. Amann, A. Meyerdierks

Department of Chemistry, University of Otago | Dunedin, New Zealand
R. Zitoun, S. Sander

National Institute for Water and Atmospheric (NIWA)/University of Otago Research Centre for Oceanography | Dunedin, New Zealand
R. Zitoun

Marine Environmental Studies Laboratory, IAEA Environment Laboratories, Department of Nuclear Science and Applications, International Atomic Energy Agency | Monaco, Principality of Monaco
S. Sander

Department of Geosciences, University of Bremen | Bremen, Germany
A. Türke, W. Bach

Department of Geosciences, Jacobs University | Bremen, Germany
C. Kleint, A. Koschinsky

NOAA/Pacific Marine Environmental Laboratory | Seattle (WA), USA
S. L. Walker

Hydrothermal vents are highly dynamic sources of energy in the deep sea. Recent studies have uncovered that the depletion of chemically rich fluids leads to spatio-temporal succession across tens of kilometers. However, the microbial diversity along these gradients and their metabolic potential is yet not fully resolved. In our interdisciplinary approach, we focused on microbial communities inhabiting hydrothermal plumes at four hydrothermally active submarine volcanos at the Kermadec Arc (South Pacific), characterized by different physical and geochemical conditions. At some vent sites, the microorganisms had already been characterized before (e. g. Brothers), others (Haungaroa, Rumble III) had been visited for the first time with a ROV on SO253 for targeted microbial sampling. Primary goal with respect to our cultivation-independent

analyses was to investigate microbial community compositions and to understand the relationship between community structure and function considering the background of the present fluid chemistry.

Apart from common inhabitants of the meso- and bathypelagial, a comparative 16S rRNA gene diversity analysis of plume samples especially revealed a high proportion of SUP05-clade bacteria in plumes at Brothers and Macauley volcano, verified by fluorescence in situ hybridization. The occurrence of this group, known for sulfur oxidation at hydrothermal vents, was in general not surprising. However, the high abundance, especially in iron rich plumes was striking. Statistical analysis, including geochemical data, supported the hypothesis that the occurrence of SUP05-clade bacteria may depend on the iron concentration. Phylogenetic analyses verified that two different subclades were present at Brothers and Macauley volcano. In order to analyse the genomic potential of these SUP05-clade bacteria, metagenomes of both plumes were sequenced and assembled. Targeted re-assembly of these metagenomes led to six 75–91 % complete genomic SUP05 bins. Apart from genes for proteins known to be involved, e. g. , in sulfur oxidation reactions, several genes for cytochromes were identified. A clear support for the capability of SUP05 to oxidize iron was not found, may be due to the still limited knowledge about this process. Nevertheless, the high fraction of genes encoding cytochromes in Macauley metagenomes compared to other metagenomes from hydrothermal vents underlines the relevance of iron in these habitats and will be further investigated.

SO253*
NOBLE GAS ISOTOPES AT THE KERMADEC ARC

AUTHORS

MARUM – Center for Marine Environmental Sciences, Universität Bremen | Bremen, Germany
M. Walter, A. Türke, J. Thal

Institute of Environmental Physics, Universitöt Bremen | Bremen, Germany
M. Walter, J. Sültenfuß

Department of Geosciences, Universität Bremen | Bremen, Germany
A. Türke, J. Thal

Institute for Chemistry and Biology of the Marine Environment (ICBM), Carl von Ossietzky Universität Oldenburg | Oldenburg, Germany
R. Neuholz, B. Schnetger

Department of Marine Sciences, GNS Science | New Zealand
C. de Ronde

NOAA/PMEL | Seattle (WA), USA
S. Walker

Primordial helium is one of the gases carried from the Earths' mantle into the ocean by hydrothermal fluids, thus hydrothermal fluids and plumes are highly enriched in helium, especially the isotope ^{3}He. The isotopic signature, the ^{3}He/^{4}He ratio, of primordial helium is significantly different from the atmospheric ratio, and can be identified with high precision in water samples. Commonly used to describe the excess ^{3}He is the parameter δ^3He, that is defined by the isotopic ratio R=^{3}He/^{4}He compared to the atmospheric ratio, RA (δ^3He = 100[(R/RA)-1] in %). As a noble gas, the concentration of helium in the sea water is only altered by physical processes as mixing, not by biological and chemical reactions or processes. Therefore, the isotopic signature of helium can be used to identify and track the output of hydrothermal fields.

During the RV Sonne expedition SO253 (Dec 2016–Jan 2107), we sampled the noble gas signature of several chemically diverse hydrothermal systems along the Kermadec arc (SW Pacific), including Macauley, Rumble III, Haungaroa, and Brothers volcano. The 100+ samples come from the water column plumes of the systems taken with a CTD/

water sampling system as well as from less diluted samples collected with an ROV based sampling device typically 1m above the vents. The noble gas samples have been taken with copper tubes, sealed air-tight with aluminium clamps and measured post-cruise in the Bremen MSS lab helis, using a combined QMS/SMS (Sültenfuß et al., 2009). In addition to the noble gas samples, radium isotopes have been determined from the same samples at Uni Oldenburg (Neuholz et al., 2019).

Island arcs exhibit considerable more variability in fluid composition than mid-oceanic ridge systems. At the Kermadec arc, especially Brothers volcano, multiple expeditions over the past two decades have lead to a large data base with regard to the fluid composition and its temporal evolution, indicative of changes in the underlying hydrothermal systems (de Ronde et al., 2001, 2005, 2007, 2011). At Brothers volcano, we thus extended the existing time series of helium isotopes that have been intermittently sampled since the late 1990s.

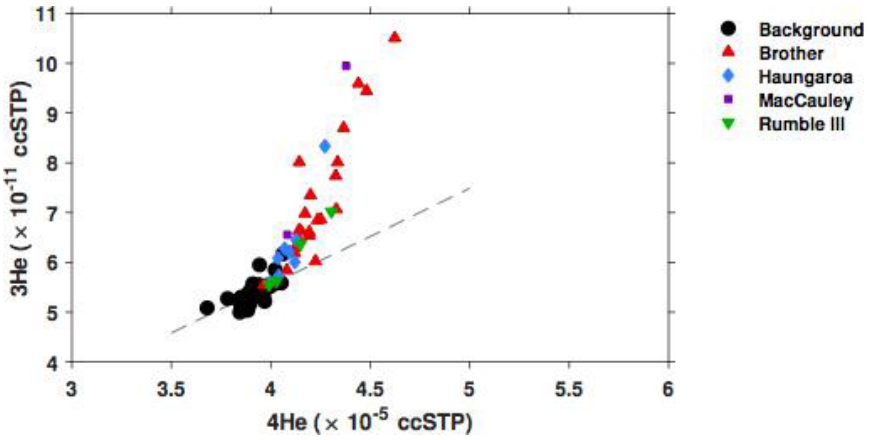

Fig. 1: ^{3}He and ^{4}He concentration from four Kermadec volcanoes. Also shown is the typical ratio for seawater (dashed).

The $^{3}He/^{4}He$ ratios at the volcanoes vary between 5.8 and 6.5 Ra. The maximum observed δ3He at the non-buoyant plume level are for Rumble III 90 %, Haungaroa 83 %, Macauley Cone site 144 %, Macauley Caldera site 16 %, Brothers Cone site 56 %, Brothers NW Caldera site 94 %. Comparison with the previously existing data sets shows in addition to this variability between individual systems a considerable amount of temporal variability. While the systems at Brothers and the Macauley Caldera site appear to be relatively stable since the late 1990s/early 2000s (de Ronde et a., 2005; 2011), the $\delta^{3}He$ at Macauley Cone has increased by a factor of 10 since the observations during the NZASRoF expedition in 2005 (de Ronde et al., 2007). This site also showed the highest recorded $\delta^{3}He$ of 445 % in a weakly diluted sample (pH = 5.0) from rising plume, less than 1m above the vent.

REFERENCES

de Ronde CEJ, et al. (2001) Intra-oceanic subduction-related hydrothermal venting, Kermadec volcanic arc, New Zealand. Earth Planet. Sci. Lett. 193, 359–369.

de Ronde CEJ, et al. (2005) Evolution of a submarine magmatic-hydrothermal system: Brothers volcano, southern Kermadec arc, New Zealand. Econ. Geol. 100, 1097–1133.

de Ronde CEJ, et al (2007) Submarine hydrothermal activity along the Mid-Kermadec Arc, New Zealand: Large-scale effects on venting. Geochem. Geophys. Geosyst. 8 (7), Q07007, doi:10.1029/2006GC001495.

de Ronde CEJ, et al. (2011) Submarine hydrothermal activity and gold-rich mineralization at Brothers volcano, Kermadec arc, New Zealand. Miner. Deposita 46, 541–584, doi:10.1007/s00126-011-0345-8.

Neuholz R, Schnetger B, Kleint C, Koschinsky-Fritsche A, Sander S, Türke A, Walter M, Zitoun R, Brumsack H-J (2019), Near-field hydrothermal plume dynamics at Brothers volcano (Kermadec arc): A short-lived radium isotope study. Chem. Geol., doi:10.1016/j.chemgeo.2019.119379.

Sültenfuß J, Rhein M, Roether W (2009) The Bremen mass spectrometric facility for the measurement of helium isotopes, neon, and tritium in water. Isotopes Environ. Health Stud. 45 (2) ,1–13

SO254

TAXONOMY, MICROBIAL AND CHEMICAL ECOLOGY OF BENTHIC DEEP-WATER INVERTEBRATES AROUND NEW ZEALAND – SONNE CRUISE SO254

AUTHORS

Carl-von-Ossietzky University Oldenburg, Institute for Chemistry and Biology of the Marine Environment (ICBM) | Wilhelmshaven, Germany
P. J. Schupp, S. Rohde, G. Steinert, M. Kellermann, A.-L. Böger, D. Versluis

Helmholtz Institute for Functional Marine Biodiversity at the University of Oldenburg (HIFMB) | Oldenburg, Germany
P. J. Schupp

GEOMAR Helmholtz Centre for Ocean Research Kiel, Marine Symbioses | Kiel, Germany
K. Busch, K. Bayer, S. Kodami, U. Hentschel

Senckenberg am Meer, German Center for Marine Biodiversity Research | Wilhelmshaven, Germany
P. Martinez Arbizu

National Institute of Water and Atmospheric Research Ltd | Auckland, New Zealand
M. Kelly

National Institute of Water and Atmospheric Research Ltd | Wellington, New Zealand
S. Mills

Department of Earth and Environmental Sciences, Paleontology & Geobiology, Ludwig-Maximilians-Universität München | München, Germany
D. Erpenbeck, G. Wörheide

SNSB-Bayerische Staatssammlung für Paläontologie und Geologie | München, Germany
M. Dohrmann, G. Wörheide

GeoBio-Center, Ludwig-Maximilians-Universität München | München, Germany
D. Erpenbeck, G. Wörheide

Christian-Albrechts University of Kiel | Kiel, Germany
C. de Ronde, G. Wörheide, U. Hentschel

One aim of the Sonne cruise SO254 was to assess the biodiversity of benthic invertebrates, including the chemical and microbial diversity associated with the collected invertebrates. One focus group during the collections were deep-water sponges. Collected sponges included 102 Hexactinellida and 101 Demospongiae specimens. Sponges were identified traditionally using morphology and spiculae composition as well as genetically by using the 16s RNA gene and 18S & 28S rDNA and the mitochondrial COI gene. Analysis of the Hexactinellida specimens revealed 3 new genera and 19 new species, while analysis of the molecular data from the Demospongiae indicated 4 new genera and 38 new species. In addition to sponges, numerous other smaller invertebrates associated with the invertebrates are also being described, several as new species, emphasizing that deep-sea benthic communities represent large unexplored biodiversity hotspots.

Associated sponge microbial communities were analyzed in the subset of thirteen phylogenetically diverse sponge species (Demospongiae and Hexactinellida) by 16S rRNA-gene amplicon sequencing. Additionally, the associated bacteria and archaea were quantified by real-time qPCR. Results showed that the bacterial communities were host-species specific similar as to what has been observed for shallow-water demosponges. The archaeal community structures in the investigated deep-sea sponges were different from the bacterial community structures in that they were almost completely dominated by a single family (ammonia-oxidizing genera within the Nitrosopumilaceae). Interestingly, the archaeal communities were rather specific to individual sponges and not sponge-species. The quantitative real-time PCR experiments indicated archaeal numbers which were up to three orders of magnitude higher than in shallow-water sponges, highlighting the importance of archaea for deep-sea sponges in general.

In addition to sponge associated bacteria we also analyzed the microbiomes of deep-water sea cucumbers using 16S rRNA-gene amplicon sequencing. Results revealed that gut bacteriomes of deep-sea benthic and nektobenthic holothurians across different species were defined by core taxa but that local environmental factors (e. g. diet and temperature) play the largest role in shaping the gut bacteriome (Fig.1).

Chemical analyses have focused so far on the toxin production in the marine gastropod Pleurobranchaea maculata, which produced the potent neurotoxin tetrodotoxin. Furthermore, screening of the microbial culture collections from the deep-water sponges, see cucumber and sediments have so far shown only limited antimicrobial activities, but efforts to identify new pharmacologically active compounds are ongoing.

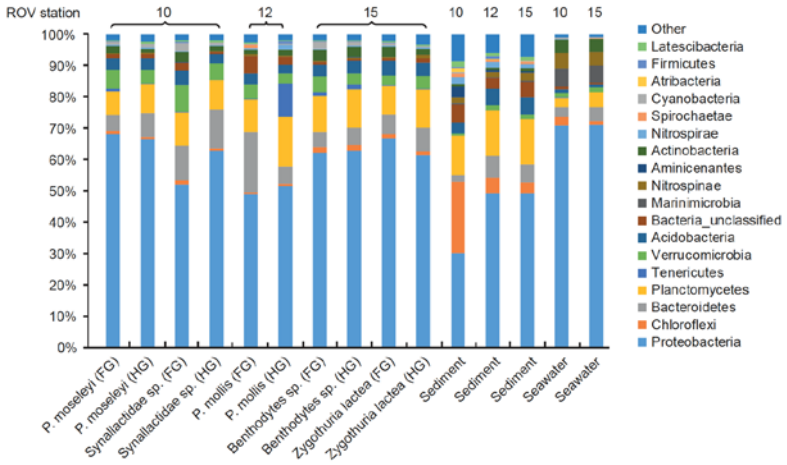

Fig. 1: The composite relative abundance profiles of the major bacterial phyla (>2%) in the sediment, seawater and the holothurian fore- and hindgut samples. FG = foregut. HG = hindgut.

SO254*

TAXONOMY AND PHYLOGENY OF GLASS SPONGES (PORIFERA: HEXACTINELLIDA) COLLECTED BY SONNE CRUISE SO254 IN THE SW PACIFIC OFF NEW ZEALAND

AUTHORS

Department of Earth and Environmental Sciences, Paleontology & Geobiology, Ludwig-Maximilians-Universität München | München, Germany
M. Dohrmann, S. Schätzle, G. Wörheide

Biology Department, University of Victoria, Natural History Section | Victoria, British Columbia, Canada
H. Resiwig

Coasts and Oceans National Centre, National Institute of Water & Atmospheric Research | Auckland, New Zealand
M. Kelly

Sadie Mills, NIWA Invertebrate Collection, National Institute of Water & Atmospheric Research, Evans Bay Parade | Wellington, New Zealand
S. Mills

GeoBio-CenterLMU, Ludwig-Maximilians-Universität München | München, Germany
C. de Ronde, G. Wörheide

SNSB – Bayerische Staatssammlung für Paläontologie und Geologie | München, Germany
S. Walker, G. Wörheide

ICBM Terramare, University of Oldenburg | Wilhelmshaven, Germany
S. Rohde, P. Schupp

ICBM Terramare, University of Oldenburg | Wilhelmshaven, Germany
P. Schupp

During cruise SO254 of R.V. SONNE in the SW Pacific around New Zealand (February 2017), 102 specimens of glass sponges (Porifera: Hexactinellida) were collected. Integrative taxonomic analysis using mitochondrial 16S rDNA sequencing and spicule

analysis revealed the presence of 40 species from 25 genera, 9 families, and 3 orders in this collection. Represented families were Aulocalycidae, Euplectellidae, Leucopsacidae, Rossellidae (Lyssacinosida); Aphrocallistidae, Euretidae, Farreidae (Sceptrulophora); Hyalonematidae, and Pheronematidae (Amphidiscosida). Of these, Euplectellidae was the most species-rich (15 spp.), followed by Rossellidae (9 spp.) and Farreidae (5 spp.); the remaining families were present with only 1–3 species. Overall, 19 species new to science were identified, which were distributed in 16 genera, including 3 new ones from the family Rossellidae. For further molecular phylogenetic analysis, nuclear 18S and 28S rRNA and mitochondrial COI gene fragments were sequenced from 37 selected species. The new sequences were added to established alignments from a previous study (Dohrmann 2019 Hydrobiologia 843:51), followed by analysis in Bayesian and Maximum-Likelihood frameworks. The greatly expanded taxon sampling allowed determining the phylogenetic position of 12 genera for the first time and further corroborated monophyly of all involved families. This was especially important for Aulocalycidae, which had so far only been sampled for 2 species. On genus level, monophyly of several taxa could be further confirmed, whereas some genera (such as the mega-diverse Farrea) were reconstructed paraphyletic, indicating the need for further taxonomic revisions. Overall, this study greatly enhances our understanding of glass sponge phylogeny and further underpins the recognition of New Zealand deep waters as a unique biodiversity hotspot of Hexactinellida.

SO254*

PRESENCE OF THE POTENT NEUROTOXIN TETRODOTOXIN IN THE GASTROPOD PLEUROBRANCHAEA MACULATA COLLECTED IN NEW ZEALAND'S MESOPELAGIC ZONE

AUTHORS

Carl-von-Ossietzky University Oldenburg, Institute for Chemistry and Biology of the Marine Environment (ICBM) | Wilhelmshaven, Germany
S. Rohde, A.-L. Böger, M. Y. Kellermann, P. Schupp

Helmholtz Institute for Functional Marine Biodiversity at the University of Oldenburg (HIFMB) | Oldenburg, Germany
H. Resiwig

The potent neurotoxin tetrodotoxin (TTX) is mostly known from and named after the order Tetraodontiformes, which includes the group of pufferfish. Although TTX was first isolated from these fish (Family Naticidae), it was also detected in other marine organisms, such as octopuses and snails. In 2009, tetrodotoxin was detected for the first time in the marine gastropod Pleurobranchaea maculata following a series of dog poisoning on beaches of New Zealand (McNabb et al. 2010).

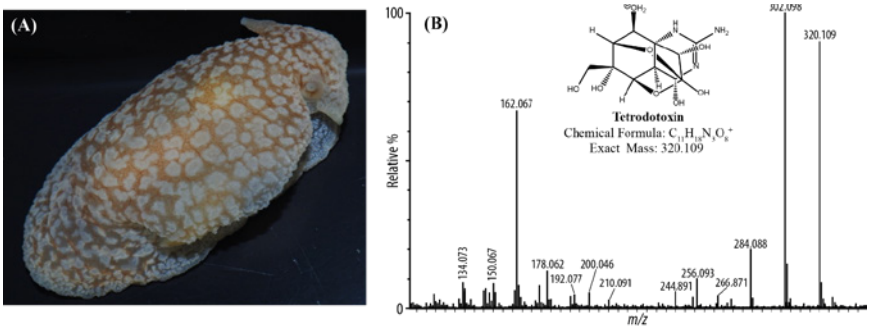

Fig. 1: Figure shows (A) the marine gastropod Pleurobranchaea maculata collected at a water depth of 851 m off the coast of Christchurch, New Zealand and (B) daughter ion mass spectra (MS2) of TTX (m/z = 320.109).

A follow up study revealed a high spatial variability of TTX concentrations in P. maculata (Wood et al. 2012). However, nearly all samples were collected from shallow water depths between 3–20 m. Only one specimen was collected from deep waters (290 m depth), which did not include TTX. Many authors support the hypothesis that metazoans incorporate TTX either through their food or by harboring TTX producing bacteria. Thus,

the absence of TTX in snails from the mesophotic zone could indicate the absence of a TTX producing diet or bacteria. On the cruise SO-254, we collected five snails at a water depth of 851 m off the coast of Christchurch, New Zealand. Specimens were directly frozen and stored at -80C until further processing. Prior to extractions sea slugs were dissected in organs and body parts and each was separately extracted and analyzed using a high resolution MALDI TOF Mass spectrometer (Waters Synapt G2). TTX concentrations were quantified to reveal variations of TTX among the different specimens and body parts. Additionally, molecular analyses of the snail's microbiome were conducted to provide indications of TTX origin. Clear evidence for TTX was found in four of the five sea slugs at concentrations ranging from 1.3 to 24.2 mg kg^{-1}. There were also significant differences between organs, with highest concentrations in the coelom and the extradermal mucus. The high TTX concentration at the body surface could indicate an ecological defensive function against predation. Even though bacteria associated with the production of TTX, like Vibrio tapetis, Alteromonas sp., Pseudomonas sp. and Pseudoalteromonas sp. were detected in all five sea slugs, we cannot conclude whether the toxin is of endogenous or exogenous origin. However, we could demonstrate for the first time that TTX is present in snails from the mesopelagic zone. Further studies are needed to reveal whether the occurrence of TTX in P. maculata involves symbiotic TTX-producing bacteria, toxin accumulation through the food chain, or if TTX is produced endogenously.

REFERENCES

McNabb P et al. (2010) Detection of tetrodotoxin from the grey side-gilled sea slug - Pleurobranchaea maculata, and associated dog neurotoxicosis on beaches adjacent to the Hauraki Gulf, Auckland, New Zealand. Toxicon 56:466–473

Wood SA, Taylor DI, McNabb P, Walker J, Adamson J, Cary SC (2012) Tetrodotoxin Concentrations in Pleurobranchaea maculata: Temporal, Spatial and Individual Variability from New Zealand Populations. Mar Drugs 10:16–176

SO254*

HYPERSPECTRAL LIGHT AVAILABILITY ACROSS AND ALONG THE PACIFIC OCEAN – FROM CHILE TO NEW ZEALAND AND UP TO ALASKA

AUTHORS

Institute for Chemistry and Biology of the Marine Environment (ICBM), University of Oldenburg | Oldenburg, Germany
O. Zielinski, R. Henkel, D. Meier, D. Voß

German Research Center for Artificial Intelligence (DFKI) | Oldenburg, Germany
O. Zielinski

The characterization of the underwater light field by in-situ observations is essential to develop and improve ocean color remote sensing algorithms as well as realistic aquatic light model parameterizations. In-situ measurements from profiling systems are commonly utilized, however, only a few datasets exist covering the Pacific Ocean, especially the southern Pacific and its gyre system. Here, surface waters are known to be the most oligotrophic and optically clearest in the global ocean. The underwater light field of the Pacific Ocean was observed on three cruises with R/V SONNE (2015–2017) by using a hyperspectral free-falling optical profiler covering the visible spectrum. We sampled waters from Antofagasta, Chile to Wellington, New Zealand (SO245, 2015) as well as waters around New Zealand down to 55° South (SO254, 2017) and from New Zealand to Dutch Harbour, Alaska USA (SO248, 2016). All cruises are illustrated in Figure 1.

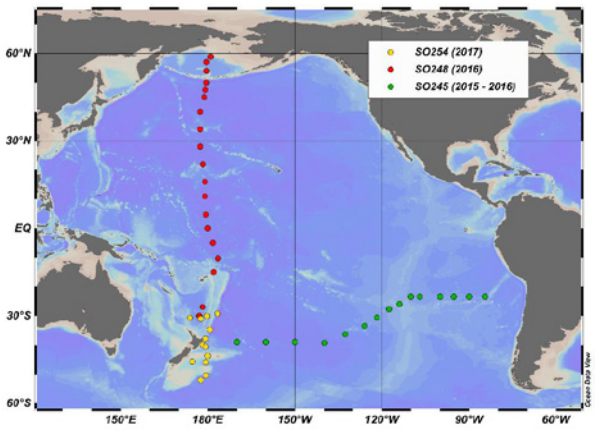

Fig.1: Cruise track of R/V Sonne cruise SO245, SO248, and SO254 covering the Pacific Ocean, stations are marked with dots, from Chile to New Zealand, around New Zealand, and from New Zealand to Alaska.

With this contribution we present a combined overview of all three R/V SONNE expeditions. The data along the meridional and zonal transect across the Pacific Ocean cover different water masses with a broad range of influencing parameters: from ultra-clear waters with deep chlorophyll maxima at 200 m depth, to temperate as well as cold near-shore and coastal waters with low light penetration depths and deep chlorophyll maxima around 30 m. Furthermore, we will connect these investigations with a study across the Pacific Ocean in 2019 (R/V SONNE SO267-2, from Suva, Fiji Islands to Manzanillo, Mexico) and highlight the observation with hyperspectral above-water radiometry and satellite data.

SO254*

ASSESSING THE COMPOSITION OF DISSOLVED ORGANIC MATTER ALONG THE PACIFIC CIRCULATION PATHWAY

AUTHORS

Institute for Chemistry and Biology of the Marine Environment (ICBM), Carl-von-Ossietzky University Oldenburg | Oldenburg, Germany
S. K. Bercovici, B. E. Noriega-Ortega, M. E. Heinrichs, H. Osterholz, T. Dittmar, J. Niggemann

Institute of Freshwater Ecology and Inland Fisheries (IGB) | Berlin, Germany
B. E. Noriega-Ortega

Leibniz Institute for Baltic Sea Research Warnemünde (IOW) | Rostock, Germany
H. Osterholz

Marine dissolved organic matter (DOM) is a complex and diverse mixture of organic molecules, with thousands of different compounds identified on a molecular level. As the carbon component of DOM comprises the largest standing stock of reduced carbon in the ocean and rivals the standing stock of atmospheric CO_2, it is important to determine the fate of this pool. While it is primarily produced in the surface ocean, the majority of DOM is stored at depth, where it is largely resistant to microbial attack and is transported along ocean currents, persisting for long timescales. One potential reason behind this recalcitrance is microbial processing and diversification. Microbial metabolites are highly diverse, and thus potentially generate and sustain the refractory nature of deep DOM. Assessing the molecular composition of DOM and how it changes with deep ocean mixing provides valuable information on the mechanisms that control persistence and fate of this important carbon pool.

Major Pacific ocean water masses were sampled along a South-North transect at 180° longitude during RV Sonne cruises SO248 (30°S–59°N) and SO254 (29°S–52°S). We amended the sample set with samples taken during RV Sonne cruise SO245 that crossed the South Pacific Gyre (Figure 1). The resulting unique sample set encompasses the major water masses of the Pacific Ocean (Figure 2). Dissolved organic matter was extracted on board via solid phase extraction (SPE; Dittmar et al. 2008) and the molecular composition of the extracted DOM was characterized via ultrahigh resolution mass spectrometry (Fourier Transform Ion Cyclotron Resonance Mass Spectrometry; FT-ICR-MS). This non-targeted analysis yields information on the relative abundance of more than 7000 different molecular formulae in each of the 485 analyzed DOM samples.

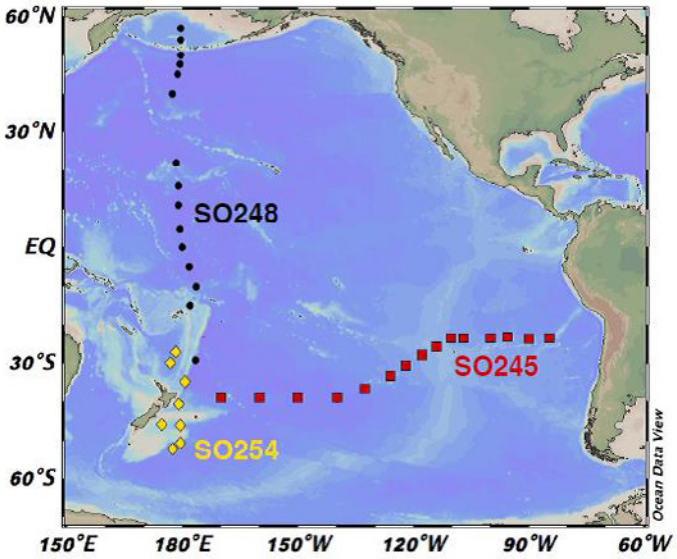

Fig. 1: Map of sampled stations during the SO248 (black dots), SO254 (yellow diamonds), and SO245 cruises (red squares).

The main research objectives of the cruises SO248 and SO254 focused on microbial ecology in different biogeographic provinces. DOM is the main carbon and energy source for heterotrophic microorganisms and as such strongly interlinked with the prevailing microbial communities. In surface waters (0–200 m), DOM composition partly reflected the physicochemical and microbiological differences of the biogeographic provinces. DOM from deeper water masses was much more similar in molecular composition and differences were mostly related to ageing and mixing of deep waters. Changes in molecular composition clearly indicated ongoing degradation of DOM as it migrates with deep Pacific currents. We applied a multiple regression approach to isolate those molecular formulae within DOM that track ocean mixing and define the characteristics of this conserved DOM. In order to assess the role of microorganisms in producing and sustaining DOM diversity, we scan the compounds detected in the Pacific DOM samples for potential microbial exometabolites. Approximately 15 to 20 % of molecular masses detected in bacterial exometabolomes (Noriega-Ortega et al. 2019) overlap with DOM from the deep Pacific. Tracing these metabolites within the deep Pacific ocean currents provides insights as to their persistence and fate relative to the bulk DOM pool.

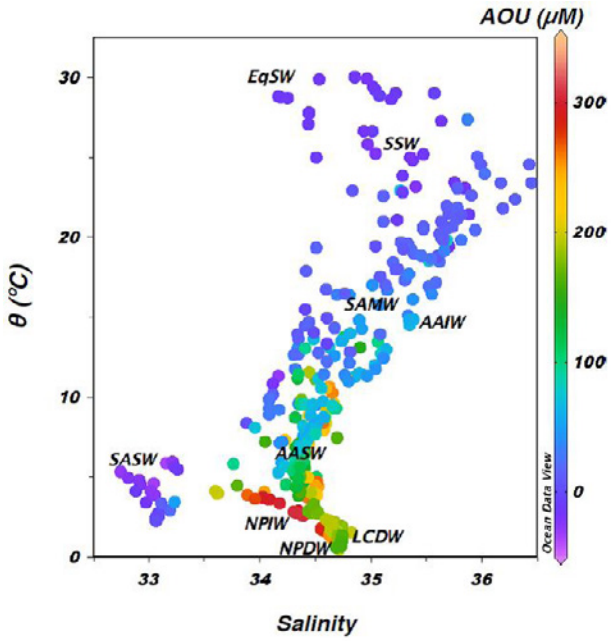

Fig. 2: Potential temperature (Θ, °C) vs. salinity, with apparent oxygen utilization (AOU, µM) in color. Each dot represents the characteristics of a DOM sample included in this study. AOU can be used as a semi-conservative tracer to distinguish water masses. The labeled water masses (black text) are Lower Circumpolar Deep Water (LCDW), North Pacific Deep Water (NPDW), North Pacific Intermediate Water (NPIW), Antarctic Intermediate Water (AAIW), Subantarctic Mode Water (SAMW), Antarctic Surface Water (AASW), Subtropical Surface water (SSW), Equatorial Surface Water (EqSW), and Subarctic Surface Water (SASW).

REFERENCES

Dittmar T, Koch BP, Hertkorn N, Kattner G, A simple and efficient method for the solid-phase extraction of dissolved organic matter (SPE-DOM) from seawater, Limnology and Oceanography Methods 2008, 6, 230–235, doi:10.4319/lom.2008.6.230.

Noriega-Ortega BE, Wienhausen G, Mentges A, Dittmar T, Simon M, Niggemann J, Does the chemodiversity of bacterial exometabolomes sustain the chemodiversity of marine dissolved organic matter? Frontiers in Microbiology, 2019, 10, 215, doi:10.3389/fmicb.2019.00215.

SO254*

MICROBIAL ABUNDANCE, DIVERSITY AND ACTIVITY IN PACIFIC DEEP-SEA SEDIMENTS

AUTHORS

Insitute for Chemistry and Biology of the Marine Environment, Carl von Ossietzky University | Oldenburg, Germany

M. Pohlner, J. Degenhardt, B. Engelen

The composition of benthic microbial communities is commonly investigated at relatively eutrophic coastal sites or high energy systems, e. g. hydrothermal vents. Now, mostly oligotrophic deep sea sediments of the Pacific Ocean were analyzed to assess the influence of nutrient availability and the viral impact on microbial community structures. Sediments were sampled during the two cruises RV Sonne SO248 (May 2016) and SO254 (February 2017). Combined, both cruises result in a transect from New Zealand (52°S) to Alaska (59°N) covering the main biogeographical provinces of the central Pacific (Fig. 1).

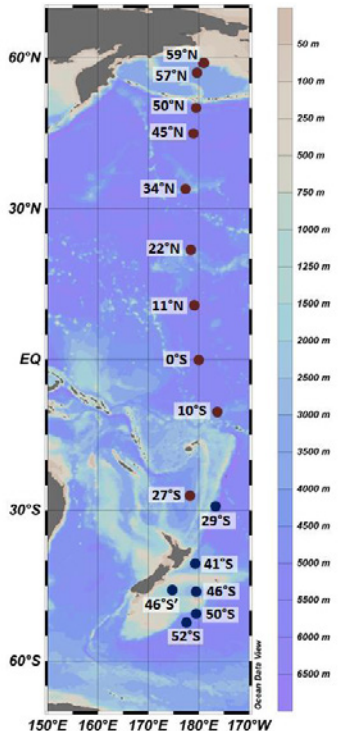

Fig. 1: Distribution of sampling sites during RV Sonne cruises SO248 (red) and SO254 (blue).

For samples from the sediment surface and 20 cm depth, geochemical measurements were combined with the analysis of microbial activity, abundance and diversity. Furthermore, the impact of deep-sea viruses on the composition of benthic microbial communities and nutrient availability was assessed by phage induction experiments. We hypothesized a distinct biogeographical distribution of benthic microbial communities linked to the productivity of the water column and nutrient availability in the different oceanic provinces and on a smaller scale also to the viral activity in those sediments.

Geochemical analyses, e. g. of nitrate, ammonia, phosphate and silicic acid, revealed increased nutrient availability in the New Zealand Province and towards the northern Pacific, but low nutrient concentrations in the Gyre regions (Fig. 2). Total cell abundances ranged between 108 and 109 cells per cm3 at the sediment surface with maximum values in the Bering Sea according to the increase of available nutrients in the northern Pacific (Fig. 3). Within the upper 20 cm, cell numbers decreased by up to 99 %. This decrease was especially pronounced in the nutrient depleted mid ocean gyres. Exoenzyme activities were measured as proxy for microbial activity in sediments. Aminopeptidase activities confirmed the trend of the varying nutrient concentrations and also showed higher values near New Zealand and in the North Pacific.

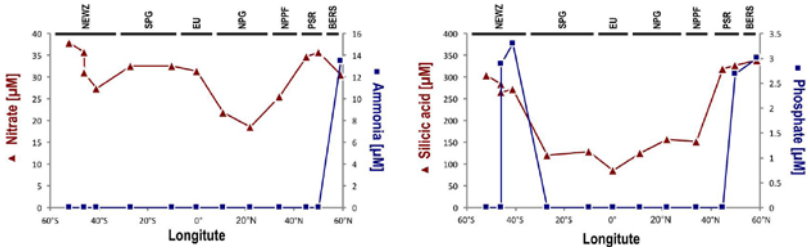

Fig. 2: Nutrient concentrations at the sediment surface of (A) nitrogen compounds as well as (B) phosphate and silicic acid in the porewaters of the different sampling sites. NEWZ: New Zealand Province, SPG: South Pacific Gyre, EU: Equatorial Upwelling, NPG: North Pacific Gyre, NPPF: North Pacific Polar Front, PSR: Pacific Subarctic Region, BERS: Bering Sea.

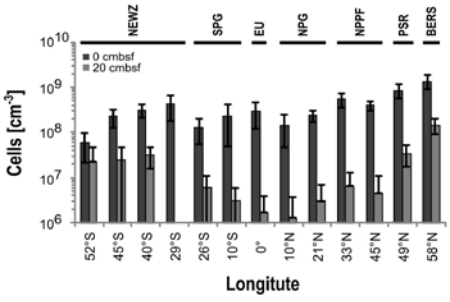

Fig. 3: Total cell counts in the sediments along the Pacific transect from the sediment surface (dark grey) and in 20 cm sediment depth (light grey). NEWZ: New Zealand Region, SPG: South Pacific Gyre, EU: Equatorial Upwelling, NPG: North Pacific Gyre, NPPF: North Pacific Polar Front, PSR: Pacific Subarctic Region, BERS: Bering Sea.

Sequencing of 16S rRNA genes and transcripts of the samples gained during RV Sonne cruise SO248 (27°N and further North) showed that Bacteria dominated the benthic communities over Archaea at most sites, while the community compositions were specific for the individual locations and sediment depths. The analysis revealed that the community structure within the different oceanic provinces depends on the nutrient availability and primary production in the water column. Thus, oceanic areas with low nutrient content such as both Pacific Gyres were characterized by specific communities, while sediments in the nutrient rich Bering Sea were inhabited by a microbial community most distinct from all others (Fig. 4).

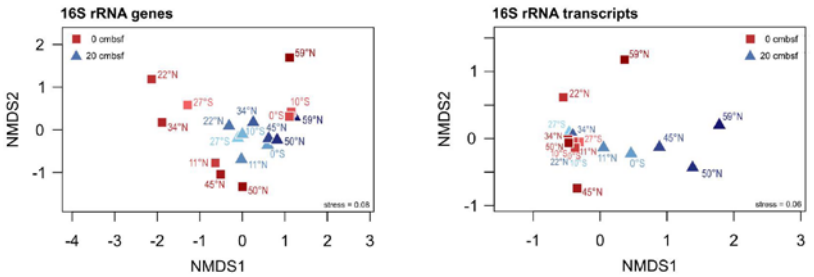

Fig. 4: Non metric multidimensional scaling plot (NMDS based on Bray Curtis distances) of bacterial communities based on 16S rRNA genes (left) and transcripts (right). Blue triangles represent communities at the sediment surface, while red squares refer to 20 cm sediment depth. The color of the symbols indicates the locations of the specific sites from South (light) to North (dark).

The impact of deep-sea viruses on the composition of benthic microbial communities and nutrient availability was assessed by phage induction experiments. To stimulate a viral infection, sediments from 0 cm and 20 cm sediment depth were treated with mitomycin C, an antibiotic inducing lysogenic viruses. In the experiment using sediment of the highly-productive Bering Sea, phages could successfully be induced in the 20 cm sediment layer, while there was no obvious increase of viruses in the surface incubations. This suggests that lysogeny becomes more prevalent in deeper, more oligotrophic sediments. Sequencing of 16S rRNA genes and transcripts showed that viral lysis resulted in a remarkable stable community composition (Fig. 5), indicating the importance of viruses for maintaining microbial diversity and ecosystem's stability. By ultra-high resolution mass spectrometry, a variety of different molecules was identified which were released upon cell lysis. Some of those were readily utilized by microorganisms, while some persisted throughout the incubation period. Currently, further phage induction experiments from other sampling sites in the Pacific are analyzed to evaluate the impact of viruses on benthic microbial communities in the different oceanic regions with different biogeochemical backgrounds.

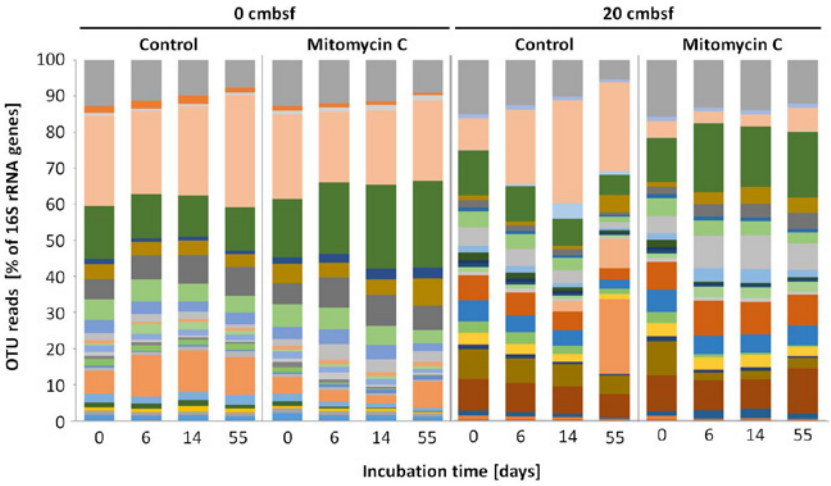

Fig. 5: Community composition on class level of the phage induction experiment using sediment from the Bering Sea.

SO255

NEW INSIGHTS FROM SO255 INTO THE FORMATION OF THE KERMADEC & COLVILLE RIDGES AND QUATERNARY KERMADEC ARC & HAVRE TROUGH THROUGH VITIAZ ARC SPLITTING

AUTHORS

GEOMAR Helmholtz Centre for Ocean Research Kiel | Kiel, Germany
K. Hoernle, F. Hauff, R. Werner, J.-A. Wartho, M. Gutjahr

Institute of Geosciences, Kiel University | Kiel, Germany
K. Hoernle, D. Garbe-Schönberg

University of California | Santa Cruz (CA), USA
J. Gill

GNS Science | Lower Hutt, New Zealand
C. Timm

University of Wisconsin | Madison (WI), USA
B. Jicha

The intra-oceanic Kermadec arc system extends ~1300 km between New Zealand and Fiji and comprises at least 30 arc front volcanoes, the Havre Trough back-arc and the remnant Colville and Kermadec Ridges, which formed the Vitiaz Arc prior to splitting. On the German RV Sonne SO255 cruise in 2017, we carried out extensive dredge sampling of the Kermadec arc system between 27–35°S latitudes (Figs. 1 and 2). Our major goal was to reconstruct the temporal (with $^{40}Ar/^{39}Ar$ age data) geochemical (major and trace element and Sr-Nd-Hf-Pb isotope) evolution of the arc system to further elucidate our understanding of the causes and consequences of arc splitting. We obtained geochemical analyses for more than 300 volcanic rocks and age data on a subset of these samples. Geochemical data from the Quaternary volcanic front and Havre Trough back-arc basin show that the local ambient mantle wedge is "Pacific" in character (Gill et al., in prep.). The slab component lies on a continuum from fluid-like to melt-like both at the volcanic front and in the back-arc, but the melt-like component increases in the back-arc where it is widely distributed, reflecting higher slab surface temperatures. The mass fraction of slab component increases southward in the back-arc as well as at the arc front, reflecting the increasing amount of sediments subducted nearer to New Zealand. Back-arc basalts generally

have less slab component and occur throughout the basin in an irregular fashion. In summary, the Kermadec arc front, including rear-arc, basalts can be explained by mixing of input (sediments and Hikurangi Seamounts) with the ambient "Pacific-like" mantle.

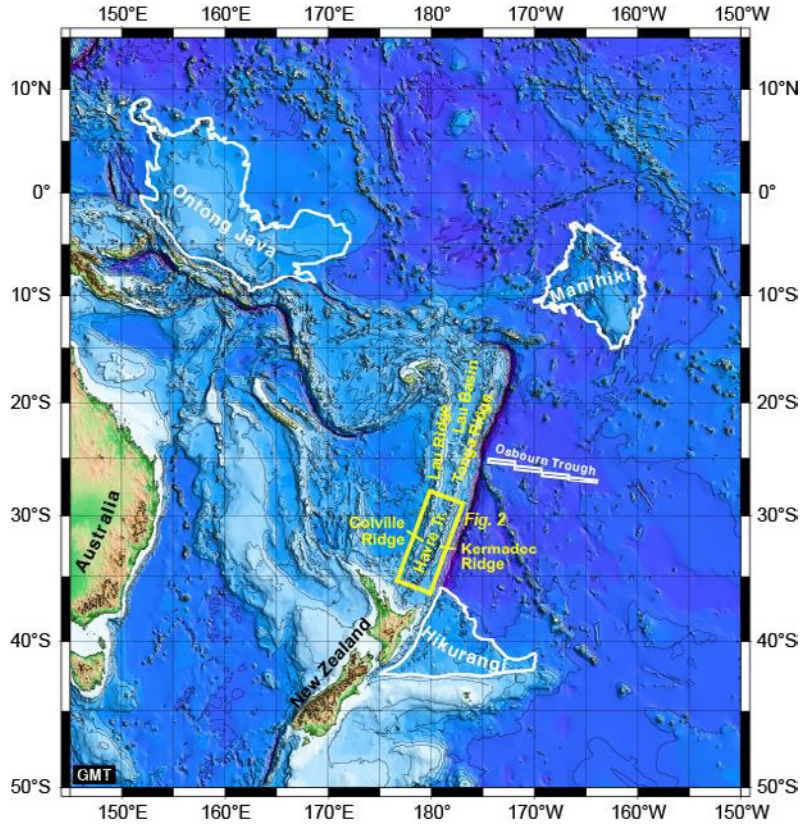

Fig. 1: Bathymetric map showing the location of the Tonga-Kermadec Arc/Backarc system and the Hikurangi, Manihiki and Ontong Java Plateaus. Yellow box shows the location of blow-up map in Fig. 2. The base map is from „The GEBCO_2014 Grid, version 20150318, http://www.gebco.net".

Most research to date on the Kermadec arc system has focused on the Kermadec arc front volcanoes, leaving the Colville and Kermadec Ridges almost completely unexplored. Our new $^{40}Ar/^{39}Ar$ ages range from ~7.5–2.6 Ma for the Colville Ridge and from ~4.4-3.4 Ma for the Kermadec Ridge (Timm et al., 2019). These preliminary age data indicate that the Colville Ridge received arc front type magmas until ~2.6 Ma ago. In contrast to the Quaternary Kermadec Arc, the Kermadec and Colville Ridges show evidence for the involvement of an enriched mantle one (EM1) type component, similar in isotopic composition to high-Ti basalts from the Manihiki Plateau, until ~3.8 Ma (Hoernle et al., in prep.).

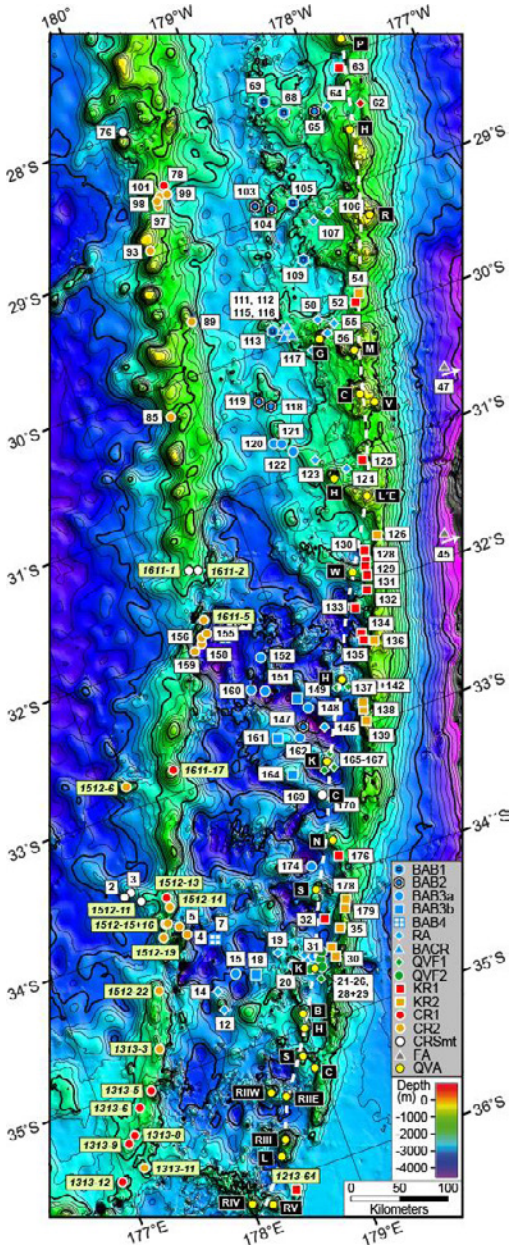

Fig. 2: Sample locations on the Kermadec and Colville Ridges, in the Havre Trough and on the Kermadec Arc. The base map is from „The GEBCO_2014 Grid, version 20150318, http://www. gebco.net". Numbered symbols represent RV SONNE (white background) and RV TANGAROA dredge sites (yellow background). The symbols for those stations identify their most common rock type and are listed in the legend (BAB, Back Arc Basalts; RA, Rear Arc; BACR, Backarc Caldera; QVF, Quaternary Volcanic Front; KR, Kermadec Ridge; CR, Colville Ridge; FA - Forearc; QVA, Quaternary volcanic arc). Present Quaternary volcanic front volcanoes are identified by numbers in black squares as follows, from south to north: RV, Rumble V; RIV, Rumble IV; L, Lille; RIII, Rumble III; RIIE, Rumble II East; RIIW, Rumble II West; C, Cotton; S, Silent; H, Healy; B, Brothers; K, Kibblewhite; S, Sonne; N, Ngatoroirangi; C, Cole; K, Kuiwai; H, Huanharoa; W, Wright; L'E, L'Esperance; H, Havre; V, Volcanolog; C, Curtis; M, Macauley; G, Giggenbach; R, Raoul; H, Hinetapeka; P, Putoto.

When fit back together, the Kermadec and Colville Ridges have surprisingly similar geographic variations in isotopic composition, deviating from the Quaternary volcanic arc compositions between 29–37°S (relative to Kermadec Ridge) with the most pronounced EM1-type composition at ~33°S. Our results confirm that the Kermadec and Colville Ridges are remnant fragments of a Miocene-Pliocene Arc that split to form the Havre Trough. The presence of the enriched signature north of a projection of the subducted Hikurangi Plateau could reflect subduction of a fracture zone, forming the western boundary of the seafloor formed at the Osbourn paleo-spreading center, which caused separation of the Manihiki and Hikurangi Plateaus. We propose that subduction of the western margin of the Hikurangi Plateau and fracture zone with fragments of the plateau in it, subparallel to the Kermadec Trench, could explain the enriched signature in the Vitiaz Arc and may have triggered arc splitting.

Most economic gold, silver and copper deposits on Earth are associated with volcanic arcs, yet little is known about the petrogenetic processes that control the sub-arc budget of these elements. In particular, what causes the enrichment of these elements in arc systems remains an enigma. High-precision Au, Ag and Cu analyses from 65 submarine glasses recovered from the length of the Kermadec Arc (27 from SO255) reveal that contents of these elements (e. g., Au <1 to 15 ppb) are highest in glasses derived from the most depleted sub-arc mantle by high degrees of partial melting (~18–30 %) at high temperatures (Timm et al., in revision). Therefore, we conclude that the magmatic Au, Ag and Cu budget is controlled by mantle wedge composition and the extent of its melting.

REFERENCES

Gill J, Hoernle K, Hauff F, Werner R, Timm C, Garbe-Schönberg D, M Gutjahr, Mantle flow and magma production during backarc basin evolution: Havre Trough and Kermadec Arc, southwest Pacific, Geochemistry Geophysics Geosystems in prep.

Hoernle K, Timm C, Gill J, Hauff F, Werner R, Garbe-Schönberg D, Gutjahr M, Geochemistry of Kermadec and Colville Ridges, SW Pacific: Implications for the origin of the enriched geochemical signature not seen in the Quaternary Kermadec Arc. Geology in prep.

Timm C, Portnyagin M, de Ronde CEJ, Hannington M, Garbe-Schönberg D, Hoernle K, Brandl P, Layton-Matthews D, Leybourne M, Arculus R, Mantle melting controls gold, silver and copper in arc magmas. Nature Geoscience in revision

Timm C, de Ronde CEJ, Hoernle K, Cousens B, Wartho JA, Tontini FC, Wysoczanski R, Hauff F, Handler M, New Age and Geochemical Data from the Southern Colville and Kermadec Ridges, SW Pacific: Insights into the recent geological history and petrogenesis of the Proto-Kermadec (Vitiaz) Arc. Gondwana Research 2019, 72, 169–193. DOI 10.1016/j.gr.2019.02.008.

SO256

TEMPERATURE AND CIRCULATION HISTORY OF THE EAST AUSTRALIAN CURRENT (TACTEAC)

AUTHORS

MARUM-Center for Marine Environmental Sciences, University of Bremen | Bremen, Germany
M. Mohtadi, M. Hollstein*

Bundesanstalt für Geowissenschaften und Rohstoffe (BGR) | Hannover, Germany
M. Hollstein*, A. Lückge

Atmosphere and Ocean Research Institute (AORI), University of Tokyo | Chiba, Japan
A. Servettaz, Y. Yokoyama

Oceanography Department, Dalhousie University | Halifax, Canada
J. Gould, M. Kienast

Department of Geological Oceanography, College of Ocean and Earth Sciences, University of Xiamen | Xiamen, China
B. Zou, S. Steinke

College of Science and Engineering, James Cook University | Cairn, Australia
R. Beaman

*Presenting author

This project is centered around the RV SONNE expedition SO-256 (TACTEAC) to eastern Australia in April/May 2017. Twenty-two scientists from 10 institutes from Germany, Australia, Japan, Canada, the Netherlands and China participated in the expedition. During the 10 working days, more than 100 m of sediment were collected by 23 gravity corer, 14 multi-corer and 3 giant box-corer deployments at 36 stations in 9 working areas off East Australia between 12°S and 26°S. In addition, the water column was sampled at 4 stations with the CTD-rosette water sampler. The dredge was deployed at 5 stations and together, more than 8 hours of video recordings were collected from the Great Barrier Reef (Mohtadi et al., 2013).

The collected sample material was used to reconstruct present and past changes in temperature and circulation of the Coral Sea, particularly from the East Australian Current

(EAC) and its influence on the climate of Northeast Australia. Radiocarbon studies on water samples show that the Antarctic Intermediate Water is transported to the study area via North and South Caledonian Jets from the east, while the deep water origins additionally from a more proximal, southern source and is transported to the Coral Sea through the Tasman Sea (Servettaz et al., accepted). In addition, this study shows that the deep water in this region is not yet contaminated by the bomb carbon of the nuclear tests released in the 1950s. Another study shows evidence of a relationship between deuterium isotopes in biomarkers (alkenones) and salinity changes in the photic zone and suggests that this proxy can be used for salinity changes as low as 1.2 psu (Gould et al., 2019).

Another study on planktic foraminiferal fauna at two multi-corer stations in the north and south of the study area suggests an increase in surface temperatures together with a decrease in productivity of the EAC during the past 400 years (Zou, 2019). Element analysis of gravity cores from the expedition SO-256 shows a relatively high terrigenous fraction in the sediments off northeast Australia during warm periods that cannot be related to changes in sea-level and therefore, reflects increased rainfall in hinterland. The generally more humid climate of the northeastern Australia together with higher surface temperatures calculated from Mg/Ca ratios in planktic foraminifera or alkenones during the warm periods support the working hypothesis of this project on long timescales (Hollstein et al., in prep.).

REFERENCES

Gould J, Kienast M, Dowd M, Schefuß E, An open-ocean assessment of alkenone □D as paleo-salinity proxy. Geochimica et Cosmochimica Acta 2019, 246, 478–497.

*Hollstein M, Lückge A, Kienast M, Mohtadi M, Temperature evolution across the Coral Sea over the last glacial-interglacial cycle. To be submitted to Paleoceanography and Paleoclimatology.

Mohtadi M, et al. R/V SONNE Cruise Report SO256, TACTEAC, Temperature And Circulation History of The East Australian Current, Auckland (New Zealand) – Darwin (Australia), 17 April – 09 May 2017. Berichte, MARUM – Zentrum für Marine Umweltwissenschaften, Fachbereich Geowissenschaften, Universität Bremen 2017, 316, p. 81, ISSN 2195-9633.

Servettaz A, Yokoyama Y, Hirabayashi S, Kienast M, Miyairi Y, Mohtadi M, Dissolved inorganic radiocarbon content of the western Coral Sea: implications for intermediate and deep water circulation. Radiocarbon, accepted, doi:10.1017/RDC.2019.122.

Zou B, Late Holocene planktic foraminiferal assemblages in the Coral Sea, southwestern Pacific. BSc. Thesis 2019, College of Ocean and Earth Sciences, Xiamen University, p.20.

SO257

AUSTRALIAN MONSOON VARIABILITY OVER THE PAST THREE GLACIAL CYCLES: PRELIMINARY RESULTS OF R/V SONNE CRUISE SO257 (WACHEIO)

AUTHORS

Institute for Geosciences, Kiel University | Kiel, Germany
W. Kuhnt, A. Holbourn, R. Pei, J. Hingst, S. Steffen, M. Koppe SO-257

And: Shipboard Scientific Party

R/V Sonne cruise SO257 (WACHEIO) retrieved a suite of sediment cores along the continental margin of Western Australia between 15° and 32°S. Coring along high resolution Parasound and multichannel seismic lines allowed recovery of high quality long gravity and piston cores closely connected to drilling sites of International Ocean Discovery Program (IODP) Expeditions 356 (Indonesian Throughflow) and 363 (West Pacific Warm Pool). These high-resolution sediment archives closely track late Pleistocene climate evolution along the southwestern margin of the Indo-Pacific Warm Pool and the variability of the Australian Monsoon. Based on the development of a high-resolution chronology using radiometric dating and benthic isotope stratigraphy, this unique climate archive allows to: (1) test the hypothesis of southward (northward) shifts of the westerlies and the southern margin of the tropical rainbelt during Southern Hemisphere warming (cooling) events; (2) test the hypothesis of a reduction in tropical convection and weakening of the Walker circulation during tropical warming, thus evaluating consequences for the prediction of tropical rainfall for future global warming; (3) explore the effects of tropical and Southern Hemisphere warming on precipitation and circulation patterns along the coast of Western Australia.

The variability in sediment discharge from northwestern Australia provides a powerful tool to monitor changes in the position and intensity of the Australian monsoonal rainbelt. We combine X-ray fluorescence (XRF) core scanner-derived estimates of changes in terrigenous sediment discharge and provenance and aeolian dust flux with foraminiferal Mg/Ca and oxygen isotope based ocean mixed layer temperature and salinity estimates to reconstruct the past variability of the Australian Monsoon on centennial to millennial timescales. Elemental composition of core-top samples retrieved during R/V Sonne cruise SO257 WACHEIO along the northwestern Australian margin closely matches elemental signatures of major river catchments. We reconstructed the displacement of climatic belts along the western coast of Australia during main Southern Hemisphere warming/cooling phases over the last four glacial cycles. This latitudinal transect includes the tropical monsoon region of Northwestern

Australia, and the arid zone, where rainfall mainly occurs during landfall of tropical cyclones (Fig. 1).

First results indicate that interglacials and suborbital Southern Hemisphere warm periods were associated with intensification and southward migration of the Australian monsoonal rain belt and heightened cyclone activity, whereas cold periods were characterized by weakened monsoon, extended aridity and intensified trade winds increasing dust fluxes. Rapid intensification of monsoonal precipitation and reduction of aeolian dust input occurred during the Younger Dryas and early Holocene and in the terminal phase of major deglaciations (Fig. 2). These short-lived monsoonal maxima in the early Holocene (~11-8 ka), early MIS 5e, MIS 7 and MIS 9 indicate southward shifts in the summer position of the Intertropical Convergence Zone (ITCZ) that coincide with peak sea surface temperatures offshore Western Australia and with maxima in temperature, carbon dioxide and methane in Antarctic ice cores. Southern Hemisphere low latitude hydroclimate and vegetation changes associated with the southward shift of the ITCZ and monsoon intensification may, thus, have additionally contributed to the global methane and pCO_2 maxima at the end of glacial terminations. Our results indicate that the intensity of Australian monsoon precipitation and the position of the Intertropical Convergence Zone (ITCZ) were strongly affected by changes in Southern Hemisphere temperatures and the interhemispheric temperature gradient during global warming at glacial terminations and suggest that the currently rising greenhouse gas concentrations will enforce local insolation over Western Australia and intensify Australian monsoon precipitation and tropical cyclone activity during austral summer.

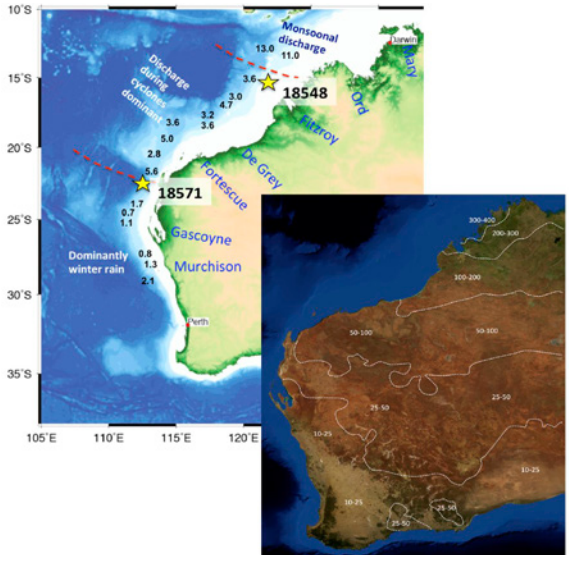

Fig. 1: A. Main climate zones, river systems, and offshore average sedimentation rates in cm/kyr from Keep et al. (2018) with position of cores SO25718548 and SO257–18571. B. February vegetation and precipitation in Western Australia (b). February precipitation based on 30 year standard climatology (1961–1990) in mm/month from Australian Bureau of Meteorology (2010). Satellite Image February 2004, NASA Blue Marble.

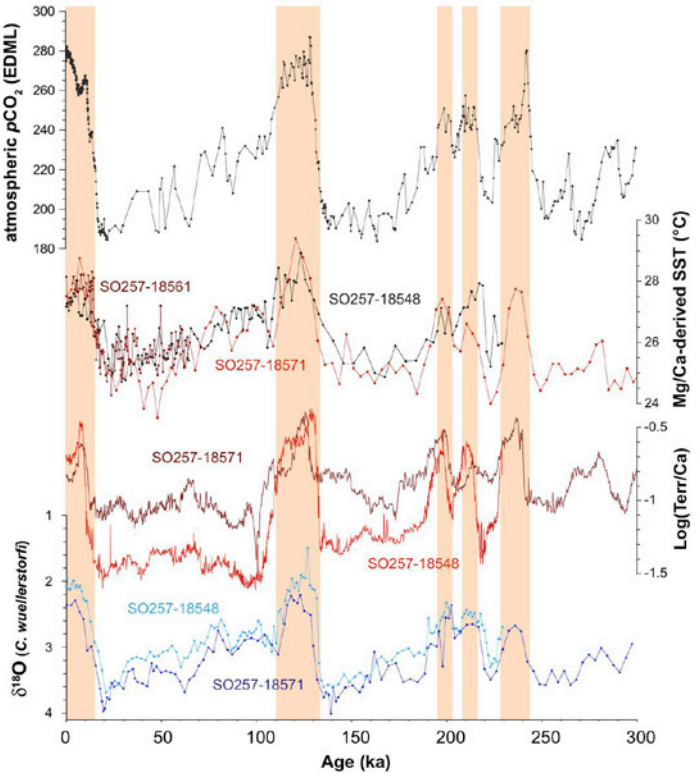

Fig. 2: Benthic $\delta^{18}O$, terrigenous runoff from XRF-scanner data (Log(Terr/Ca) and sea surface temperatures (SST) in comparison to atmospheric pCO_2 changes over the last three glacial cycles (Pei et al., in preparation).

REFERENCES

Keep, M., Holbourn, A., Kuhnt, W., and Gallagher, S., 2018. Progressing Western Australian collision with Asia: implications for regional orography, oceanography, climate and marine biota. Journal of the Royal Society of Western Australia, 101, 1–17.

Kuhnt, W., A. Holbourn, J. Xu, B. Opdyke, P. De Deckker, U. Röhl, and M. Mudelsee, 2015. Southern Hemisphere control on Australian monsoon variability during the late deglaciation and Holocene. Nature Communications, 6, 5916, doi:10.1038/ncomms6916.

Kuhnt, W., Holbourn, A., Schönfeld, J., Lindhorst, K. and the SO257 Shipboard Scientific Party, 2017, West Australian climate history from Eastern Indian Ocean Sediment Archives (WACHEIO). SO257 Cruise Report.

Pei, R., Kuhnt, W., Holbourn A., Hingst, J., Koppe, M. and Andresen, N., in preparation. Monitoring the latitudinal migration of the Intertropical Convergence Zone and Australian Monsoon variability during the last four glacial cycles.

SO258/1*

NEW INSIGHTS INTO THE TEMPORAL AND GEOCHEMICAL EVOLUTION OF THE 85°E RIDGE IN THE MID-INDIAN OCEAN

AUTHORS

GEOMAR Helmholtz-Zentrum für Ozeanforschung Kiel | Kiel, Germany
S. Homrighausen, K. Hoernle, F. Hauff, J-A. Wartho, M. Portnyagin, R. Werner, J. Geldmacher

Institut für Geowissenschaften, Christian-Albrechts Universität zu Kiel | Kiel, Germany
K. Hoernle

V.I. Vernadsky Institute of Geochemistry and Analytical Chemistry | Moscow, Russia
M. Portnyagin

The R/V SONNE expedition SO258/1 is part of the research project INGON, which aims to investigate magmatic and tectonic processes that trigger continental break-up and the formation of ocean basins. SO258/1 focused on mapping and sampling of the proposed 85°E Ridge hotspot track in the Mid-Indian Ocean basin. The 85°E Ridge, composed of the Buried Hills, Partly Buried Hills, Afanasy Nikitin Plateau and Southern Seamounts Chain (Fig. 1), is associated with either the Crozet, Marion or the Conrad Rise hotspot (Curray and Munasinghe, 1991; Kent et al., 1992; Müller et al., 1993). Curray and Munasinghe (1991) proposed that the 85°E Ridge was formed by a classical mantle plume that may have formed the Rajmahal Traps flood basalt province and may have triggered the Indian-Antarctic break-up. Alternatively, these features may have been produced by shallow recycling of subcontinental lithospheric mantle and/or lower crust, delaminated during continental breakup and brought to the surface by upwelling near mid-ocean ridges, as proposed for the Christmas Island Seamounts in the eastern Indian Ocean sampled during the SO211 cruise (Hoernle et al., 2011). Apart from the Afanasy Nikitin Plateau, which gained a certain publicity as the most "enriched mantle 1" (EMI) end member thus far discovered in the ocean basins (Mahoney et al., 1996), the entire structure was previously unsampled. The pronounced EMI-type signature is of particular interest, because the potential source material has also been proposed to be responsible for the global-scale geochemical DUPAL-anomaly (named after the French geochemists DUPré and ALlègre) observed in the South Atlantic and Indian Ocean (e. g. , Hart, 1984). In order to test these models and to characterize any possible spatial and temporal geochemical evolution, 39 dredge hauls along the 85°E Ridge and the neighboring 86°E Fracture Zone were carried out during SO258/1. The recovered lavas and fresh (!) volcanic glasses represent the most comprehensive rock collection from the Mid-Indian Ocean to date. Here we present the results of geochemical (major and trace element data, Sr-Nd-Pb isotope ratios) and geochronological ($^{40}Ar/^{39}Ar$ age dating) analyses of these rocks.

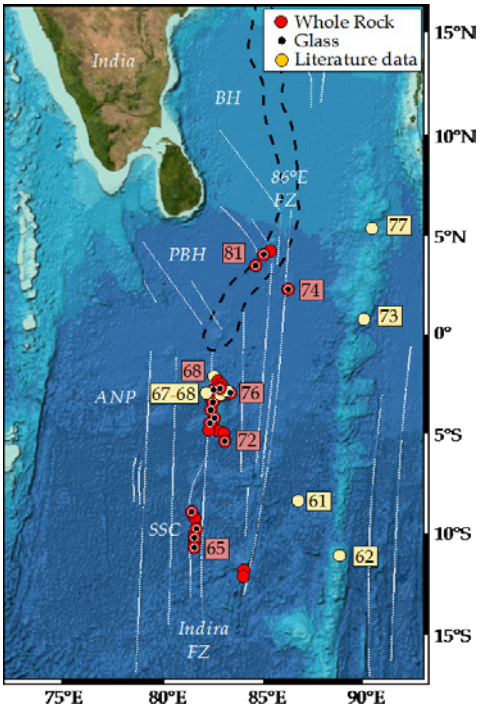

Fig.1: Bathymetric map of the Mid-Indian Ocean basin with fracture zones (white lines) and the negative gravity anomaly difining the Buried Hills (black dashed line). SO258/1 sampling sites with $^{40}Ar/^{39}Ar$ ages have red background color and material analyzed is divided into whole-rock lavas (red circles) and fresh glasses (black dots). The literature data (yellow color with $^{40}Ar/^{39}Ar$ ages from Krishna et al., 2012) are shown for comparison. Note that the low gravity anomaly of the Buried Hills lie on the northward extension of the 86°E Fracture Zone (FZ), which could indicate a purely tectonic origin for the Buried Hills (e. g., Liu et al., 1982; Kent et al., 1992) Abbreviations: BH = Buried Hills, PBH = Partly Buried Hills, ANP = Afanasy Nikitin Plateau, SSC = Southern Seamounts Chain; bathymetric map from http://www.geomapapp.org.

Our age data show a general N to S younging trend from the Partly Buried Hills to the Afanasy Nikitin Plateau and to the Southern Seamounts Chain (Southern 85°E Ridge track), which could indicate the formation by a stationary melt anomaly (Fig. 1). However, if the age data from the Partly Buried Hills are combined with recent plate motion models (e. g., Seton et al., 2012) an origin of the Southern 85°E Ridge track, the Buried Hills and the Rajmahal Traps by the same hotspot is not supported. Based on age data, plate motion and isostatic models, the southern 85°E Ridge most likely share a co-genetic evolution with the Conrad Rise. Plate reconstructions of the southern 85°E Ridge eruptive sites place them close to the proposed site of the Conrad Rise hotspot.

The geochemical variability of the recovered Mid-Indian Ocean lavas requires at least three distinct compositional types: 1) a depleted upper mantle component, similar to the Central Atlantic mid ocean ridge basalt (MORB), 2) an Indian hotspot component with prevalent mantle (PREMA)-like composition, and 3) an EMI-type component (Fig. 2). The Indian hotspot component may suggest a mantle plume origin of the southern 85°E Ridge

track. The EMI-type component is characterized by high Ba/Nb ratios (up to 40), low Ce/Pb ratios (7–20) depletion in Th, U, Nb, and Ta and enrichment in Sr and K, which is similar to average lower continental crust (Fig. 2; e. g., Rudnick and Gao, 2003). This EMI compositional type is also documented at the 39–41°E Southwest Indian Ridge and for Antarctic/West Australian lamproites, which indicates a shallow upper mantle origin.

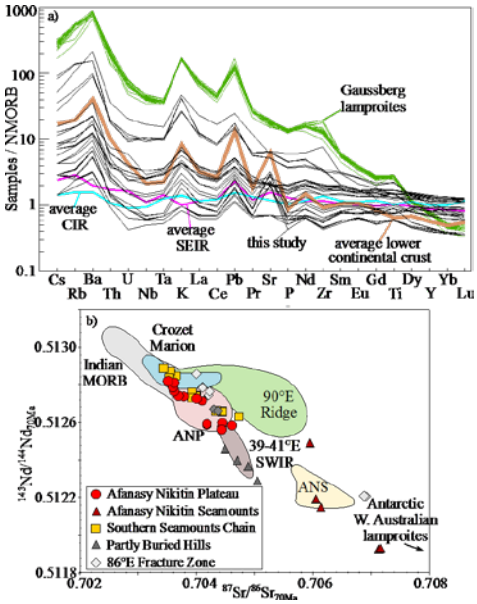

Fig. 2: a) N-MORB normalized multi-element diagram and b) 87Sr/86Sr70Ma vs. 143Nd/144Nd70Ma isotope ratios of SO258/1 samples along with fields of Indian MORB and hotspots projected to 70Ma. Note, the Afanasy Nikitin Seamounts (ANS) represent late-stage volcanism (~10 Ma after the ANP formation) and possess the strongest EMI signature. Abbreviations: CIR = Central Indian Ridge, SEIR = Southeast Indian Ridge, SWIR = Southwest Indian Ridge. Literature data are taken from GEOROC Database (http://georoc.mpch-mainz.gwdg.de/georoc/).

It appears that the EMI-type signature of the Indian Ocean DUPAL anomaly decreases with time, whereas the South Atlantic DUPAL anomaly remains relatively constant over time. These contrasting temporal evolutions could reflect two distinct source origins. The crustal signature in the Indian Ocean is most likely derived from delamination of continental lithosphere and/or lower continental crust dispersed in the upper mantle after the fragmentation of Gondwana (e. g., Dupré and Allègre, 1983; Hawkesworth et al., 1986; Hoernle et al., 2011). In contrast, the crustal signature in the South Atlantic most likely derives from deep-rooted mantle plumes (e. g., Homrighausen et al., 2019).

REFERENCES

Curray, J.R. and Munasinghe, T. (1991) Origin of the Rajmahal Traps and the 85°E Ridge: Preliminary reconstructions of the trace of the Crozet hotspot. Geology 19, 1237–1240.

Dupré, B. and Allègre, C.J. (1983) Pb–Sr isotope variation in Indian Ocean basalts and mixing phenomena. Nature 303, 142–146.

Hart, S.R. (1984) A large-scale isotope anomaly in the Southern Hemisphere mantle. Nature 309, 753–757.

Hawkesworth, C.J., Mantovani, M.S.M., Taylor, P.N. and Palacz, Z. (1986) Evidence from the Parana of south Brazil for a continental contribution to Dupal basalts. Nature 322, 356.

Hoernle, K., Hauff, F., Werner, R., van den Bogaard, P., Gibbons, A.D., Conrad, S. and Muller, R.D. (2011) Origin of Indian Ocean Seamount Province by shallow recycling of continental lithosphere. Nature Geosci 4, 883–887.

Homrighausen, S., Hoernle, K., Hauff, F., Wartho, J.-A. and Garbe-Schönberg, C.D. (2019) New age and geochemical data from the Walvis Ridge: The temporal and spatial diversity of South Atlantic intraplate volcanism and its possible origin. Geochimica et Cosmochimica Acta 245, 16–34.

Kent, R.W., Storey, M., Saunders, A.D., Ghose, N.C. and Kempton, P.D. (1992) Comment and Reply on "Origin of the Rajmahal Traps and the 85°E Ridge: Preliminary reconstructions of the trace of the Crozet hotspot". Geology 20, 957–959.

Krishna, K.S., Abraham, H., Sager, W.W., Pringle, M.S., Frey, F., Gopala Rao, D. and Levchenko, O.V. (2012) Tectonics of the Ninetyeast Ridge derived from spreading records in adjacent oceanic basins and age constraints of the ridge. Journal of Geophysical Research: Solid Earth 117.

Liu, C.-S., Sandwell, D.T. and Curray, J.R. (1982) The negative gravity field over the 85°E ridge. Journal of Geophysical Research: Solid Earth 87, 7673–7686.

Mahoney, J.J., White, W.M., Upton, B.G.J., Neal, C.R. and Scrutton, R.A. (1996) Beyond EM-1: Lavas from Afanasy-Nikitin Rise and the Crozet Archipelago, Indian Ocean. Geology 24, 615–618.

Müller, R.D., Royer, J.-Y. and Lawver, L.A. (1993) Revised plate motions relative to the hotspots from combined Atlantic and Indian Ocean hotspot tracks. Geology 21, 275–278.

Rudnick, R.L. and Gao, S. (2003) 3.01 - Composition of the Continental Crust in: Turekian, K.K. (Ed.), Treatise on Geochemistry. Pergamon, Oxford, pp. 1–64.

Seton, M., Müller, R.D., Zahirovic, S., Gaina, C., Torsvik, T., Shephard, G., Talsma, A., Gurnis, M., Turner, M., Maus, S. and Chandler, M. (2012) Global continental and ocean basin reconstructions since 200 Ma. Earth-Sci Rev 113, 212–270.

SO259*

EXPLORING THE INDIAN OCEAN – RESULTS FROM CRUISE SO259

AUTHORS

Bundesanstalt für Geowissenschaften und Rohstoffe | Hannover, Germany
U. Schwarz-Schampera, R. Freitag

University Hamburg | Hamburg, Germany
N. Harms, N. Lahajnar

Deutsches Zentrum für Marine Biodiversitätsforschung Senckenberg am Meer | Wilhelmshaven, Germany
T. Kihara

Laurentian University | Greater Sudbury, Kanada
H. Gibson

The SO259 expedition (INDEX 2017) of BGR with TFS SONNE targeted the German license area for polymetallic sulfides in the Indian Ocean. Cruise participants included the Universities at Bremen, Hamburg, HCU Hamburg, Erlangen, the DZMB Senckenberg Am Meer Wilhelmshaven and GEOMAR in Kiel. Trainees from Egypt, Thailand, Cook Islands, Ghana and Nigeria represented the International Seabed Authority. The cruise focused on the detailed bathymetric, geophysical and geological exploration for active vents and inactive sulfide fields in the clusters #10, #11 and #12. The wider license area, the clusters #1, #3#, #4, #5 and #7 and the clusters of interest were also sampled for environmental, i.e., (paleo) oceanographic, sedimentary and faunal base line studies. Very few environmental and geological studies exist in this part of the Indian Ocean so far. Our work contributes to the understanding of regional oceanographic and sedimentation processes and to the faunal census.

Cruise SO259 (INDEX 2017) performed 109 stations. Site survey, observation and sampling operations were completed and 14 different operational tools were used for diverse and extensive exploration and environmental studies in transit and within the license area, including

- 17 vertical CTD rosette casts for environmental, water masses and sedimentary studies,
- 7 multicorer and five gravity corer stations for paleooceanographic and biogeochemical studies,

- 4 heat flow probe measurements for crustal temperature regime estimations,
- 27 wax corer and 13 dredge stations for petrological reconnaissance and spreading ridge evolution studies,
- 8 sediment trap and one ADCP mooring operations for biogeochemistry, particle flux and ocean current measurements,
- 6 deep-towed HOMESIDE surveys for high-resolution bathymetric mapping, magnetics and water anomaly surveys (total of 329 km in 147 hours),
- 8 tow-yo stations with the SOPHI sensor sled for plume hunting (125 km, 119 hours),
- 4 STROMER video sled ocean floor observations,
- 3 Golden Eye operations for electromagnetic measurements (4 km, 22 hours),
- 2 TV-guided grab survey and sampling operations,
- 4 bathymetric, magnetic and gravity surveys (total of 783 km and 60 hours for 14 profiles).

Additionally, two transit profiles in the license area (450 km, 24 hours) for bathymetry and magnetics, a total of 9,430 km of swath bathymetric mapping (776 hours) and 9,955 km (1,005 hours) of scientific echosounder measurements for water column imaging were carried out. The biodiversity was studied and sampled at 51 stations with 630 samples and 3,232 individuals, and 5:29 hours of video material and 4522 photos were collected. Molecular work produced a number of 422 cell extractions and 305 PCR DNA products from different species.

Four plumes were detected during eight tows with the plume sled SOPHI (125 km) and a new site of hydrothermal venting was localized by HOMESIDE and STROMER surveys on the eastern graben flank of cluster #11, and named "NEW SONNE" field. The site was studied in greater detail during cruise INDEX2018 on board R/V PELAGIA and with the Canadian ROV ROPOS. NEW SONNE is located at the outer graben wall of a 300 m wide fault bound plateau. The area consists of sedimented talus and heavily fractured steep basalt outcrops with pillow flows. The area close to the main graben flank is strongly fractured with steep and wide fault scarps in the massive basalts. Talus fans change with massive basalt outcrops. Flow tops occur at different water depths (e. g., 2937 m, 2927 m). Ferruginous sediments indicate the presence of hydrothermal venting and sulfide blocks and crusts close to tube lava and pillow lavas indicate the pillow-basalt hosted hydrothermal system and site. Fluid pathways are likely to vent through the pillow interstices. The NEW SONNE field consists of three areas with diffuse discharge

and two prominent sulfide mounds. All sulfide sites are within the +/-2920 m water depth contour line. The active sites show numerous venting spots and the chimneys have multiple orifices with temperatures up to 334°C (2919 m water depth), with well-developed characteristic vent fauna and the venting of clear, probably phase-separated hydrothermal fluids. The sampled orifice has massive chalcopyrite mineralization. The opening of a beehive structure still produces clear fluids and the beehive consists out of chalcopyrite as well. The fluid exit temperature is 323°C (2916 m) suggesting phase separation processes at depth. Secondary copper mineral phases in an area of eroded stockwork mineralization indicate high fluid temperatures in the subsurface. An area of basalt pillars, associated with ropy lava and indicative for a cooling lava lake from a proximal volcanic vent site, was observed nearby.

Features prospective for active and inactive sulfide sites were identified in all three clusters, both on the eastern and western graben valleys. Our findings attest to the high potential for sulfide mineralization in all three clusters. During subsequent cruises INDEX2018 and INDEX2019 (SO271) additional sulfide occurrences were identified. The cluster #12 hosts at least two large scale sulfide areas, named PENUMBRA and HUNA, found during INDEX2018 and extending for more than 2 km and hosting 7–12 sulfide mounds and fields, respectively. Cruise INDEX2019 (SO271) identified two additional areas in cluster #06 (SURYA) and cluster #07 (SOORAJ). The current status of BGR`s exploration activities in the German license area in the western central Indian Ocean is ten sulfide areas with 25 active vent fields and 31 inactive sulfide sites.

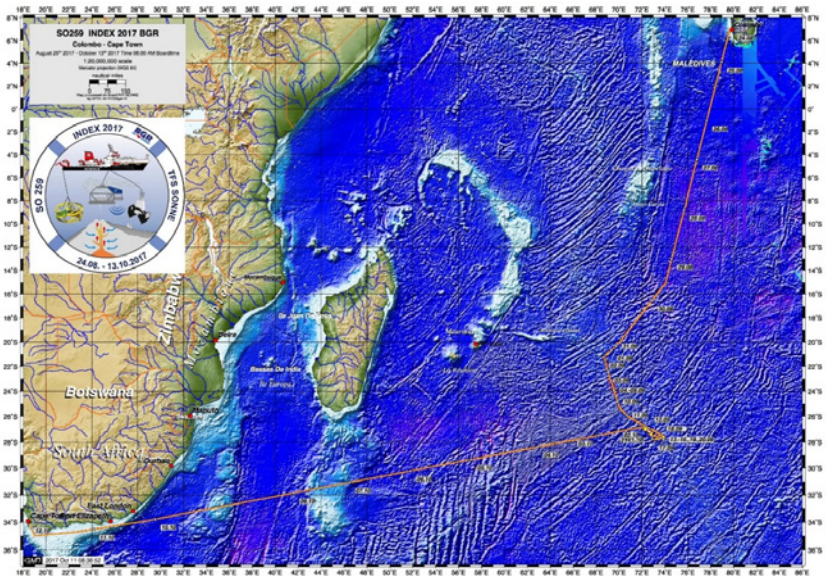

Fig. 1: Overview of the SO259 (INDEX 2017) working area, the cruise plot and courses along the southern Central and the northern Southeast Indian Ridge, Central Indian Ocean. The cruise started in Colombo, Sri Lanka and ended in Cape Town, South Africa.

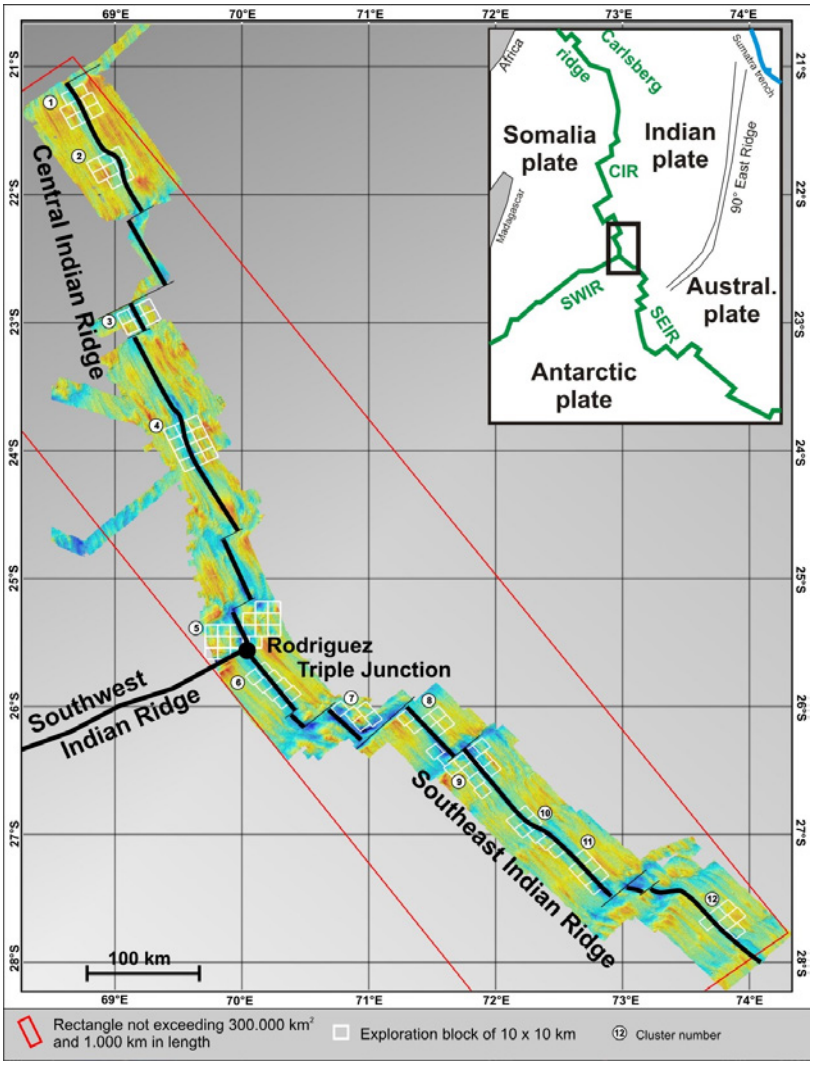

Fig. 2: The German exploration license area along the southernmost Central Indian Ridge and the northernmost Southeast Indian Ridge. Cruise SO259 (INDEX 2017) with FS SONNE addressed the clusters #1, #3#, #4, #5, #7, #10, #11 and #12 along the southern Central and the northern Southeast Indian Ridges.

SO259/3*
COLLECTING REFERENCE DATA OVER OCEANS

AUTHORS

MPI-Meteorologie
S. Kinne

The Xmas 2017 and 2018 New-Year transit of the RV Sonne from Emden, via Brest to Buenos Aires allowed the opportunity to sample with light carry-on meteorological instruments latitudinal cross-sections for aerosol, trace-gases and clouds across the Atlantic. Such references are needed to explore required assumptions in interpretations of satellite sensor data and in model parameterizations and to improve coverage and quality in global data-sets. Sample highlights were a very intense dust event off the Sahara for several days from the Cape Verde Islands to the equator and the passing of a squall line with intense precipitations structures off Rio de Janeiro. In addition, French ARGO floats (collected at Brest) were deployed and bathymetric data in non-national waters were analyzed for the Seabed 2030 data-base.

SO260

DYNAMICS OF SEDIMENTATION PROCESSES AND THEIR IMPACT ON BIOGEOCHEMICAL REACTIONS ON THE CONTINENTAL SLOPE OFF ARGENTINA AND URUGUAY "DOSPROBIO"– RESULTS OF RV SONNE CRUISE SO260

AUTHORS

Alfred Wegener Institute Helmholtz Centre for Polar and Marine Research | Bremerhaven, Germany
S. Kasten

MARUM – Center for Marine Environmental Sciences, University of Bremen | Bremen, Germany
S. Kasten

University of Bremen, Faculty of Geosciences | Bremen, Germany
S. Kasten, T. Schwenk, L. Steinmann

And: participants of RV SONNE cruise SO260

RV SONNE cruise SO260 "DosProBio" was carried out in two legs from January 12th until February 14th 2018 (Kasten et al., 2019). The study area was the continental margin off Argentina and Uruguay, which represents a highly dynamic depositional environment and is also a key location of the global thermohaline circulation due to the confluence of northward and southward flowing contour currents. With a multidisciplinary team of geoscientists from various disciplines, biologists and oceanographers the objectives of the cruise were to study the fundamental interaction between bottom currents and sediment deposition as well as to assess how sedimentation processes control biogeochemical reactions and element cycling in the seabed. Moreover, the sediments deposited in contourites and canyons were targeted as high-resolution archives to study paleo-oceanographic changes. In order to reach these scientific aims, detailed sediment echosounder and seismic surveys were conducted. Based on these mappings we chose suitable sites for sediment and water column sampling. The water column was sampled using a Rosette/CTD system and in situ pumps. The sediment surface and the uppermost meters of the sediments were sampled by means of multiple corer, giant box corer, sediment grab, and gravity corer. In order to retrieve older/deeper sediments the MARUM MeBo70 drill rig was deployed. The expedition contributed to and was carried out in the framework of the DFG-funded Cluster of Excellence MARUM "The Ocean in the Earth System" (MARUM – Center for Marine Environmental Sciences, University of Bremen).

A major outcome of the cruise was the discovery of a so far unknown giant cold-water coral province. Detailed, integrated analysis of multibeam bathymetry, sediment echosounder, and Acoustic Doppler Current Profiler (ADCP) data allowed the characterization of its morphological, stratigraphic, and hydrodynamic setting. It could be shown that its distribution is linked to both, the submarine geomorphology and the interfaces of water masses. The existence of buried coral mounds points to vertical shifts of the water mass boundaries in the past (Fig. 1; Steinmann et al., in review).

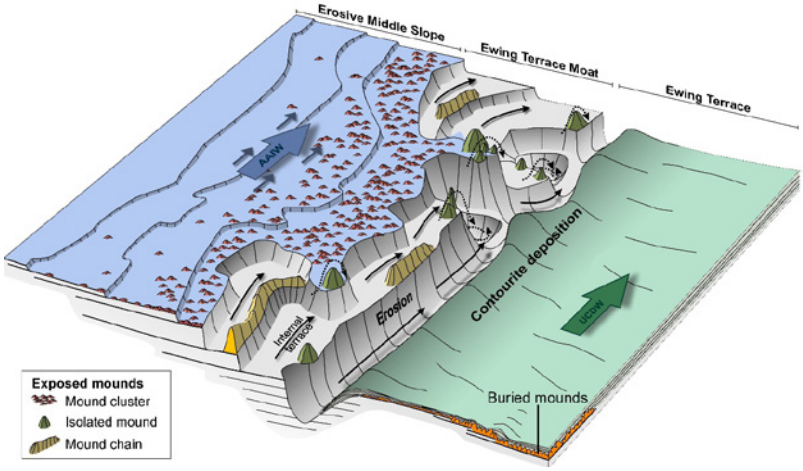

Fig. 1: Perspective view on the Coral-Contourite System as identified along the northern Argentine continental margin. The distribution of coral mounds in relation to the regional morphosedimentary setting and oceanography is illustrated. (Steinmann et al., in review).

Moreover, for the first time, a submarine, quantitative geomorphometric analysis of multibeam data from the Uruguayan slope has been carried out. As a result, a distribution map of surface sediment grain sizes was calculated showing a clear along-slope trend from SE to NE and the impact of local canyon systems on sediment distribution by contour currents. We also succeeded in retrieving high-resolution/high sedimentation records from an intra-canyon terrace, which – based on first radiocarbon results represents the last 9.000 years. This sediment record will serve as an archive to reconstruct the dynamics of intermediate and deep-water circulation throughout the Holocene in the study area.

Several gravity cores and MeBo cores were taken from different depositional environments along the continental margin off Argentina and Uruguay, which are currently subject to detailed inorganic and organic geochemical, biogeochemical, microbiological, sedimentological and rock-magnetic analyses. The aim of these investigations is to assess how the different depositional conditions – including sedimentation/accumulation rate, quantity and quality of organic matter and iron mineral phases as well as intensity of upward methane fluxes - control the pathways and rates of biogeochemical processes

and diagenetic signal formation in these highly dynamic marine sediments. First results obtained from two contrasting depositional settings – i. e. a site at the contourite system of the Northern Ewing Terrace and a site at the lower continental slope – already demonstrate significant differences in geochemical zonation, biogeochemical processes and element fluxes (also c.f. Melcher et al., this volume)

REFERENCES

Kasten, S. and cruise participants of RV SONNE expedition SO260 (2019) Dynamics of sedimentation processes and their impact on biogeochemical reactions on the continental slope off Argentina and Uruguay – DosProBio. Cruise Report of RV SONNE Cruise SO260, 97 pp.

Steinmann, L, Baques, M, Wenau, S, Schwenk, T, Spiess, V, Piola, AR, Bozzano, G, Violante, R, Kasten, S. Discovery of a giant cold-water coral mound province along the northern Argentine margin and its linkage to the oceanographic and morphosedimentary setting, Marine Geology, in review.

SO260*

IMPACT OF DEPOSITIONAL REGIMES ON BIOGEOCHEMICAL CYCLING OF IRON IN SEDIMENTS OF THE ARGENTINA CONTINENTAL MARGIN: FIRST RESULTS OF RV SONNE EXPEDITION SO260

AUTHORS

Alfred Wegener Institute Helmholtz Centre for Polar and Marine Research | Bremerhaven, Germany
A.-C. Melcher, S. Henkel, M. Köster, J. Volz, S. Kasten

MARUM – Center for Marine Environmental Sciences, University of Bremen | Bremen, Germany
S. Henkel, T. Pape, A. Meixner, S. Kasemann, T. Frederichs, E. Miramontes, S. Kasten

University of Bremen, Faculty of Geosciences | Bremen, Germany
T. Pape, A. Meixner, S. Kasemann, T. Frederichs, E. Miramontes, S. Kasten

The Argentina Continental Margin represents a unique geologic setting where fundamental interactions between bottom currents, sediment deposition and their impact on biogeochemical processes and element cycling, in particular iron, can be studied. The aims of this study were to investigate 1) the consequences of various depositional conditions on biogeochemical processes and 2) the preservation and diagenetic cycling of Fe mineral phases in sediments. Furthermore, it was 3) studied how sedimentary stable Fe isotope signatures (δ^{56}Fe) are affected during early diagenesis and 4) evaluated whether δ^{56}Fe represents a reliable proxy for microbial Fe reduction in methanic sediments. During RV SONNE expedition SO260, two different depositional environments were sampled using a 10 m long gravity corer (GC) as well as a multi corer (MUC) for the retrieval of surface sediments. The first study site is located on the lower continental slope at 3605 m water depth (Biogeochemistry Site, cores GeoB22708-3/GeoB22709-1), while the second site is situated in a contourite system on the Northern Ewing Terrace at 1078 m water depth (Contourite Terrace Site, cores GeoB22722-3/GeoB22722-5) as shown in Figure 1. A sequential extraction protocol was applied on the collected sediments to determine four operationally defined reactive Fe phases targeting Fe carbonates, (easily) reducible Fe (oxyhydr) oxides and hardly reducible Fe oxides (Poulton and Canfield, 2005). Purification of extracts for δ^{56}Fe analysis of the Fe carbonates and easily reducible Fe (oxyhydr)oxide fractions followed protocols described in Henkel et al. (2016).

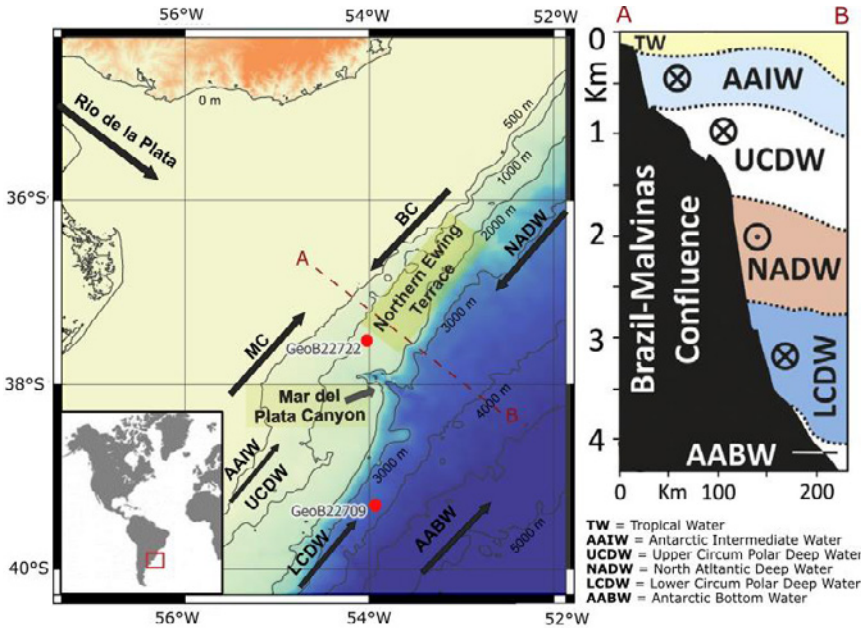

Fig. 1: (Left) Bathymetric map of the Coast of Argentina and Uruguay including water masses (The Gebco_2014grid, version20150318). MC (Malvinas Current) and BC (Brazil Current) form the Brazil-Malvinas Confluence. The study sites are highlighted. (Right) The water mass stratification modified after Preu et al. (2012) shows the distribution along the continental margin.

The dataset was combined with pore-water data obtained during the cruise and complemented by concentrations and stable carbon isotope data of dissolved methane determined post-cruise (Figs. 2 and 3). The redox zonation and depth location of the sulfate-methane-transition (SMT) differ at both sites. It is suggested that sedimentation rates at the lower continental slope are low with steady state conditions, leading to a strong diagenetic overprint of sedimentary Fe phases. This is in contrast to the sediments collected from the contourite system, that are characterized by high sedimentation rates and did not show a pronounced diagenetic overprint (e. g. Hensen et al., 2003, Kasten et al., 2003, Riedinger et al., 2005). Fe extraction data indicate that reactive Fe phases are subject to reductive dissolution at the SMT. Nevertheless, significant amounts of reactive Fe oxides are preserved below the SMT for deep Fe reduction (possibly through Fe mediated anaerobic oxidation of methane), which is evidenced by the presence of dissolved Fe in the methanic sediments. The δ^{56}Fe of reactive Fe phases in methanic sediments were determined here for the first time. These data suggest significant microbial fractionation of Fe isotopes during deep Fe reduction at the lower continental slope, whereas at the contourite site δ^{56}Fe signatures do not indicate remarkable microbial Fe isotope fractionation. It is concluded that the applicability of δ^{56}Fe signatures as tracer for microbial Fe reduction might be sensitive to the depositional regime, and thus may be limited in high sedimentation areas.

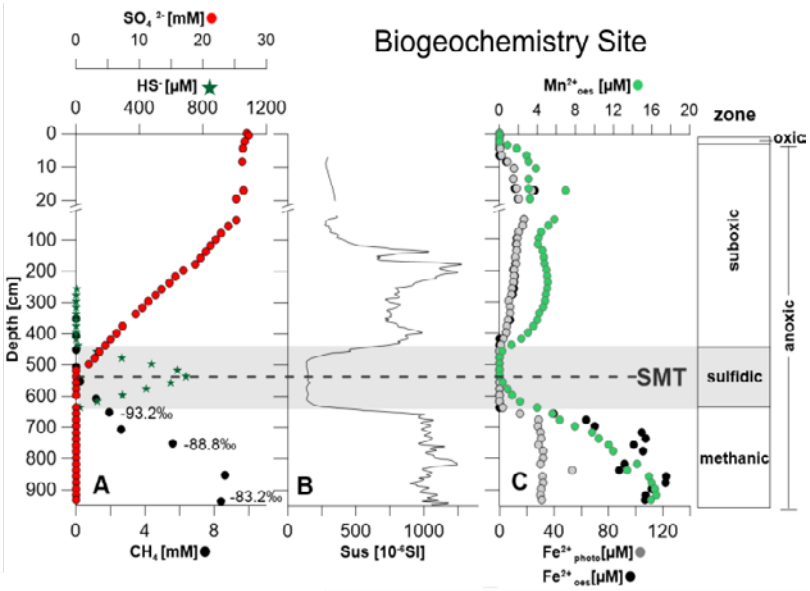

Fig. 2: Pore-water profiles analyzed during and after cruiseSO260 at the Biogeochemistry Site. Note break of vertical axis: data for the upper 20 cm is from MUC GeoB22708-3, data below is from GC GeoB22709-1. (A) CH_4, HS^-, SO_4^{2-}including $\delta^{13}C$-CH_4. (B) Magnetic susceptibility (Kasten et al., 2019). (C) Photometrically determined Fe^{2+}_{photo} and ICP-OES determined Fe^{2+}_{oes} along with Mn^{2+} profile (Melcher, 2019).

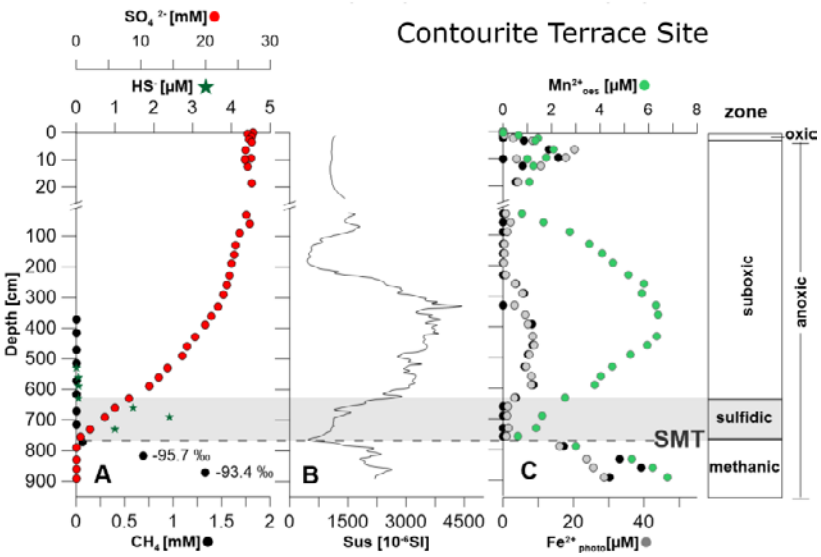

Fig. 3: Pore-water profiles analyzed during and after SO260 at the Contourite Terrace Site. Note break of vertical axis: data for the upper 25 cm is from MUC GeoB22722-3, below is from GC GeoB22722-5. (A) CH_4, HS^-, SO_4^{2-} including $\delta^{13}C$-CH_4. (B) Magnetic susceptibility (Kasten et al., 2019). (C) photometrically determined Fe^{2+}_{photo} and ICP-OES determined Fe^{2+}_{oes} along with Mn^{2+} profile (Melcher, 2019).

REFERENCES

Henkel S, Kasten S, Poulton S, Staubwasser M, Determination of the stable iron isotopic composition of sequentially leached iron phases in marine sediments. Chemical Geology 2016, 421, 93–102. doi: 10.1016/j.chemgeo.2015.12.003

Hensen C, Zabel M, Pfeifer K, Schwenk T, et al. Control of sulfate pore-water profiles by sedimentary events and the significance of anaerobic oxidation of methane for the burial of sulfur in marine sediments. Geochimica et Cosmochimica Acta 2003, 67, 2631–2647. doi: 10.1016/S0016-7037(03)00199-6

Kasten S, Zabel M, Heuer V, Hensen C, Processes and signals of nonsteady-state diagenesis in deep-sea sediments and their pore waters. In the South Atlantic in the Late Quaternary: reconstruction of material budget and current systems. Springer 2003, 431–459. doi: 10.1007/978-3-642-18917-3_20

Kasten et al., Dynamics of sedimentation processes and their impact on biogeochemical reactions on the continental slope off Argentina and Uruguay – DosProBio. Cruise Report of RV SONNE Cruise SO260 2019, 97p.

Melcher A, Impact of depositional regimes on biogeochemical cycling of iron in sediments of the Argentina Continental Margin. University of Bremen, Faculty of Geosciences 2019, 82p, unpublished master thesis.

Poulton SW, Canfield DE, Development of a sequential extraction procedure for iron: implications for iron partitioning in continentally derived particulates. Chemical Geology 2015, 214, 209–221. doi: 10.1016/j.chemgeo.2004.09.003

Riedinger N, Pfeifer K, Kasten S, Garming JFL, et al., Diagenetic alteration of magnetic signals by anaerobic oxidation of methane related to a change in sedimentation rate. Geochimica et Cosmochimica Acta 2005, 69, 4117–4126, doi: 10.1016/j.gca.2005.02.004

SO261

ECOLOGY AND BIOGEOCHEMICAL PROCESSES OF THE ATACAMA TRENCH SYSTEM

AUTHORS

Alfred Wegener Institute Helmholtz-Center for Polar and Marine Research, HGF-MPG Group for Deep Sea Ecology and Technology | Bremerhaven, Germany
F. Wenzhöfer

Max Planck Institute for Marine Microbiology | Bremen, Germany
F. Wenzhöfer

MARUM – University of Bremen, Germany
M. Zabel

University of Southern Denmark, Department of Biology | Odense, Denmark
R. N. Glud

And: science party SO261

Hadal trenches are the most remote parts of our global oceans, representing the most extreme and scantly explored habitats on Earth. However, recent investigations have shown that hadal trenches act as important depocenters for organic material and biological deep-sea hotspots with intensified diagenesis. However, the sources, transport and lability of the deposited material and the pathways responsible for the carbon degradation remain largely unknown. Furthermore, current investigations are based on very few measurements that typically target one spot in the central deposition basin. The main goal of expedition SO261 was to get a new understanding of biogeochemical processing and community structure of the Atacama Trench (AT) system which is underlying highly productive surface waters. The integrated multidisciplinary investigations were carried out at 6 sites along the trench axis from 24° to 20° S and are compared to 3 abyssal reference sites next to the trench. The key focus of the investigations was on benthic biogeochemical and biological sampling and observations, including the composition of the benthic communities (all size classes) as well as ecosystem functions (e. g. remineralization rates). Additionally, observations of the physicochemical characteristics of the water column and biological sampling from the surface to hadal depth were performed.

In situ O_2 microprofiles document intensified diagenetic activity along the trench axis as compared to the adjacent abyssal plain – and higher overall activity in the AT as compared to the few other trench environments that have been studied (Lou et al., 2018;

Wenzhöfer et al., 2016, Glud et al., 2013). However, our measurements also reflect a large variation in O_2 consumption along the trench axis presumably reflecting the local deposition dynamics. Porewater profiles and onboard incubations of AT sediments also reveal variable but substantial manganese and iron redox cycling and microbial sulfate respiration. Experimental ^{15}N-based rate measurements indicate active N_2 production and anaerobic ammonium oxidation below the oxic surface layer. We conclude that denitrification and anammox are substantial sinks for fixed nitrogen in hadal sediments with most of the loss conveyed by piezotolerant anammox bacteria. Preliminary microbial community analyses further indicate distinct communities in the trench system. These communities were more similar to communities from other trench systems (e. g. Kermadec Trench) than to their adjacent abyssal counterparts. Our results indicate that diagenetic gradients and the resulting biogeochemical zonation play a dominant role in shaping the overall community composition. Meiofauna communities also show a high variability within the trench axis site, p<resumably reflecting the variability in the dominant biogeochemical processes and organic matter availability. However, an elevated density and biomass in trench sediments compared to neighboring abyssal sites, as previously indicated, could not be confirmed. Elevated $^{210}Pb_{ex}$ inventories along the trench axis, as compared to other deep-sea sites, indicate sediment focusing and downslope transport to the trench bottom. However, differences between the investigated trench sites suggest varying transport processes along the axis affecting both the quality and quantity of the hadal food supply.

Using this multidisciplinary, concerted and quantitative approach in comparing carbon and nutrient fluxes as well as the connection, composition and structure of hadal communities we gained new knowledge on eutrophic trench ecosystems and deep sea ecosystems in general.

This study is part of the ERC project "Diagenesis and microbiology of Hadal trenches" (Grant 669947).

REFERENCES

Glud RN, Wenzhöfer F, Middelboe M, Oguri K Turnewitsch R, Canfield DE, Kitazato H (2013) High rates of benthic microbial activity at 10.900 meters depth: Results from the Challenger Deep (Mariana Trench), Nature Geoscience 2013 6, 284–288, DOI: 10.1038/NGEO1773

Luo M, Glud RN, Pan B, Cui W, Wenzhöfer F, Xu Y, Lin G, Chen D, Benthic carbon mineralization in hadal trenches: Insights from in-situ determination of benthic oxygen consumption. Geophysical Research Letters 2018, 45, 2752–2760. https://doi.org/10.1002/ 2017GL076232

Wenzhöfer F, Kazumasa O, Middelboe M, Turnewitsch R, Toyofuku T, Kitazato H, Glud RN, Benthic carbon mineralization in hadal trenches: Assessment by in situ O_2 microprofile measurements. Deep Sea Research I 2016, 116, 276–286.

SO261*

DISTRIBUTION AND DRIVERS OF BENTHIC BIODIVERSITY IN HADAL AND ABYSSAL REALMS THROUGH EDNA BASED INVENTORIES

AUTHORS

IFREMER | Plouzané, France
S. Arnaud-Haond, B. Trouche

IFREMER, MARBEC | Sète, France
M. Brandt

Sorbonne Université, CNRS, Station Biologique de Roscoff | Roscoff, France
H. Nicolas

CNRS, MARBEC | Sète, France
A. Atteia

Genoscope | Evry, France
J. Poulain

CEA-Institut de Génomique, GENOSCOPE | Evry, France
P. Wincker

Station Biologique de Roscoff, Sorbonne Université & CNRS | Roscoff, France
C. de Vargas

University de Bremen | Bremen, Germany
M. Zabel

Alfred Wegener Institute Helmholtz-Center for Polar and Marine Research Bremerhaven, HGF-MPF Group for Deep Sea Ecology and Technology | Bremerhaven, Germany
F. Wenzhöfer

University of Southern Denmark, Department of Biology | Odense, Denmark
R. N. Glud

IFREMER, EEP-LEP | Plouzané, France
D. Zeppilli

Biodiversity in the marine environment still mostly remains to be revealed. However, the difficulty to access it, particularly in the deep sea, and the time needed to deliver rigorous morphological descriptions of the many new species discovered during each oceanographic expedition render this task unrealistic at the scale of human lifetime. Environmental DNA (eDNA) offers, adopting a phylogenetic species concept, a parallel avenue to deliver rapid and standardized biodiversity inventories of the different biotic compartments forming deep sea communities, including prokaryotic and eukaryotic diversity. In the framework of the project "Pourquoi Pas les Abysses" (Ifremer) and its twin project eDNAbyss (CEA, Génoscope), we adopted a standardized protocol to sample and analyse molecularly and bioinformatically eDNA from sediment of bathyal, abyssal and hadal environments. Our main goal was to contribute to a molecular inventory of the deep sea biodiversity, in relation with abiotic descriptors of the environments. This protocol was deployed in several abyssal areas of the Atlantic and the Pacific, and in hadal environments during the Sonne cruise So261 on Atacama trench, in collaboration with the HADES (EU, ERC, Nordcee) project. Our aim was to explore the compared the levels and taxonomic composition of eukaryotic biodiversity along the trench axis and in reference abyssal areas. The first results showed decreasing biodiversity with site depth, despite a trend toward higher biomass in hadal than in abyssal systems. The relative influence of site and sediment depth on benthic communities, as well as geography (latitude/distance) was also shown to vary significantly depending on taxa. We will provide an overview of the extend of hadal versus abyssal biodiversity, the composition of communities, and the main relationship emerging with abiotic descriptors of the environment.

SO261*

AUTONOMOUS HADAL BENTHIC LANDER FOR IN SITU TRACER INCUBATIONS AND SEDIMENT RECOVERY TO STUDY BENTHIC COMMUNITY ACTIVITIES

AUTHORS

Alfred Wegener Institute Helmholtz-Center for Polar and Marine Research Bremerhaven | Bremerhaven, Germany
J. Lemburg

Alfred Wegener Institute Helmholtz-Center for Polar and Marine Research, HGF-MPG Group for Deep Sea Ecology and Technology | Bremerhaven, Germany
F. Wenzhöfer

Max Planck Institute for Marine Microbiology | Bremen, Germany
F. Wenzhöfer

University of Southern Denmark, Department of Biology | Odense, Denmark
M. Larsen, B. Thamdrup, R. N. Glud

Hadal trenches are the most remote parts of our global oceans, representing the most extreme and scantly explored habitats on Earth. However, recent investigations have shown that these ecosystems are biological hot spots compared to neighboring abyssal sites. A major challenge to investigate these habitats is the recovery of intact and undisturbed sediment samples. Hydrostatic pressure changes during sediment recovery will influence the activity of organisms and also the composition of the pore water (e. g. lysis of labile organic matter). Additionally, not many research vessels are capable to collect sediment samples from such depth.

Here we present an autonomous lander system for in situ sediment incubation and core recovery from hadal depth. Insertion of core liners and retraction of sediment cores is motor driven, providing mechanically undisturbed sediment samples and ensuring a safe instrument recovery. The lander is designed to collect 6 sediment cores and to vertically inject tracers in the sediment for in situ incubations. In each core we can apply 1 to 3 needles for injection over 10–20cm depending on the sediment penetration depth of the core liners. The tracers are injected in each core at a regular time interval of 2–6 hours (depending on bottom time) and a total volume of 100–250ml is injected along a vertical track at pre-programmed depth resolution. After injection the sediment cores are retracted into the bottom water for incubation until the end of the program. During a recent cruise

to the Atacama trench system (RV SONNE cruise So268, 2018) we injected $^{15}NO_{3^-}$, $^{15}NO_{2^-}$ and $^{15}NH_{4+}$ to quantify key processes in the benthic nitrogen cycle. Additionally, we also injected Br^- as an inert tracer for documenting the ability to evenly inject tracers in the sediment and explore to what extent lander recovery and core handling affected tracer distribution.

This study is part of the ERC project "Diagenesis and microbiology of Hadal trenches" (Grant 669947).

SO261*

BENTHIC NITROGEN CYCLING IN HADAL TRENCHES: HIGH RATES AND LARGE CONTRIBUTIONS FROM ANAMMOX

AUTHORS

University of Southern Denmark, Department of Biology | Odense, Denmark
B. Thamdrup, C. Schauberger, M. Larsen, A. Glud, R. N. Glud

Alfred Wegener Institute Helmholtz-Center for Polar and Marine Research Bremerhaven, HGF- MPG Group for Deep Sea Ecology and Technology | Bremerhaven, Germany
F. Wenzhöfer

Due to low input of reactive organics and resulting deep oxygen penetration, nitrogen cycling in abyssal sediments is generally dominated by aerobic nitrification and the benthic release of nitrate, while relatively little bioavailable N is converted to N_2 by anaerobic denitrification and anammox. By contrast, hadal sediments may represent hot spots of organic deposition and hence favor anaerobic processes to a larger extent, but little is known about the pathways of N cycling there. We investigated benthic nitrogen cycling along the axis of the Kermadec and Atacama trenches based on geochemical and biomolecular analyses as well as experimental ^{15}N-based rate measurements. Pore water extraction and microsensor profling both revealed steep decreases in NO_3-concentrations below the depth of O_2 penetration, with depletion of NO_3- already at 5–10 cm depth in the Atacama Trench compared to 15 cm in the Kermadec Trench. As NO_{2-} concentrations remained low and NH_{4+} only accumulated below the NO_{3-} zone, these profiles indicate active N_2 production and anaerobic ammonium oxidation. Shipboard incubations with $^{15}NO_{3-}$, $^{15}NO_{3-}$ or $^{15}NH_{4+}$ confirmed denitrification and anaerobic NH_{4+} oxidation activity with highest potential rates in the nitrogenous zone. Isotope pairing in N_2 further implied that NH_{4+} was oxidized through the anammox process, which was substantiated by a close correlation between rates and copy numbers of the anammox specific hydrazine synthase (hzs) gene. At most sites, anammox dominated N_2 production with contributions reaching 70 %. Based on hzs gene sequences, hadal anammox bacteria are closely related to “Ca. Scalindua” from shallower marine habitats. Judged from their activity during the incubations at surface pressure, these bacteria were not heavily impaired by decompression. This was substantiated by in situ incubations with ^{15}N tracers in the seafloor by means of a benthic lander, which generated patterns and rates of N_2 production consistent with those obtained in the laboratory. We conclude that denitrification and anammox are substantial sinks for fixed nitrogen in hadal sediments with most of the loss conveyed by anammox bacteria that appear to be piezotolerant. Our results demonstrate that high rates of biogeochemical activity persist beyond the oxic surface layer of these systems.

SO261*

MICROBIAL RESPIRATION IN HADALPELAGIC REALM OF ATACAMA TRENCH

AUTHORS

Shenzhen Key Laboratory of Marine Archaea Geo-Omics, Department of Ocean Science and Engineering, Southern University of Science and Technology | Shenzhen, China
Xinxin L., Xin Z.

University of Southern Denmark, Department of Biology | Odense M, Denmark
R. N. Glud

Departamento de Oceanografía, Universidad de Concepción | Concepción, Chile
O. Ulloa, I. Fernández Urruzola

Instituto Milenio de Oceanografía, Universidad de Concepción | Concepción, Chile
O. Ulloa, I. Fernández Urruzola

State Key Laboratory of Marine Environmental Science, Institute of Marine Microbes and Ecospheres, College of Ocean and Earth Sciences, Xiamen University | Xiamen, China
Wenpeng L.

Trenches are the "last front" in marine science research. Fully understanding organic carbon (OC) recycling in the water column is essential to understand the trench sediment being a depocenter of OC. Here we presented the first integrated study of size fractionated microbial community respiration (MCR) rate and dark dissolved inorganic carbon (DIC) fixation rate from epipelagic to hadalpelagic water as well as their potential linkages with primary production in Atacama Trench. Depth profiles of DIC fixation rate at most sites showed a decrease from 5m to 6000 m and went up in hadal trenches indicating the importance of DIC fixation in dark ocean. MCR were notably decreased from epi-to meso-pelagic zone (~1000m) and kept constant in bathy- and abyssopelagic zones, but varied in hadal-pelagic water significantly from overlying water column, with some extremely high rates in bottom depths. Relatively, over 60 % (71.00±12.10 %, n=123) of the total MCR was contributed from particle attached (PA) fractions (>0.8 μm) rather than the free-living (FL) fraction (0.2–0.8 μm). Overall, the dark DIC fixation rates were too little compared to 3 magnitude higher MCR to be counted as important energy sources in Atacama Trench. Comparation between integrated-MCR at different layers

and 8-year average net primary production (NPP) indicated unique carbon sources in hadal pelagic water besides primary production. This first quantitative exploit of the study will provide basic understanding of processes in trench storage of OC and marine OC cycling.

SO261*

INTRA- AND INTER-TRENCH HETEROGENEITY OF SEDIMENTARY ORGANIC CARBON REVEALED BY COMPOSITION, SOURCES, AND AGE IN KERMADEC TRENCH AND ATACAMA TRENCH

AUTHORS

Shanghai Ocean University, College of Marine Sciences | Shanghai, China
Yunping X., Min L.

South University of Science and Technology, Department of Ocean Science and Engineering | Shenzhen, China
Xinxin L.

University of Southern Denmark, Department of Biology | Odense, Denmark
R. Glud

The biogeochemistry of sedimentary organic matter exerts profound influences on the life and ecology of the hadal zone, the deepest ocean realm with water depth of 6000–11,000 m. However, our knowledge on the hadal zone is rudimentary due to the great sampling and monitoring challenges. Here, we investigated several short cores collected from oligotrophic Kermadec Trench (KT) and upwelling-induced high productive Atacama Trench (AT). By analyzing elementary compositions (TOC, TN, TOC/TN), stable isotopes ($\delta^{13}C$, $\delta^{15}N$), radiocarbon (^{14}C) age and biomarkers (such as alkanes, alkanols, fatty acids, sterols), we attempted to understand spatial variability in concentration, composition and source of sedimentary organic carbon at intra- and inter-trench scales. Trench axis sites generally showed higher TOC contents than adjacent abyssal sites in each trench, whereas the AT has higher concentrations of sedimentary TOC and biomarkers than KT, consistent with their primary productivity. The $\delta^{13}C$, TOC/TN and biomarkers reveal a mixed contribution of terrestrial and marine-derived organic matter, but the enrichment terrestrial organic matter was a common phenomenon along trench axis, likely attributed to better preservation of terrestrial OC during transport processes. The vertical profiles of ^{14}C age and other parameters suggest relatively stable depositional conditions at the abyssal sites with post-depositional decay of OC, but unstable depositional conditions at the hadal sites (e. g., reversal of ^{14}C, large amplitude changes in TOC, TOC/TN and $\delta^{13}C$ and biomarkers). These abrupt changes were caused by earthquake-triggered turbidity currents. Overall, our study provided evidence that the heterogeneity of sedimentary organic matter between trenches and within the trench. More investigations are needed for better understanding the biogeochemistry of organic matter in the hadal zone and its role in global ocean carbon cycling.

SO261*

HIGH BENTHIC TRANSFER RATES WITH LOW CONCENTRATIONS OF ORGANIC CARBON – NO CONTRADICTION IN THE ATACAMA TRENCH

AUTHORS

MARUM – University of Bremen | Bremen, Germany
M. Zabel, E. Okuma

GEOMAR Helmholtz Centre for Ocean Research Kiel | Kiel, Germany
Chuang Pei-Chuan

MARUM – Center for Marine Environmental Sciences, University of Bremen | Bremen, Germany
M. Elvert, M. Kölling

Sediments of abyssal plains and in deep-sea trenches have long been considered relatively inactive from a microbiological point of view. High abundances of benthic organisms (Danovaro et al. 2003) and high microbial carbon turnover rates at the seafloor surface (Glud et al. 2013) have already corrected this assumption for some deep-sea ditches. Obviously, partial ocean trenches function as a kind of trap for particulate organic material, which is transported by currents or debris flow from the steep edges into trenches. So far, biogeochemical investigations in deep-sea trenches have only been available for surface sediments. Here we present the first results of deep buried sediments. The samples were collected on a cruise of the RV SONNE in spring 2018 to the Atacama Trench. They prove that even several meters below the seabed the microbial activity can reach an intensity comparable to that known from coastal high production areas. Despite significantly lower total carbon contents in the sediments of the trench, considerable flow rates were observed. We assume that the main original ash for this finding is in the sediment dynamics in the vicinity of the trench. The sediments are characterized by a large number of smaller and more powerful turbidite layers and therefore show very high accumulation rates. Obviously, reactive organic material is buried relatively fast and is therefore preferentially available for anoxic degradation processes.

REFERENCES

Danovaro R, Croce ND, Dell'Anno A, Pusceddu A. (2003). A depocenter of organic matter at 7800m depth in the SE Pacific Ocean. Deep-Sea Res. I 2003, 50, 1411–1420.

Glud RN, Wenzhöfer F, Middelboe M, Oguri K, Turnewitsch R, Canfield DE, Kitazato H, High rates of microbial turnover in sediments in the deepest oceanic trench on Earth. Nature 2013, 6, 284–288.

SO262

NODULE RESOURCES, BIODIVERSITY AND ENVIRONMENT OF THE GERMAN LICENSE AREA FOR THE EXPLORATION OF POLYMETALLIC NODULES IN THE EQUATORIAL NOTHEAST PACIFIC

AUTHORS

Bundesanstalt für Geowissenschaften und Rohstoffe | Hannover, Germany
C. Rühlemann, T. Kuhn, K. Schmidt, A. Vink

Deutsches Zentrum für Marine Biodiversitätsforschung, Senckenberg am Meer | Wilhelmshaven, Germany
P. Martínez Arbizu, N. Mercado Salas, K. Uhlenkott

Jacobs University Bremen | Bremen, Germany
B. Gillard

The Lyell Centre for Earth and Marine Science and Technology, Heriot-Watt University | Edinburgh, Scotland, UK
R. Harbour

And: cruise participants

The MANGAN 2018 cruise with R/V SONNE to the eastern part of the German license area for the exploration of polymetallic nodules in the East Pacific (Fig. 1) was carried out from 6 April to 29 May 2018, starting in Guayaquil (Ecuador) and ending in Suva (Fiji). During this period, we investigated three working areas (WA-1 to WA-3) in the east of the license area. The cruise had three major aims: (1) exploration of a new prospective manganese nodule field, (2) recovery of manganese nodule mass samples for metallurgical experiments at pilot plant scale, and (3) acquisition of high-resolution baseline environmental data in preparation for a collector test in April 2019. The environmental investigations included (i) detailed studies of the benthic biodiversity, (ii) measurements of metal concentrations in (sub)bottom waters, (iii) mooring of three ADCP current meters for the analysis of the bottom current regime until April 2019, and (iv) mooring of a sediment trap until April 2019 in order to determine background particle fluxes. Furthermore, we continued the sampling of time series for biodiversity analysis in the two reference areas for which annual samples for the period between 2013 and 2016 were already available.

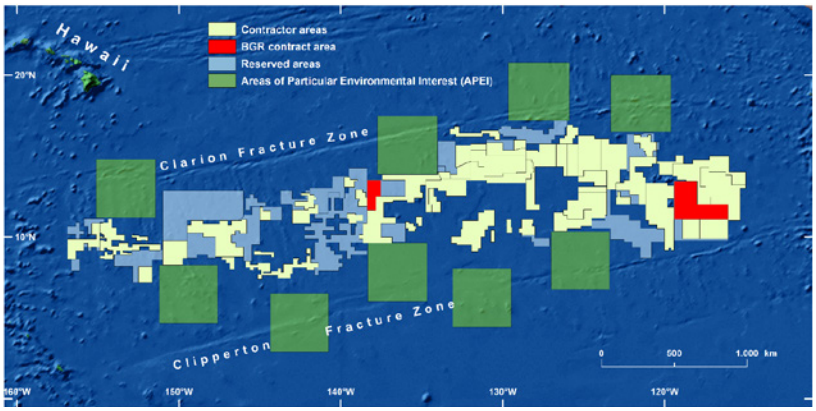

Fig. 1: Locations of the two parts of the BGR contract area for polymetallic nodules exploration (highlighted in red) within the Clarion-Clipperton Fracture Zone of the Pacific Ocean. Other contractor areas are shown in yellow, Reserved Areas are displayed in blue-grey and Areas of Particular Environmental Interest are shown in green.

The northern part of working area WA-1 includes the nodule field selected for the collector test of the Belgian company DEME-GSR in April 2019. Within an area of 4 x 5 km, we recovered multicorer (MUC) samples at 26 stations for the investigation of meiofaunal biodiversity, the geochemical composition of porewater and sediments and the particle size distribution. Furthermore, we collected seawater for the analysis of trace elements and sinking particulate matter with a Rosette water sampler equipped with a CTD (ROS/CTD) and a marine snow catcher (MSC) to study the effects of a sediment plume release in the upper water column during potential future deep-sea mining. Along two 10-kilometre-long video sledge profiles, we obtained data on manganese nodule coverage and size distribution and studied the diversity of megafaunal organisms. The benthic lander "Anonyx", equipped with a bait and a high-resolution camera, was deployed three times for 24-36 hours each to analyse the diversity and behaviour of scavengers. Our work in the collector test area was completed by two multinet (MN) stations to recover plankton throughout the water column and the mooring of a sediment trap equipped with current meters for one year.

In the southern part of WA-1, which includes the "Impact Reference Zone" of the German license area, we recovered MUC samples at six stations and carried out two epibenthic sledge (EBS) deployments in order to continue a time series of annually repeated sampling for biodiversity studies from 2013 to 2016. We used the ROS/CTD to collect water samples for particle and metal concentration analyses at three stations and the MSC to sample aggregates at two stations. Along a short video sledge transect we mapped the area close to a three year old EBS track and found that the sediment blanketing of nodules up to 40 m north and 100 m south of the track, as observed in 2015 shortly after the disturbance due to the EBS deployment, is no longer present. This suggests re-suspension of the thin sediment layer during periods of enhanced current velocities, in agreement with experimental results showing that resettled particle aggregates are

re-suspended at velocities >8 cm/s. Furthermore, we deployed the Anonyx lander two times and recovered 11.5 tons of nodules (wet weight) with 13 dredge deployments for future metallurgical experiments at pilot plant scale.

In working area WA-2, located about 80 km east of WA-1, we explored the economic potential of a nodule field of 350 km^2 size with 41 box core samples and two transects of high-resolution video sledge mapping. WA-2 is predominantly covered with big nodules larger than 4 cm in diameter. The seafloor samples and onboard XRF measurements showed consistently high nodule abundances of 23 kg/m^2 on average and high mean metal concentrations of 3% nickel, copper and cobalt in total. The total quantity of manganese nodules in this area amounts to eight million metric tons (mt) wet weight, which is equivalent to 79,000 mt Ni, 66,000 mt Cu, 9500 mt Co, and 1,7000,000 mt Mn. This amount of nodules could potentially sustain two to three years of deep-sea mining. In addition, we deployed the Anonyx lander at four stations and the ROS/CTD at two stations. Seven MUC stations, two EBS tracks, four MSC stations, and one MN station complemented our work in WA-2. Afterwards, we sailed 44 nm north to the license area of UK Seabed Resources Ltd where we recovered two moored sediment traps that were deployed in 2015.

Working area WA-3 represents the "Preservation Reference Zone" of the German license area, where we likewise continued a biodiversity time series of four consecutive years started in 2013 by sampling at six MUC sites and two EBS tracks. We further deployed a mooring with two current meters. During the mapping of a 13.5 km long transect of the seafloor with the video sledge, we were able to detect three 1.5 m wide EBS tracks from previous years and a fresh track from the day before. As already observed in WA-1, resettled sediment on nodules in proximity to the old EBS tracks has obviously been re-suspended and drifted away, likely during phases of enhanced current velocities. We further deployed a MSC at one station, carried out a full depth CTD station and a MN station. With one more Anonyx lander station in this working area, we finished nine lander deployments in total during the MANGAN 2018 cruise. A preliminary evaluation of these nine video records showed that relatively few species dominate the bait-attended population, which appear in arrival sequence on the bait.

Further working areas were chosen for individual stations: a prominent seamount of 2100 m height between WA-1 and WA-2 served to obtain oceanographic data required for hydrodynamic models on sediment plume dispersion. Two gravity corer stations in the south of the license area were selected to obtain long sediment cores at sites where sediment echo sounder recordings from previous cruises revealed buried nodules at about 7 m sediment depth. The cruise ended after 30 working days and 177 stations with the successful completion of all planned activities of the exploration program.

First results of the biodiversity sampling revealed that the megafauna is dominated by Xenophyophora, Echinodermata, Anthozoa and Porifera. During the MANGAN 2018

cruise, 43 megafaunal taxa (morphological identification) were documented. Regarding the macrofauna, most abundant taxa are Copepoda and Polychaeta, followed by Chaetognatha, Bivalvia and Ostracoda. In 2013, a time series of two EBS stations has been initiated, that was sampled for the fifth time during this cruise. Comparing relative abundances, the community is dominated by Copepoda in 2018 and 2015, whereas Polychaeta comprise the most abundant taxon in all other years. Zooplankton, investigated across the complete water column, revealed changes in community with increasing depth. The number of taxa and the diversity decreased in the oxygen minimum zone (150–700 m) as compared to the surface community. Below 700 m, we observed typical deep-water taxa.

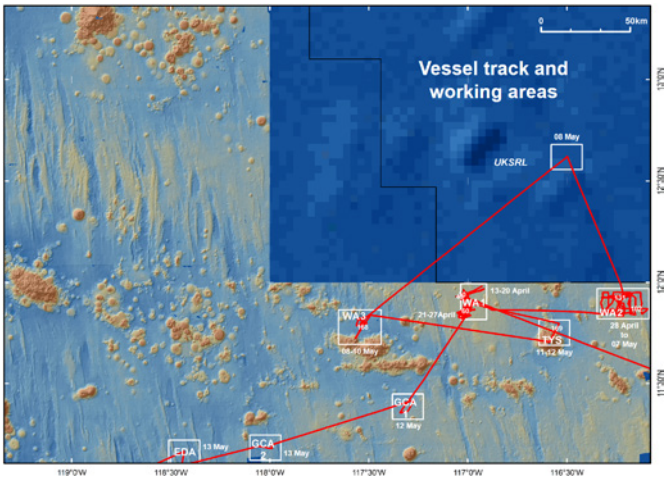

Fig. 2: Bathymetric map of the eastern part of the German license area with the track of R/V SONNE during cruise MANGAN 2018 in red. Labels WA-1 to WA-3 represent the three main working areas (CHAPTER 2.5 and onwards in the cruise report).The dates specify the time periods spent in each of the working areas.

SO262*

PRELIMINARY RESULTS FROM OCEAN BOTTOM MOORINGS: NEAR-BOTTOM CURRENTS AND PARTICLE FLUXES IN THE NE EQUATORIAL PACIFIC (MANGAN2018, SO262)

AUTHORS

Bundesanstalt für Geowissenschaften und Rohstoffe (BGR) | Hannover, Germany
M. Hollstein, A. Vink, C. Rühlemann

MARUM – Center for Marine environmental Sciences, University of Bremen | Bremen, Germany
K. Purkiani

The globally increasing demand for metals and rare earth elements has raised the interest for potential mining of deep-sea mineral resources such as polymetallic nodules. One important field of polymetallic nodules is located in the northeastern equatorial Pacific, within the Clarion-Clipperton Fracture Zone (CCZ). On behalf of the German Federal Ministry for Economics and Energy, the Federal Institute for Geosciences and Natural Resources (BGR) has held a license for the exploration of manganese nodules in the CCZ with the International Seabed Authority (ISA) since 2006. Against this background and in addition to carrying out resource assessments, BGR, in cooperation with partners from national and international research institutes, has the obligation to conduct detailed environmental studies in its license area.

To assess the environmental impacts of potential future mining activities, a nodule pre-prototype collector test is scheduled to occur in the German license area in autumn 2020, and will be accompanied by an extensive environmental monitoring program (joint effort between BGR and the European research project JPI-Oceans "MiningImpact2"). However, to assess the impact of mining activities on the deep-sea environment, for example due to the development of an operational sediment plume on the seafloor, prior knowledge on the bottom current regime and variability of particle flux and composition within the CCZ under natural conditions is a prerequisite. One major goal of the SO262 expedition was the acquisition of high-resolution, pre-impact baseline environmental data from the study area. This included the deployment of Ocean Bottom Moorings (OBM) equipped with current and turbidity meters for the analysis of the bottom current regime between April 2018 and April 2019, and a sediment trap to determine background particle fluxes and composition. Here, we present first results of these oceanographic and sedimentological datasets and analyses, and compare the results with other available information deriving from the region.

SO264*

SONNE-EMPEROR: THE PLIO/PLEISTOCENE TO HOLOCENE DEVELOPMENT OF THE PELAGIC NORTH PACIFIC FROM SURFACE TO DEPTH – ASSESSING ITS ROLE FOR THE GLOBAL CARBON BUDGET AND EARTH´S CLIMATE

AUTHORS

GEOMAR Hemholtz Centre for Ocean Research Kiel | Kiel, Germany
D. Nürnberg

Alfred-Wegener-Institut Hemholtz-Zentrum für Polar- und Meeresforschung, Bhv | Bremerhaven, Germany
R. Tiedemann, L. Lembke-Jene

And: SO264 Shipboard Scientific Party

The North (N) Pacific increasingly attracts attention due to its prime role in shaping the Earth's climate. The RV SONNE-EMPEROR cruise SO264 aiming at the Emperor Seamount Chain in the N Pacific (Fig. 1, 2) focussed on scientific questions closely linking paleoceanographic, paleoclimatic, chemical-oceanographic, and marine biological studies in an integrated approach to advance the dynamic and three-dimensional process-oriented understanding of the complex N Pacific's role for regulating ocean-atmosphere greenhouse gas exchanges prior to anthropogenic timescales.

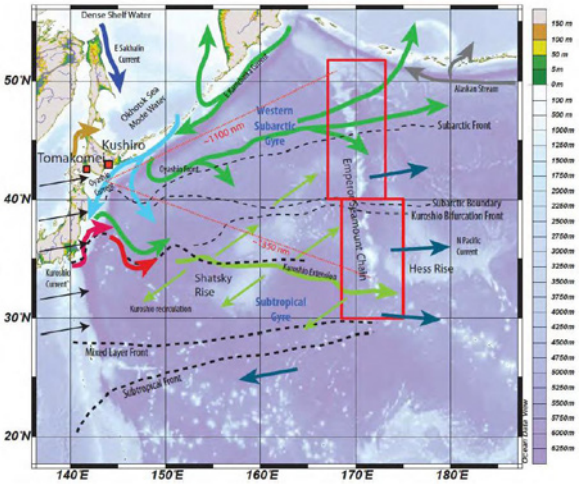

Fig. 1: Bathymetric chart of the N Pacific showing the SO264 study area.

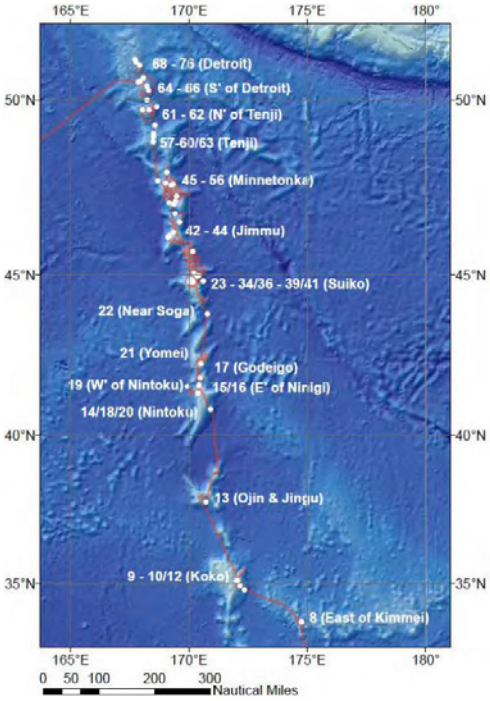

Fig. 2: Bathymetric chart showing GEO-stations sampled during SO264.

RV SONNE cruise SO264 took place in the framework of the BMBF-funded joint project "SONNE EMPEROR" coordinated by GEOMAR and AWI (June 30–August 24, 2018, Suva – Yokohama). SO264 blogs and videos are available at www.bmbf.de, www.oceanblogs.org, and www.youtube.com.

In a so far unique approach, we recovered closely-spaced high-quality sediment records (~640 m core recovery from ~1100 m to ~5700 m water depth) from a broad meridional transect along the Emperor Seamount Chain (~170°E), spanning subtropical to subarctic ocean climate regimes from ~30°N to ~50°N, and crossing major oceanographic and climatic patterns (e. g. the Kuroshio Extension, the Kuroshio Bifurcation Front, the Subarctic Boundary, the Subarctic Front). The deep-sea deposits are important climate archives, which shed light on the long-term Plio/Pleistocene oceanographic and climatic development of the pelagic N Pacific, and will allow exact statements on e. g. changes in ocean physical properties, stratification of the water column and deep ocean ventilation in the past.

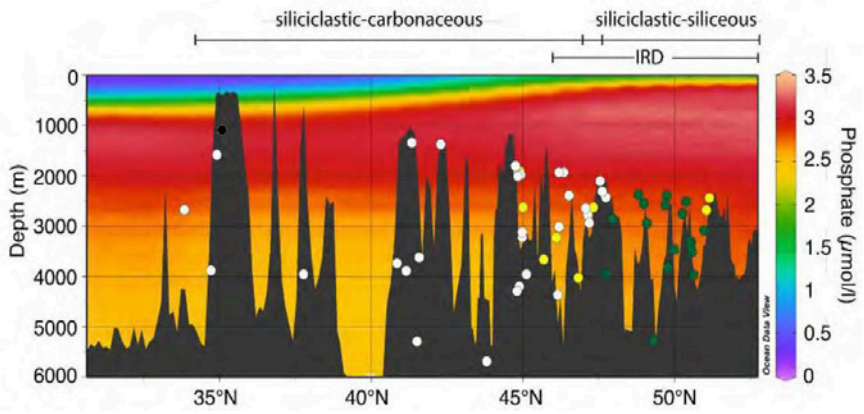

Fig. 3: North-south oriented SO264 core transect along the Emperor Seamount Chain. White dots – siliciclastic-carbonaceous sediments; green dots – siliciclastic-siliceous (opaline) sediments; yellow dots – bent sediment cores. IRD – ice-rafted debris. Color shading indicates phosphate concentrations in seawater from WOA (Garcia et al., 2009). Section done with ODV4 (Schlitzer, 2014).

The suite of proxy data we are currently working with will allow us to yield a comprehensive understanding of the interdynamic development of surface, subsurface, and deep water masses, and will provide clues on atmosphere-ocean exchange processes, the evolution of the cryosphere, interhemispheric coupling, and inter-ocean exchange. We will present high-resolution (isotope) geochemical proxy records from cores, which have meanwhile been stratigraphically classified.

REFERENCES

Garcia H E., Locarnini R A., Boyer, T P et al. World Ocean Atlas 2009, Volume 4: Nutrients (phosphate, nitrate, silicate). S. Levitus, Ed. NOAA Atlas NESDIS 71, 2010, U.S. Government Printing Office, Washington, D.C., 398 pp.

Nürnberg D ed. RV SONNE Fahrtbericht / Cruise Report SO264 - SONNE-EMPEROR: The Plio/Pleistocene to Holocene development of the pelagic North Pacific from surface to depth – assessing its role for the global carbon budget and Earth's climate, Suva (Fiji) – Yokohama (Japan), 30.6.–24.8.2018. GEOMAR Report, N. Ser. 046, 2018, 284 pp. DOI 10.3289/GEOMAR_REP_NS_46_2018.

Schlitzer R Ocean Data View, 2014, http://odv.awi.de

SO268/3*

ISOLATION AND QUANTIFICATION OF MICROPLASTIC PARTICLES FROM WATER AND SEDIMENT SAMPLES COLLECTED DURING SO268/3 ON THE PACIFIC OCEAN

AUTHORS

Helmholtz Centre for Environmental Research – UFZ, Department of Analytical Chemistry | Leipzig, Germany

R. Rynek, P. Klöckner, T. Reemtsma, S. Wagner

In 2018 the global plastic production exceeded 340 million tons (PlasticsEurope, 2018). Due to insufficient waste management and deliberately incorrect waste disposal it is estimated that up to 10 % of the annual produced plastic mass reaches the oceans (Thompson, 2007). Assuming there is no change in the way plastic waste is handled, more than 250 million tons of plastic could have reached the oceans by 2025 where it accumulates in different zones due to the influence of wind and ocean currents (Maximenko, Hafner and Niiler, 2012; Jambeck et al., 2015). One of these accumulation zones is the Great Pacific Garbage Patch between California (USA) and Hawaii. It is expected that there is also a vertical distribution of plastic across the water column in the ocean. The aim of this study is to determine the lateral and vertical distribution of plastic particles in the Pacific Ocean, to identify possible material- or size-specific sinks and to compare the concentration of plastic particles between accumulation zones and remote regions. Therefore, samples from surface and near-surface waters, the water column at different depths and the sea sediment were taken during the cruise SO268/3 between Vancouver and Singapore from May to July 2019. (Fig. 1)

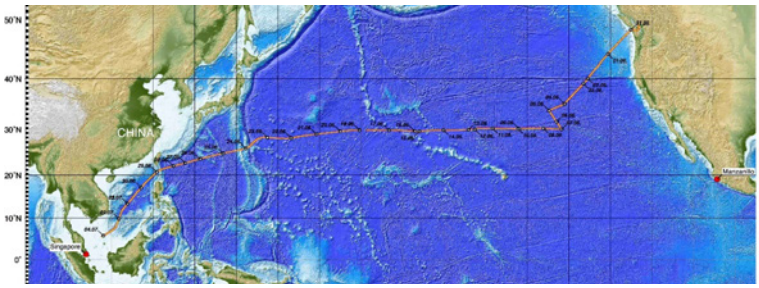

Fig. 1: Track of cruise SO268/3 on research vessel SONNE

Here we present the planned workflow from sampling to quantification of plastic particles in different matrices and some preliminary results on recovery experiments and methodical tests for the isolation of plastic particles from different matrices.

The upper 5 cm of sediment samples taken with a multicorer in depths > 5000 m will be used for micro plastic analysis. To isolate polymer particles from the sediment matrix a density separation approach with sodium polytungstate is used, where our preliminary experiments show recovery rates > 90 % for polystyrene particles in the size range of 45–63 µm and a concentration of 10 particles per g of sediment. After isolation, residual organic matter may be removed by an enzymatic cleanup procedure if there are interferences with the used FT-IR detection (Löder et al., 2017). Remaining particles will then be filtrated on Anodisc membranes and subjected to FT-IR analysis.

Suspended matter from water was sampled by catamaran trawling (surface water, > 330 µm), cascade filtration (surface-near water, > 500 µm–10 µm) and in situ pumps (water column, > 30 µm–0,45 µm). After resuspending the particles by rinsing the used sampling devices or filters, the organic matrix is removed by enzymatic or chemical cleanup and the residual particles are deposited on Anodisc filters. Preliminary experiments show that the cleanup is necessary to measure the samples with FT-IR imaging because the high abundance of natural particles interferes with the detection of polymer particles. The enzymatic cleanup procedure clearly decreases the amount of natural organic particles on the filter surface, enables the measurement of polymer particles and increases the quality of measured spectra. (Fig. 2) Further experiments will be conducted to evaluate the cleanup procedure in terms of recovery, influence on particle size distribution and changes in specta of different reference materials. The final protocol will then be applied to the suspended matter samples from the Pacific Ocean.

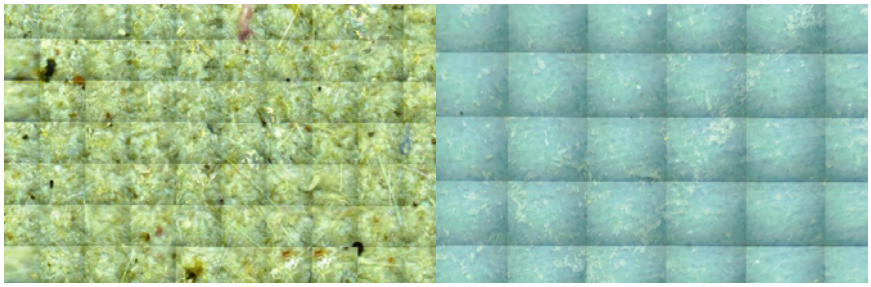

Fig. 2: Microscope image without cleanup (left) and after enzymatic digestion (right)

Focal plane array-based transmission mode FT-IR imaging combined with database comparison is then used to determine the number, size and composition of the isolated polymer particles < 500 µm on the membrane filters from both sediment and suspended matter samples. Plastic particles > 500 µm will be sorted out visually and identified by ATR-FT-IR spectroscopy.

REFERENCES

Jambeck, J. R. et al. (2015) 'Plastic waste inputs from land into the Ocean', Science, 347(6223), pp. 768–771. doi: 10.1126/science.1260352.

Löder, M. G. J. et al. (2017) 'Enzymatic Purification of Microplastics in Environmental Samples', Environmental Science and Technology, 51(24), pp. 14283–14292. doi: 10.1021/acs.est.7b03055.

Maximenko, N., Hafner, J. and Niiler, P. (2012) 'Pathways of marine debris derived from trajectories of Lagrangian drifters', Marine Pollution Bulletin. Elsevier Ltd, 65(1–3), pp. 51–62. doi: 10.1016/j.marpolbul.2011.04.016.

PlasticsEurope (2018) 'Plastics - the Fact 2018', 71(1–2), pp. 299–306. doi: 10.1016/j.marpolbul.2013.01.015.

Thompson, R. C. (2007) 'Plastic debris in the marine environment: consequences and solutions', Marine Nature Conservation in Europe 2006, (May 2006), pp. 107–116.

PS118*

INFLUENCE OF ICE COVER AND LATITUDE ON ANTARCTIC PERACARID CRUSTACEANS IN A CHANGING ENVIRONMENT

AUTHORS

Senckenberg Naturmuseum | Frankfurt am Main, Germany
D. Di Franco, H. Saaedi, A. Brandt

British Antarctic Survey (BAS) | Cambridge, United Kingdom
K. Linse, H. Griffiths

Alfred Wegener Institute, Helmholtz Centre for Polar and Marine Research | Bremerhaven, Germany
C. Haas

In February 2019 the RV Polarstern sailed towards the Larsen-C ice-shelf from which in 2017 a huge portion of ice (iceberg A68) calved exposing the underlying seafloor to new environmental conditions (Hogg and Gudmundsson 2017). The aim of the expedition (PS118) was to investigate the communities of peracarid crustaceans which lived under the ice-shelf and assess the influence of the latter on their composition and diversity. The samples would therefore be compared to those collected during previous expeditions in other areas characterised by different extents of ice-cover (Figure 1A): Prince Gustav Channel (JR17003a) where the ice shelf collapsed in 1995, the seasonally ice-covered Filchner Trough (JR275), the ice free South Orkney Islands (JR15005). Unfortunately, during the expedition PS118 it was not possible to reach the Larsen-C due to heavy ice conditions, therefore samples were collected in other locations along the Antarctic Peninsula, following a latitudinal gradient and leading to new scientific questions.

The aim of the study is to investigate the influence of ice cover and latitude on peracarid abundance and species composition comparing areas characterised by different ice cover regime and latitudinal gradients. Besides the influence of other environmental parameters (e. g. depth, temperature, salinity, type of sediments, primary production) is also assessed.

A total of 64766 peracarids were sorted and identified at order level (Amphipoda, Isopoda, Cumacea, Tanaidacea and Mysidacea).

The calculated trawling distances were normalised to 1000 m hauls in order to carry out comparative analyses.

Filchner Trough (JR275) showed the highest abundance with 51 079 individuals per 1000 m hauls, while South Orkney Islands (JR15005) were the least populated with only 7714 individuals (Figure 2B). In total Cumacea were the most abundant taxon with 33,700 individuals per 1000 m hauls, representing the 31 % of the total abundance, followed by Amphipoda (32,815 individuals, 30 %) and Isopoda (31,360 individuals, 29 %). Tanaidacea and Mysidacea showed 4,955 and 4,908 individuals per 1000m respectively, both representing the 5 % of the total abundance (Figure 2A).

Statistical analysis showed a significant correlation between the total abundance of peracarids from different areas and environmental parameters such as chlorophyll concentration, depth, ice cover, phytoplankton, salinity and temperature ($p<0.05$; Figure 5C-H). In particular, higher values of chlorophyll, phytoplankton and ice cover result in an increase of peracarid abundance, whereas at higher temperature, salinity and depth the abundances decrease. At the present stage no correlation between abundance of peracarids and latitude was found, although the future inclusion of previous published data of peracarid abundances in the analysis may provide us additional information. Our study shows the interaction between environmental parameters and macrobenthic peracarids providing us useful information on how possible changes of such parameters could have an influence on their actual distribution and abundance. A better understanding of the aforementioned interactions can be an important factor to predict the ecological impact induced by the on-going climate change.

REFERENCES

Hogg, Anna E., and G. Hilmar Gudmundsson. "Impacts of the Larsen-C Ice Shelf calving event." Nature Climate Change 7.8 (2017): 540

Figure 1: Expeditions and sampling stations (A); Amphipoda, Eusirus perdentatus Chevreux,1912 (B); Isopoda, Ceratoserolis trilobitoides (Eights, 1833) (C); Cumacea, Campylaspis G.O. Sars, 1865 (D).

Figure 2: Pearson correlation between abundance of peracarids from all the stations and environmental parameters, $p < 0.05$.

SCHRIFTENREIHE PROJEKTTRÄGER JÜLICH

1. Technologie- und Erkenntnistransfer aus der Wissenschaft in die Industrie
   Eine explorative Untersuchung in der deutschen Material- und Werkstoffforschung
   hrsg. von A. Pechmann, F. Piller und G. Schumacher (2010), 230 Seiten
   ISBN: 978-3-89336-624-8

2. STATUSTAGUNG SCHIFFFAHRT UND MEERESTECHNIK
   Tagungsband der Statustagung 2010 (2010), 173 Seiten
   ISBN: 978-3-89336-677-4

3. STATUSTAGUNG SCHIFFFAHRT UND MEERESTECHNIK
   Tagungsband der Statustagung 2011 (2011), 227 Seiten
   ISBN: 978-3-89336-745-0

4. STATUSTAGUNG SCHIFFFAHRT UND MEERESTECHNIK
   Tagungsband der Statustagung 2012 (2012), 206 Seiten
   ISBN: 978-3-89336-832-7

5. STATUSTAGUNG MARITIME TECHNOLOGIEN
   Tagungsband der Statustagung 2013 (2013), 188 Seiten
   ISBN: 978-3-89336-922-5

6. STATUSTAGUNG MARITIME TECHNOLOGIEN
   Tagungsband der Statustagung 2014 (2014), 179 Seiten
   ISBN: 978-3-95806-006-7

7. STATUSTAGUNG MARITIME TECHNOLOGIEN
   Tagungsband der Statustagung 2015 (2015), 196 Seiten
   ISBN: 978-3-95806-104-0

8. STATUSTAGUNG MARITIME TECHNOLOGIEN
   Tagungsband der Statustagung 2016 (2016), 220 Seiten
   ISBN: 978-3-95806-187-3

9. STATUSSEMINAR MEERESFORSCHUNG mit FS SONNE
   14.–15. Februar 2017 in Oldenburg–Tagungsband (2017), 221 Seiten
   ISBN: 978-3-95806-207-8

10. STATUSTAGUNG MARITIME TECHNOLOGIEN
    Tagungsband der Statustagung 2017 (2017), 224 Seiten
    ISBN: 978-3-95806-277-1

11. STATUSTAGUNG MARITIME TECHNOLOGIEN
    Tagungsband der Statustagung 2018 (2018), 224 Seiten
    ISBN: 978-3-95806-366-2

12. STATUSTAGUNG MARITIME TECHNOLOGIEN
Tagungsband der Statustagung 2019 (2018), 187 Seiten
ISBN: 978-3-95806-439-3

13. STATUS CONFERENCE RESEARCH VESSELS 2020
Conference transcript
Online-Publikation (2020), 411 Seiten
ISBN: 978-3-95806-479-9


Projektträger Jülich
Forschungszentrum Jülich


HELMHOLTZ
RESEARCH FOR GRAND CHALLENGES